

AMMONIUM THIOSULPHATE LEACHING OF GOLD FROM PRINTED CIRCUIT BOARD WASTE

by

Pierre Wouter Albertyn

Thesis presented in partial fulfilment
of the requirements for the Degree

of

MASTER OF ENGINEERING
(EXTRACTIVE METALLURGICAL ENGINEERING)



in the Faculty of Engineering
at Stellenbosch University

Supervisor
Prof. Christie Dorfling

March 2017

Plagiarism Declaration

By submitting this thesis electronically, I declare that the entirety of the work contained therein is my own, original work, that I am the sole author thereof (save to the extent explicitly otherwise stated), that reproduction and publication thereof by Stellenbosch University will not infringe any third party rights and that I have not previously in its entirety or in part submitted it for obtaining any qualification.

Date: March 2017

Copyright © 2017 Stellenbosch University

All rights reserved

Abstract

Technological innovation leads to a reduced lifespan of older electrical and electronic equipment, which in turn leads to the generation of vast quantities of electronic waste (e-waste). The recycling of e-waste is becoming increasingly important as it provides certain economic benefits apart from the obvious environmental benefits. Printed circuit boards (PCBs) are found in most forms of e-waste and contain especially high concentrations of base and precious metals.

Hydrometallurgy is one of the major processing routes for the recovery of valuable metals from e-waste. This processing route normally implements several leaching stages to selectively recover certain metals. A two-step base metal leaching stage was implemented that utilized two different lixivants. The first step used nitric acid to mainly recover Pb and Fe, while the second step used sulphuric acid in combination with hydrogen peroxide to mainly recover Cu, Zn and Ni. The Au and Ag were subsequently recovered in an additional leaching stage with ammonium thiosulphate in the presence of copper(II) sulphate. This study focused on the use of a less environmentally hazardous lixiviant than the traditional alternative, cyanide, to promote the development of a more sustainable recovery process.

The primary objective of this study was to determine how the variation of copper in the first stage residue will affect the gold leaching in the second stage. The extent of interactions between process conditions was also studied. These process conditions included temperature, thiosulphate concentration, ammonium concentration, cupric ion concentration, pH and pulp density. The secondary objective of this study was to determine how the degradation of thiosulphate was affected by the change in certain process conditions.

The screening phase determined that only a change in $S_2O_3^{2-}$ concentration, pH range and pulp density had a statistically significant effect on the Au extraction. Statistically significant interactions existed between the Cu on the PCBs and Cu(II) concentration; and the Cu on the PCBs and pulp density. These results were used together with recommendations from literature to determine what factors to include in the full factorial design. The $S_2O_3^{2-}$ concentration (0.1 and 0.2 M), NH_3 concentration (0.2 and 0.4 M), pH range (9 – 9.5 and 10 – 10.5) and pulp density (25 and 50 g/L) were chosen.

The investigation of the $S_2O_3^{2-}$ and NH_3 concentrations determined that Au leaching was dependent on the $S_2O_3^{2-}/NH_3$ ratio. $S_2O_3^{2-}$ concentrations that were too high relative to NH_3 resulted in the $Cu(S_2O_3^{2-})_3^{5-}$ complex becoming more prominent, which hindered Au dissolution. NH_3 concentrations that were too high resulted in a decrease in the oxidation potential of the Cu(II)-Cu(I) couple, which in turn reduced the driving force for the Au leaching reaction. NH_3 concentrations that were too low reduced the amount of $Cu(NH_3)_4^{2+}$ (oxidizing agent for gold) that was available, which in turn also reduced Au leaching. The optimum $S_2O_3^{2-}/NH_3$ ratio for the range of parameters that were investigated was found to be 0.5.

A change in NH_3 concentration was found to have a more significant effect on Au extraction at the lower pH range of 9 – 9.5. This was believed to be due to a higher concentration of NH_4^+ relative to NH_3 being present at lower pH values, which caused faster Au leaching. The lower pH range of 9 – 9.5 also generally produced better Au leaching. An increase in pulp density from 25 to 50 g/L resulted in a decrease in Au extraction, which could be attributed to the fact that the amount of reagent per unit weight of PCB decreased.

The importance of the interactions between $\text{S}_2\text{O}_3^{2-}$ and NH_3 ; and pH range and NH_3 were confirmed in the statistical analysis of the full factorial design. The statistical analysis produced a model with a R^2 value of 0.94 that predicted an optimum Au extraction of 78.04 % at the same conditions that produced the optimum Au extraction during testing. The predicted an optimum compared well with actual value of 78.47 %, which was obtained at 0.2 M $\text{S}_2\text{O}_3^{2-}$, 0.4 M NH_3 , 0.02 M Cu(II), 25 g/L, 25°C, 1 – 10 % leftover Cu and pH range of 9 – 9.5.

The optimum conditions were used to determine the effect of a variation in Cu in the first stage residue, temperature and Cu(II) concentration. Au extraction decreased with an increase in Cu leftover content, temperature and Cu(II) concentration. Increased amounts of Cu inhibited Au leaching through the dissolution of Cu to $\text{Cu}(\text{NH}_3)_2^+$ with the consumption of $\text{Cu}(\text{NH}_3)_4^{2+}$. Increased rates of thiosulphate consumption/degradation were encountered at higher temperatures, Cu(II) concentrations and leftover Cu.

Opsomming

Tegnologiese vordering lei tot 'n verkorte lewensduur van ouer elektriese en elektroniese toerusting. Dit lei tot die opgaar van groot hoeveelhede van elektroniese afval (e-afval). Die herwinning van e-afval word toenemend belangrik aangesien dit sekere ekonomiese voordele benewens die ooglopende voordele vir die omgewing het. Gedrukte stroombaan borde (GSBe) is 'n algemene vorm van e-afval en bevat veral hoë konsentrasies van basis- en edelmetale.

Hidrometallurgie is een van die primêre prosesroetes vir die herwinning van waardevolle metale uit e-afval. Hierdie prosesroete maak gewoonlik gebruik van 'n paar logingsfases om die metale selektief te herwin. Tydens hierdie studie is die basismetale herwin deur 'n twee-stap logingsfase. In die eerste stap is salpetersuur aangewend om hoofsaaklik Pb en Fe te herwin, terwyl in die tweede stap swaelsuur aangewend is in kombinasie met waterstofperoksied om hoofsaaklik Cu, Zn en Ni te herwin. Die Au en Ag is daarna herwin in 'n bykomende logingsfase met ammonium tiosulfaat in die teenwoordigheid van koper (II) sulfaat. Hierdie studie fokus op die gebruik van 'n minder gevaarlike logingsoplossing as die tradisionele alternatief, sianied, met die oog om die ontwikkeling van 'n meer volhoubare herwinningsproses te bevorder.

Die primêre doel van hierdie studie was om vas te stel hoe die variasie van oorblywende koper in die eerste logingsfase residu, die goud logging in die tweede logingsfase sal beïnvloed. Die mate van interaksie tussen proestoestande is ook bestudeer. Die proestoestande het temperatuur, tiosulfaat konsentrasie, ammonium konsentrasie, koper ioon konsentrasie, pH en pulpdigtheid ingesluit. Die sekondêre doel van hierdie studie was om vas te stel hoe die degradering van tiosulfaat beïnvloed word deur die verandering in sekere proestoestande.

Die keuringsfase het bepaal dat slegs 'n verandering in $S_2O_3^{2-}$ konsentrasie, pH en pulpdigtheid statistiese beduidende effekte gehad op die Au ekstraksie. Statistiese beduidende interaksies bestaan tussen die Cu op die GSB en Cu (II) konsentrasie; en die Cu op die GSB en pulpdigtheid. Hierdie resultate is saam met aanbevelings uit die literatuur gebruik om te bepaal watter proestoestande in die faktoriaaleksperimente ingesluit moet word. Die $S_2O_3^{2-}$ konsentrasie (0.1 en 0.2 M), NH_3 konsentrasie (0.2 en 0.4 M), pH (9 – 9.5 en 10 – 10.5) en pulpdigtheid (25 en 50 g/L) is gekies.

Die faktoriaal eksperimente het bepaal dat Au logging afhanklik is van die $S_2O_3^{2-}/NH_3$ verhouding. $S_2O_3^{2-}$ konsentrasies wat te hoog is in vergelyking met NH_3 het veroorsaak dat die $Cu(S_2O_3^{2-})_3^{5-}$ komplekse meer prominent geraak het. Dit het die Au ekstraksie belemmer. NH_3 konsentrasies wat te hoog is het gelei tot 'n afname in die oksidasie potensiaal van die Cu(II) – Cu(I) koppeling, wat op sy beurt die dryfkrag vir die Au loggingreaksie verminder het. NH_3 konsentrasies wat te laag is, het die hoeveelheid $Cu(NH_3)_4^{2+}$ (oksideermiddel vir goud) wat beskikbaar was verminder. Dit het gevolglik die Au logging verminder. Die optimale $S_2O_3^{2-}/NH_3$ verhouding vir die toestand wat ondersoek is, is 0.5.

'n Verandering in NH_3 konsentrasie het 'n meer beduidende effek op Au ekstraksie gehad by die laer pH reeks van 9 – 9.5. Daar is veronderstel dat dit te danke was aan 'n hoër konsentrasie van NH_4^+ relatief tot NH_3 , wat teenwoordig was by laer pH waardes, wat vinniger Au loging veroorsaak het. Die laer pH reeks van 9 – 9.5 het ook oor die algemeen beter Au loging produseer. 'n Toename in pulpdigtheid van 25 – 50 g/L het 'n afname in Au ekstraksie tot gevolg gehad, wat toegeskryf kan word aan die feit dat die hoeveelheid reagens per eenheidsgewig van GSBe afgeneem het.

Die belangrikheid van die interaksies tussen $\text{S}_2\text{O}_3^{2-}$ en NH_3 ; en pH en NH_3 is bevestig in die statistiese analise van die faktoriaal eksperimente. Die statistiese analise het 'n model produseer met 'n R^2 waarde van 0.94, wat 'n optimale Au ekstraksie van 78.04 % voorspel het by dieselfde toestande wat die optimale Au ekstraksie geproduseer het tydens eksperimente. Die voorspelde optimum het goed vergelyk met die werklike optimum van 78.47 % wat behaal is by 0.2 M $\text{S}_2\text{O}_3^{2-}$, 0.4 M NH_3 , 0.02 M Cu(II), 25 g/L, 25°C, 1 – 10 % oorblywende Cu en 'n pH reeks van 9 – 9.5.

Die optimale toestande is gebruik om die effek van 'n verandering in oorblywende Cu in die eerste logingsfase, temperatuur en Cu(II) konsentrasie vas te stel. Au ekstraksie het afgeneem met 'n toename in oorblywende Cu, temperatuur en Cu(II) konsentrasie. Verhoogde hoeveelhede van Cu inhibeer Au loging deur die ontbinding van Cu na $\text{Cu}(\text{NH}_3)_2^+$, met die verbruik van $\text{Cu}(\text{NH}_3)_4^{2+}$. 'n Verhoogde tempo van tiosulfaat verbruik/degradering is ondervind by hoër temperature, Cu(II) konsentrasies en oorblywende Cu vlakke.

Acknowledgements

I would like to firstly thank my supervisor, Prof. Christie Dorfling, of the Department of Process Engineering at the University of Stellenbosch. He provided guidance whenever it was necessary and was always available when I wanted to discuss my research. Thank you for your patience.

I would also like to express my gratitude to the National Research Foundation of South Africa and the SAIMM Outotec Postgraduate Scholarship for their financial support. Any opinion, finding and conclusion or recommendation expressed in this material is that of the author and the NRF and other funding organisations do not accept any liability in this regard.

Finally, I would like to acknowledge my family for their support and encouragement throughout the duration of this project.

Table of Contents

Plagiarism Declaration	ii
Abstract	iii
Opsomming	v
Acknowledgements	vii
List of Tables.....	xi
List of Figures	xiii
Nomenclature	xvi
1. Introduction	1
1.1. Motivation	1
1.2. Objectives and Scope	1
1.3. Approach	2
1.4. Document Outline	2
2. Literature Review	3
2.1. Background	3
2.2. Lixiviant Types.....	8
2.2.1. Base Metal Lixiviants.....	8
2.2.2. Precious Metal Lixiviants.....	12
2.3. Base Metal Leaching.....	15
2.3.1. Nitric Acid Leaching.....	16
2.3.2. Sulphuric Acid Leaching.....	17
2.4. Thiosulphate Leaching of Precious Metals	18
2.4.1. Gold Leaching	18
2.4.2. Silver Leaching.....	21
2.4.3. Thiosulphate Stability.....	21
2.4.4. Thiosulphate Regeneration.....	22
2.4.5. Reaction Kinetics	22
2.5. Thermodynamics	24
2.6. Results from Previous Literature.....	29

2.6.1.	Thiosulphate Leaching Parameters.....	29
2.6.2.	Summary	33
3.	Experimental Method.....	35
3.1.	Size Reduction.....	35
3.2.	PCB Characterisation	35
3.3.	Base Metal Leaching.....	36
3.3.1.	Experimental Strategy	36
3.3.2.	Equipment	37
3.3.3.	Materials.....	40
3.3.4.	Procedure.....	40
3.4.	Precious Metal Leaching.....	43
3.4.1.	Experimental Strategy	43
3.4.2.	Equipment	45
3.4.3.	Materials.....	45
3.4.4.	Procedure.....	46
3.5.	Analysis.....	47
4.	Results and Discussion.....	48
4.1.	PCB Characterisation	48
4.2.	Base Metal Leaching.....	50
4.3.	Precious Metal Leaching.....	54
4.3.1.	Screening Phase.....	54
4.3.2.	Full Factorial Phase.....	68
4.3.3.	Optimization Phase.....	77
5.	Conclusions and Recommendations.....	83
5.1.	Conclusions	83
5.2.	Recommendations	84
6.	References	85
7.	Appendices	94
7.1.	Appendix A: PCB Characterisation.....	94

7.1.1.	Aqua Regia Preparation.....	94
7.1.2.	Experimental Data.....	94
7.1.3.	Aqua Regia Safety.....	95
7.2.	Appendix B: Base Metal Leaching.....	96
7.2.1.	Initial Base Metal Leaching Tests.....	96
7.2.2.	Large-Scale HNO ₃ Leaching.....	96
7.2.3.	Small Scale H ₂ SO ₄ Leaching.....	97
7.3.	Appendix C: Precious Metal Leaching.....	98
7.3.1.	Screening Phase.....	98
7.3.2.	Full Factorial Phase.....	110
7.3.3.	Optimisation Phase.....	121

List of Tables

Table 1: E-waste categories and examples [10]	3
Table 2: Toxic substances commonly contained within e-waste and associated health impacts (adapted from [14] & [10])	4
Table 3: PCB metal content as reported by various authors.....	6
Table 4: Energy savings from the use of recycled materials over virgin materials (adapted from [40])	6
Table 5: Summary of several base metal leaching studies conducted on PCBs.....	9
Table 6: Advantages and disadvantages of cyanide alternatives [66]	12
Table 7: Standard reduction potentials (25°C)	15
Table 8: Gibbs free energies (25°C) of non-oxidative and oxidative leaching of certain metals.....	16
Table 9: Reagent concentrations for Cu-NH ₃ -S ₂ O ₃ , Au-NH ₃ -S ₂ O ₃ and Ag-NH ₃ -S ₂ O ₃ systems	24
Table 10: Summary of conditions implemented for precious metal leaching by various authors	33
Table 11: Effect of most prominent parameters on Au leaching.....	33
Table 12: Optimum conditions implemented in previous studies on precious metal leaching	34
Table 13: Initial experimental parameters of the small-scale base metal leaching stage	37
Table 14: Figure 12 component designations.....	39
Table 15: Figure 13 component designations.....	40
Table 16: Base metal leaching – Chemical stock information	40
Table 17: Base metal leaching – Required chemical quantities for leaching steps	40
Table 18: Parameters selected for investigation.....	43
Table 19: Precious metal leaching screening design.....	44
Table 20: Precious metal leaching parameter settings	44
Table 21: Precious metal leaching – Chemical information.....	45
Table 22: Precious metal leaching – Required chemical quantities per test.....	45
Table 23: Average metal content of PCBs	50
Table 24: Cu extraction of 5 replicate tests with residence times of 180 minutes	53
Table 25: Screening test parameters.....	54
Table 26: Average difference in total Au content for screening tests as grouped in Figure 21 to Figure 24.....	57
Table 27: Comparison of Au and Ag detection capabilities ICP-OES and ICP-MS.....	65
Table 28: Initial ANOVA table of 2 ⁽⁷⁻³⁾ fractional factorial design phase.....	66
Table 29: 2 ⁴ full factorial experimental design	67
Table 30: Comparison of three different rate limiting models	73
Table 31: Initial ANOVA table for 2 ⁴ full factorial design phase.....	74
Table 32: Adjusted ANOVA table of 2 ⁴ full factorial phase.....	75
Table 33: Adjusted regression coefficients of 2 ⁴ full factorial phase.....	76

Table 34: Calculation of required quantities of aqua regia components per 200 mL digestion.....	94
Table 35: Results of Aqua Regia residence time tests of 6 different PCB samples	94
Table 36: Initial base metal leaching tests.....	96
Table 37: Base metal leaching comparison	96
Table 38: Amount of metals leached from 2 kg of PCBs during large scale HNO ₃ leaching step	96
Table 39: Metal extraction at various times during large scale HNO ₃ leaching step	97
Table 40: Amount of metals leached from 80 g of PCBs during small scale H ₂ SO ₄ leaching step	97
Table 41: Metal extraction at various times during small scale H ₂ SO ₄ leaching step.....	97
Table 42: Calculating the Au extraction at the end of the screening phase.....	98
Table 43: Calculating the Ag extraction at the end of the screening phase.....	99
Table 44: Extent of Au and Ag leaching during the screening phase experiments	99
Table 45: Extent of Au and Ag leaching during the screening phase repeat experiments	103
Table 46: Thiosulphate degradation/consumption of screening tests.....	105
Table 47: Calculation of Au and Ag extraction (ICP-MS).....	108
Table 48: Confounding of effects in the screening analysis.....	109
Table 49: Redundant effects in the screening analysis.....	109
Table 50: Calculating the Au extraction at the end of the full factorial phase	110
Table 51: Calculating the Ag extraction at the end of the full factorial phase	111
Table 52: Change in pH and Eh during full factorial tests	112
Table 53: Test conditions for the optimization phase	121
Table 54: Calculating the Au extraction at the end of the optimization phase.....	121
Table 55: Calculating the Ag extraction at the end of the optimization phase.....	121
Table 56: Extent of Au and Ag leaching during the optimization phase experiments	122
Table 57: Thiosulphate degradation/consumption of optimization phase tests.....	123
Table 58: Change in pH during optimization phase test	124

List of Figures

Figure 1: Metallurgical process routes for e-waste recycling [adapted from [41]]	7
Figure 2: Electrochemical-catalytic mechanism model for gold leaching with ammonium thiosulphate (adapted from [52])	18
Figure 3: Electrochemical-catalytic mechanism model for gold leaching with ammonium thiosulphate (adapted from [76])	20
Figure 4: Pourbaix diagram for Cu-NH ₃ -S ₂ O ₃ ²⁻ system at high reagent concentrations [adapted from [52]]	25
Figure 5: Pourbaix diagram for Au-NH ₃ -S ₂ O ₃ ²⁻ system at high reagent concentrations [adapted from [52]]	25
Figure 6: Pourbaix diagram for Ag-NH ₃ -S ₂ O ₃ ²⁻ system at high reagent concentrations [adapted from [52]]	26
Figure 7: Pourbaix diagram for Cu-NH ₃ -S ₂ O ₃ ²⁻ system at low reagent concentrations [adapted from [52]]	27
Figure 8: Pourbaix diagram for Au-NH ₃ -S ₂ O ₃ ²⁻ system at low reagent concentrations [adapted from [52]]	28
Figure 9: Pourbaix diagram for Ag-NH ₃ -S ₂ O ₃ ²⁻ system at low reagent concentrations [adapted from [52]]	28
Figure 10: Schematic representation of the size reduction procedure	35
Figure 11: Schematic representation of the base metal leaching procedure	36
Figure 12: Small-scale leaching equipment for base metal leaching stage	38
Figure 13: Large-scale leaching equipment for base metal leaching stage	39
Figure 14: Base metal leaching behaviour as a function of time during Aqua Regia digestion for (a) test 1, (b) test 2, (c) test 3 and (d) test 4	48
Figure 15: Precious metal leaching behaviour during Aqua Regia residence time tests	49
Figure 16: Base metal leaching comparison of step 1	51
Figure 17: Base metal leaching comparison of step 2	51
Figure 18: Leaching behaviour of metals during large-scale HNO ₃ leaching (step 1)	52
Figure 19: Leaching behaviour of metals during small-scale H ₂ SO ₄ leaching (step 2)	53
Figure 20: Final Au extraction during the screening phase tests	55
Figure 21: Final Ag extraction during screening phase tests	55
Figure 22: Gold extraction during tests 1 (Cu: 10 %, S ₂ O ₃ ²⁻ : 0.1 M, Cu(II): 0.02 M, NH ₃ : 0.2 M, pH: 9 – 9.5, 25°C, 25 g/L), 2 (Cu: 20 %, S ₂ O ₃ ²⁻ : 0.1 M, Cu(II): 0.02 M, NH ₃ : 0.2 M, pH: 9 – 9.5, 40°C, 50 g/L), 3 (Cu: 10 %, S ₂ O ₃ ²⁻ : 0.2 M, Cu(II): 0.02 M, NH ₃ : 0.2 M, pH: 10 – 10.5, 40°C, 25 g/L), 4 (Cu: 20 %, S ₂ O ₃ ²⁻ : 0.2 M, Cu(II): 0.02 M, NH ₃ : 0.2 M, pH: 10 – 10.5, 25°C, 50 g/L) and their repeat runs	56

Figure 23: Gold extraction during tests 5 (Cu: 10 %, $S_2O_3^{2-}$: 0.1 M, Cu(II): 0.1 M, NH_3 : 0.2 M, pH: 10 – 10.5, 40°C, 50 g/L), 6 (Cu: 20 %, $S_2O_3^{2-}$: 0.1 M, Cu(II): 0.1 M, NH_3 : 0.2 M, pH: 10 – 10.5, 25°C, 25 g/L), 7 (Cu: 10 %, $S_2O_3^{2-}$: 0.2 M, Cu(II): 0.1 M, NH_3 : 0.2 M, pH: 9 – 9.5, 25°C, 50 g/L), 8 (Cu: 20 %, $S_2O_3^{2-}$: 0.2 M, Cu(II): 0.1 M, NH_3 : 0.2 M, pH: 9 – 9.5, 40°C, 25 g/L) and their repeat runs.....	57
Figure 24: Gold extraction during tests 9 (Cu: 10 %, $S_2O_3^{2-}$: 0.1 M, Cu(II): 0.02 M, NH_3 : 0.4 M, pH: 10 – 10.5, 25°C, 50 g/L), 10 (Cu: 20 %, $S_2O_3^{2-}$: 0.1 M, Cu(II): 0.02 M, NH_3 : 0.4 M, pH: 10 – 10.5, 40°C, 25 g/L), 11 (Cu: 10 %, $S_2O_3^{2-}$: 0.2 M, Cu(II): 0.02 M, NH_3 : 0.2 M, pH: 9 – 9.5, 40°C, 50 g/L), 12 (Cu: 20 %, $S_2O_3^{2-}$: 0.2 M, Cu(II): 0.02 M, NH_3 : 0.4 M, pH: 9 – 9.5, 25°C, 25 g/L) and their repeat runs ...	58
Figure 25: Gold extraction during tests 13 (Cu: 10 %, $S_2O_3^{2-}$: 0.1 M, Cu(II): 0.1 M, NH_3 : 0.4 M, pH: 9 – 9.5, 40°C, 25 g/L), 14 (Cu: 20 %, $S_2O_3^{2-}$: 0.1 M, Cu(II): 0.1 M, NH_3 : 0.4 M, pH: 9 – 9.5, 25°C, 50 g/L), 15 (Cu: 10 %, $S_2O_3^{2-}$: 0.2 M, Cu(II): 0.1 M, NH_3 : 0.4 M, pH: 10 – 10.5, 25°C, 25 g/L), 16 (Cu: 20 %, $S_2O_3^{2-}$: 0.2 M, Cu(II): 0.1 M, NH_3 : 0.4 M, pH: 9 – 9.5, 40°C, 50 g/L) and their repeat runs	58
Figure 26: Silver extraction during tests 1 (Cu: 10 %, $S_2O_3^{2-}$: 0.1 M, Cu(II): 0.02 M, NH_3 : 0.2 M, pH: 9 – 9.5, 25°C, 25 g/L), 2 (Cu: 20 %, $S_2O_3^{2-}$: 0.1 M, Cu(II): 0.02 M, NH_3 : 0.2 M, pH: 9 – 9.5, 40°C, 50 g/L), 3 (Cu: 10 %, $S_2O_3^{2-}$: 0.2 M, Cu(II): 0.02 M, NH_3 : 0.2 M, pH: 10 – 10.5, 40°C, 25 g/L), 4 (Cu: 20 %, $S_2O_3^{2-}$: 0.2 M, Cu(II): 0.02 M, NH_3 : 0.2 M, pH: 10 – 10.5, 25°C, 50 g/L) and their repeat runs	59
Figure 27: Silver extraction during tests 5 (Cu: 10 %, $S_2O_3^{2-}$: 0.1 M, Cu(II): 0.1 M, NH_3 : 0.2 M, pH: 10 – 10.5, 40°C, 50 g/L), 6 (Cu: 20 %, $S_2O_3^{2-}$: 0.1 M, Cu(II): 0.1 M, NH_3 : 0.2 M, pH: 10 – 10.5, 25°C, 25 g/L), 7 (Cu: 10 %, $S_2O_3^{2-}$: 0.2 M, Cu(II): 0.1 M, NH_3 : 0.2 M, pH: 9 – 9.5, 25°C, 50 g/L), 8 (Cu: 20 %, $S_2O_3^{2-}$: 0.2 M, Cu(II): 0.1 M, NH_3 : 0.2 M, pH: 9 – 9.5, 40°C, 25 g/L) and their repeat runs.....	60
Figure 28: Silver extraction during tests 9 (Cu: 10 %, $S_2O_3^{2-}$: 0.1 M, Cu(II): 0.02 M, NH_3 : 0.4 M, pH: 10 – 10.5, 25°C, 50 g/L), 10 (Cu: 20 %, $S_2O_3^{2-}$: 0.1 M, Cu(II): 0.02 M, NH_3 : 0.4 M, pH: 10 – 10.5, 40°C, 25 g/L), 11 (Cu: 10 %, $S_2O_3^{2-}$: 0.2 M, Cu(II): 0.02 M, NH_3 : 0.2 M, pH: 9 – 9.5, 40°C, 50 g/L), 12 (Cu: 20 %, $S_2O_3^{2-}$: 0.2 M, Cu(II): 0.02 M, NH_3 : 0.4 M, pH: 9 – 9.5, 25°C, 25 g/L) and their repeat runs ...	60
Figure 29: Silver extraction during tests 13 (Cu: 10 %, $S_2O_3^{2-}$: 0.1 M, Cu(II): 0.1 M, NH_3 : 0.4 M, pH: 9 – 9.5, 40°C, 25 g/L), 14 (Cu: 20 %, $S_2O_3^{2-}$: 0.1 M, Cu(II): 0.1 M, NH_3 : 0.4 M, pH: 9 – 9.5, 25°C, 50 g/L), 15 (Cu: 10 %, $S_2O_3^{2-}$: 0.2 M, Cu(II): 0.1 M, NH_3 : 0.4 M, pH: 10 – 10.5, 25°C, 25 g/L), 16 (Cu: 20 %, $S_2O_3^{2-}$: 0.2 M, Cu(II): 0.1 M, NH_3 : 0.4 M, pH: 9 – 9.5, 40°C, 50 g/L) and their repeat runs	61
Figure 30: Thiosulphate degradation during tests which used 0.1 M $S_2O_3^{2-}$	63
Figure 31: Thiosulphate degradation during tests which used 0.2 M $S_2O_3^{2-}$	63
Figure 32: Copper behaviour as a function of time during (a) tests 1 to 4 and (b) tests 5 to 10	64
Figure 33: Copper behaviour as a function of time during (a) tests 9 to 12 and (b) tests 13 to 16	65
Figure 34: Effect of change in thiosulphate concentration on gold leaching	68
Figure 35: Effect of change in thiosulphate concentration on silver leaching	69
Figure 36: Effect of change in ammonia concentration on gold leaching.....	70
Figure 37: Effect of change in ammonia concentration on silver leaching	71
Figure 38: Effect of change in pulp density on gold leaching.....	71

Figure 39: Effect of change in pulp density on silver leaching.....	72
Figure 40: Effect of change in pH range on gold leaching.....	72
Figure 41: Effect of change in pH range on silver leaching.....	73
Figure 42: Initial normal probability plot.....	75
Figure 43: Normal probability plot of residuals.....	76
Figure 44: Raw residuals vs case numbers.....	77
Figure 45: Repeatability test of optimum Au extraction.....	78
Figure 46: Effect of temperature on Au extraction.....	79
Figure 47: Effect of temperature on thiosulphate degradation.....	79
Figure 48: Effect of Cu(II) concentration on Au extraction.....	80
Figure 49: Effect of Cu(II) concentration on thiosulphate degradation.....	80
Figure 50: Effect of leftover Cu on Au extraction.....	81
Figure 51: Effect of leftover Cu on thiosulphate degradation.....	81
Figure 52: PCB metal content.....	95
Figure 53: Thiosulphate degradation during tests which used 0.1 M $S_2O_3^{2-}$ (extended).....	105
Figure 54: Thiosulphate degradation during tests which used 0.2 M $S_2O_3^{2-}$ (extended).....	106
Figure 55: Change in pH for tests 1, 2, 7 and 8.....	106
Figure 56: Change in pH for tests 11, 12, 13 and 14.....	107
Figure 57: Change in pH for tests 3, 4, 5 and 6.....	107
Figure 58: Change in pH for tests 9, 10, 15 and 16.....	108
Figure 59: Initial Pareto chart of standardized effects.....	110
Figure 60: Rate controlled by surface chemical reaction.....	113
Figure 61: Rate controlled by diffusion in the boundary layer.....	113
Figure 62: Rate controlled by diffusion in the porous product layer.....	114
Figure 63: $NH_3 - S_2O_3^{2-}$ fitted surface plot (pH 9 – 9.5, 25 g/L).....	114
Figure 64: $NH_3 - S_2O_3^{2-}$ fitted surface plot (pH 10 – 10.5, 50 g/L).....	115
Figure 65: pH – $S_2O_3^{2-}$ fitted surface plot (0.2 M NH_3 , 25 g/L).....	115
Figure 66: pH – $S_2O_3^{2-}$ fitted surface plot (0.4 M NH_3 , 50 g/L).....	116
Figure 67: Pulp density – $S_2O_3^{2-}$ fitted surface plot (pH 9 – 9.5, 0.2 M NH_3).....	116
Figure 68: Pulp density – $S_2O_3^{2-}$ fitted surface plot (pH 10 – 10.5, 0.4 M NH_3).....	117
Figure 69: pH – NH_3 fitted surface plot (0.1 M $S_2O_3^{2-}$, 25 g/L).....	117
Figure 70: pH – NH_3 fitted surface plot (0.2 M $S_2O_3^{2-}$, 50 g/L).....	118
Figure 71: Pulp density – NH_3 fitted surface plot (pH 9 – 9.5, 0.1 M $S_2O_3^{2-}$).....	118
Figure 72: Pulp density – NH_3 fitted surface plot (pH 10 – 10.5, 0.2 M $S_2O_3^{2-}$).....	119
Figure 73: Pulp density – pH fitted surface plot (0.1 M $S_2O_3^{2-}$, 0.2 M NH_3).....	119
Figure 74: Pulp density – pH fitted surface plot (0.2 M $S_2O_3^{2-}$, 0.4 M NH_3).....	120
Figure 75: Silver extraction during optimization phase tests.....	123

Nomenclature

General

Symbol	Meaning
BFR	Brominated flame retardants
CRT	Cathode ray tube
EEE	Electric and electronic equipment
E-waste	Electronic waste
PCBs	Printed circuit boards
S/L	Solid to liquid
WEEE	Waste electrical and electronic equipment
SCWO	Supercritical water oxidation

Reaction Kinetics

Symbol	Meaning	Units
b	Stoichiometric factor for surface reaction products	
C	Reagent concentration	mol/m ³
K	Surface reaction intrinsic rate constant	m/s
k	Apparent rate constant for shrinking sphere model	s ⁻¹
ρ	Gold molar density	mol/m ³
r	Spherical particle radius	m
X	Gold fraction reacted after time t	

1. Introduction

1.1. Motivation

With the rate at which newer technologies are being developed nowadays, the environment is experiencing an increased burden due to the accumulation of electronic waste (e-waste). This, however, creates the opportunity for economic benefit through the recycling of valuable metals contained within the waste. Printed circuit boards (PCBs) are a common form of e-waste that contain higher concentrations of base and precious metals than primary metal resources.

One of the possible processing routes for the recycling of e-waste is hydrometallurgy. This route generally involves disassembly, size reduction, physical separation and leaching phases before the metals can be extracted into a usable form through electrometallurgical means. The focus of this study is centred around the leaching phase that consists of multiple leaching stages to ensure selective metal recovery. Extensive research has been done on the base metal leaching stage (first stage) and subsequent cyanide leaching stage (second stage) for the recovery of precious metals. Recently, attention has shifted to the use of less environmentally hazardous lixiviants in the precious metal leaching stage.

Thiosulphate leaching is considered to be one of the possible cyanidation alternatives, as this form of leaching provides a thermodynamically stable gold complex, which other non-cyanide lixiviants do not. This process also has a high selectivity, is non-toxic and non-corrosive [1]. This study aims to assist in the development of a favourable process pathway for ammonium thiosulphate leaching of precious metals in PCBs.

1.2. Objectives and Scope

Various studies have been conducted on the second leaching stage to determine the effects of different process conditions on the thiosulphate leaching of gold and accompanying precious metals contained in PCBs [2], [3], [4], [5], [6], [7], [8], [9]. The effect of varying the resultant copper content in the solid residue from the first stage has not been investigated sufficiently.

The primary objective of this study was to determine how the variation of copper in the first stage residue affected the gold leaching from PCBs in the second stage, when a lixiviant comprised of thiosulphate, ammonia and copper (II) sulphate was used. The extent of interactions between process conditions was also studied. These process conditions included temperature, thiosulphate concentration, ammonium concentration, cupric ion concentration, pH and pulp density. The secondary objective of this study was to determine how the change in certain process conditions affected the thiosulphate degradation. The data obtained from the tests were used to develop an empirical model to help identify optimum conditions for gold recovery.

1.3. Approach

The recovery process was handled in a two-stage leaching process. The first stage involved base metal leaching from PCBs in two steps. The first step utilized nitric acid (HNO_3), while the second step utilized sulphuric acid (H_2SO_4) and hydrogen peroxide (H_2O_2). The residence time was varied to obtain different amounts of unleached copper in the solid residue. The solid residue was used as the feed material for the second stage, in which precious metals were leached with ammonium thiosulphate in the presence of copper (II) sulphate. This stage was divided into three sets of experiments. The first set of experiments was implemented according to a screening design which was intended to determine the most significant main effects (test parameters that had the largest effect on gold recovery). Once the most significant main effects were identified, the second set of experiments was designed according to a full factorial design. The final experimental phase was planned to attempt to improve the optimum Au extraction obtained during the full factorial phase. During this optimization phase the effect that a change in certain parameters had on thiosulphate degradation/consumption were also investigated. Aqua regia digestion tests were completed after each test to dissolve any remaining metals. Samples were taken for the analysis of precious metal extraction and for the analysis of thiosulphate degradation where appropriate. The gold and silver content in liquid samples were measured through ICP-OES, after which the recoveries were determined by means of mass balances. The thiosulphate degradation was determined by measuring the thiosulphate concentration of liquid samples over time using High Performance Liquid Chromatography (HPLC).

1.4. Document Outline

This paper consists of a literature review in chapter 2 and experimental methodology in chapter 3. The literature review explores the chemistry of both base and precious metal leaching of PCBs. It also contains results from previous literature which were used for the identification of test parameters. The experimental methodology outlines the experimental strategy, equipment, materials and procedure of each leaching stage. The discussion of experimental results is included in chapter 4, while chapter 5 consists of the conclusions and recommendations.

2. Literature Review

2.1. Background

Increasingly advanced electrical and electronic equipment (EEE) are constantly being developed due to great demand for superior equipment, the rapid growth of the market and fierce competition between manufacturing companies. Technological advancement results in a reduced lifespan of older EEE, which in turn leads to the generation of vast quantities of electronic waste (e-waste) or Waste Electrical and Electronic Equipment (WEEE). Table 1 illustrates the different categories of e-waste according to the e-waste guide [10]. The highest potential for e-waste generation can be connected to the first four categories shown in Table 1.

Table 1: E-waste categories and examples [10]

Categories	Examples
Large Household Appliances	Washing Machines, Dryers, Refrigerators, Air-conditioners, etc.
Small Household Appliances	Vacuum Cleaners, Coffee Machines, Irons, Toasters, etc.
Office, Information and Communication Equipment	PCs, Laptops, Mobiles, Telephones, Fax Machines, Copiers, Printers, etc.
Entertainment and Consumer Electronics	Televisions, VCR/DVD/CD Players, Hi-Fi Sets, Radios, etc.
Lighting Equipment	Fluorescent Tubes, Sodium Lamps, etc.
Electric and Electronic Tools	Drills, Electric Saws, Sewing Machines, Lawn Mowers, etc.
Toys, Leisure, Sports and Recreational Equipment	Electric Train Sets, Coin Slot Machines, Treadmills, etc.
Medical Instruments and Equipment	X-ray Machine, Heart Machine, Lung Machine, etc.
Surveillance and Control Equipment	CCTV cameras, Scanning Equipment, etc.
Automatic Issuing Machines	Parking Ticket Machine, etc.

In 2005 the e-waste discarded in the UK amounted to approximately 940 000 tons [11]. A study conducted by eWASA (e-Waste Association of South Africa) [12] estimated that the total household potential e-waste tonnage amounted to 875 687 tons for South Africa. This shows that even in developing countries e-waste can be generated in large quantities.

E-waste consists of an intricate mixture of ferrous, non-ferrous, plastic and ceramic materials. The Association of Plastics Manufacturers in Europe (APME) indicates that the major components of E&E equipment are ferrous (38 %), non-ferrous (28 %) and plastic (19 %) [13]. These materials can potentially be environmentally hazardous. Toxic substances contained within e-waste can contaminate the surrounding environment through disposal and primitive recycling operations, thereby impacting human health both directly and indirectly. Direct impact can be caused by toxic combustion gasses emitted during incineration, while indirect impact may be caused from groundwater contamination from landfill and recycling operations [14]. Table 2 contains toxic substances most commonly found in e-waste and some of the health impacts associated with them. These substances illustrate the danger that e-waste poses for society if it is not properly handled. Kiddee et al. [14] mentioned various sources that

demonstrated the detrimental effects of e-waste on local communities of China ([15], [16], [17], [18], [19], [20], [21]), Ghana [22] and India [23], [24].

Table 2: Toxic substances commonly contained within e-waste and associated health impacts (adapted from [14] & [10])

E-Waste Constituent	Application in e-waste	Human Health Impact
Heavy Metals and Other Metals		
Antimony (Sb)	Solder alloy in cabling and a melting agent in cathode ray tube (CRT) glass	Antimony has been known to cause vomiting, stomach ache, stomach ulcers and diarrhoea when inhaled for extended periods of time and has been classified as a substance with carcinogenic properties
Arsenic (As)	Light emitting diodes contain gallium arsenide	Arsenic has also been classified as a carcinogen as it is known to cause lung cancer through chronic exposure. Skin disease and decreased nerve conduction velocity have also been linked to this poisonous metallic element
Barium (Ba)	CRT gutters, sparkplugs and fluorescent lamps	Acute exposure to barium may cause muscle weakness, brain swelling, heart-, spleen- and liver damage
Beryllium (Be)	Motherboards and power supply boxes	Lung cancer, chronic beryllium disease and skin disease are caused by exposure to beryllium
Cadmium (Cd)	Semiconductor chips, rechargeable Ni-Cd batteries, inks and toners used for printers, infrared detectors and printer drums in photocopiers	Chronic exposure to cadmium can lead to kidney damage and lung cancer. Cadmium has also been known to cause flu-like symptoms through acute exposure
Chromium VI (Cr VI)	Floppy disks, hard discs, data tapes and pigment colourant	Chromium VI can cause permanent eye damage and DNA damage through chronic exposure
Lead (Pb)	PCBs, CRT screens, lead-acid batteries and solder	Chronic exposure to lead can lead to kidney-, brain-, nervous system- and reproductive system damage. Acute exposure to high levels has been known to cause coma, diarrhoea, vomiting, convulsions and death.
Lithium (Li)	Lithium batteries	Common side effects of lithium exposure include headache, muscle weakness, vomiting and diarrhoea
Mercury (Hg)	Thermostats, certain alkaline batteries, switches and fluorescent bulbs used for backlighting	Mercury has been known to damage the kidneys and brain
Nickel (Ni)	PCBs, Ni-Cd batteries, CRT and computer housings	Large quantities of nickel can lead to lung embolism, respiratory failure, birth defects, asthma, chronic bronchitis, heart disorders, allergic reactions and lung cancer
Rare Earth Elements (REE)	Fluorescent layer in CRT screens	Liver function decline may be related to high levels of exposure to REE
Selenium (Se)	Photoreceptor drums in photocopiers	Selenium can cause selenosis through exposure to high concentrations

Table 2 continued

Halogenated Substances		
PBR (Polybrominated Biphenyls)	These substances are used as fire retardants for PCBs, thermoplastic components and cable insulation. They are commonly referred to as brominated flame retardants (BFR).	The combustion of PCBs and halogenated case material releases toxic vapours that can cause hormonal disorders
PBDE (Polybrominated Diphenyl Ethers)		
TBBPA (Tetrabromobisphenol-A)		
CFC (Chlorofluorocarbons)	Insulation foam and cooling units	CFC have detrimental effect on the ozone layer which in turn increases the occurrence of skin cancer
Polychlorinated Biphenyls	Transformers, condensers as well as heat transfer fluids	Exposure to polychlorinated biphenyls can cause damage to the liver, immune system, reproductive system, nervous system and endocrine system
PVC (Polyvinyl Chloride)	Cable insulation, computer housings, keyboards and monitors	Ultimately leads to respiratory problems when burned, due to the formation of hydrogen chloride gas and subsequent formation of hydrochloric acid
Radio-Active Substances		
Americium (Am)	Fire detectors, medical equipment and smoke detectors	The accumulation of americium in the human body poses the risk of cancer developing

The recycling of e-waste is becoming increasingly important as an alternative to landfilling and incineration. Recycling e-waste does not only provide environmental benefits, but economic benefits as well, as valuable constituents are present in e-waste. PCBs are found in most forms of e-waste and are normally composed of 40 % metals, 30 % plastics and 30 % ceramics [25]. PCBs, which are the selected feed material for recycling in this study, contain especially high concentrations of both base metals and precious metals.

The exact composition of PCBs varies considerably, but two main flame retardant (FR) types exist within which the compositions are more closely related. FR-4 circuit boards consist of multi-layered fibreglass coated with copper, while FR-2 circuit boards consist of a single layer of phenolic material/fibreglass/cellulose paper coated with copper [26]. The FR-4 circuit boards are implemented in small E&E equipment such as mobile phones, while FR-2 circuit boards are implemented in larger E&E equipment such as computers [27]. The quality of each PCB also effects the composition. For example, more gold is used in higher quality PCBs as it is a better conductor than copper. Table 3 contains information on the metal content of PCBs as reported by various authors.

Table 3: PCB metal content as reported by various authors

Author	Source	Cu [%]	Al [%]	Pb [%]	Zn [%]	Ni [%]	Fe [%]	Sn [%]	Au [ppm]	Ag [ppm]	Pd [ppm]
[28]	Mixed	23.7	4.7	4.5	0.8	3.3	7.5	3.7	800	800	210
[29], [30], [31]	Mobile phone	23.5	1.3	1.0	1.5	2.4	1.2	1.5	570	3300	290
[32]	Mobile phone	20.0	5.0	1.5		1.0	7.0		250	1000	110
[33]	Mobile phone	20.0	2.0	2.0	1.0	2.0	8.0	4.0	1000	2000	50
[34]	Mixed	17.9	4.8	4.2	2.2	1.6	2.0	5.3	350	1300	250
[2]	Mobile phone	56.7	1.4		0.2		0.2	1.4	210	1000	100
[3]	Mixed	47.5	2.7	1.4	1.1	0.9	10.4	3.3	140	800	30
[35]	PC	25.3		0.1		0.02	0.2	0.3	105	7	
[36]	Mixed								11	18	90
[37]	PC	30.6	11.7	6.7	1.9	1.6	15.2	7.4	240	690	
[38]	Mixed	26.8	4.7	5.3	1.5	0.5		1.0	80	3300	
[39]	Mixed	16.0	5.0	2.0	1.0	1.0	5.0	3.0	250	1000	100
[40]	Mixed	16.0				2.0	3.0		300	500	100

PCBs are considered to be a secondary metal resource, while primary metal sources are ores and concentrates obtained from mining operations. When these metal sources are compared, it is apparent that PCBs generally contain more of both precious and important base metals. Primary metal sources have a gold content between 1 – 10 g/ton and a copper content between 0.5 – 1 % [41]. PCBs on the other hand can contain gold and copper in ranges of 10.6 – 1000 g/ton and 16 – 56.7 % respectively (from Table 3). Recycling of this waste contributes to the conservation of primary metal resources by supplementing metal supplies. In this way continued environmental impacts from mining operations and connected purification operations can possibly be decreased.

In addition to the environmental and economic benefits of recycling PCBs, a large amount of energy can be saved by using recycled materials in comparison to virgin materials. Energy savings from the use of recycled materials rather than virgin materials are summarised in Table 4 [40].

Table 4: Energy savings from the use of recycled materials over virgin materials (adapted from [40])

Material	Aluminium	Copper	Iron and Steel	Lead	Zinc	Paper	Plastics
Energy Savings [%]	95	85	74	65	60	64	>80

The major processing routes for the extraction of valuable metals from e-waste are hydrometallurgy and pyrometallurgy. Each of these routes has their own advantages and disadvantages. Figure 1 shows potential processes and their pathways. The dotted lines represent optional pathways. Pyrometallurgy involves the use of thermal energy and metallurgical/chemical properties of substances in order to liquefy secondary materials with the goal of simultaneously concentrating wanted metals and separating unwanted materials into a slag phase [42]. Pyrometallurgical routes are relatively simplistic and useful for heterogeneous material feeds. The largest drawback to using this route is the environmental impact

due to the production of slag and hazardous gases. This route also requires the use of subsequent hydrometallurgical/electrochemical techniques, as precious metals are only partly recovered through pyrometallurgical routes and need to be separated from the base metals. The presence of ceramics on PCBs produce increased slag volumes, which in turn increases the chance of losing precious metals. Certain substances on PCBs, such as BFRs, produce toxic gasses when incinerated. This increases plant costs as additional equipment is required to control the gas emissions [27].

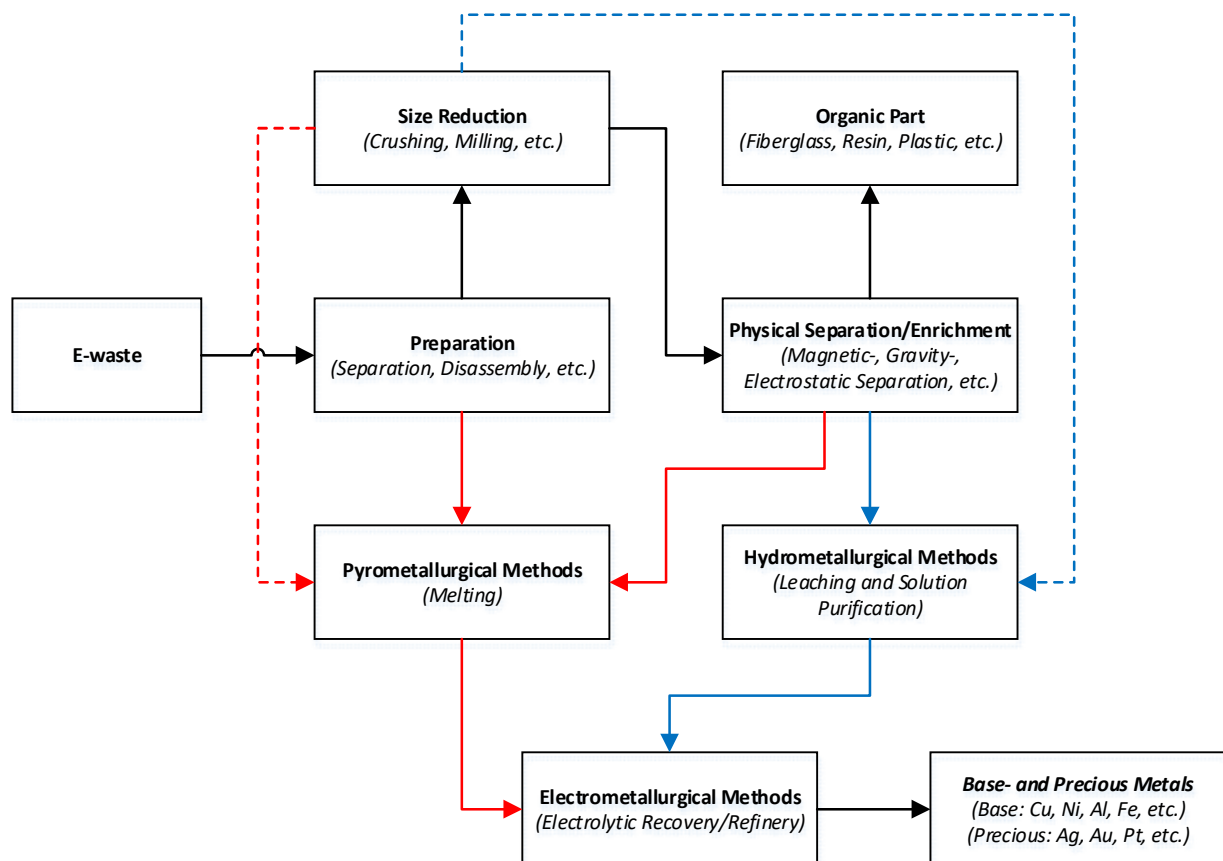


Figure 1: Metallurgical process routes for e-waste recycling [adapted from [41]]

Hydrometallurgical routes are claimed to be more easily controlled, more precise and most importantly, less environmentally harmful [43]. This route involves the use of a leaching solution to selectively dissolve desired metals from feed materials. Hydrometallurgy should be the preferred method for the recovery of precious metals according to Akcil et al. [41], as it produces low gas and dust emissions, has low energy consumption and is known for high precious metal recovery. High precious metal recovery from PCBs was reported by a number of researchers ([3], [44], [45], [46], [4], [5]), some of which reported almost complete gold extraction [4].

Unfortunately, this route is time consuming and requires pre-processing for efficient recovery of base and precious metals from PCBs. Physical pretreatment is the pre-processing step that follows the removal of electronic components and entails the use of mills or crushers to mechanically break PCB waste into smaller sized particles. Once the PCB waste has gone through physical pretreatment it is put

through certain separation processes to enrich the metals and non-metals. Separation processes used include screening, magnetic separation and electrostatic separation, to name a few [47]. After the pre-processing steps are done the hydrometallurgical process begins.

The general hydrometallurgical process for the recovery of precious metals involves two stages. The first stage involves the recovery of base metals using a lixiviant such as H_2SO_4 , HCl or HNO_3 , in combination with an oxidant such as H_2O_2 if necessary. The solid residue produced in the first stage is used as feed material for the second stage in which precious metals are recovered through an additional leaching operation. The general lixiviant used for precious metal recovery, cyanide, is dangerous and can contaminate water sources. Various alternatives exist, such as halide leaching, thiourea leaching and thiosulphate leaching [27].

Various methods have been implemented for the purification of leaching solutions to obtain pure precious metals. A few examples include solvent extraction, adsorption, chemical treatment and electrolysis [48]. Kasper et al. [49] investigated the potential of gold electrowinning from an ammoniacal thiosulphate solution (which was applied for the recycling of waste PCBs). They found that 99 % of the gold contained within the solution could be recovered with electrowinning, even in the presence of copper.

The focus of this study is precious metal recovery (gold and silver mostly) through thiosulphate ($\text{S}_2\text{O}_3^{2-}$) leaching, in the presence of copper (II) sulphate (CuSO_4) and ammonia (NH_3). The reason for this choice of lixiviant is explored in section 2.2.2. Various authors investigated and reviewed the thiosulphate leaching process and reported its success as an alternative to the cyanidation process [50], [51], [52], [53], [54], [55], [56], [57], [6], [58], [4].

2.2. Lixiviant Types

Leaching is an important step in the hydrometallurgical process for the recovery of metals. It is therefore important to choose a lixiviant that can selectively extract valuable metals and provide rapid solubility of said metals. The choice of lixiviant also depends on the environmental impact and cost of the lixiviant, as well as its ability to be regenerated. Lower environmental impact and lixiviant cost are favored.

2.2.1. Base Metal Lixiviants

Numerous studies have been conducted on the base metal leaching of PCBs. The most common base metal lixiviants, as previously mentioned, are H_2SO_4 , HNO_3 and HCl . To assist with the selection of optimum base metal leaching conditions, a few studies will be briefly discussed. Table 5 contains a summary of several studies that focussed on base metal leaching of PCBs.

Table 5: Summary of several base metal leaching studies conducted on PCBs

Author	Metal Focus	Base Metal Lixiviant	Particle Sizes [mm]	T [°C]	Pulp Density [g/L]	Agitation Rate [rpm]	Residence Time [h]	Optimum Base Metal Recovery [%]
[43]	1 Stage (2 step): Cu	H ₂ SO ₄ : 2 M H ₂ O ₂ : 25 mL (35 wt%)	≤ 0.3	25	100	200	3	Cu: 99.75
[3]	1st Scenario: Cu, Zn, Fe, Al, Ni	H ₂ SO ₄ : 2 M H ₂ O ₂ : 0.2 M	≤ 0.8	80	100	500	8	Cu: 85 Zn: 76 Fe:82 Al: 77 Ni:70
	2nd Scenario: Pb, Sn	NaCl: 0.5 M	≤ 0.8	25	75.56	500	2	Pb: 88 Sn: 83
[59]	Cu	H ₂ SO ₄ : 2 M H ₂ O ₂ : (15 wt%)	0.5 x 0.5 - 0.7 mm	150	30	-	1.5	Cu: 97.01
[60]	Cu	CuSO ₄ : 0.3 M NH ₃ : 5 M (NH ₄) ₂ SO ₄ : 1 M	≤ 1.5	25	10	200	2.5	Cu: 93
[61]	Cu	HNO ₃ : 1.25 - 7 M	≤ 1	30 - 60	20 - 160	300	0.75 - 1	Cu: 99.99
[36]	Cu, Pb, Sn	HNO ₃ : 6 M	≤ 2.5	80	333.3	-	6	Cu: >99
	Pb	HNO ₃ : 2 - 6 M	≤ 2.5	23	333.3	-	6	Pb: >99
	Sn	HNO ₃ : 2 M	≤ 2.5	23	333.3	-	6	Sn: 65
[62]	Cu	HCl: 3 M HNO ₃ : 1 M	≤ 0.2	60	100	-	2	Cu: 92.7
[35]	Cu	H ₂ SO ₄ : 5 - 35 wt% H ₂ O ₂ : 5 - 25 mL (30 wt%)	0.5 - 8	25 - 50	33.33 - 200	-	0.5 - 4	Cu: 95

In a study conducted by Behnamfard et al. [43], PCBs were mechanically pre-processed before being subjected to a three-stage leaching process. The first stage consisted of a two-step copper leaching process with H₂SO₄ and H₂O₂, which is the focus of this section. The solid residue from the first step was leached in the second step at identical test conditions. The first and second steps yielded copper recoveries of 85.76 % and 13.99 % (total recovery 99.75 %) respectively. Additionally, some silver was recovered in the first (0.86 %) and second steps (11.30 %), which means that the total silver recovery for the first stage amounted to 12.16 %. The increase in silver recovery can be attributed to the decreased base metal content of the solid residue, which enabled more silver to be exposed to the lixiviant.

The study conducted by Ficeriova et al. [3] focused on the development of a hydrometallurgical process to recover the maximum amount of metal types found in PCBs. The effect of sample crushing on gold, silver and the remaining metal recovery was also investigated. All semiconductors, condensers and resistances were removed from the PCBs before crushing and physical separation. They investigated two different base metal leaching scenarios that are illustrated in Table 5. The first scenario resulted in recoveries of 76 % Zn, 85 % Cu, 82 % Fe, 77 % Al and 70 % Ni after 8 h of leaching, while the second scenario resulted in recoveries of 88 % Pb and 83 % Sn after 2 h of leaching.

Jha et al. [59] conducted leaching operations on PCBs with H_2SO_4 under atmospheric and pressurised conditions for the recovery of copper. The PCBs were prepared for leaching in two different ways to compare different pre-processing techniques. Some of the PCBs, with a copper content of 17.05 %, were crushed to a thickness 2 – 3 mm and sizes of 1 – 1.5 cm to represent the first pre-processing technique. The rest of the PCBs were exposed to a swelling organic process that liberated metal sheets within the PCBs. These metal sheets were crushed to a thickness of 0.5 mm and sizes of about 0.5 – 0.7 cm. This pre-processing technique concentrated the copper content of the feed material from 17.05 % (crushed PCBs) to 74.76 % (crushed metal sheets) copper and improved the copper recovery from leaching. The optimal copper recovery of 97.01 % was achieved with the crushed metal sheets at an oxygen pressure of 20 bar. The amount of H_2O_2 added was not mentioned.

Koyama et al. [60] investigated the copper leaching behaviour from PCBs in an ammoniacal alkaline solution. They tested the effect of varying various parameters on the recovery of copper. The tests concluded that increased copper recovery is obtained when the residence time is increased from 2 to 4 h, particle diameter is decreased from 3.4 to 1.5 mm, initial Cu(II) concentration is increased from 0 to 0.3 M, initial Cu(I) concentration is zero and temperature is increased from 25 to 55°C. The optimum copper recovery of 97.01 % was obtained after only 2.5 h of leaching when the average particle size was decreased to 1.5 mm.

In a study conducted by Le et al. [61], PCBs were shredded and crushed to particle sizes smaller than 1 mm and fed into a column type air separator to remove the non-metallic components. The samples were leached in a HNO_3 solution at different conditions that are given in Table 5. The results indicated that increased copper recovery is obtained when temperature is increased, pulp density is kept below 120 g/L and HNO_3 concentration is increased. Almost total copper recovery (99.99 %) was obtained at all tests after 1 h, except for tests in which 1.25 and 2.5 M HNO_3 were used.

Mecucci & Scott [36] investigated the leaching of Cu, Pb and Sn from PCBs using HNO_3 . The results indicated that Cu dissolution increased both with an increase in HNO_3 concentration and with an increase in temperature. Increased Cu dissolution due to an increase in temperature was most prominent at lower HNO_3 concentrations. The Pb dissolution increased with an increase in HNO_3 concentration, but temperature had no prominent effect on Pb dissolution. The Sn dissolution rate increased from 1 M

HNO₃ to 2 M HNO₃, after which it decreased. The decrease after 2 M HNO₃ was attributed to Sn corrosion up to 4 M and Sn passivation beyond 4 M. The optimum Cu recovery of roughly 99 % was achieved with 6 M HNO₃ at 80°C.

Vijayaram et al. [62] investigated the effect of leaching Cu from PCBs with different lixiviant mixtures for a single cell setup. Seven different lixiviant mixtures were investigated: (1) 1.09 M H₂SO₄ + 3 M HCl; (2) 3 M HCl + 1 M HNO₃; (3) 3 M HCl; (4) 2 M HCl + 2 M HNO₃; (5) 3 M HCl + 2 M HNO₃; (6) 3 M HNO₃; (7) 2.5 M HCl + 2.5 M HNO₃. The results showed that that lixiviants 6 and 2 produced the most efficient copper recovery of 86.95 % and 92.7 % respectively. The first lixiviant produced the lowest amount of copper recovery (8.5 %).

In 2011 Yang et al. [35] conducted a study on the leaching of copper from shredded PCBs with H₂SO₄ and H₂O₂. Several parameters were investigated that are listed in Table 5. The results showed that Cu recovery increased when H₂SO₄ concentration increased, H₂O₂ addition increased (up to 10 mL), the solid/liquid ratio decreased, residence time increased and particle size decreased. A change in temperature did not have any significant effect on copper recovery. They also investigated if the presence of Cu(II) as an oxidant would increase Cu leaching from the PCBs. A Cu(II) concentration below 13 g/L did not have any significant effect on Cu recovery, but any further increase led to a decrease in Cu recovery.

One other study worth mentioning was done by Reyes et al. [44]. They conducted leaching experiments with the purpose of characterizing certain PCBs by SEM-EDS and recovering gold contained within. This was done by firstly dissolving the copper, zinc and nickel substrate through acid dynamic leaching using oxygen and sulphuric acid. The gold was then physically separated from the polymer components. After characterization through SEM-EDS, the gold bearing parts of the PCBs were used in leaching tests conducted at atmospheric pressure. It was determined that the PCBs can be characterized by a polymer layer, metal layer (Cu, Zn, Ni) and a gold substrate.

In a more recent study focused on determining selective and complete base metal recovery, a two-step leaching process was suggested. The first step involves HNO₃ leaching of the crushed PCBs to ensure the removal of Fe and Pb, while the second step entails H₂SO₄ leaching in combination with H₂O₂ addition to remove the majority of the Cu and Zn. HNO₃ leaching can be manipulated to minimize the extraction of Cu. Mecucci and Scott [36] reported that at 23°C and 1 M HNO₃, the Cu extraction only reached 8 % after 360 minutes of leaching. Rossouw [63] reported that H₂SO₄ had difficulty leaching Pb, while nitric acid was highly effective. The inability of H₂SO₄ to leach Pb can be attributed to the formation of a passivation layer of protective lead sulphate on the surface [64]. This supports the use of the two-step procedure.

The first step uses 1M HNO₃, a temperature of 25°C, pulp density of 100 g/L, agitation rate of 500 rpm and residence time of 8 h. The second test uses 2.5 M H₂SO₄, a H₂O₂ (30 wt%) flowrate of 1.2 mL/min for a 500 mL lixiviant, temperature of 25°C, pulp density of 160 g/L, agitation rate of 600 rpm and residence time of 8 h. This process is favorable as a pre-processing step for precious metal leaching, as the Au and Ag content should remain unaffected [63]. These are the conditions that were implemented in this study.

2.2.2. Precious Metal Lixiviants

Cyanide has been the leading choice for gold extraction since 1970, but in more recent times, several projects have endeavored to test alternative lixiviants and develop new processes. The driving force behind the development of alternatives is the need for sustainability. Cyanide leaching is considered to be effective for the leaching of gold and silver only at the surface of PCBs. The cyanidation process also generates large quantities of wastewater, making it a liability to the environment. This study aims to contribute to the growing knowledge base of non-cyanide lixiviants. This means that several studies were considered to assist with the choice of non-cyanide lixiviant for the precious metal leaching stage. Gos & Rubo [65] investigated the advantages and disadvantages of a few cyanide alternatives, which are listed in Table 6.

Table 6: Advantages and disadvantages of cyanide alternatives [65]

Cyanide Alternative	Advantages	Disadvantages
Thiourea	Fast rate of gold dissolution	Recyclability is limited due to rate of decomposition
	Reduced consumption through redox control	Substantial detoxification costs
	Availability	Applicability is limited
	Proven technology	High reagent consumption
		Questionable selectivity for gold
		Intrinsically unstable and decomposes rapidly
		Chemistry is difficult to control
		Toxicity profile not favorable
		Categorized as a suspected carcinogenic compound
Thiosulphate	Leaching performance is good	High reagent cost
	Availability	Limited recyclability due to instability
	Proven technology	Substantial detoxification costs
	Relatively low lethal toxicity and ecotoxicity when compared to cyanide	Limited applicability
		High reagent consumption
	Control is difficult	

Table 6 continued

Thiocyanate	Covers a wide pH range for leaching	Limited availability
	Partly recyclable	Substantial detoxification costs
	Ecotoxicity is favorable when compared to cyanide	High capital and operating costs
		High temperatures are required
Ammonia	Availability	Cannot be detoxified, must be recycled
	Recyclable	High temperatures and pressures are required
	Reagent cost	High capital and operating costs
		Toxicity profile not favorable
		Selectivity uncertain
Halogens	Availability	Control is difficult
	Proven technology	Requires oxidant
	Good leaching performance	Higher capital costs
		Cannot be detoxified, must be recycled

Gos & Rubo [65] concluded that none of the current cyanide alternatives showed any significant advantage and could not be considered as a definite replacement for cyanide. This illustrates the need for further research into these alternatives. Zhang et al. [47] discussed the current research on leaching precious metals from waste PCBs up to the year 2012. This led to the consideration of some of the various non-cyanide leaching processes. Like Gos & Rubo [65], Zhang et al. [47] concluded that thiourea is more expensive than cyanidation and requires more development of the gold recovery stage.

Thiosulphate leaching is normally done with either ammonium thiosulphate or sodium thiosulphate. This means that thiosulphate leaching can be either environmentally acceptable (sodium thiosulphate leaching) or economically viable (ammonium thiosulphate leaching) depending on the choice of thiosulphate cation [65]. The information provided by Zhang et al. [47] supports this statement as the authors concluded that the environmental benefits do not make thiosulphate leaching an economical process overall. Thiosulphate leaching does, however, have the advantage of a thermodynamically stable gold complex, which other non-cyanide lixivants do not have. The gold thiosulphate complex is the closest in stability to the gold cyanide complex. This process has a high selectivity, is non-toxic and non-corrosive [1].

Gos & Rubo [65] also considered halide leaching, which includes chloride-, bromide- and iodide leaching. Halide leaching provides higher leaching rates, but each form also has their own drawbacks. Chloride leaching requires the use of special equipment due to the corrosive nature of the process, while bromide leaching is restricted due to the health and safety hazard the process poses (even with specialized equipment). Iodide leaching is the most promising halide leaching process. It has increased leaching, no corrosion, no toxicity, good selectivity and is easy to regenerate. The disadvantages of the process include high consumption and high cost. The efficiency of electrolytic deposition of gold must also be improved. This reiterates the problem of not having a process that is both environmentally acceptable and economically viable. Zhang et al. [47] concluded that the best alternatives for cyanide

leaching are thiourea leaching and iodide leaching. These conclusions were investigated by consulting a few papers on thiourea and iodide leaching.

In the study conducted by Behnamfard et al. [43] the second stage focussed on acidic thiourea leaching in the presence of ferric iron (oxidant), with the goal of recovering gold and silver. The solid residue from the first stage was leached with a lixiviant comprised of 20 g/L thiourea, 10 g/L sulphuric acid and 6 g/L ferric iron, in a 1/10 solid to liquid ratio. The mixture was leached at ambient temperature ($\pm 25^{\circ}\text{C}$) at a constant agitation speed of 200 rpm for 3 h. The resultant gold, silver and palladium recoveries were 84.31 %, 71.36 % (total recovery 83.52 %) and 2.13 % respectively.

Birloaga et al. [37] also implemented thiourea for the recovery of gold from waste PCBs. In this study the experimental conditions were 20 g/L thiourea, 6 g/L ferric ion, 10 g/L sulphuric acid and 600 rpm. Tests were conducted to determine the effect of temperature, particle size and copper on the PCBs. When 90 % copper was removed in a pre-treatment stage, the gold recovery amounted to 45 % for particle sizes between 2 and 3 mm. When the particle sizes were reduced to below 2 mm and only 75 % copper was removed the gold recovery amounted to 69 %. The results proved that improved leaching is encountered for smaller particle sizes and when more copper is removed in a pre-treatment stage. Two leaching tests were conducted with 2.5 g pins from the PCBs in which temperatures of 25°C and 40°C were used. The results showed that the higher temperature causes the decomposition of thiourea which decreased the gold leaching considerably.

Iodine-iodide leaching was implemented in a study conducted by Xiu et al. [66] after the supercritical water oxidation (SCWO) pre-treatment of PCBs (<4mm) and base metal leaching with HCl. The goal of the pre-treatment step was to decompose toxic organic matters, like BFRs, and enrich metals contained within the PCBs. SCWO was remarkably efficient for improving Cu and Pb leaching with HCl, but detrimental for the leaching of Sn and Cr with HCl [67]. Xiu et al. [66] investigated the influence of multiple parameters, from both the SCWO pre-treatment step and the iodide leaching step, on the Au, Ag and Pd recovery. The results showed that Ag reached a maximum leaching efficiency of 99 % faster than Au (98.5 %) and Pd (97.2 %), which could be attributed to the fact that the conversion efficiency of zero-value Ag to its oxidation state was higher. The iodide and iodine concentrations were evaluated simultaneously to find an optimum ratio for the oxidant (iodine) and complexant (iodide). They found that an iodine/iodide mole ratio of 1:5 resulted in the maximum leaching efficiency for Au and Pd, while a mole ratio of 1:6 resulted in the maximum leaching efficiency for Ag. This was due to the fact that Ag has a lower oxidation potential. The optimum S/L ratio was found to be between 1:8 and 1:10, and a pH value of 9 resulted in the highest recoveries of Ag, Au and Pd.

It is clear that both thiourea and iodide leaching are able to produce good precious metal leaching results, given the right process pathway. Thiosulphate leaching also has the potential to be considered as a viable alternative lixiviant if more research is done to develop a favourable process pathway. Thiourea leaching

has more significant environmental and health risks involved when compared to thiosulphate leaching and is more expensive [41]. Iodide leaching is also more expensive than thiosulphate leaching, as specialized equipment is required [47].

Various researchers have endeavored to understand the ammonium thiosulphate leaching system over the last 20 years, mainly due to the environmental and health benefits. Early results showed low gold recoveries when compared to cyanide leaching, but decreased lixiviant consumption. The direct leaching processes produced such low gold recoveries due to the adverse effect of copper present in the feed material (decomposition of thiosulphate). More recent studies showed improved recoveries of gold with the addition of a pre-leaching stage for base metal recovery [41]. Ammonium thiosulphate was chosen as the lixiviant for the precious metal leaching stage, since there exists a potential for further development, especially with regards to computer PCBs.

2.3. Base Metal Leaching

In order to obtain the required feed material for the precious metal leaching stage, the PCBs must be pre-treated in a base metal leaching process. This leaching process eliminates base metal impurities from the PCBs, which can inhibit the extent of precious metal leaching. In the Cu-NH₃-S₂O₃ system (in the precious metal leaching stage) the presence of copper on the PCBs inhibits gold leaching. This happens with the dissolution of copper to Cu(NH₃)₂⁺ through the consumption of the oxidising agent for gold, Cu(NH₃)₄²⁺. With a decreased concentration of Cu(NH₃)₄²⁺, less gold will be leached [4].

As previously mentioned, the base metal leaching stage was conducted in a two-step leaching process, with the first step being HNO₃ leaching and the second step being H₂SO₄ and H₂O₂ leaching. Before going into the leaching chemistry involved, standard reduction potentials (25°C) of elements present in the PCBs are listed in Table 7.

Table 7: Standard reduction potentials (25°C)

Acidic Solution Reduction Half Reaction	E ⁰ [V]
Au³⁺(aq) + 3e⁻ → Au(s)	1.5
Pt²⁺(aq) + 2e⁻ → Pt(s)	1.2
Pd²⁺(aq) + 2e⁻ → Pd(s)	0.99
Ag⁺(aq) + e⁻ → Ag(s)	0.8
Cu²⁺(aq) + 2e⁻ → Cu(s)	0.34
Pb²⁺(aq) + 2e⁻ → Pb(s)	-0.13
Sn²⁺(aq) + 2e⁻ → Sn(s)	-0.14
Ni²⁺(aq) + 2e⁻ → Ni(s)	-0.25
Co²⁺(aq) + 2e⁻ → Co(s)	-0.28
Fe²⁺(aq) + 2e⁻ → Fe(s)	-0.44
Zn²⁺(aq) + 2e⁻ → Zn(s)	-0.76
Al³⁺(aq) + 3e⁻ → Al(s)	-1.66

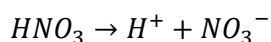
Gibbs free energies (ΔG_R^0) of non-oxidative and oxidative leaching are given in Table 8. The Gibbs free energy of a reaction can be perceived as a measure of the thermodynamic driving force that makes a reaction occur. Positive ΔG_R^0 values indicate that a reaction cannot proceed spontaneously, while negative values indicate that it will.

Table 8: Gibbs free energies (25°C) of non-oxidative and oxidative leaching of certain metals

Non-oxidative Leaching	
Reaction	ΔG_R^0 [kJ/mol]
$Au^0 + 3H^+(aq) \rightarrow Au^{3+}(aq) + \frac{3}{2}H_2(g)$	434.18
$Pt^0 + 2H^+(aq) \rightarrow Pt^{2+}(aq) + H_2(g)$	231.56
$Pd^0 + 2H^+(aq) \rightarrow Pd^{2+}(aq) + H_2(g)$	191.04
$Ag^0 + H^+(aq) \rightarrow Ag^+(aq) + \frac{1}{2}H_2(g)$	77.11
$Cu^0 + 2H^+(aq) \rightarrow Cu^{2+}(aq) + H_2(g)$	65.49
$Pb^0 + 2H^+(aq) \rightarrow Pb^{2+}(aq) + H_2(g)$	-24.43
$Sn^0 + 2H^+(aq) \rightarrow Sn^{2+}(aq) + H_2(g)$	-27.39
$Ni^0 + 2H^+(aq) \rightarrow Ni^{2+}(aq) + H_2(g)$	-46.4
$Co^0 + 2H^+(aq) \rightarrow Co^{2+}(aq) + H_2(g)$	-51.5
$Fe^0 + 2H^+(aq) \rightarrow Fe^{2+}(aq) + H_2(g)$	-78.90
$Zn^0 + 2H^+(aq) \rightarrow Zn^{2+}(aq) + H_2(g)$	-147.1
$Al^0 + 3H^+(aq) \rightarrow Al^{3+}(aq) + \frac{3}{2}H_2(g)$	-485
Oxidative Leaching	
Reaction	ΔG_R^0 [kJ/mol]
$Au^0 + \frac{3}{4}O_2(g) + 3H^+(aq) \rightarrow Au^{3+}(aq) + \frac{3}{2}H_2O(l)$	78.38
$Pt^0 + \frac{1}{2}O_2(g) + 2H^+(aq) \rightarrow Pt^{2+}(aq) + H_2O(l)$	-5.64
$Pd^0 + \frac{1}{2}O_2(g) + 2H^+(aq) \rightarrow Pd^{2+}(aq) + H_2O(l)$	-46.16
$Ag^0 + \frac{1}{4}O_2(g) + H^+(aq) \rightarrow Ag^+(aq) + \frac{1}{2}H_2O(l)$	-41.49
$Cu^0 + \frac{1}{2}O_2(g) + 2H^+(aq) \rightarrow Cu^{2+}(aq) + H_2O(l)$	-171.71
$Pb^0 + \frac{1}{2}O_2(g) + 2H^+(aq) \rightarrow Pb^{2+}(aq) + H_2O(l)$	-261.63
$Sn^0 + \frac{1}{2}O_2(g) + 2H^+(aq) \rightarrow Sn^{2+}(aq) + H_2O(l)$	-264.59
$Ni^0 + \frac{1}{2}O_2(g) + 2H^+(aq) \rightarrow Ni^{2+}(aq) + H_2O(l)$	-283.6
$Co^0 + \frac{1}{2}O_2(g) + 2H^+(aq) \rightarrow Co^{2+}(aq) + H_2O(l)$	-288.7
$Fe^0 + \frac{1}{2}O_2(g) + 2H^+(aq) \rightarrow Fe^{2+}(aq) + H_2O(l)$	-316.1
$Zn^0 + \frac{1}{2}O_2(g) + 2H^+(aq) \rightarrow Zn^{2+}(aq) + H_2O(l)$	-384.3
$Al^0 + \frac{3}{4}O_2(g) + 3H^+(aq) \rightarrow Al^{3+}(aq) + \frac{3}{2}H_2O(l)$	-840.8

2.3.1. Nitric Acid Leaching

HNO_3 is a strong oxidizing reagent with the ability to dissolve most of the base metals present in PCBs. It also provides the possibility for regeneration and re-use. HNO_3 is preferred over HCl , due to the possible formation of precipitates during HCl acid leaching [68], [69], [36]. HNO_3 is a strong acid which dissociates according to Reaction 1.



Reaction 1

HNO₃ can be reduced to various degrees. The degree of reduction is dependent on the reductant and HNO₃ concentration. Concentrated HNO₃ is reduced to NO₂, while dilute HNO₃ is reduced to NO [70]. Dilute HNO₃ was used in this study. To illustrate that dilute HNO₃ should not leach precious metals, the reduction potential of the reduction reaction of NO₃⁻ (0.96 V) is compared to the values in Table 7.



The reduction potentials of the base metals are lower than 0.96 V, while the reduction potentials of Au, Pt and Pd are higher. The reduction potential of Ag, however, is lower and suggests that it might also be leached. The dissolution reactions of Cu, Co, Zn, Fe, Pb, Ni and Sn occur according to the following general reaction, where M represents the metal element:



The dissolution reaction for Al is given below:



At higher concentrations of HNO₃, Ahn et al. [68] and Meccuci & Scott [36] reported that the passivation of Sn occurs during leaching, which leads to the formation of a protective β-SnO₂ film that decreases the rate of Sn dissolution. This β-SnO₂ film also causes the formation of metastannic acid according to Reaction 5.



2.3.2. Sulphuric Acid Leaching

Base metals were leached with H₂SO₄ and H₂O₂ as this combination of lixiviant and oxidant have proven to be successful in previous literature. This also eliminates the energy requirements for heating as the leaching process can be operated at ambient temperature. The positive Gibbs energy of non-oxidative Cu leaching in Table 8 indicate that H₂SO₄ would not be able to leach Cu without an oxidant. The chemical reactions used to describe the dissolution of base metals with H₂SO₄ and H₂O₂ are mostly similar and can be illustrated with Reaction 6.



The dissolution reaction for Al is given in Reaction 7.



The dissolution reactions for Cu, Zn, Fe, Ni and Sn have ΔG_R⁰ values of -326.1, -535.4, -484.7, -423.6 and -572.8 kJ/mol respectively, which indicate spontaneous reactions [37].

H_2O_2 is one of the more common oxidants used for leaching copper from PCBs and is known to have a higher oxidation potential (1.77 V) than other oxidants [71]. Unfortunately, H_2O_2 is a thermodynamically unstable compound that decomposes spontaneously. The decomposition of H_2O_2 produces oxygen gas as shown in Reaction 8.



The rate of oxygen formation must be controlled as an overly high rate will cause the oxygen to escape to the atmosphere before absorption to the aqueous phase can take place, while an overly slow rate will disable leaching. The rate of H_2O_2 decomposition increases with rising temperatures, concentrations and pH [72]. The decomposition rate was controlled by using a temperature of 25°C and adding H_2O_2 (30 wt%) slowly at rate of 1.2 mL/min to a 500 mL lixiviant.

2.4. Thiosulphate Leaching of Precious Metals

2.4.1. Gold Leaching

Aylmore & Muir [51], [52] suggested an electrochemical-catalytic mechanism for gold leaching with ammonium thiosulphate. During the gold leaching process, a cathodic and anodic area form on the surface of the gold particles according to the mechanism shown in Figure 2.

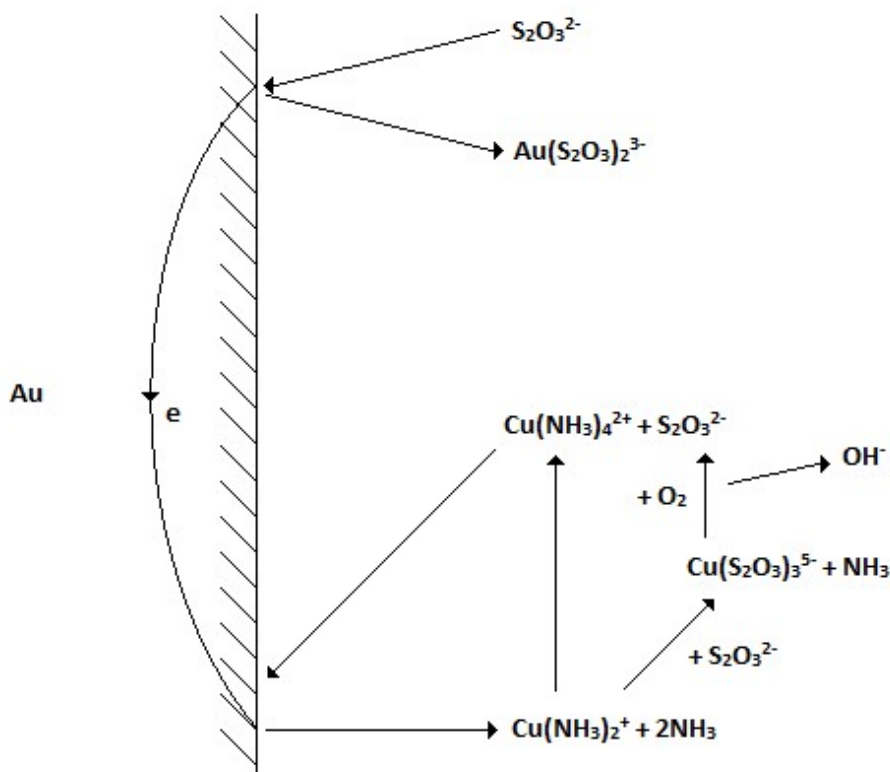


Figure 2: Electrochemical-catalytic mechanism model for gold leaching with ammonium thiosulphate (adapted from [52])

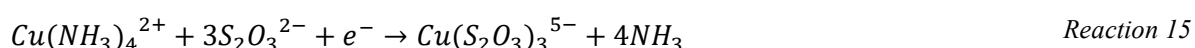
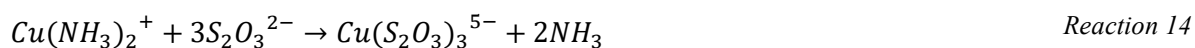
Oxidation occurs at the anodic portion of the gold surface which leads to the release of gold ions (Au^+). The gold ions then react with either thiosulphate or ammonia to form $Au(S_2O_3)_2^{3-}$ or $Au(NH_3)_2^+$ respectively. Reaction 9 to Reaction 11 illustrate the process of gold complex formation on the anodic surface of gold [51].



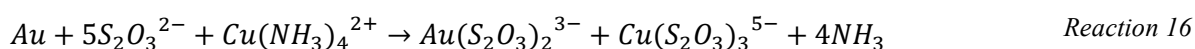
The $Au(S_2O_3)_2^{3-}$ is believed to be the more stable gold complex. This means that the oxidation half reaction can be summarized by combining Reaction 9 and Reaction 10 [41], [54], [73].



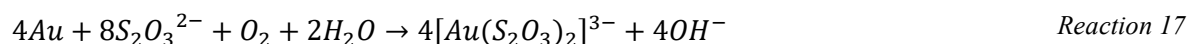
At the same time $Cu(NH_3)_4^{2+}$ in solution acquires electrons from the cathodic surface of gold and is reduced directly to $Cu(NH_3)_2^+$, after which thiosulphate present in solution converts $Cu(NH_3)_2^+$ to $Cu(S_2O_3)_3^{5-}$. The $Cu(S_2O_3)_3^{5-}$ and any leftover $Cu(NH_3)_2^+$ are then oxidised into $Cu(NH_3)_4^{2+}$ by oxygen. The relative concentrations of the species present in solution will determine what the predominant cathodic reaction is. The main cathodic reactions are given in Reaction 13 and Reaction 14, which can be combined to form Reaction 15 [51]. The reaction has a reduction potential of 0.225 V [74], [75].



The overall reaction for the leaching of gold can be summarized by combining Reaction 12 to Reaction 14. In this electrochemical reaction Cu(II) ions are used as the oxidant rather than oxygen.



The leaching of gold can also be described as shown in Reaction 17, where thiosulphate is the ligand and oxygen the oxidant [52]. After the gold-thiosulphate complex has formed it is exceptionally stable.



Crundwell [76] suggests that the classic diagram illustrated in Figure 2, that depicts separate positions for anodic and cathodic sites, is flawed for two reasons. The first reason being that Figure 2 suggests that the anodic and cathodic sites are physically separated, which requires that each site possesses a different electrical potential to provide the necessary driving force to facilitate electron transfer. Crundwell [76] claims that the electrochemical mechanism of dissolution requires that the material

surface universally possesses the same potential and that the anodic and cathodic reactions take place simultaneously on the entire surface. The electrochemical mechanism of the dissolution of a metal M in an aqueous solution containing an oxidant B^{2+} can be illustrated by Reaction 18.



It is suggested that Reaction 18 shows no accumulation of charge due to the instantaneous acceptance of every electron (donated by the dissolution half reaction of the metal) during the reduction half reaction of the oxidant. The second reason is that Figure 2 suggests that a flow of electrons exists within the bulk of the material between the separate sites due to the difference in potential. Crundwell [76] claims that this reasoning is flawed as there is no driving force when the entire surface is at the same mixed potential. Dissolution also does not require bulk flow of electrons as it occurs at the surface of the material. This means that Figure 2 can be redrawn as Figure 3.

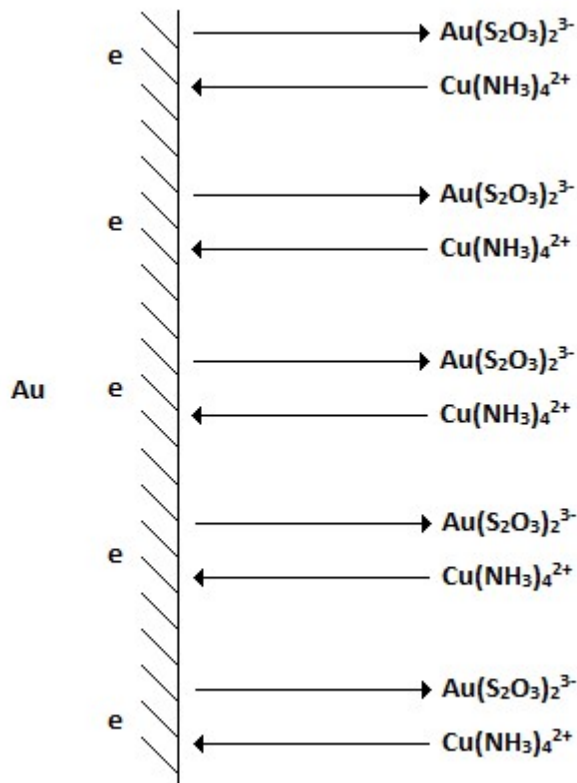


Figure 3: Electrochemical-catalytic mechanism model for gold leaching with ammonium thiosulphate (adapted from [76])

The effect that various parameters have on the gold dissolution in an ammonium thiosulphate lixiviant will be discussed in section 2.6.1.

2.4.2. Silver Leaching

The leaching of silver in the Ag-NH₃-S₂O₃ system is similar to that of the leaching of gold in the Au-NH₃-S₂O₃ system. The reactions used to describe gold dissolution can be used for silver. The rate at which silver is leached is known to improve with increasing concentrations of copper and thiosulphate, while the rate is reduced with increasing ammonia concentrations. The optimisation of the thiosulphate/ammonia ratio can be used to control the silver leaching reaction. The occurrence of silver on the PCBs also increases the dissolution of gold. When purely gold is leached with the same solution the resultant gold dissolution is at least 6 times less [52]. Silver leaching occurs rapidly but is limited by the mass transfer of Cu(II) to the surface of metallic silver [74].

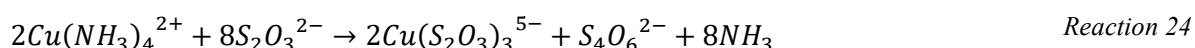
2.4.3. Thiosulphate Stability

A major problem associated with the recovery of gold through thiosulphate leaching is the high rate of thiosulphate consumption. The metastable nature of thiosulphate is largely responsible for the high rate of thiosulphate consumption, as it readily undergoes chemical decomposition in aqueous solutions. The stability of thiosulphate is influenced by the solution concentration and pH, amount of exposure to ultraviolet light and the presence of certain metals and sulphur metabolising bacteria. It is known that thiosulphate becomes more unstable at higher temperatures [75]. Concentrated solutions of thiosulphate (>0.1 M) are known to decompose more slowly than dilute solutions (<0.01 M) [52]. In an acidic environment thiosulphate decomposes much faster when compared to alkaline environments.

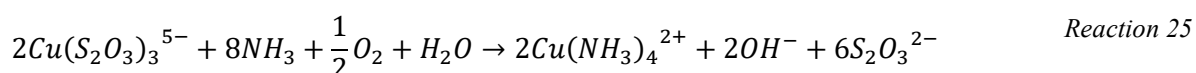
The complexity of the gold leaching mechanism mentioned in section 2.4.1 is increased by the oxidation of thiosulphate to tetrathionate (S₄O₆²⁻) and other sulphur species. Depending on the conditions present, thiosulphate will: oxidise to sulphate (SO₄²⁻) (Reaction 19) or tetrathionate (Reaction 20); disproportionate into sulphate and elemental sulphur (Reaction 21); disproportionate to sulphite and sulphide ions (Reaction 22 or Reaction 23) [52].



The oxidation of thiosulphate to tetrathionate characteristically takes place between pH values of 4 and 6. With the addition of ammonia and copper to the system, however, the oxidation of thiosulphate to tetrathionate occurs according to Reaction 24 in a pH range of 8 to 10 [52].



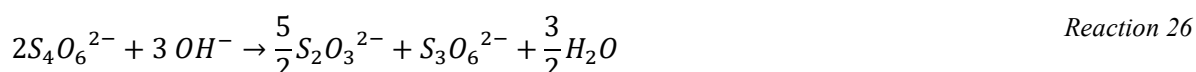
Reaction 24 also illustrates that the Cu(II) complex is reduced to a Cu(I) complex. Decreased concentrations of Cu(II) ions and thiosulphate will cause decreased gold dissolution. The degradation of thiosulphate is promoted by an increased Cu(II) concentration, but inhibited by increased ammonia concentrations. The ratio between copper and ammonia is an important factor that simultaneously affects the extent of gold dissolution and the stability of thiosulphate. Apart from the oxidation of thiosulphate, the presence of oxygen also leads to a rise in Eh and the rapid oxidation of the Cu(I) complex to Cu(II) complex. This means that only the necessary oxygen must be used to regenerate Cu(II) according to Reaction 25 in order to prevent substantial loss of thiosulphate.



When ammonium thiosulphate leaching solutions are used to extract gold, an increase in thiosulphate concentration is known to result in increased thiosulphate consumption [77].

2.4.4. Thiosulphate Regeneration

Thiosulphate can be regenerated under non-oxidising conditions through the decomposition of tetrathionate, which is illustrated in Reaction 26.



Reaction 26 can be divided into a step wise reaction scheme (Reaction 27 to Reaction 29) that is catalysed by thiosulphate ions [52].



2.4.5. Reaction Kinetics

The rate of gold leaching is chemically controlled according to various sources [78], [54], [5]. This means that increased temperatures should increase the gold leaching rate. It is important to know that the Cu(II) reduction reaction (through thiosulphate) is also chemically controlled and has a larger activation energy than the gold leaching reaction. This suggests that the system should not be operated at much higher temperatures than 25°C to avoid the unwanted consumption of thiosulphate. The gold leaching rate has also been found to slow down with time as Cu(II) concentrations decrease [54].

Senanayake [79] found that the leaching of gold from sulphide ores/concentrates in a Cu(II)-NH₃-S₂O₃ lixiviant follows the shrinking sphere kinetic model for the first 60 min. The chemical reaction limiting shrinking sphere model is illustrated in equation (1).

$$1 - (1 - X)^{1/3} = \left(\frac{bKC}{\rho r}\right)t = kt \quad (1)$$

Where

b = Stoichiometric factor for surface reaction products

C = Reagent concentration [mol/m³]

K = Surface reaction intrinsic rate constant [m/s]

k = Apparent rate constant for shrinking sphere model [s⁻¹]

r = Spherical particle radius [m]

X = Gold fraction reacted after time t

ρ = Gold molar density [mol/m³]

Jeffrey [74] found that the steady state gold leaching rate was dependent on the concentrations of ammonia, thiosulphate and copper in the system. It was concluded that the reaction rate was chemically controlled at high copper concentrations, but copper diffusion controlled at 30°C and low copper concentrations. The reaction rate of gold leaching reached a steady state value after a transient film was dissolved. This transient film was believed to hinder the reaction rate of gold leaching.

In order to clarify what the rate limiting step was for gold leaching at the conditions that were investigated during this study, three common mechanisms were considered. According to Prosser [80] the premises for these mechanisms are that the rate is controlled by:

- “mass transport of a dissolved reactant from the bulk solution to the solid-solution interface via a boundary layer in which there is laminar flow”, or
- “some chemical reaction occurring at the solid-solution interface”, or
- “mass transport of a dissolved reactant through an adhering layer of inert mineral or solid product containing continuous pores”.

The rate equations for these mechanisms are illustrated in Equation (1) for chemical reaction, Equation (2) for mass transport in the boundary layer and Equation (3) for mass transport in the porous product layer.

$$1 - (1 - X)^{2/3} = kt \quad (2)$$

$$1 - 2(X/3) - (1 - X)^{2/3} = kt \quad (3)$$

2.5. Thermodynamics

Gold and silver leaching with ammonium thiosulphate, in the presence of CuSO_4 , creates a complex chemical system. The Cu(II)-Cu(I) redox couple, the simultaneous presence of ammonia and thiosulphate ligands as well as the possibility of oxidative decomposition of thiosulphate, all contribute to the difficulty in understanding the system [52]. In order to successfully leach gold and silver these substances must dissolve and form soluble complexes.

To assist with the identification of optimal conditions in which these soluble complexes exist and to better understand the system, thermodynamic analyses were conducted by Aylmore & Muir [51], [52]. Two sets of Pourbaix (Eh-pH) diagrams were constructed for high and low ammonia, thiosulphate and Cu(II) concentrations. The reagent concentrations used for the construction of Cu-NH₃-S₂O₃, Au-NH₃-S₂O₃ and Ag-NH₃-S₂O₃ systems are given in Table 9.

Table 9: Reagent concentrations for Cu-NH₃-S₂O₃, Au-NH₃-S₂O₃ and Ag-NH₃-S₂O₃ systems

Concentration	System	Au [M]	Ag [M]	S ₂ O ₃ ²⁻ [M]	NH ₃ /NH ₄ ⁺ [M]	Cu ²⁺ [M]
High	Au-NH ₃ -S ₂ O ₃ / Cu-NH ₃ -S ₂ O ₃	5×10 ⁻⁴		1	1	0.05
	Ag-NH ₃ -S ₂ O ₃		5×10 ⁻⁴	1	1	
Low	Au-NH ₃ -S ₂ O ₃ / Cu-NH ₃ -S ₂ O ₃	5×10 ⁻⁴		0.1	0.1	5×10 ⁻⁴
	Ag-NH ₃ -S ₂ O ₃		5×10 ⁻⁴	0.1	0.1	

The Pourbaix diagrams illustrate the region of stability for various species associated with the aforementioned systems in pH and reduction potential. Figure 4 to Figure 6 show the species distribution of the high reagent concentration systems, while figures Figure 7 to Figure 9 show the species distribution for the low reagent concentration systems. When evaluating these systems conditions must be chosen where the Cu(II) ammine complex ($\text{Cu}(\text{NH}_3)_4^{2+}$) is stable and gold and silver dissolution occur. Gold dissolution is enhanced through the formation of $\text{Cu}(\text{NH}_3)_4^{2+}$, which occurs due to the stabilisation of the oxidant Cu(II) by ammonia [52].

Figure 4 shows that for high reagent concentrations the pH range of stability for $\text{Cu}(\text{NH}_3)_4^{2+}$ is roughly between 7.7 - 10.7. When operating at pH levels above 9.2 inside the stability region, the reduction potential must be above 0.17 V. As the pH decreases below 9.2, a higher potential is required to maintain stability. Shifting the pH outside of these bounds will result in the formation of CuO. At low potential values copper sulphides will precipitate. The stability region for $\text{Cu}(\text{S}_2\text{O}_3)_3^{5-}$ has a much wider pH range than that of $\text{Cu}(\text{NH}_3)_4^{2+}$.

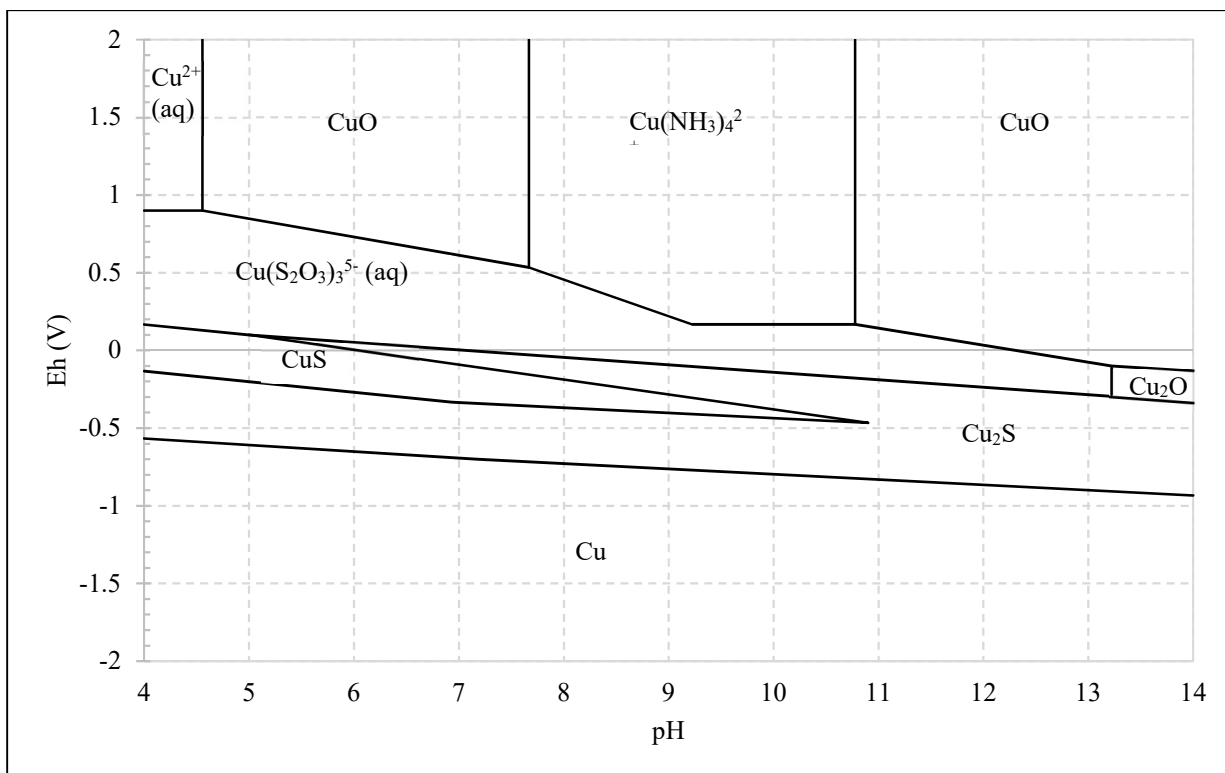


Figure 4: Pourbaix diagram for $\text{Cu-NH}_3\text{-S}_2\text{O}_3^{2-}$ system at high reagent concentrations [adapted from [52]]

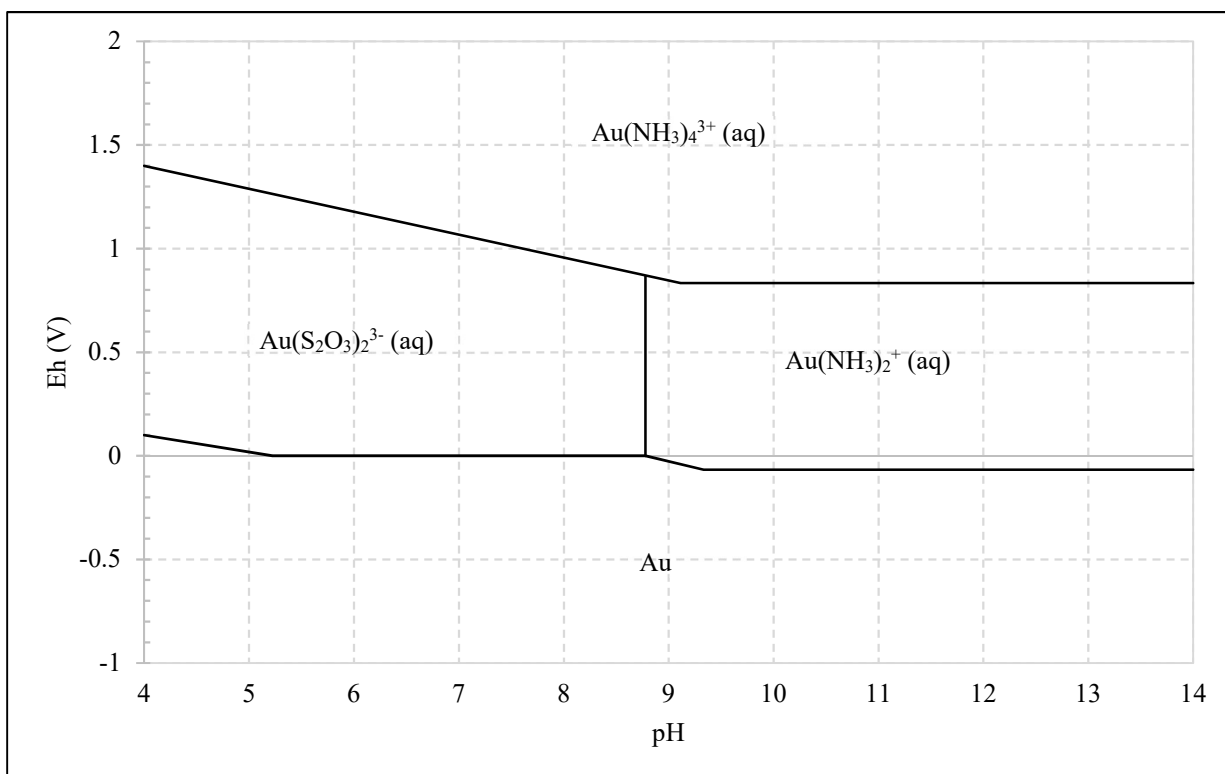


Figure 5: Pourbaix diagram for $\text{Au-NH}_3\text{-S}_2\text{O}_3^{2-}$ system at high reagent concentrations [adapted from [52]]

Figure 5 illustrates the importance of a high enough potential for gold dissolution. Generally, if the potential is below 0 V, the gold will remain undissolved across the entire pH range. In order to obtain the preferred gold (I) thiosulphate complex ($\text{Au}(\text{S}_2\text{O}_3)_2^{3-}$) the pH level must be kept below roughly 8.7. The predominate gold complex becomes gold (I) diamine ($\text{Au}(\text{NH}_3)_2^+$) when the pH rises above 8.7. Another, less stable, gold thiosulphate complex known to form is $\text{Au}(\text{S}_2\text{O}_3)^-$ [81]. Stability constants predicted by Hancock et al. [82], however, show higher values for $\text{Au}(\text{S}_2\text{O}_3)_2^{3-}$ than $\text{Au}(\text{NH}_3)_2^+$. Certain measurements at pH levels above 9 indicated that gold rest potentials do not change with ammonia concentration, but rather with thiosulphate concentration [53], [83]. Aylmore & Muir [51], [52] suggest that this means that the prime gold complex is $\text{Au}(\text{S}_2\text{O}_3)_2^{3-}$ rather than $\text{Au}(\text{NH}_3)_2^+$ and that Pourbaix diagrams generated with the predicted stability constants result in a stable region over the entire pH range for $\text{Au}(\text{S}_2\text{O}_3)_2^{3-}$.

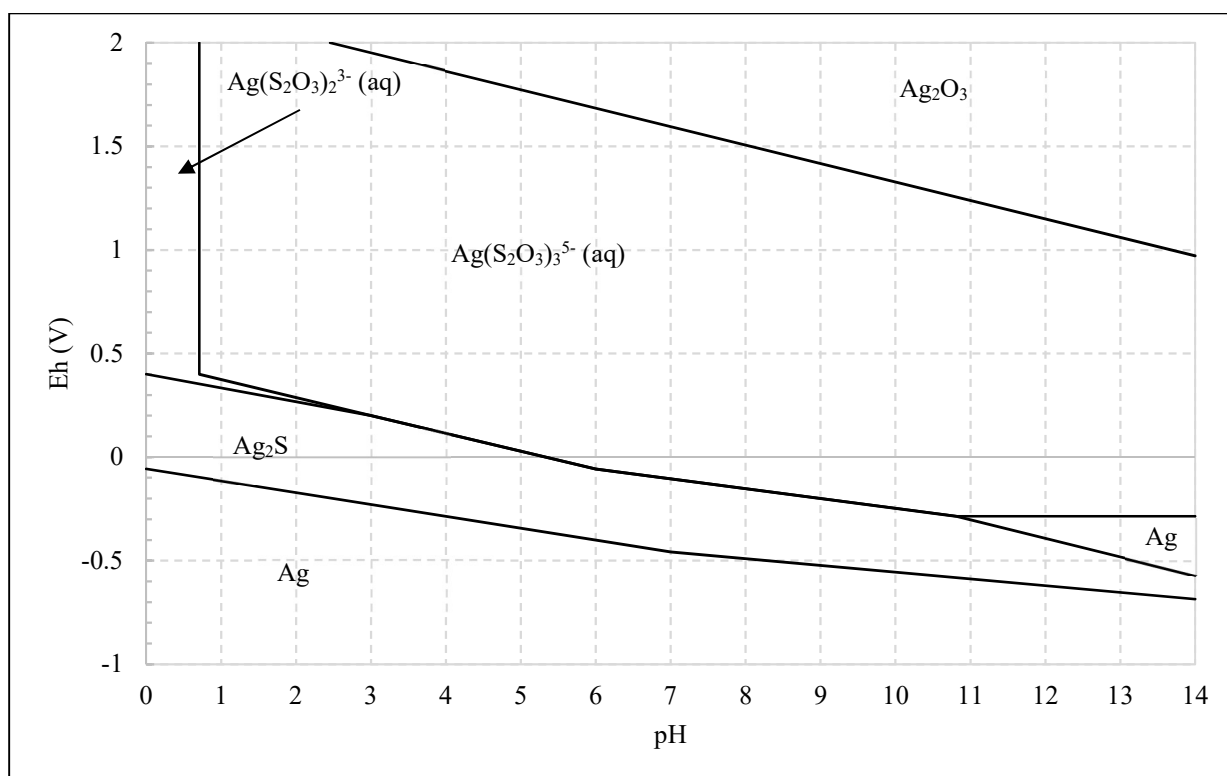


Figure 6: Pourbaix diagram for $\text{Ag-NH}_3\text{-S}_2\text{O}_3^{2-}$ system at high reagent concentrations [adapted from [52]]

The large area occupied by $\text{Ag}(\text{S}_2\text{O}_3)_3^{5-}$ in Figure 6 shows that silver preferentially combines with thiosulphate. Like gold, silver will not dissolve if the potential is too low. This will result in the precipitation of Ag_2S over the entire pH range. When both the pH and potential are high, Ag_2O_3 will precipitate.

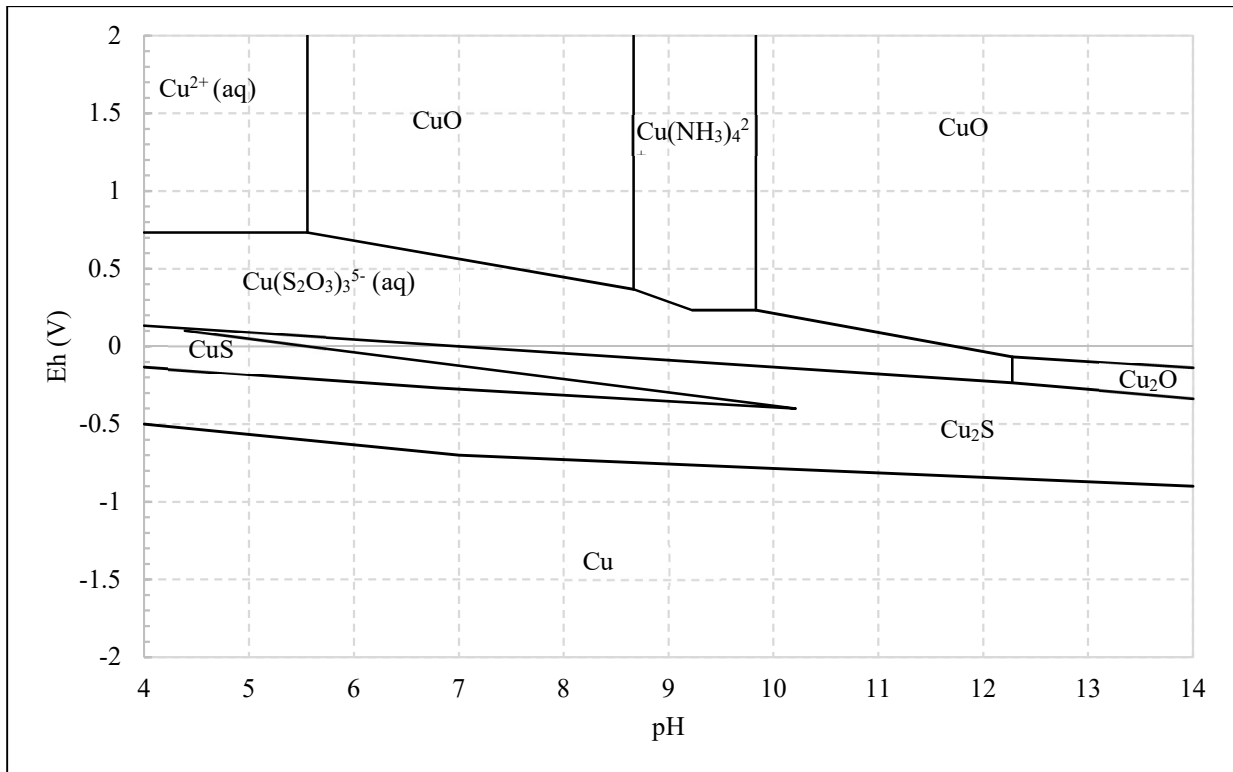


Figure 7: Pourbaix diagram for $\text{Cu-NH}_3\text{-S}_2\text{O}_3^{2-}$ system at low reagent concentrations [adapted from [52]]

Figure 7 shows that at lower reagent concentrations the stability region for CuO , Cu_2O and Cu_2S is much larger, while the stability region for $\text{Cu}(\text{NH}_3)_4^{2+}$ is much smaller. Both the pH and reduction potential range for $\text{Cu}(\text{NH}_3)_4^{2+}$ stability are smaller. The pH range has decreased to roughly 8.7 - 9.8, while the potential must be kept above 0.25 V to 0.38 V, depending on the pH level. An increase in potential, with O_2 for example, will result in a decrease of $\text{Cu}(\text{S}_2\text{O}_3)_3^{5-}$ and an increase of $\text{Cu}(\text{NH}_3)_4^{2+}$ when all other reagent concentrations are kept constant. It is important to note that high $\text{Cu}(\text{NH}_3)_4^{2+}$ concentrations will result in a higher amount of thiosulphate being converted to tetrathionate. Aylmore & Muir [51], [52] also noticed through the construction of speciation diagrams that by increasing total ammonia concentration, the stability region for $\text{Cu}(\text{NH}_3)_4^{2+}$ increases. An increase in thiosulphate concentration, however, resulted in increased stability for $\text{Cu}(\text{S}_2\text{O}_3)_3^{5-}$. When copper concentration is increased the $\text{Cu}(\text{S}_2\text{O}_3)_3^{5-}$ complex is favoured as well. High ammonia to thiosulphate concentration will therefore increase the stability of $\text{Cu}(\text{NH}_3)_4^{2+}$ over $\text{Cu}(\text{S}_2\text{O}_3)_3^{5-}$, but will result in higher thiosulphate consumption.

With a decrease in reagent concentrations the stability regions of the gold and silver species undergo minor changes. Figure 8 illustrates that at extremely high pH and potential values AuO_2 forms.

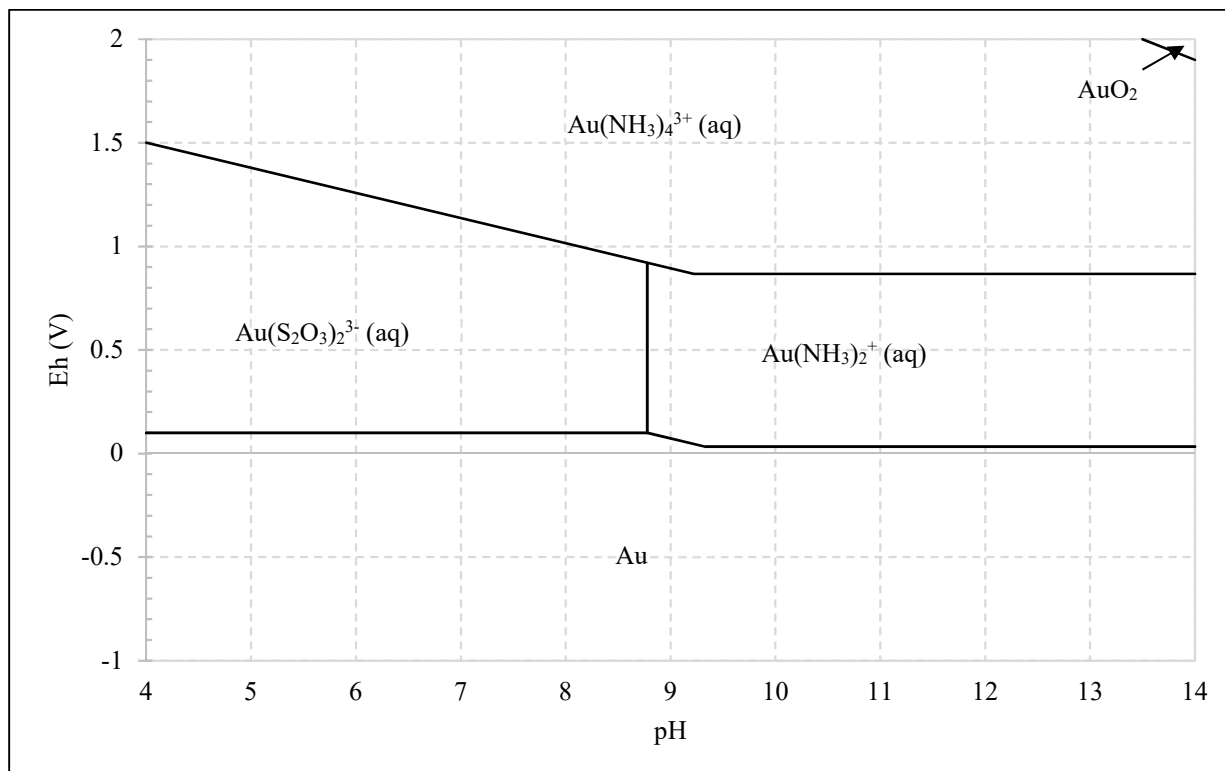


Figure 8: Pourbaix diagram for $\text{Au-NH}_3\text{-S}_2\text{O}_3^{2-}$ system at low reagent concentrations [adapted from [52]]

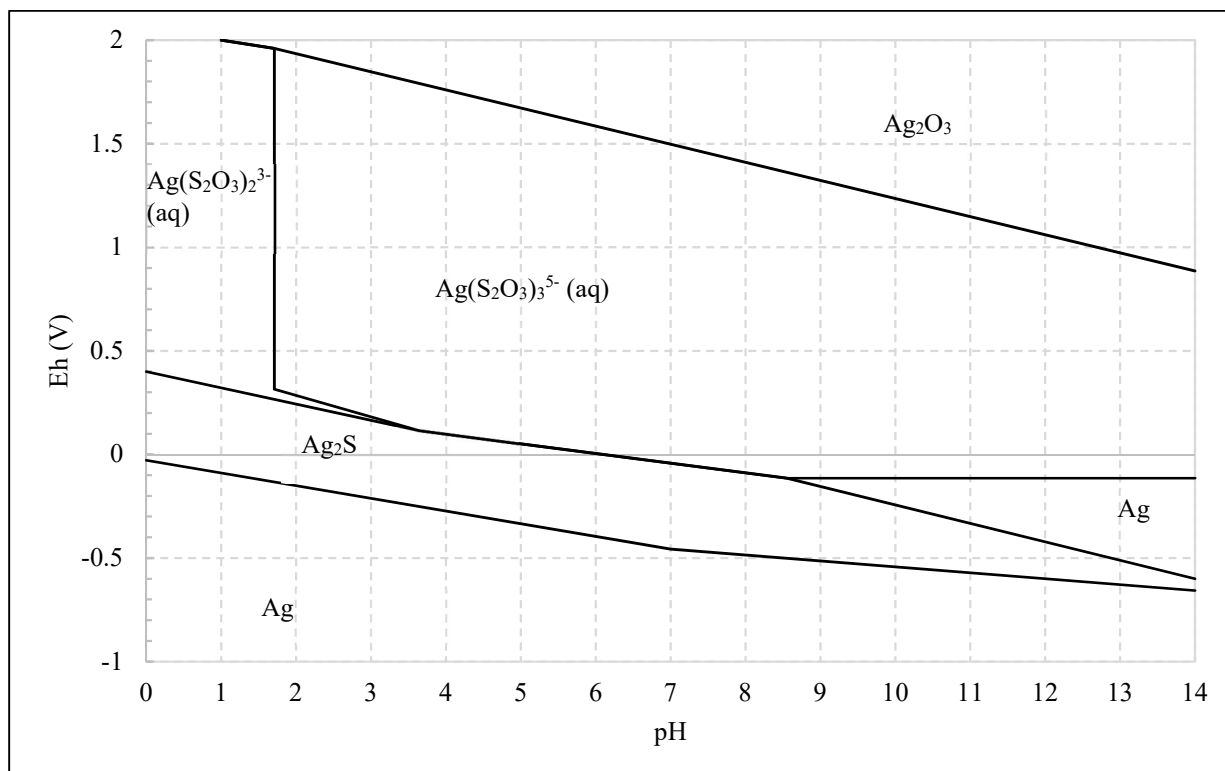


Figure 9: Pourbaix diagram for $\text{Ag-NH}_3\text{-S}_2\text{O}_3^{2-}$ system at low reagent concentrations [adapted from [52]]

2.6. Results from Previous Literature

In order to clarify certain aspects of the leaching process and determine which variables require further investigation, a number of previous studies will be discussed.

2.6.1. Thiosulphate Leaching Parameters

The base metal leaching section of the study conducted by Ficeriova et al. [3] was discussed in section 2.2.1. This is a continuation of that study, with the focus shifting to precious metal leaching in the second scenario. The second scenario implemented 0.5 M $(\text{NH}_4)_2\text{S}_2\text{O}_3$, 0.2 M CuSO_4 and 1 M NH_3 to leach 40 g of crushed PCB at a pH of 9 for 2880 min at 40°C. This resulted in Au and Ag recoveries of 98 % and 93 % respectively. A test under similar conditions was repeated with untreated PCBs (not crushed) which resulted in Au and Ag recoveries of only 16 % and 12 % respectively. This means that by decreasing the PCB particle size, a significant increase in Au and Ag leaching can be obtained. This is most likely due to the increased particle surface area available for interaction with the lixiviant. It is also known that Cu layers cover most of the surface of a PCB, which means Au and Ag will leach with more difficulty from whole PCBs.

A paper published by Oh et al. [6] studied the selective leaching of valuable metals from waste PCBs. The base metals found in the PCBs consisted of Cu (10.9 %), Fe (7.7 %), Ni (2.5 %), Sn (3.9 %), Pb (1.5 %), Al (1.7 %) and Zn (1.1 %). The precious metals were Au (0.005 %), Ag (0.008 %) and Pd (0.002 %). The PCBs were crushed (<1 mm) by a shredder and separated according to conductivity through electrostatic separation, after which the conductive materials were then separated magnetically. The non-magnetic materials were then pre-leached with H_2SO_4 and H_2O_2 to separate the base metals. The residue was leached in a 0.2 M $(\text{NH}_4)_2\text{S}_2\text{O}_3$, 0.02 M CuSO_4 and 0.4 M NH_4OH solution at 40°C, 150 rpm and 5 g/L for 48 h to recover the precious metals. The Ag recovery was 100 % after 24 h, while the Au recovery was 95 % after 48 h.

In a study conducted by Tripathi et al. [2] the effects that varying several parameters have on the gold leaching of mobile phone PCBs with $(\text{NH}_4)_2\text{S}_2\text{O}_3$ were investigated. All leaching tests were conducted for 8 h on shredded PCBs (0.5 to 3mm). The Cu, Au and Ag content of the PCBs were 56.68 wt%, 0.021 wt% and 0.1 wt% respectively. The pH (8 – 11), CuSO_4 concentration (0 – 0.05 M), $(\text{NH}_4)_2\text{S}_2\text{O}_3$ concentration (0.05 – 0.25 M) and pulp density (10 – 60 g/L) were varied, while the temperature (25°C) and agitation rate (250 rpm) were kept constant.

An increase in Au leaching was observed in the tests in which CuSO_4 was increased, which can be attributed to the catalyzing effect of Cu(II) ions. Cu(II) ions in solution enhance Au dissolution through the formation of Cu(II) amine complexes. Similar results were reported by other researchers [54], [84]. Au recovery only increased up to 0.1 M $(\text{NH}_4)_2\text{S}_2\text{O}_3$, which was indicative of the fact that higher $(\text{NH}_4)_2\text{S}_2\text{O}_3$ concentrations promote the formation of undesired products [4]. Increasing the pH level

from 8 to 10.5 led to increased Au leaching, while any further increase led to a decrease in Au leaching. The tests also concluded that lower pulp densities enhance Au leaching, which is attributed to the higher quantity of the reagent per unit weight of PCBs.

At the optimum leaching conditions of 0.040 M CuSO₄, 0.1 M (NH₄)₂S₂O₃, 10 g/L and a pH level between 10 – 10.5 the Au recovery amounted to 56.7 %. When a whole PCB (not crushed) was used and leached under the same optimum leaching conditions the Au recovery amounted to 78.8 %. Cu is situated above the Au on the PCB, therefore it will be leached before Au. When the PCB is crushed to granules it increases the available surface area for Cu leaching. Increased rates of Cu dissolution will result in higher losses of S₂O₃²⁻ ions through its conversion to S₄O₆²⁻ and additional polythionates, which are not helpful for Au dissolution. This proves the importance of a base metal pre-leaching stage to remove base metal impurities.

Ha et al. [4] investigated the leaching of Au from mobile phone PCBs in a Cu-NH₃-S₂O₃ solution to determine the influence of S₂O₃²⁻, NH₃ and Cu(II) concentrations. The metals of interest in the PCBs were Au (0.12 %), Cu (35.1 %), Sn (4 %) and Pb (2.7 %). The tests were conducted at 25°C, 200 rpm, pH range of 10 – 10.5 for 2 h. The S₂O₃²⁻, NH₃ and Cu(II) concentrations were varied between 0.06 – 0.2 M, 0.1 – 0.4 M and 0.005 – 0.03 M respectively.

The experimental results indicated that as the S₂O₃²⁻ concentration increased the Au leaching increased initially, reached a maximum and decreased afterward. The results were not uniform as the change in Cu(II) ion and NH₃ concentration also affected the system in a complicated manner. This can be explained due to the change in stability region of the Au species with a change in pH and potential. If the potential is too low, Au will not dissolve and Cu will precipitate as a sulphide. Furthermore, the increase in S₂O₃²⁻ concentration causes increased consumption, which in turn leads to an increased presence of degradation products such as S₄O₆²⁻.

An increase in Au leaching was witnessed up to 0.015 M Cu(II), after which the leaching of Au was nearly independent of Cu(II) concentration in the tests conducted by [4]. Jeffrey [74] suggested that Au leaching is Cu(II) diffusion limited at low concentrations, but chemically controlled at higher concentrations. The experimental results further revealed that NH₃ stabilizes the Cu in the cupric state for the oxidation of Au. An increase in Au leaching efficiency was experienced up to 0.3 M NH₃, after which the Au leaching decreased.

NH₃ has several functions in/effects on the Cu-NH₃-S₂O₃ system:

- Drastically slows the rate of S₂O₃²⁻ degradation
- Increasing the NH₃ concentration while maintaining constant pH, potential and other reagent concentrations results in an increased stability region for Cu(NH₃)₄²⁺ [52], which in turn causes slower Au leaching due to lower driving force according to Reaction 16 [57]

- Prevents the formation of sulphur coatings on the surface of Au that passivate Au dissolution [52]

Ha et al. [4] also investigated the leaching potential of mobile PCBs against mobile scrap. The mobile scrap was obtained from keyboards of waste mobile phones, while the PCBs were obtained from damaged or non-functional mobile phones. The mobile scrap showed rapid Au leaching, while the PCB leaching was much slower. After only 2 h 98 % of Au was leached from the mobile scrap, while 10 h were required to leach 90 % of the Au from the PCBs. This highlights the exceptional uncertainty of PCB composition.

In a study conducted by Ha et al. [5] one of the aims were to determine the effect that increased temperatures have on the leaching of Au from mobile phone PCBs. These PCBs (average Au content of 440 g/t) were leached in a solution comprised of 0.01 M CuSO_4 , 0.06 M $\text{Na}_2\text{S}_2\text{O}_3$, 0.2 M NH_4Cl and 0.26 M NH_3 for 10 min at 400 rpm. High purity N_2 was also sparged into the solution at 10 mL/min. The results show that the Au recovery increased when the temperature was increased from 20 to 40°C. The initial Au recovery rate was the highest at a temperature of 50°C, but the rate decreased drastically after 1 min.

Ha et al. [5] explained that the significant effect of temperature was due to the Au leaching reaction being chemically controlled, as an activation energy of 78.6 kJ/mol was acquired and since reactions that are diffusion controlled typically obtain activation energies smaller than 25 kJ/mol [54]. The particularly low reagent concentrations and addition of N_2 significantly shortened the residence time required to leach Au from the mobile PCBs. N_2 bubbling has been reported to reduce the consumption of $\text{S}_2\text{O}_3^{2-}$ and provide better overall Au leaching, while O_2 bubbling results in higher $\text{S}_2\text{O}_3^{2-}$ consumption and leaching passivation [85].

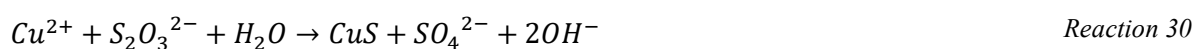
One of the objectives of a study conducted by Petter et al. [7] was to investigate the extraction of Au and Ag, from the PCBs of mobile phones, with different $\text{S}_2\text{O}_3^{2-}$ solutions. Separate tests were conducted on whole PCBs with $\text{Na}_2\text{S}_2\text{O}_3$ and $(\text{NH}_4)_2\text{S}_2\text{O}_3$ in combination with NH_4OH . In each set of tests either CuSO_4 or H_2O_2 were used as catalysts. The test constants were $\text{S}_2\text{O}_3^{2-}$ concentration (0.1 M), NH_4OH concentration (0.2 M), temperature (25°C), residence time (4 h), solid to liquid ratio (1/20) and pH range (9 and 11.5). In each set of tests the CuSO_4 and H_2O_2 concentrations were varied between 0.015 and 0.05 M; and 0.01 and 0.1 M respectively.

The results indicated that low amounts of Au and Ag were extracted, which is expected due to no prior PCB size reduction or base metal pre-leach. The best Au extraction (11 %) was achieved with $\text{Na}_2\text{S}_2\text{O}_3$ and the addition of 0.1 M H_2O_2 , while 9 % of Au was extracted with $(\text{NH}_4)_2\text{S}_2\text{O}_3$ and 0.05 M H_2O_2 . The addition of 0.05 M CuSO_4 resulted in similar Au extraction (± 8 %) for both $\text{S}_2\text{O}_3^{2-}$ types. The best Ag extraction (21 %) was achieved with $\text{Na}_2\text{S}_2\text{O}_3$ and 0.03 M CuSO_4 . H_2O_2 was not efficient for the recovery of Ag.

Abbruzzese et al. [8] investigated the ammoniacal thiosulphate leaching of Au bearing ore in the presence of CuSO₄. They investigated the influence of S₂O₃²⁻ concentration, Cu(II) concentration, NH₃ concentration and temperature for a residence time of 3h. They found that the Au recovery increased when the S₂O₃²⁻ concentration was increased from 0.125 M to 2 M, in a 4 M NH₃ and 0.1 M Cu(II) leach solution. The Cu(II) concentration was varied from 0.03 M to 0.1 M with 2 M thiosulphate and 4 M NH₃. The initial Au extraction is enhanced with increased Cu(II) concentrations, but the resultant Au extraction after 2 h was not influenced significantly. At 0.1 M Cu(II) the Au extraction increased slowly after 1 h up to 80 %.

It was determined that the Au recovery increased when the NH₃ concentration was increased from 1 M to 4 M, in a 2 M S₂O₃²⁻ and 0.1 M Cu(II) solution. NH₃ concentrations above 4 M resulted in a drastic decrease of Au leaching. When the NH₃ concentration is increased the pH becomes higher until the stability regions for Cu(NH₃)₄²⁺ and Cu(S₂O₃)₃⁵⁻ become smaller, while the stability regions for solid Cu species (CuO, Cu₂O) become larger.

In the experiments to determine the effect of temperature Abbruzzese et al. [8] used a 2 M thiosulphate, 4 M ammonium and 0.1 M copper sulphate leaching solution. The results indicated that a rise in temperature from 25 to 60°C decreased the Au extraction. This is believed to be due to the passivation of the Au surface as a result of CuS film formation, which is very fast at 60°C.



Molleman & Dreisinger [75] studied the application of (NH₄)₂S₂O₃ for the recovery of Au from Cu-Au ores. They suggest that the system should be operated at low S₂O₃²⁻ concentrations ranging from 0.1 to 0.2 M to decrease S₂O₃²⁻ consumption; at S₂O₃/NH₃ ratios between 0.5 and 1 to provide sufficient stability for Cu(NH₃)₄²⁺ while still providing an adequate rate of Au leaching; temperatures ranging from 25 to 50°C; pH levels between 9 and 11 and low Cu(II) concentrations to prevent accelerated S₂O₃²⁻ degradation. Significantly higher Cu(II) concentrations also inhibit Au leaching due to a deficiency of lixiviant for Au complexing. This deficiency is caused due to the combination of Cu(II) with the majority of the NH₃ and S₂O₃²⁻ present in solution. According to Kozin & Melekhin [86] a thiosulphate leaching solution is usually comprised of 0.1 – 0.2 M (NH₄)₂S₂O₃, and 0.05 – 0.1 M CuSO₄ or Na₂S₂O₃ and CuSO₄. They believe the pH of the system should be between 9.2 and 10.

The effect of varying the level of copper impurities present in the precious metal feed has not been investigated as a factor.

2.6.2. Summary

A summary of the conditions implemented in a few previous studies on thiosulphate leaching is given in Table 10. The effect that these parameters have on Au leaching is given in Table 11. The optimum conditions and resultant recoveries are given in Table 12 on the next page.

Table 10: Summary of conditions implemented for precious metal leaching by various authors

Author	S ₂ O ₃ ²⁻ [M]	Cu(II) [M]	NH ₃ [M]	Temperature [°C]	pH	Pulp Density [g/L]	Agitation Rate [rpm]	Residence Time [h]
[8]	0.125 - 2	0.03 - 0.1	1 - 4	25 - 60	8.5 - 10.5	400	400	3
[6]	0.2	0.02	0.4	40	10	5	150	48
[4]	0.06 - 0.2	0.005 - 0.03	0.1 - 0.4	25	10 - 10.5	66.67	200	2 - 10
[3]	0.5	0.2	1	40	9	88.89	500	48
[2]	0.05 - 0.25	0 - 0.048		25	8 - 11	10 - 60	250	8
[7]	0.1	0.015 - 0.05	0.2	25	9 - 11.5	50		4
[9]	0.07 - 0.19	0.02	0.1 - 0.2	20	10	50	180	2

Table 11: Effect of most prominent parameters on Au leaching

Test Parameters	Effect on precious metal recovery
Particle Size	Lower particle sizes increase precious metal recoveries.
Residence Time	Longer residence times generally increase precious metal recoveries until equilibrium has been established.
Copper Content	Lower base metal content in the feed has been known to increase precious metal recoveries. This has not been investigated as a factor however.
Thiosulphate Concentration	Higher thiosulphate concentrations lead to increased precious metal recoveries up to a point, after which it decreases precious metal recovery.
Ammonia Concentration	Increasing the ammonia concentration produces similar results to an increase in thiosulphate concentration.
Copper(II) Ion Concentration	Higher copper(II) ion concentrations lead to increased precious metal recoveries up to a point, after which it has no further effect. Too high concentrations may contaminate the metallic product, which complicates downstream processes like electrowinning and devaluates the product [47].
Temperature	Increased temperatures result in increased precious metal recoveries up to a point, beyond which it becomes difficult to maintain ammonium hydroxide in the leach solution. This leads to the passivation of gold particles that will decrease gold recovery.
Pulp Density	Lower pulp densities increase precious metal recoveries.
Agitation Rate	The agitation rate must be fast enough to ensure sufficient mixing. Solids must be kept in suspension to ensure effective leaching.
pH	The pH must be between 8 and 10.5 to produce acceptable precious metal recoveries. Higher and lower pH values will result in decreased Au and Ag recoveries. The pH changes with time as reactions take place making it a nuisance variable.

Table 12: Optimum conditions implemented in previous studies on precious metal leaching

Author	S ₂ O ₃ ²⁻ [M]	Cu(II) [M]	NH ₃ [M]	T [°C]	pH	Pulp Density [g/L]	Agitation Rate [rpm]	Residence Time [h]	Optimum Recovery [%]	
									Au	Ag
[8]	2	0.1	4	25	8.5 - 10.5	400	400	3	80	
[6]	0.2	0.02	0.4	40	10	5	150	48	95	100
[4]	0.12	0.02	0.2	25	10 - 10.5	66.67	200	6	98	
[3]	0.5	0.2	1	40	9	88.89	500	48	98	
[2]	0.1	0.04		25	10 - 10.5	10	250	8	56.7	
[7]	0.1	0.05	0.2	25	9 - 11.5	50		4	11	21
[9]	0.13	0.02		20	10	50	180	2	70	

3. Experimental Method

3.1. Size Reduction

Various studies have proven the importance of the particle size reduction step in the hydrometallurgical process for the recycling of waste PCBs. Computer PCBs were the selected feed for this study. The size reduction stage consisted of several steps which are illustrated in Figure 10.

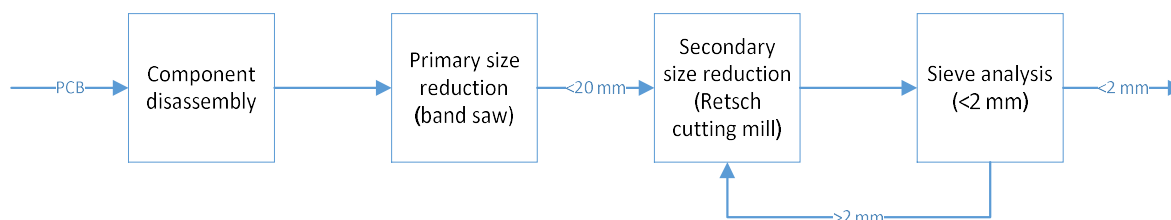


Figure 10: Schematic representation of the size reduction procedure

The PCBs were partially disassembled to remove certain large components, such as heat sinks, that could prove harmful to the equipment in subsequent size reduction steps. Smaller components such as capacitors, batteries and piezo buzzers, that consisted primarily of base metals and other unwanted materials, were also removed as the focus of this study was the recovery of precious metals. Batteries should be removed to prevent firing and explosion during size reduction [87]. The PCBs were then introduced to a band saw to produce square pieces of approximately 20 x 20 mm each. Minor feed losses were encountered due to the formation of PCB dust, originating from the cutting process.

These pieces were then gradually fed into a Retsch cutting mill to produce material with all particles passing 2 mm. Progressively smaller mill sieves were used to reduce the particle size from 20 mm to 10 mm, 8 mm, 4 mm and eventually 2 mm. In between each size step a sieve analysis was conducted to separate pieces that required further milling from those already smaller than 2 mm. Similar to the primary size reduction step, some feed losses were encountered due to the formation of PCB dust. Not all of the dust could be collected. In order to obtain representative samples from the crushed PCBs a rotating sample splitter was used. A total of 4 kg of computer PCBs were processed in the size reduction step.

3.2. PCB Characterisation

The exact composition of PCBs is known to be inconsistent as the metal composition varies considerably from one circuit board to the next. This fact is illustrated in Table 3 as previously mentioned. The non-homogeneous distribution of metals inside the PCBs also make it difficult to quantify the composition of samples that have been through size reduction. One of the methods commonly used to determine the composition of PCBs is aqua regia digestion, followed by elemental analysis of the liquor using ICP-AES or similar analytical techniques.

Aqua regia is a solution comprised of HNO_3 and HCl in a molar ratio of 1:3. Aqua regia digestions were carried out on several samples that were taken at the following time instances:

- After the size reduction of the PCBs to determine the initial metal content and required residence time for Aqua Regia digestions (20 g samples)
- After the base metal leaching stage to assist with mass balances (entire test residues)
- After the precious metal leaching stage to complete mass balances (entire test residues)

Each sample was digested in a 1 L vessel at a temperature of 55°C and a pulp density of 100 g/L. The results from aqua regia digestions were used as an indication of the amount of metals present in the computer PCBs.

3.3. Base Metal Leaching

3.3.1. Experimental Strategy

The recovery of base metals was handled in a two-step leaching process that is illustrated in Figure 11. The first step utilized HNO_3 to extract most of the Pb and Fe from the crushed PCBs, while the second step utilized H_2SO_4 and H_2O_2 to extract most of the Cu and Zn from the PCB residue produced by the HNO_3 leaching step. After each step the solids and liquids were separated through filtration.

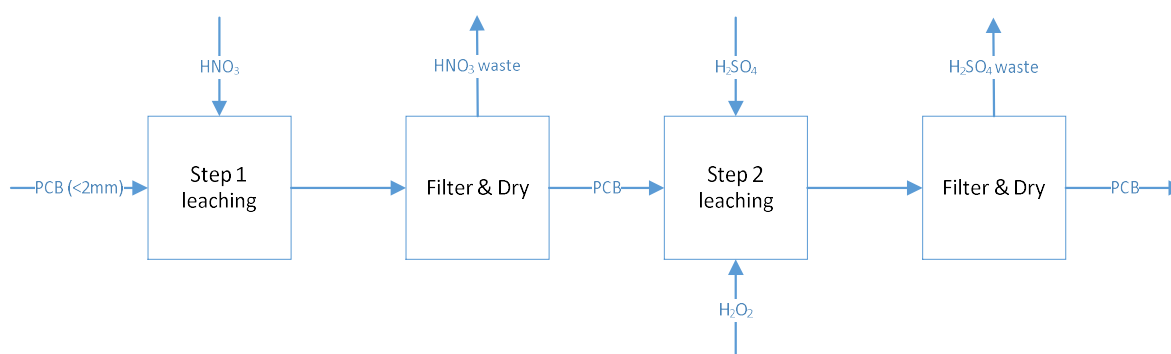


Figure 11: Schematic representation of the base metal leaching procedure

A few experiments were initially conducted on a small scale to test the claims of [63], namely that mostly Pb is leached in step 1, while mostly Cu is leached in step 2. In the small-scale tests, 800 mL lixiviant was used in the first step and 500 mL lixiviant was used in the second step. During these experiments, samples were taken periodically to determine at which point the desired amount of Cu was left on the PCBs. The samples were also used to illustrate the behaviour of gold and silver during the base metal leaching stage. The experimental parameters of each step are illustrated in Table 13. It is important to note that the H_2O_2 flow rate is for a 500 mL solution.

Table 13: Initial experimental parameters of the small-scale base metal leaching stage

Step	HNO ₃ [M]	H ₂ SO ₄ [M]	H ₂ O ₂ (30 wt%) [mL/min]	T [°C]	Pulp Density [g/L]	Agitation Rate [rpm]	Residence Time [h]
1	1	-	-	25	100	600	8
2	-	2.5	1.2	25	160	600	8

The results from the tests were used to determine the residence time required to produce two batches of PCBs. One with lower Cu content and the other with higher Cu content. These batches were used in the precious metal leaching stage to test the effect of Cu content in the PCBs on three dependent factors, namely the dissolution of Au and Ag and the degradation of S₂O₃.

After the initial experiments the HNO₃ leaching step was completed on a larger scale, as this form of leaching does not require cooling. For each large scale experiment a 20 L HNO₃ solution was prepared. The agitation rate was adjusted to ensure that all particles were kept in suspension. These experiments were not heated externally, so the residence time was increased until Pb extraction similar to the first step in the small-scale experiments was achieved. This was checked through atomic absorption spectroscopy (AAS) during the tests. Once all the PCBs had been treated with HNO₃, the residue was split into representative samples for the next step. The H₂SO₄ leaching step was completed using the same smaller scale equipment that was used in the initial experiments. The equipment is illustrated in section 3.3.2. The rotating sample splitter was also used for the residue from this step to prepare the samples for the precious metal leaching step.

3.3.2. Equipment

Two different setups were used in the base metal leaching stage, as mentioned before. Figure 12 illustrates the equipment that was implemented for small-scale leaching experiments, which required the control and regulation of temperature and agitation speed through a hotplate and overhead stirrer respectively.

This setup consisted of a 1.7 L jacketed glass reaction vessel that was secured to a metal stand to provide stability. Cooling water at a temperature of about 18°C was fed through the jackets that surrounded the reaction vessel to provide the necessary cooling for exothermic reactions. The reaction vessel was covered with a glass lid that could also be secured to the metal stand. Fittings were created on the lid for a condenser, temperature probe, pH probe, impeller and sampling port. The condenser was used to recycle any escaping gasses produced by the leaching processes and to provide access for the peristaltic pump line for H₂O₂ dosing. Efficient agitation was provided with an overhead stirrer, Teflon impeller and set of Teflon baffles that were introduced into the reaction vessel. The Teflon baffles decreased the amount of energy required from the overhead stirrer for efficient mixing, by limiting the swirling effect produced by normal agitation processes. Teflon impellers and baffles were used to ensure that the components do not degrade due to prolonged exposure to lixiviants. The temperature probe was

connected to a hotplate which provided the desired temperature control. The pH probe shown in Figure 12 was excluded in the base metal leaching stage.

The large scale HNO_3 leaching experiments were conducted in a 40 L chemically resistant barrel with a lid. The lid had apertures for an impeller and sampling. The agitation was provided by an overhead stirrer and unique Teflon impeller, as illustrated in Figure 13.

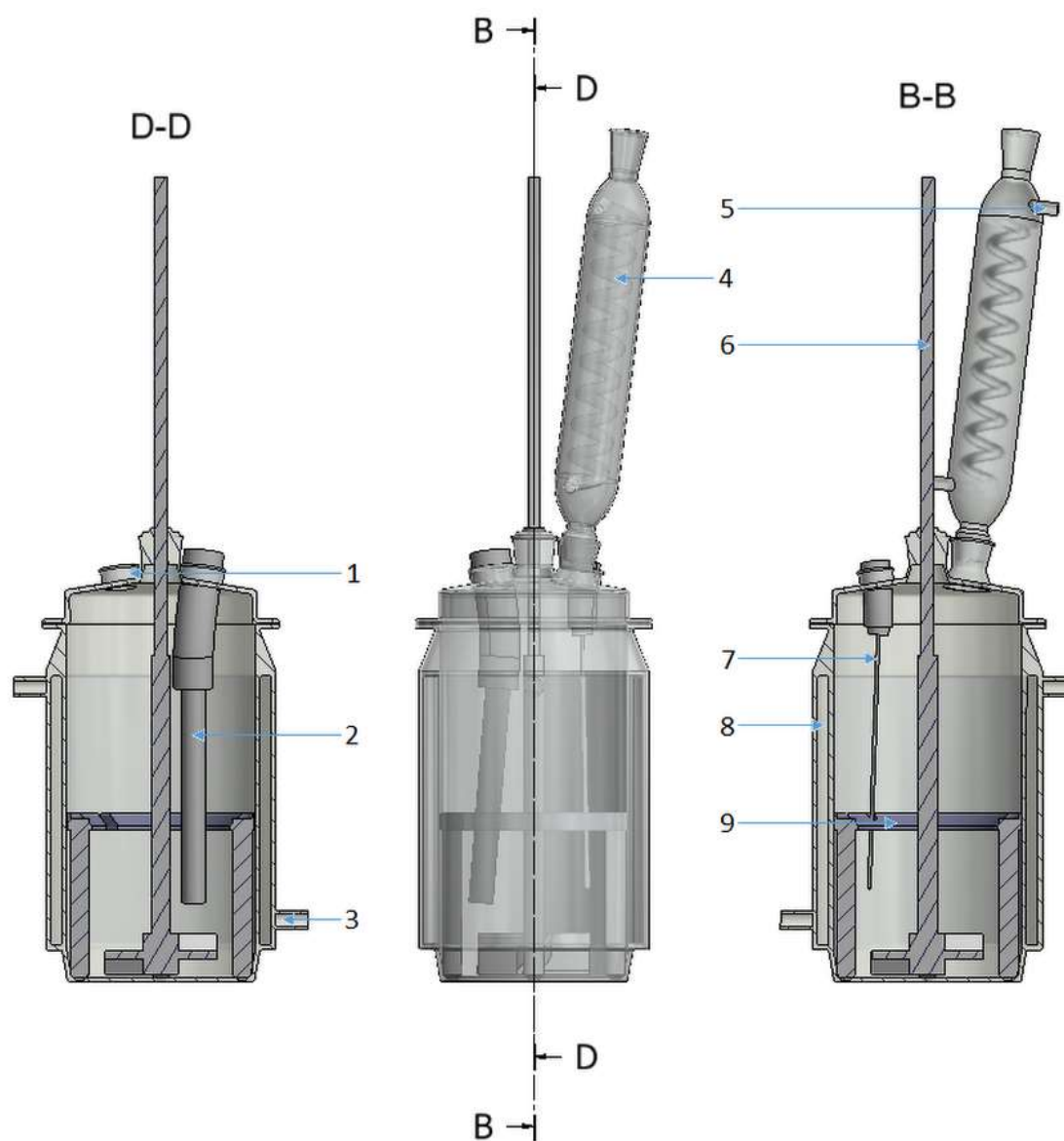


Figure 12: Small-scale leaching equipment for base metal leaching stage

Table 14: Figure 12 component designations

Number	Description
1	Sampling port
2	pH probe encased in glass
3	Vessel jacket inlet for cooling water
4	Condenser
5	Condenser outlet for cooling water
6	Teflon impeller
7	Temperature probe
8	Vessel jacket for cooling water
9	Teflon baffles

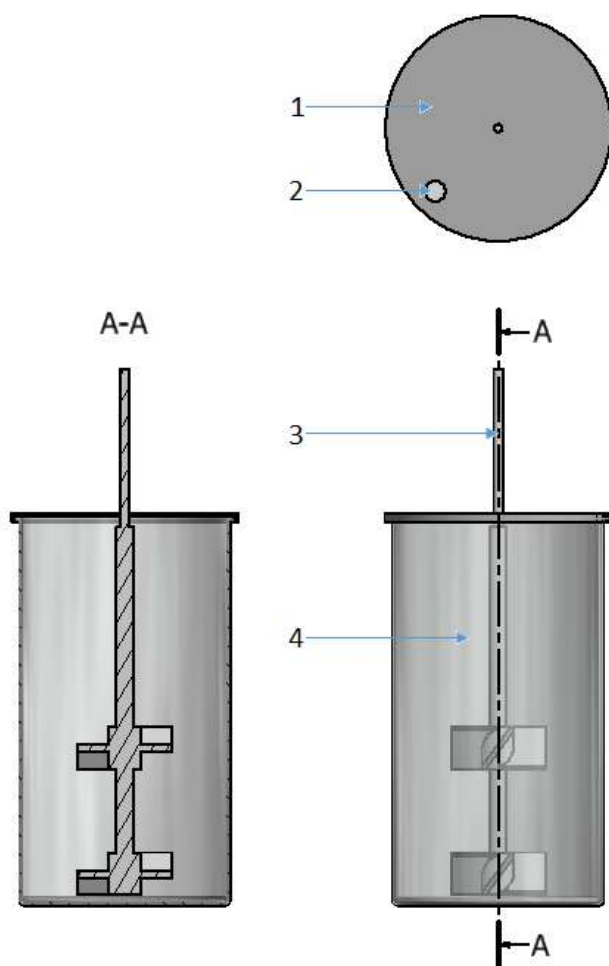


Figure 13: Large-scale leaching equipment for base metal leaching stage

Table 15: Figure 13 component designations

Number	Description
1	Vessel lid
2	Sampling port
3	Double bladed Teflon impeller
4	40 L vessel

3.3.3. Materials

The chemicals that were used for the preparation of the lixivants in the base metal leaching steps are listed in Table 16. The concentrated acids were diluted to the desired lixiviant concentrations in demineralised water. The required quantities for the preparation of lixivants at the different test settings are shown in Table 17. At a residence time 8h, 576 mL H₂O₂ is required.

Table 16: Base metal leaching – Chemical stock information

Substance	Purity [wt%]	Purity [M]	Molar Mass [g/mol]	Density [g/L]
H ₂ SO ₄	98	18.385	98.079	1840
H ₂ O ₂	30	9.701	34.015	1100
HNO ₃	55	11.690	63.010	1339

Table 17: Base metal leaching – Required chemical quantities for leaching steps

Small Scale Leaching (500 mL)			
Step	Substance	Concentration [M]	Stock Addition [mL]
1	HNO ₃	1	42.77
2	H ₂ SO ₄	2.5	67.99
Large Scale Leaching (20 L)			
Step	Substance	Concentration [M]	Stock Addition [mL]
1	HNO ₃	1	1710.8

3.3.4. Procedure

3.3.4.1. General preparation

To successfully complete each test, the following pieces of additional lab equipment were used:

- Sample bottles for liquid samples (15 mL)
- Buchner flask & funnel
- Filter paper ($\phi = 12.5$ cm) for small scale test filtration
- Syringes (10 mL) and syringe filters (0.22 μ m)

3.3.4.2. Start-up

Small scale experiments

The first step was to secure the jacketed vessel to the metal stand by inserting it into a ring attached to the structure. The height of this ring could be adjusted. The hot plate was placed below the vessel, which was then lowered onto the hot plate. Now the Teflon baffles and impeller were inserted into the vessel and the water cooling pipes were connected to the jackets and condensers. The lixiviant was then prepared and added to the vessel. For the H_2SO_4 leaching tests, H_2O_2 was added to a separate container which was connected to a peristaltic pump. The impeller shaft was pushed through the aperture in the vessel lid, before the lid was secured on the vessel through bolts and screws located on the sides of the ring.

Once the vessel lid was in place, the impeller was attached to the overhead stirrer which was secured to the metal stand. The gap between the impeller and the bottom of the vessel was never more than 2 cm. The temperature probe was inserted through the lid and connected to the hot plate. The condenser was then connected to the lid and the cooling water was switched on for both the condenser and vessel jacket. The peristaltic pump pipe was fed through the condenser into the vessel.

Finally, the hot plate, peristaltic pump and overhead stirrer were switched on and the temperature was set to the desired value. The agitation speed was set to a low speed setting to assist with the heating procedure of the lixiviant. Once the set temperature was reached, the required amount of crushed PCBs were fed into the vessel through the sampling port. The sampling port was then closed with a stopper and the agitation- and peristaltic pump speed were set to the desired values.

Large Scale Experiments

The large-scale experiment start-up began with the preparation of the required lixiviant in the 40 L barrel. This was done by firstly filling the barrel with 5 L of demineralised water. The Teflon impeller was pushed through the aperture in the barrel lid and the lid was placed on the barrel. The impeller was then connected to the overhead stirrer and the required amount of concentrated acid was added to the barrel through the sampling port. The solution was topped up to 20 L with demineralised water. At this point the overhead stirrer was switched on and the agitation rate was set to a low value to achieve proper mixing of the lixiviant. After about 10 min, the required amount of PCBs was fed into the barrel through the sample port and the agitation rate was set to a value that provides particle suspension. The sampling port was closed with a stopper.

3.3.4.3. Sampling method

Small scale experiments

At 15, 30, 45, 90, 180, 240, 300, 360, 420 and 480 minutes 5 mL samples were taken through the sampling port with a syringe. The stirring rate was decreased for sampling if excessive splashing was present. The samples were filtered through 0.22 µm syringe filters to ensure clear liquid samples.

Large Scale Experiments

Samples were taken at 1 h intervals after 4h of leaching, until the required amount of Pb was leached. The samples were also filtered through 0.22 µm syringe filters, before being sent for analysis.

3.3.4.4. Shutdown

Small Scale Experiments

At the end of each test the peristaltic pump, hot plate, overhead stirrer and cooling water to the condenser were switched off. The cooling water to the vessel was kept on to allow the vessel contents to cool down if necessary, before being switched off. Now every connection to the vessel lid was disconnected and the impeller was unscrewed from the overhead stirrer. The lid, impeller and baffles were subsequently removed. The vessel was then weighed and the contents were filtered using a Buchner funnel, filter paper and vacuum pump to separate the solid and liquid phases. The solid residue was dried at room temperature and weighed, whereas the volume of the liquid phase was determined before being disposed of in an allocated waste container. Each piece of equipment was cleaned after the necessary tasks were completed.

Large-Scale Experiments

Once the test was completed, the overhead stirrer was switched off and the impeller was disconnected from the stirrer. The barrel lid and impeller were then removed and the vessel was weighed. The bulk of the liquid phase was removed before continuing with filtration. The remaining solids and liquids were separated using a Buchner funnel, filter paper and vacuum pump. The solid residue was dried in an oven at 60°C and weighed once completely dried. The separated liquid phase was added to the rest of the liquid that was previously removed and the total volume was measured. The entire liquid phase was then disposed of in an allocated waste container, after which all equipment was cleaned.

3.4. Precious Metal Leaching

3.4.1. Experimental Strategy

Table 18: Parameters selected for investigation

Factors	Parameter
Variable	Copper Content
	Thiosulphate Concentration
	Ammonia Concentration
	Copper(II) Ion Concentration
	Temperature
	pH
	Pulp Density
Fixed	Agitation Rate
	Particle Size
	Residence Time

One of the objectives of this study was to determine the significance of interactions that exist between the Cu content in the solid feed and other test parameters of interest. The effects that the most prominent test parameters (main effects) have on precious metal recovery are given in Table 11. According to literature the parameters that affect the system most significantly are thiosulphate concentration, ammonia concentration, cupric ion concentration, temperature and pH. No optimum agitation rate to pulp density relation has been identified. Literature also suggests that gold leaching is chemically controlled, which means the agitation rate should not have a prominent effect on gold leaching. It only needs to be fast enough that the mass transfer through the boundary layer does not become rate limiting. Agitation rate was therefore included as a fixed nuisance parameter. Pulp density on the other hand was included as a variable factor, as lower values are known to result in increased precious metal leaching due to the increased amount of reagent per unit weight of PCBs. Residence time and particle size distribution were constants and were not included in the experimental design.

To determine the most significant main effects, an initial screening design was implemented to evaluate the seven factors at two levels. This was a resolution IV screening design that consisted of 16 runs [2^{7-3}_{IV}]. In this design, no main effects were confounded with any 2-factor interactions. The main effects were confounded with 3-factor interactions and higher. One replicate of each run was done to assess repeatability, which meant that the screening design amounted to 32 runs. The screening design is illustrated in Table 19, with the test parameter settings given in Table 20.

Table 19: Precious metal leaching screening design

Test Run Number	Replicate	A	B	C	D	E	F	G
1	1	-1	-1	-1	-1	-1	-1	-1
2	1	1	-1	-1	-1	1	-1	1
3	1	-1	1	-1	-1	1	1	-1
4	1	1	1	-1	-1	-1	1	1
5	1	-1	-1	1	-1	1	1	1
6	1	1	-1	1	-1	-1	1	-1
7	1	-1	1	1	-1	-1	-1	1
8	1	1	1	1	-1	1	-1	-1
9	1	-1	-1	-1	1	-1	1	1
10	1	1	-1	-1	1	1	1	-1
11	1	-1	1	-1	1	1	-1	1
12	1	1	1	-1	1	-1	-1	-1
13	1	-1	-1	1	1	1	-1	-1
14	1	1	-1	1	1	-1	-1	1
15	1	-1	1	1	1	-1	1	-1
16	1	1	1	1	1	1	1	1
17	2	-1	-1	-1	-1	-1	-1	-1
18	2	1	-1	-1	-1	1	-1	1
19	2	-1	1	-1	-1	1	1	-1
20	2	1	1	-1	-1	-1	1	1
21	2	-1	-1	1	-1	1	1	1
22	2	1	-1	1	-1	-1	1	-1
23	2	-1	1	1	-1	-1	-1	1
24	2	1	1	1	-1	1	-1	-1
25	2	-1	-1	-1	1	-1	1	1
26	2	1	-1	-1	1	1	1	-1
27	2	-1	1	-1	1	1	-1	1
28	2	1	1	-1	1	-1	-1	-1
29	2	-1	-1	1	1	1	-1	-1
30	2	1	-1	1	1	-1	-1	1
31	2	-1	1	1	1	-1	1	-1
32	2	1	1	1	1	1	1	1

Table 20: Precious metal leaching parameter settings

Setting	A	B	C	D	E	F	G
	Copper Content [%]	S ₂ O ₃ ²⁻ [M]	Cu(II) [M]	NH ₃ [M]	Temperature [°C]	pH	Pulp Density [g/L]
High (+1)	11 - 20	0.2	0.1	0.4	40	10-10.5	50
Low (-1)	1 - 10	0.1	0.02	0.2	25	9-9.5	25

The particle size and residence time used for each test were 2 mm and 8 h respectively. The agitation rate was set to 500 rpm. Once the most significant main effects were identified, a full factorial design was considered. The full factorial phase had the goal to determine the effect that these significant parameters have on Au extraction. A final experimental phase was planned to attempt to improve the optimum Au extraction obtained during the full factorial phase. During this optimization phase the effect that a change in certain parameters had on thiosulphate degradation/consumption were also investigated.

3.4.2. Equipment

The precious metal leaching stage implemented the same setup that is illustrated in Figure 12. The only difference from the base metal leaching stage was that the peristaltic pump and pump line were excluded.

3.4.3. Materials

In each individual precious metal leaching test 12.5 g or 25 g of PCB residue was recovered from the base metal leaching tests and leached with 500 mL of lixiviant. The dry chemicals, $(\text{NH}_4)_2\text{S}_2\text{O}_3$ and $\text{CuSO}_4 \cdot 5\text{H}_2\text{O}$, were dissolved in demineralised water and mixed with NH_4OH to prepare the required lixiviant. Table 21 contains the chemical information and Table 22 shows the required quantities for the preparation of a 500 mL lixiviant at the different test settings.

Table 21: Precious metal leaching – Chemical information

Dry Chemicals				
Substance	Purity [wt%]	Purity [M]	Molar Mass [g/mol]	Density [g/L]
$(\text{NH}_4)_2\text{S}_2\text{O}_3$	98	-	148.210	1679
$\text{CuSO}_4 \cdot 5\text{H}_2\text{O}$	98	-	250.699	2284
Wet Chemicals				
Substance	Purity [wt%]	Purity [M]	Molar Mass [g/mol]	Density [g/L]
NH_4OH	30	7.704	35.046	900
NaOH	50	18.939	39.997	1515

Table 22: Precious metal leaching – Required chemical quantities per test

Dry Chemicals						
Substance	Low Setting			High Setting		
	Concentration [M]	Chemical Addition [g]		Concentration [M]	Chemical Addition [g]	
$\text{S}_2\text{O}_3^{2-}$	0.1	$(\text{NH}_4)_2\text{S}_2\text{O}_3$	7.411	0.2	$(\text{NH}_4)_2\text{S}_2\text{O}_3$	14.821
Cu(II)	0.02	$\text{CuSO}_4 \cdot 5\text{H}_2\text{O}$	2.507	0.1	$\text{CuSO}_4 \cdot 5\text{H}_2\text{O}$	12.535
Wet Chemicals						
Substance	Low Setting			High Setting		
	Concentration [M]	Chemical Addition [mL]		Concentration [M]	Chemical Addition [mL]	
NH_3	0.2	NH_4OH	6.308	0.4	NH_4OH	12.616

3.4.4. Procedure

3.4.4.1. General preparation

To successfully complete each test, the following pieces of additional lab equipment were used:

- Sample bottles for liquid samples (15 mL)
- Buchner flask & funnel
- Filter paper ($\phi = 12.5$ cm)
- Syringes (10 mL) and syringe filters (0.22 μm)

The required amounts of $(\text{NH}_4)_2\text{S}_2\text{O}_3$, $\text{CuSO}_4 \cdot 5\text{H}_2\text{O}$ and NH_4OH were prepared before the start of each test. Information on the required chemicals for low and high setting tests are provided in Table 22. Enough H_2SO_4 and NaOH were kept at hand to adjust and control the pH of the lixiviant.

3.4.4.2. Start-up

The start-up procedure was similar to what was explained in section 3.3.4.2 for the small-scale experiments, as a similar setup was used for these tests. To prevent confusion, the complete start-up procedure will be mentioned again while incorporating the differences.

The first step was to secure the jacketed vessel to the metal stand by inserting it into an adjustable ring attached to the structure. The hot plate was placed below the vessel, which was then lowered unto the hot plate. Now the Teflon baffles and impeller were inserted into the vessel and the water cooling pipes were connected to the jackets and condensers. The lixiviant was prepared and added to the vessel, after which the impeller shaft was pushed through the aperture in the vessel lid, before the lid was secured on the vessel through bolts and screws located on the sides of the ring.

Once the vessel lid was in place, the impeller was attached to the overhead stirrer which is secured to the metal stand. The temperature and pH probes were then inserted through the lid in their respective apertures and connected to the corresponding devices (hot plate and pH monitor). The condenser was connected to the lid and the cooling water was switched on for both the condenser and vessel jacket.

Finally, the hot plate, pH monitor and overhead stirrer were switched on and the temperature was set to the desired value. The agitation speed was set to a low speed setting to assist with the heating procedure of the lixiviant. Once the set temperature was reached, the pH was adjusted to the desired value and the required amount of PCB residue was fed into the vessel through the sampling port. The sampling port was then closed with a stopper and the agitation speed was set to the desired value.

3.4.4.3. Sampling method

Samples were taken periodically during the screening tests and full factorial tests. For the screening tests, 4 mL samples were taken at 15, 30, 45, 90, 180, 240, 300, 360, 420 and 480 minutes. For the repeat tests of the screening phase and full factorial tests, 4 mL samples were taken at 120, 240, 360 and 480 minutes. As with the base metal leaching tests, the agitation rate was briefly switched off for sampling. Every sample was filtered through a 0.22 µm syringe filter to ensure clear liquid samples. 2 mL were separated from the 120, 240, 360 and 480 minute samples for thiosulphate degradation analysis with high pressure liquid chromatography (HPLC)

3.4.4.4. Shutdown

The shutdown procedure was similar to what was explained in section 3.3.4.4 for the small-scale experiments.

3.5. Analysis

The metal analysis of liquid samples was done in the analytical laboratory, which is situated in the Department of Process Engineering at the University of Stellenbosch. The metal content in liquid samples were analyzed through inductively coupled plasma optical emission spectrometry (ICP-OES). The 0.22 µm syringe filters were used during sampling to ensure that no solid particles were present in the liquid samples. The sensitive nature of the ICP machine requires solid free liquid samples. All liquid samples were diluted with 5 wt% HNO₃. The required dilution ratios for the analysis of the base and precious metal leaching stages were 1:100 and 1:40 respectively.

Additional samples were sent for metal analysis to the Department of Geology of the University of Stellenbosch. These samples were analyzed with a more sensitive analysis method, namely inductively coupled plasma mass spectrometry (ICP-MS), in order to verify that ICP-OES provided reliable analysis of Au and Ag.

The thiosulphate degradation was determined by measuring the thiosulphate concentration of samples over time using HPLC. To ensure reliable results, the samples had to be analyzed shortly after each experiment was completed. Further degradation and regeneration takes place with time which affects the accuracy of the results.

4. Results and Discussion

4.1. PCB Characterisation

The goal of this stage was to determine the average metal content of the PCBs by Aqua Regia digestion. Four tests were conducted to determine the residence time required for Aqua Regia to digest virtually all the metals inside PCBs. The amount of metals leached from 20 g PCB samples are shown in Table 35 in Appendix A.

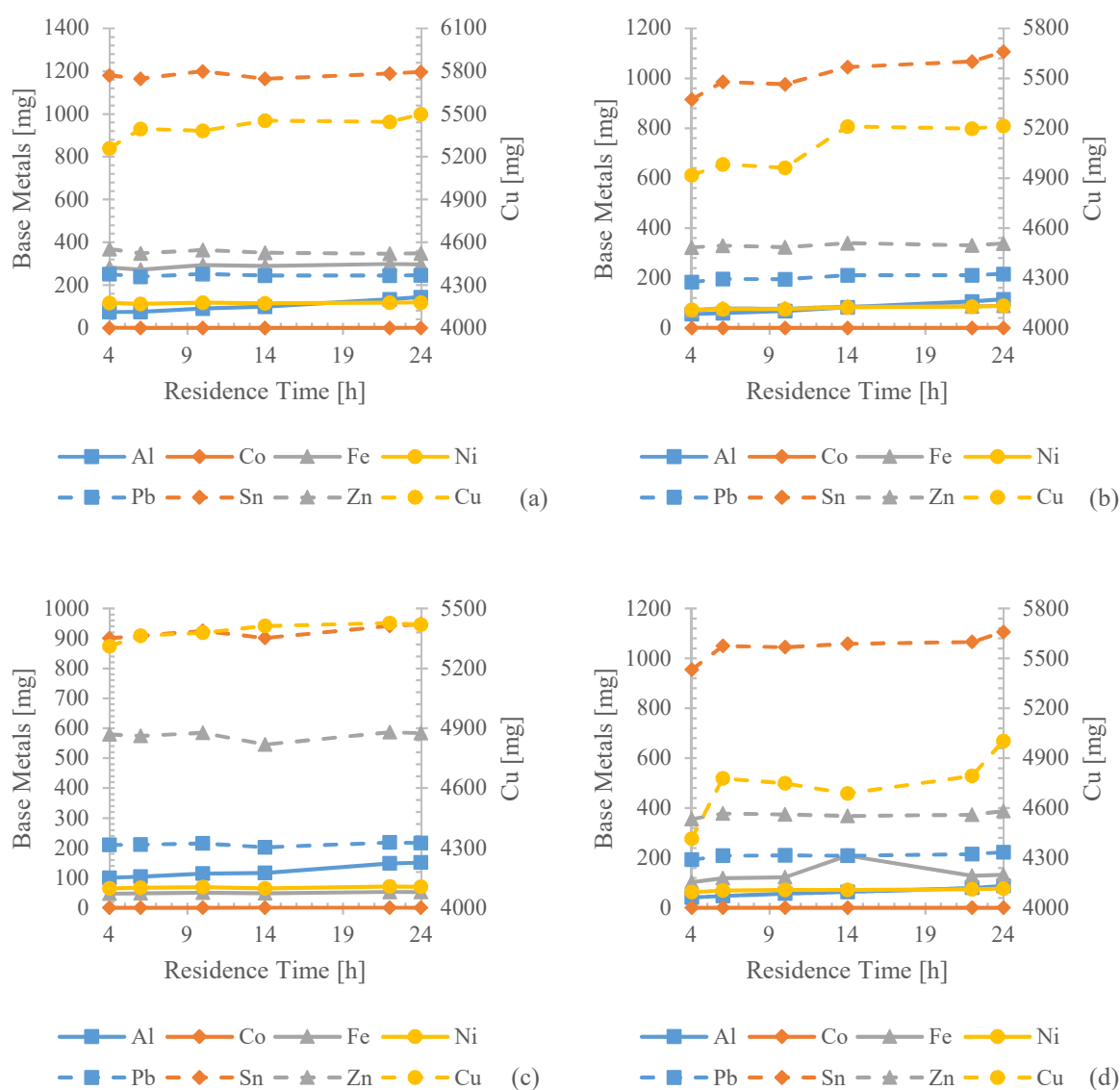


Figure 14: Base metal leaching behaviour as a function of time during Aqua Regia digestion for (a) test 1, (b) test 2, (c) test 3 and (d) test 4

Figure 14 illustrates that most of the base metals are already leached after 4 h of digestion, except for Cu and Sn. Sn leaching reached equilibrium after 4 h in tests 1 and 3, but not tests 2 and 4. Cu leaching

steadily increased from 4 h to 24 h and seemed to reach equilibrium in test 3 after 22 h. The other three tests, however, seem to indicate that Cu is still being leached and longer residence times are required. The precious metal leaching behaviour is illustrated in Figure 15.

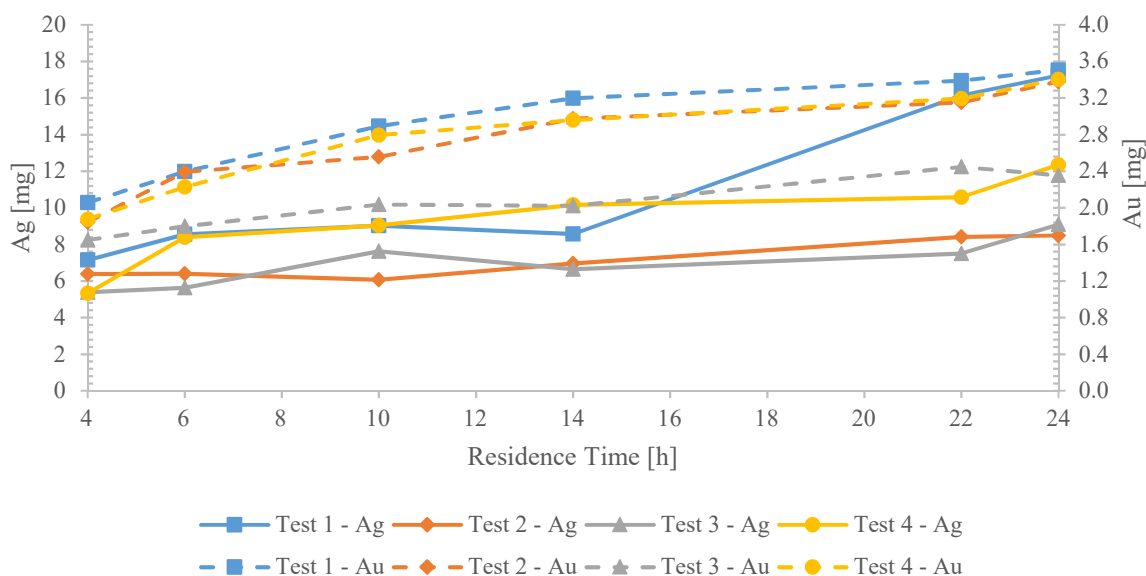


Figure 15: Precious metal leaching behaviour during Aqua Regia residence time tests

Figure 15 seems to indicate that Au leaching is still increasing at 24 h in tests 1, 2 and 4, while test 3 shows that equilibrium has been reached after 22 h. Tests 2, 3 and 4 indicate a slow increase in Ag leaching from 4 h to 24 h, while test 1 shows a large sudden increase in Ag leaching after 14 h. The only test in which Ag leaching seems to reach equilibrium is test 2. These irregularities all point to the heterogeneous nature of PCBs. Each sample of crushed PCBs does not contain the same amount of metals and the metals are not arranged in a similar manner, no matter how much sample splitting is implemented. The sudden increase in Ag leaching is probably due to the acid reaching a level in the PCB particles that contain higher concentrations of Ag, as metals are deposited unto PCBs in various layers during manufacturing. The decision was made to digest any future samples in Aqua Regia for 30 h.

Two additional digestions were conducted to provide more data for the calculation of the average metal content of the PCBs. The data from these tests are also shown in Table 35 in Appendix A. The average metal content found in PCBs from these six tests are given in Table 23 with standard deviations. The values are split into metal content (based only on mass of metals) and PCB metal content (based on mass of entire PCB). The Cu, Au, Ag, Zn and Sn content in these computer PCBs were comparable to what Birloaga et al. [37] found. They found that computer PCBs contained 30.57 % Cu, 0.02 % Au, 0.07 % Ag, 1.86 % Zn and 7.36 % Sn. The Fe, Pb and Al content differed by 14.47 %, 5.46 % and 10.97 % respectively. The large difference in Al could be attributed to the fact that all heat sinks were removed

before PCB size reduction. PCB heat sinks are primarily made from Al alloys. Yang et al. [35] reported comparable values for Cu, Pb and Fe of 25.30 %, 0.14 % and 0.15 %.

Table 23: Average metal content of PCBs

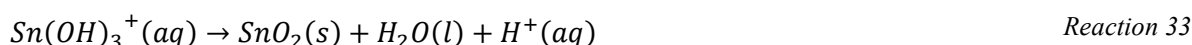
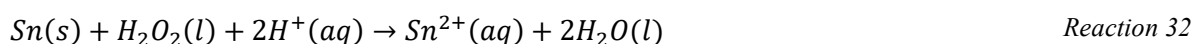
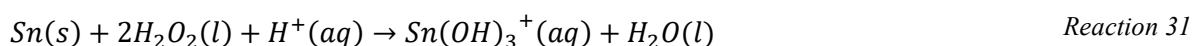
Metal	Ag	Al	Au	Co	Cu	Fe	Ni	Pb	Sn	Zn
Metal	0.17 ±	1.81 ±	0.04 ±	0.01 ±	70.36 ±	1.86 ±	1.13 ±	3.10 ±	16.01 ±	5.51 ±
[%]	0.04	0.37	0.01	0.01	2.93	1.05	0.23	0.13	2.84	1.23
PCB	0.07 ±	0.72 ±	0.02 ±	0.004 ±	28.15 ±	0.74 ±	0.45 ±	1.24 ±	6.40 ±	2.20 ±
[%]	0.02	0.15	0.00	0.000	1.17	0.42	0.09	0.05	1.13	0.49

The irregular leaching behaviour of Ag during the aqua regia digestion tests suggested that aqua regia might be inefficient for the characterisation of Ag. Further research identified that aqua regia digestion of PCBs is accompanied by the formation of an insoluble compound, AgCl [45]. This means that in order to acquire a better indication of the total Ag content of PCBs, an alternative leaching step or a combination of different lixivants are required. Petter et al. [45] used HNO₃ leaching (on un-leached PCB) to determine a reference value for the Ag content in PCBs. The presence of AgCl was only identified after the completion of all experimental work. This means that the Ag content determined during aqua regia digestions from PCB residues were only a rough indication of the remaining Ag after the BML and PML stages.

4.2. Base Metal Leaching

The process pathway suggested by [63] was implemented to determine the extent of base metal leaching during this stage. The average of two replicates is compared to the results of [63] in Figure 16 and Figure 17. The tabulated data can be found in Appendix B, Table 37.

The initial tests showed comparable results to what [63] obtained for total Ag, Au, Cu, Fe, Pb and Zn extraction. The total Al extraction was relatively close to what [63] obtained (33.7 %) and differed only by 4.53 %. A Pourbaix diagram of Al in a H₂SO₄ and H₂O₂ environment suggests that complete dissolution of Al is expected [63]. The total Ni extraction was a bit lower (84.63 %), but still comparable to what Rossouw [63] obtained (91.40 %). The total Sn extraction was slightly higher, but the low recoveries support what [63] found during this stage. Rossouw [63] suggests that Sn possibly oxidizes to Sn(OH)₃⁺ or Sn²⁺ and subsequently precipitates as SnO₂ per Reaction 31 to Reaction 34.



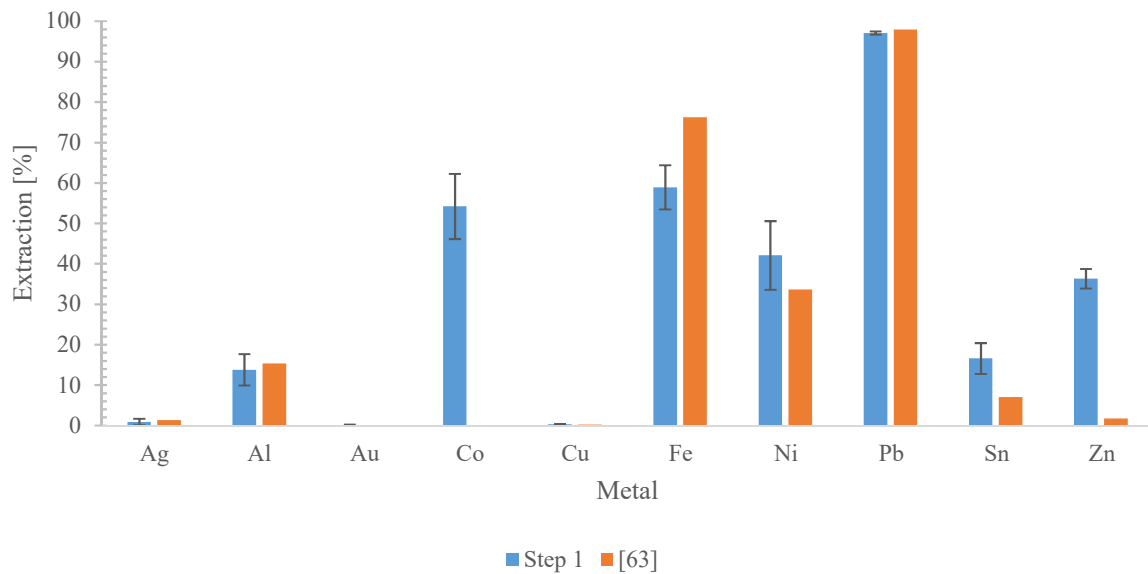


Figure 16: Base metal leaching comparison of step 1

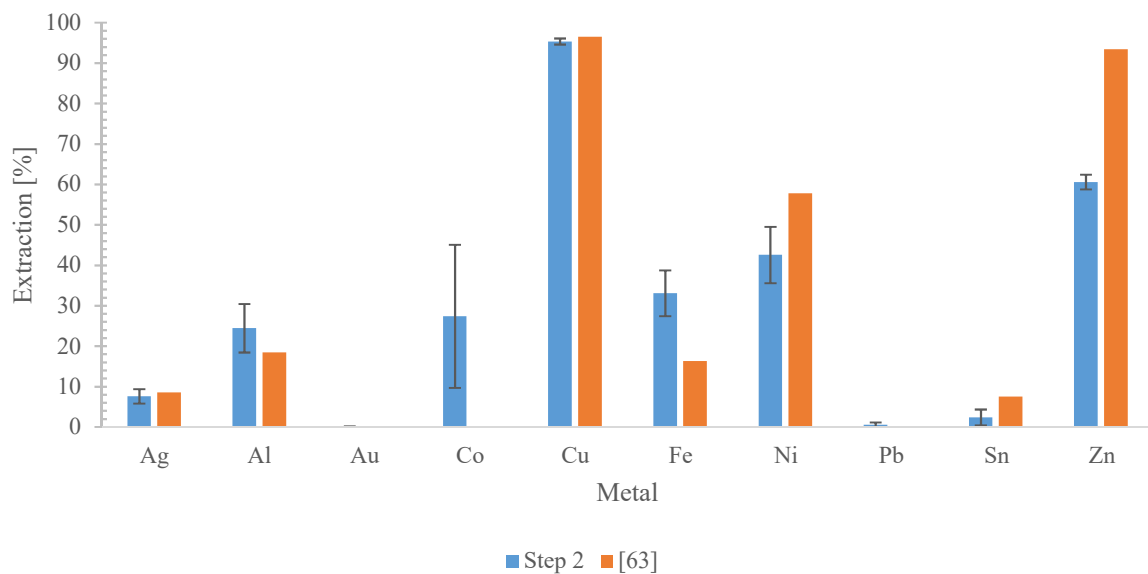


Figure 17: Base metal leaching comparison of step 2

The results of step 1 and 2 indicated good repeatability, which meant that these conditions were suitable for the preparation of feed for the precious metal leaching stage. The first step was implemented on a larger scale to shorten the time required for feed preparation. As mentioned before, samples were taken periodically to measure the Pb content with AAS to determine at which point the experiment needed to be stopped (when sufficient Pb was leached). It was found that a residence time of 600 minutes provided Pb extraction of about 95 % (according to AAS). The residence time was extended by 60 minutes to increase the probability of complete Pb dissolution. The results obtained from ICP-OES are illustrated

in Figure 18. The leaching behaviour observed in Figure 18 compares well with what [63] obtained. The extraction and precipitation of Sn that was previously mentioned can be seen here. The results from the large-scale test are shown in Table 39 in Appendix B.

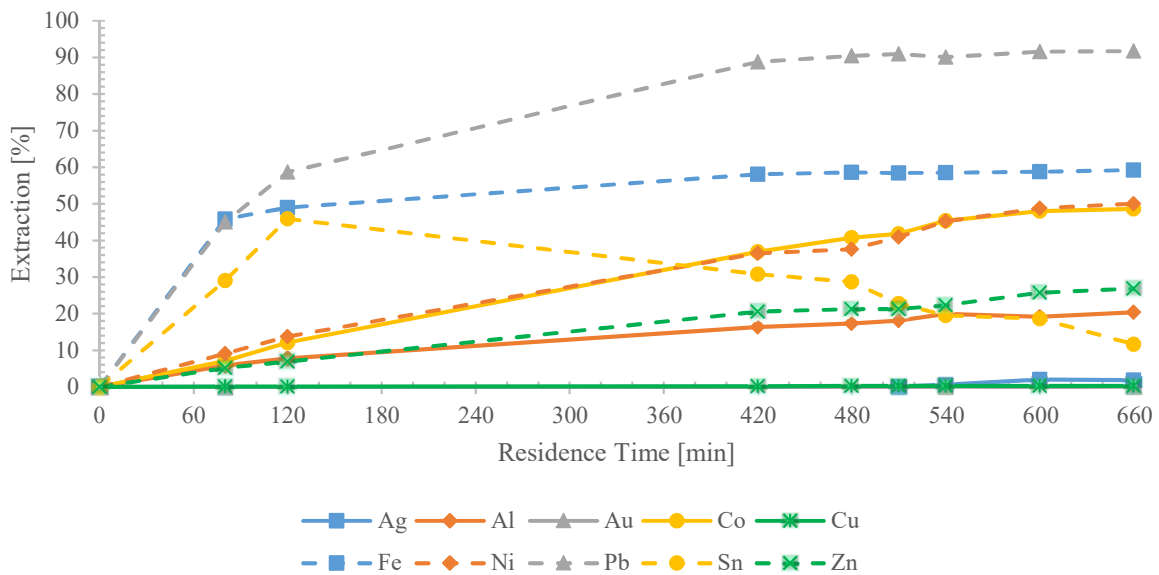


Figure 18: Leaching behaviour of metals during large-scale HNO₃ leaching (step 1)

Recall that the second step in the base metal leaching stage had to produce two batches of PCBs for the precious metal leaching stage. One with lower Cu content and the other with slightly higher Cu content. To achieve this a H₂SO₄ leaching step was conducted with an 80 g sample taken from the PCB residue of the completed large scale HNO₃ leaching step (after sample splitting). The resultant leaching behaviour is illustrated in Figure 19. The results are once again similar to what [63] reported. The small amount of Ag that was leached started to precipitate at around 360 minutes, which [63] encountered at 240 minutes. The behaviour of Ag is attributed to the HNO₃ leaching step which changed the state of Ag, as [63] did not encounter this behaviour in H₂SO₄ experiments with no prior HNO₃ leaching step.

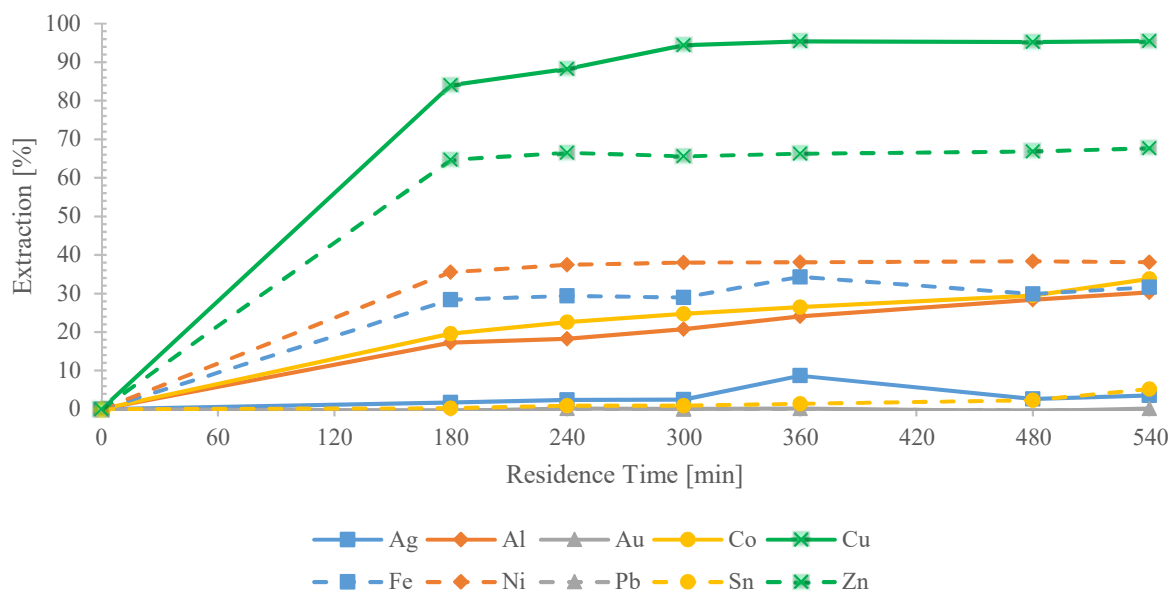


Figure 19: Leaching behaviour of metals during small-scale H₂SO₄ leaching (step 2)

A residence time of 180 minutes was chosen to produce samples with leftover Cu content between 11 and 20 %. To produce samples with leftover Cu content between 1 and 10 %, the original residence time of 480 minutes would suffice. A few H₂SO₄ leaching tests were conducted on samples that have undergone prior HNO₃ leaching to determine if the residence time of 180 minutes did in fact produce Cu extraction of between 11 and 20 %. Aqua Regia digestions were performed on these samples to complete the mass balance. The Cu extracted during the HNO₃ leaching step was estimated for an 80 g sample, from the large scale HNO₃ leaching step data. For a 80 g sample, 53.49 mg of Cu is extracted. a. The results of the tests are shown in Table 24.

Table 24: Cu extraction of 5 replicate tests with residence times of 180 minutes

Test	Cu content [mg]		Cu Extraction [%]	Cu leftover [%]
	H ₂ SO ₄ Leaching Step	Aqua Regia		
1	13661.40	2098.30	86.73	13.27
2	13034.68	2541.18	83.74	16.26
3	12101.87	3113.99	79.61	20.39
4	13545.48	1756.86	88.56	11.44
5	11538.56	2558.56	81.92	18.08

Four out of the five tests showed leftover Cu to be between 11 and 20 %. The third replicate produced a Cu recovery of 79.61 %, which is a bit lower than expected. Not all the tests were expected to fall within the range of 11 – 20 % due to the irregular and heterogeneous nature of the feed, but the result is still acceptable. Once all the tests were completed for each group (high and low Cu content), the solid residue was mixed in two separate groups and split into representative samples for the precious metal leaching stage. Two groups of representative samples were produced for each batch of base metal leaching residues (low and high Cu). Groups of 25 g and 50 g samples were produced.

4.3. Precious Metal Leaching

4.3.1. Screening Phase

The screening phase aimed to determine the most significant main effects to carry on to the next experimental phase, in which a set of full factorial tests was conducted. The test parameters are listed in Table 25 for clarification. Tests 17 to 32 are repeat runs of tests 1 to 16.

Table 25: Screening test parameters

Test	Parameter						
	Leftover Cu [%]	S ₂ O ₃ [M]	Cu(II) [M]	NH ₃ [M]	T [°C]	pH	Pulp Density [g/L]
1	1 - 10	0.1	0.02	0.2	25	9 - 9.5	25
2	11 - 20	0.1	0.02	0.2	40	9 - 9.5	50
3	1 - 10	0.2	0.02	0.2	40	10 - 10.5	25
4	11 - 20	0.2	0.02	0.2	25	10 - 10.5	50
5	1 - 10	0.1	0.1	0.2	40	10 - 10.5	50
6	11 - 20	0.1	0.1	0.2	25	10 - 10.5	25
7	1 - 10	0.2	0.1	0.2	25	9 - 9.5	50
8	11 - 20	0.2	0.1	0.2	40	9 - 9.5	25
9	1 - 10	0.1	0.02	0.4	25	10 - 10.5	50
10	11 - 20	0.1	0.02	0.4	40	10 - 10.5	25
11	1 - 10	0.2	0.02	0.4	40	9 - 9.5	50
12	11 - 20	0.2	0.02	0.4	25	9 - 9.5	25
13	1 - 10	0.1	0.1	0.4	40	9 - 9.5	25
14	11 - 20	0.1	0.1	0.4	25	9 - 9.5	50
15	1 - 10	0.2	0.1	0.4	25	10 - 10.5	25
16	11 - 20	0.2	0.1	0.4	40	10 - 10.5	50

The final Au and Ag extraction from the screening phase tests are illustrated in Figure 20 and Figure 21. For more information on the calculation of the Au and Ag extraction, refer to Table 42 and Table 43 in Appendix C. The final Au extraction was chosen as the dependent factor in the statistical analysis as Au is the more valuable metal. To simplify the analysis, the final Ag extraction was assumed to behave in a similar way to changes in parameters as the final Au extraction and was not selected as a second dependent factor. Figure 20 shows that the final Au and Ag extraction did in fact generally follow the same trend in between tests (trend refers to increases/decreases in between tests). Literature did report that the leaching chemistry of Ag is similar to the leaching chemistry of Au [52], [88].

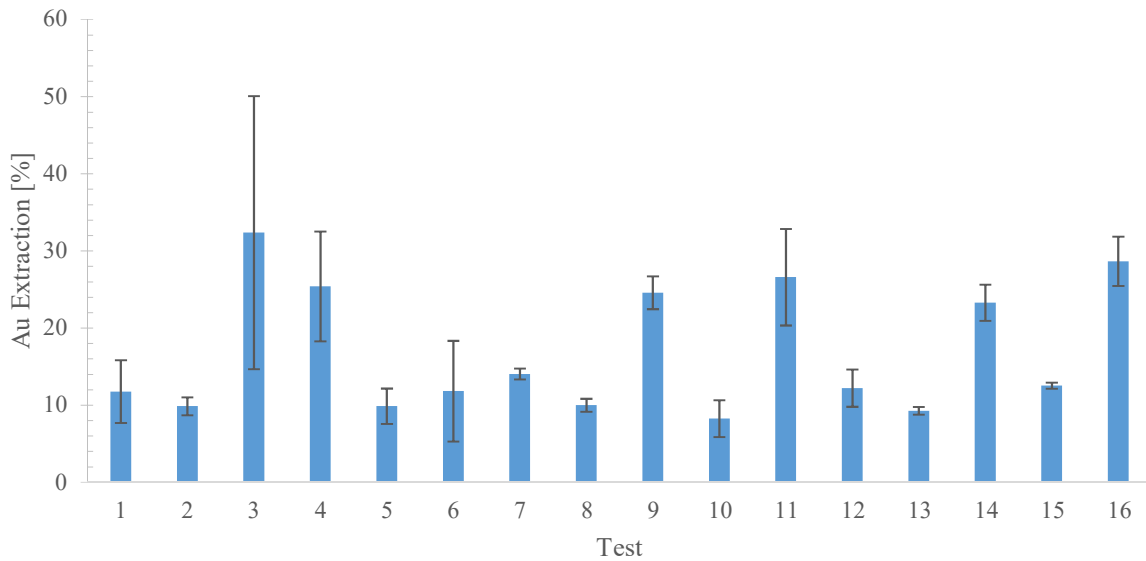


Figure 20: Final Au extraction during the screening phase tests

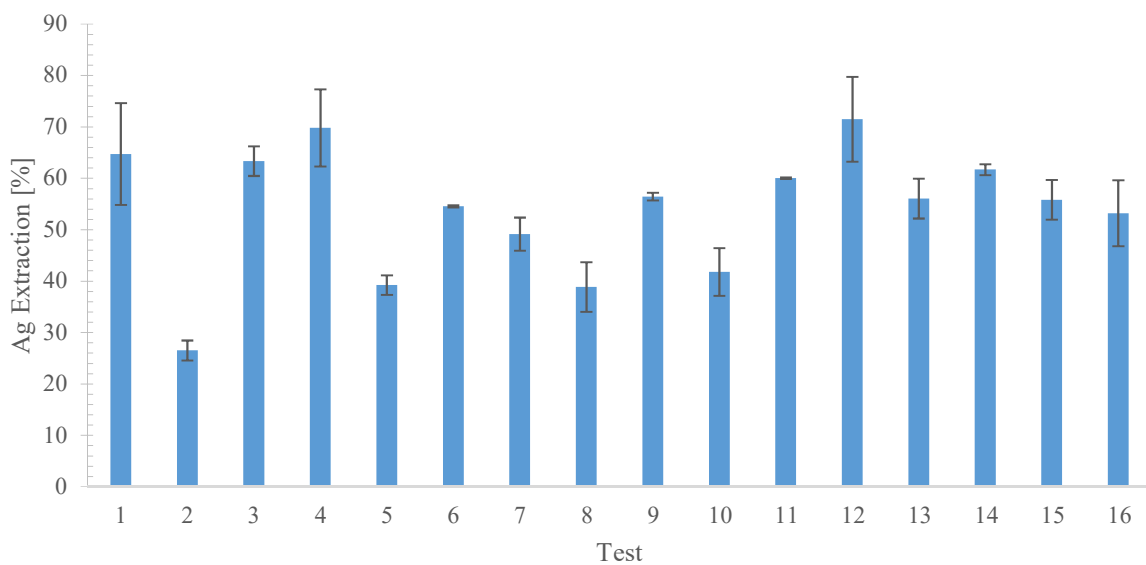


Figure 21: Final Ag extraction during screening phase tests

There were a few cases in which Ag extraction did not change in the same manner as Au extraction due to a change in test parameters. It is difficult to determine why differences existed during the screening phase, as multiple parameters were changed simultaneously. The effect of changes in certain process parameters is explored in sections 4.3.2 and 4.3.3.

4.3.1.1. Gold Behaviour

During tests 1 to 16 frequent sampling was done to check the initial behaviour of Au. The extent of Au leaching during screening test 1 - 16 and test 17 – 32 are given in Table 44 and Table 45 in Appendix C.

The results for Au leaching during the screening phase were used to identify any strange behaviour and check the repeatability of tests. Due to the small amount of Au present in the samples of crushed PCBs and the heterogeneous nature of PCBs, the repeatability was not expected to be good.

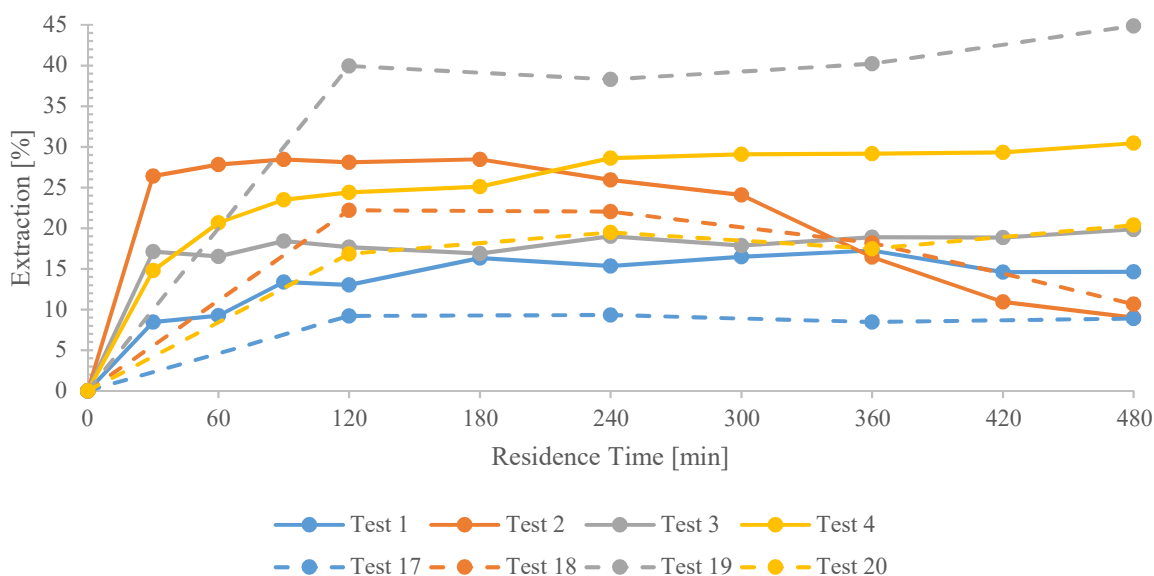


Figure 22: Gold extraction during tests 1 (Cu: 10 %, $S_2O_3^{2-}$: 0.1 M, Cu(II): 0.02 M, NH_3 : 0.2 M, pH: 9–9.5, 25°C, 25 g/L), 2 (Cu: 20 %, $S_2O_3^{2-}$: 0.1 M, Cu(II): 0.02 M, NH_3 : 0.2 M, pH: 9–9.5, 40°C, 50 g/L), 3 (Cu: 10 %, $S_2O_3^{2-}$: 0.2 M, Cu(II): 0.02 M, NH_3 : 0.2 M, pH: 10–10.5, 40°C, 25 g/L), 4 (Cu: 20 %, $S_2O_3^{2-}$: 0.2 M, Cu(II): 0.02 M, NH_3 : 0.2 M, pH: 10–10.5, 25°C, 50 g/L) and their repeat runs

Figure 22 shows that test 1 and test 17 followed the same trend but did not achieve the same amount of Au leaching. Test 2 and test 18 also followed the same general trend of initial leaching and subsequent precipitation. Au precipitation began after 180 minutes in test 2 and after 240 minutes in test 18. The precipitation was most likely due to the disproportionation of the Au(I) complexes. Au(I) has been found to be unstable in the absence of thiosulphate ions in alkaline ammoniacal leaching solutions [89]. The disproportionation or decomposition of unstable gold(I) complexes could be explained by Reaction 35.



The final Au extraction of these two tests differed only by 1.65 %. According to Table 46 in Appendix C, no $S_2O_3^{2-}$ was present at 360 minutes in test 2, which meant that Reaction 35 was probably the cause for the precipitation. The conditions implemented for tests 2 and 18 included higher temperature, higher pulp density and higher Cu leftover, all of which are believed to be detrimental for Au leaching. The most prominent extraction curve on Figure 22 was generated by test 19, during which 39.9 % Au was extracted in the first 120 minutes of leaching. This was more than double the Au extraction encountered during test 3 (19.8 %), which implemented the same parameters. The most likely explanation for this would be that a more superficial Au layer was available in the residue that was used for leaching in test 19. The Au leaching trends in tests 4 and 20 are similar but the extent of leaching differed once again.

Table 26: Average difference in total Au content for screening tests as grouped in Figure 22 to Figure 25

Tests	1 - 4	5 - 8	9 - 12	13 - 16
Average Difference in Au Content [mg]	0.964	0.540	0.516	0.570

Figure 23 showed closer final Au extraction values between screening tests and repeat runs than Figure 22. This could be attributed to the smaller average difference in total Au content of the PCB samples, as shown in Table 26. Similar final Au extraction was obtained by test 7 and 23 and test 8 and 24. The Au leaching trends in Figure 23 are generally the same between screening tests and repeat runs. Test 5 and 21 followed the same trend in the sense that both had an initial leaching phase, after which precipitation occurred. Test 21 had more aggressive leaching and precipitation but reached a similar Au extraction after 420 minutes. Test 7 had a slower initial leaching rate than test 23, but the Au extraction converged after 480 minutes. Test 22 followed the same trend as test 6 up to 360 minutes, after which it seemed like precipitation occurred. This was probably due to the lack of $S_2O_3^{2-}$, as the degradation tests indicated that no $S_2O_3^{2-}$ was present after 360 minutes. Table 46 (Appendix C) also shows almost zero $S_2O_3^{2-}$ at 240 minutes and no $S_2O_3^{2-}$ at 360 minutes for test 5.

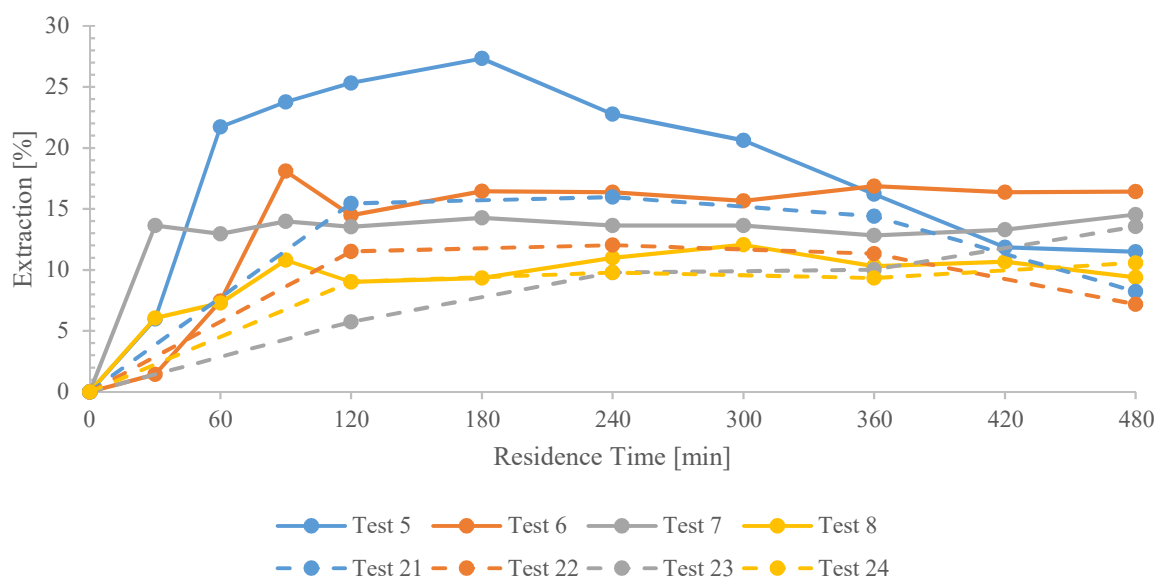


Figure 23: Gold extraction during tests 5 (Cu: 10 %, $S_2O_3^{2-}$: 0.1 M, Cu(II): 0.1 M, NH_3 : 0.2 M, pH: 10 – 10.5, 40°C, 50 g/L), 6 (Cu: 20 %, $S_2O_3^{2-}$: 0.1 M, Cu(II): 0.1 M, NH_3 : 0.2 M, pH: 10 – 10.5, 25°C, 25 g/L), 7 (Cu: 10 %, $S_2O_3^{2-}$: 0.2 M, Cu(II): 0.1 M, NH_3 : 0.2 M, pH: 9 – 9.5, 25°C, 50 g/L), 8 (Cu: 20 %, $S_2O_3^{2-}$: 0.2 M, Cu(II): 0.1 M, NH_3 : 0.2 M, pH: 9 – 9.5, 40°C, 25 g/L) and their repeat runs

The screening tests and repeat runs in Figure 24 and Figure 25 also showed similar Au leaching trends. Precipitation occurred at tests 10 and 26, which could once again be attributed to the lack of $S_2O_3^{2-}$. Table 46 shows no $S_2O_3^{2-}$ at 360 minutes for test 10.

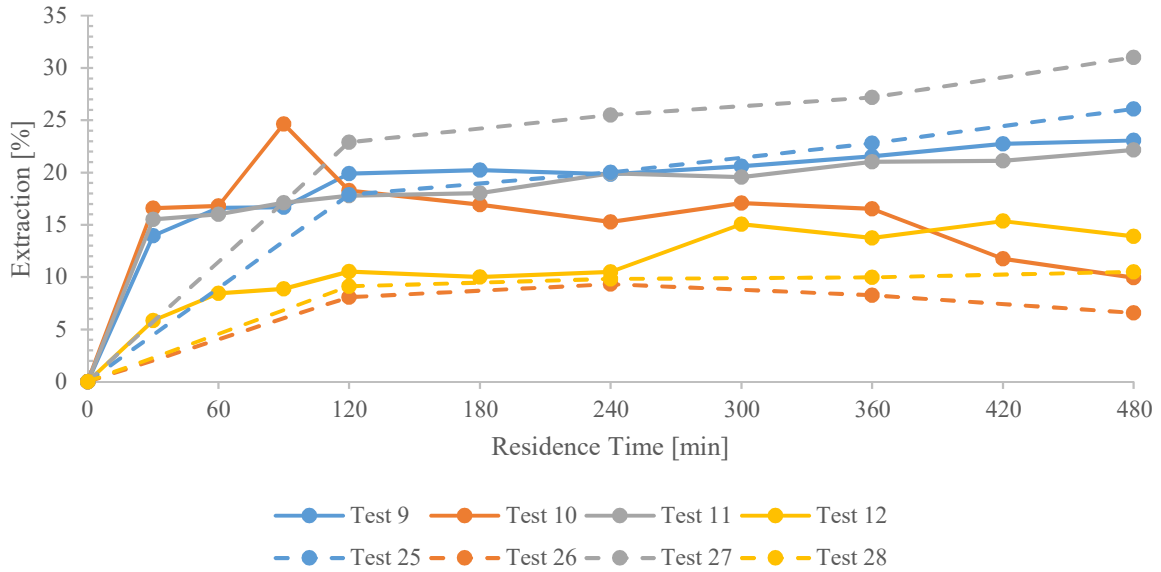


Figure 24: Gold extraction during tests 9 (Cu: 10 %, $S_2O_3^{2-}$: 0.1 M, Cu(II): 0.02 M, NH_3 : 0.4 M, pH: 10 – 10.5, 25°C, 50 g/L), 10 (Cu: 20 %, $S_2O_3^{2-}$: 0.1 M, Cu(II): 0.02 M, NH_3 : 0.4 M, pH: 10 – 10.5, 40°C, 25 g/L), 11 (Cu: 10 %, $S_2O_3^{2-}$: 0.2 M, Cu(II): 0.02 M, NH_3 : 0.2 M, pH: 9 – 9.5, 40°C, 50 g/L), 12 (Cu: 20 %, $S_2O_3^{2-}$: 0.2 M, Cu(II): 0.02 M, NH_3 : 0.4 M, pH: 9 – 9.5, 25°C, 25 g/L) and their repeat runs

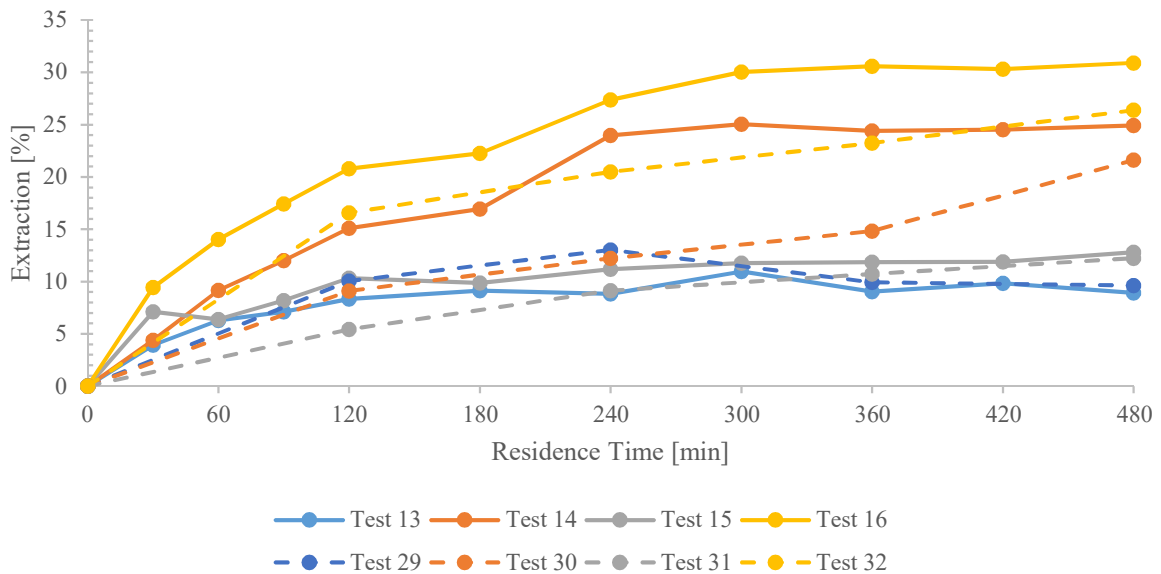


Figure 25: Gold extraction during tests 13 (Cu: 10 %, $S_2O_3^{2-}$: 0.1 M, Cu(II): 0.1 M, NH_3 : 0.4 M, pH: 9 – 9.5, 40°C, 25 g/L), 14 (Cu: 20 %, $S_2O_3^{2-}$: 0.1 M, Cu(II): 0.1 M, NH_3 : 0.4 M, pH: 9 – 9.5, 25°C, 50 g/L), 15 (Cu: 10 %, $S_2O_3^{2-}$: 0.2 M, Cu(II): 0.1 M, NH_3 : 0.4 M, pH: 10 – 10.5, 25°C, 25 g/L), 16 (Cu: 20 %, $S_2O_3^{2-}$: 0.2 M, Cu(II): 0.1 M, NH_3 : 0.4 M, pH: 9 – 9.5, 40°C, 50 g/L) and their repeat runs

4.3.1.2. Silver Behaviour

The repeatability of tests was expected to be better for Ag extraction, as aqua regia test 5 estimated that PCBs could contain almost 6 times more Ag than Au (refer to Table 35 in Appendix A). Table 44 and Table 45 in Appendix C contain the Ag extraction values during the screening phase tests. The repeatability of tests 2 and 3 in Figure 26 was relatively good. Tests 1 and 17 had a final Ag extraction difference of 14.02 %, but they both still followed the same trend that seemed to reach equilibrium at 120 minutes. The same could be said for tests 4 and 20.

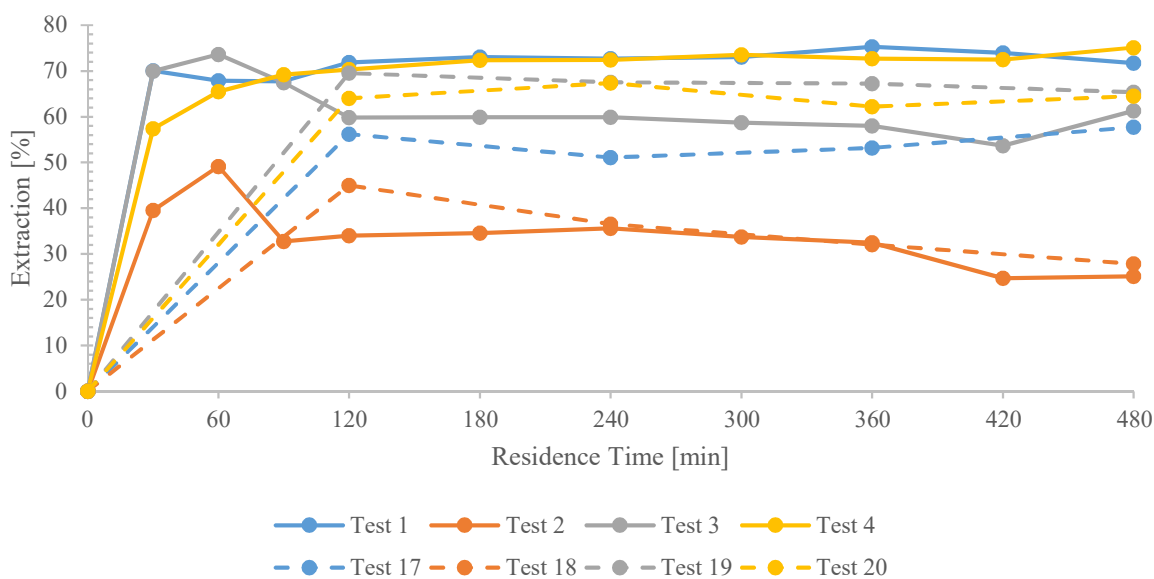


Figure 26: Silver extraction during tests 1 (Cu: 10 %, $S_2O_3^{2-}$: 0.1 M, Cu(II): 0.02 M, NH_3 : 0.2 M, pH: 9 – 9.5, 25°C, 25 g/L), 2 (Cu: 20 %, $S_2O_3^{2-}$: 0.1 M, Cu(II): 0.02 M, NH_3 : 0.2 M, pH: 9 – 9.5, 40°C, 50 g/L), 3 (Cu: 10 %, $S_2O_3^{2-}$: 0.2 M, Cu(II): 0.02 M, NH_3 : 0.2 M, pH: 10 – 10.5, 40°C, 25 g/L), 4 (Cu: 20 %, $S_2O_3^{2-}$: 0.2 M, Cu(II): 0.02 M, NH_3 : 0.2 M, pH: 10 – 10.5, 25°C, 50 g/L) and their repeat runs

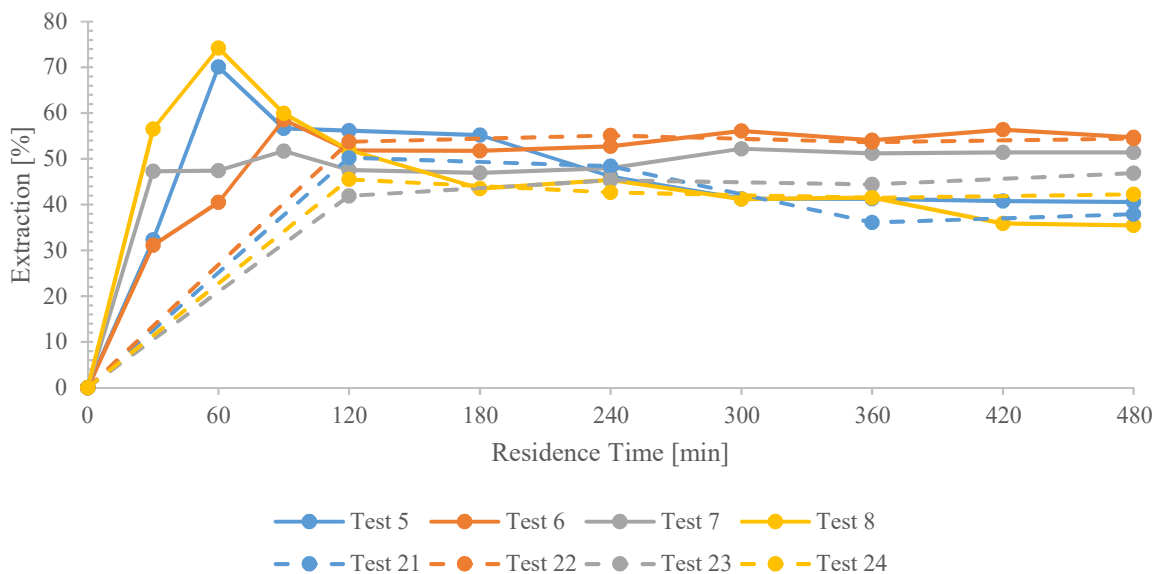


Figure 27: Silver extraction during tests 5 (Cu: 10 %, $S_2O_3^{2-}$: 0.1 M, Cu(II): 0.1 M, NH_3 : 0.2 M, pH: 10 – 10.5, 40°C, 50 g/L), 6 (Cu: 20 %, $S_2O_3^{2-}$: 0.1 M, Cu(II): 0.1 M, NH_3 : 0.2 M, pH: 10 – 10.5, 25°C, 25 g/L), 7 (Cu: 10 %, $S_2O_3^{2-}$: 0.2 M, Cu(II): 0.1 M, NH_3 : 0.2 M, pH: 9 – 9.5, 25°C, 50 g/L), 8 (Cu: 20 %, $S_2O_3^{2-}$: 0.2 M, Cu(II): 0.1 M, NH_3 : 0.2 M, pH: 9 – 9.5, 40°C, 25 g/L) and their repeat runs

The repeatability of tests in Figure 27 and Figure 28 was good, as tests followed similar trends after 120 minutes and ended with similar Ag extraction values. Test 12 in Figure 28 did however differ from the general trend of test 28 after 240 minutes. The increase in Ag extraction is most likely due to the exposure of a layer of metallic Ag which was inaccessible before 240 minutes of leaching, due to a layer of Cu. An increase in $S_2O_3^{2-}$ consumption/degradation was consequently witnessed in Figure 31.

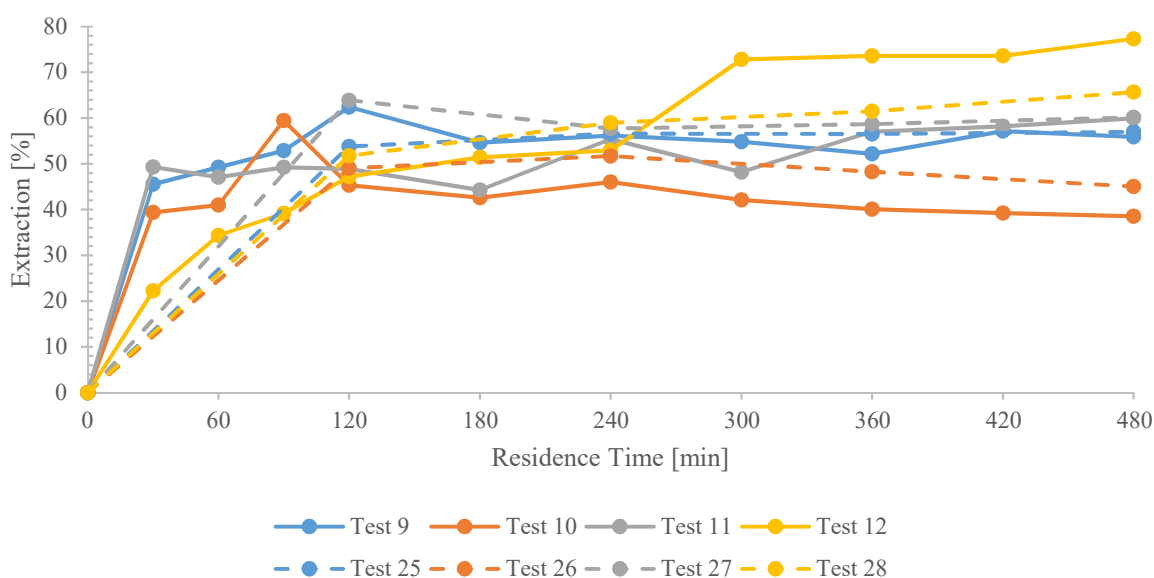


Figure 28: Silver extraction during tests 9 (Cu: 10 %, $S_2O_3^{2-}$: 0.1 M, Cu(II): 0.02 M, NH_3 : 0.4 M, pH: 10 – 10.5, 25°C, 50 g/L), 10 (Cu: 20 %, $S_2O_3^{2-}$: 0.1 M, Cu(II): 0.02 M, NH_3 : 0.4 M, pH: 10 – 10.5, 40°C, 25 g/L), 11 (Cu: 10 %, $S_2O_3^{2-}$: 0.2 M, Cu(II): 0.02 M, NH_3 : 0.2 M, pH: 9 – 9.5, 40°C, 50 g/L), 12 (Cu: 20 %, $S_2O_3^{2-}$: 0.2 M, Cu(II): 0.02 M, NH_3 : 0.4 M, pH: 9 – 9.5, 25°C, 25 g/L) and their repeat runs

The repeatability of tests in Figure 29 was good after 120 minutes of leaching. Tests 16 and 32 were the only set that showed a large difference in Ag extraction (9.05 %).

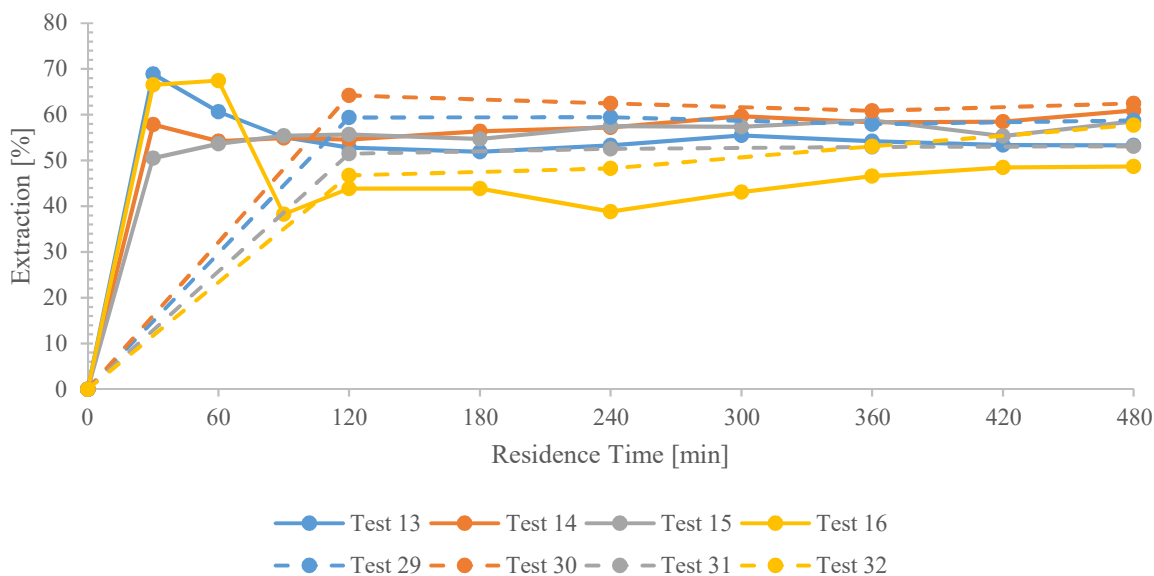
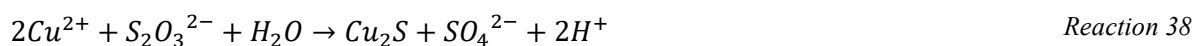


Figure 29: Silver extraction during tests 13 (Cu: 10 %, $S_2O_3^{2-}$: 0.1 M, Cu(II): 0.1 M, NH_3 : 0.4 M, pH: 9 – 9.5, 40°C, 25 g/L), 14 (Cu: 20 %, $S_2O_3^{2-}$: 0.1 M, Cu(II): 0.1 M, NH_3 : 0.4 M, pH: 9 – 9.5, 25°C, 50 g/L), 15 (Cu: 10 %, $S_2O_3^{2-}$: 0.2 M, Cu(II): 0.1 M, NH_3 : 0.4 M, pH: 10 – 10.5, 25°C, 25 g/L), 16 (Cu: 20 %, $S_2O_3^{2-}$: 0.2 M, Cu(II): 0.1 M, NH_3 : 0.4 M, pH: 9 – 9.5, 40°C, 50 g/L) and their repeat runs

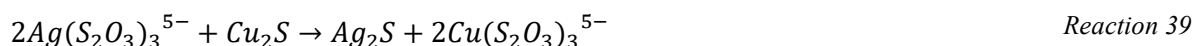
During most tests in which a temperature of 40°C was implemented, the Ag extraction reached a maximum value after which it decreased due to precipitation. This suggested that a higher temperature produced an unstable leaching system [90]. During the initial leaching process, several reactions may occur simultaneously. These reactions include Ag dissolution, cupric ion reduction, oxidative decomposition of S_2O_3 and precipitation of CuS and Cu_2S . Ag dissolution and cupric ion reduction may have occurred per Reaction 36 and Reaction 15 respectively [8].



The precipitation of CuS and Cu_2S possibly occurred per Reaction 37 and Reaction 38.



The silver thiosulphate complex ($Ag(S_2O_3)_3^{5-}$) possibly reacted with Cu_2S to form Ag_2S as a precipitate per Reaction 39 [90], [88]. Ag may precipitate in a manner similar to the copper sulphides, but no literature sources were found.



The possible redissolution of Ag_2S and consequent formation $\text{Ag}(\text{S}_2\text{O}_3)_3^{5-}$ per Reaction 40 to Reaction 41 could explain the oscillations present in the Ag extraction curves [52].



4.3.1.3. Thiosulphate Degradation/Consumption

In order to distinguish between what part of the decrease in $\text{S}_2\text{O}_3^{2-}$ is due to degradation and what part is due to metal complex formation, a robust method of analysis would be required that could determine all of the degradation products. All the required salts for the determination of the degradation products could not be obtained. The thiosulphate degradation/consumption results are illustrated in Figure 30 and Figure 31. The degradation analyses could not be done directly after each test due to time constraints, which had significant effects on the results from 240 minutes onward. Refer to Appendix C for more information on the difficulties encountered during the thiosulphate degradation analyses.

From the tests that implemented 0.1 M $\text{S}_2\text{O}_3^{2-}$, test 9 showed the slowest degradation/consumption. Not much can be said about the effect of the change in parameters, as multiple parameters are changed simultaneously in between tests during the screening phase. From the tests that implemented 0.2 M $\text{S}_2\text{O}_3^{2-}$, test 12 showed the slowest degradation/consumption up to 240 minutes, after which it increased. This was most likely due to the increased Au and Ag leaching that was seen after 240 minutes in Figure 24 and Figure 28 respectively. The data in Table 46 in Appendix C shows that test 15 ended with the highest $\text{S}_2\text{O}_3^{2-}$ concentration of 0.016 M, despite showing the 4th fastest initial degradation/consumption rate between 0 and 120 minutes. Test 19 had the fastest consumption rate between 0 and 120 minutes, which was probably caused by the high amount of gold leaching encountered from 0 to 120 minutes in Figure 22.

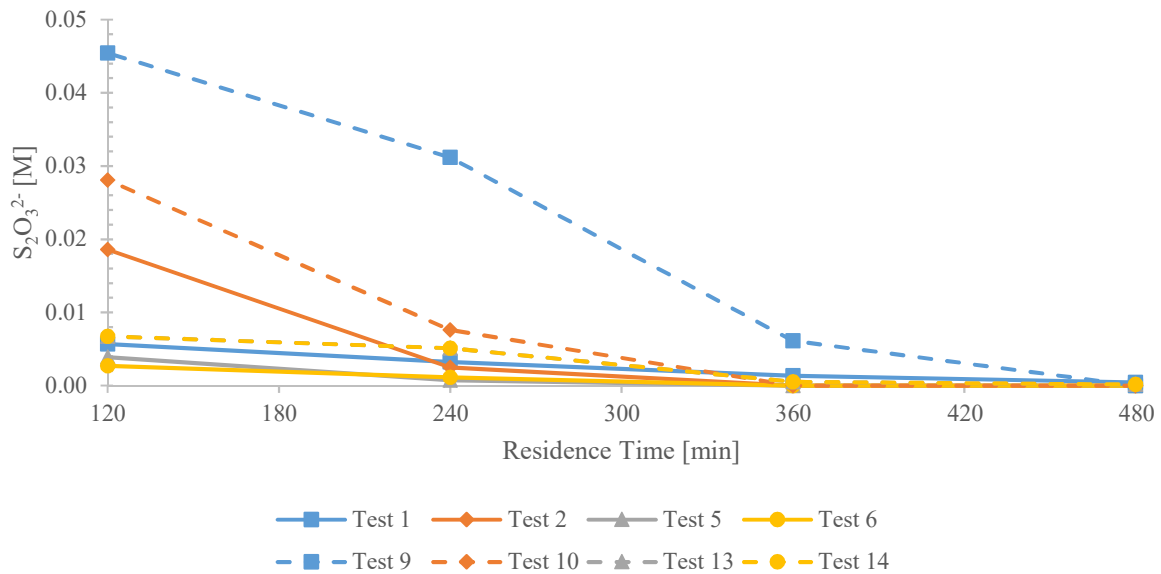


Figure 30: Thiosulphate degradation during tests which used $0.1 \text{ M S}_2\text{O}_3^{2-}$

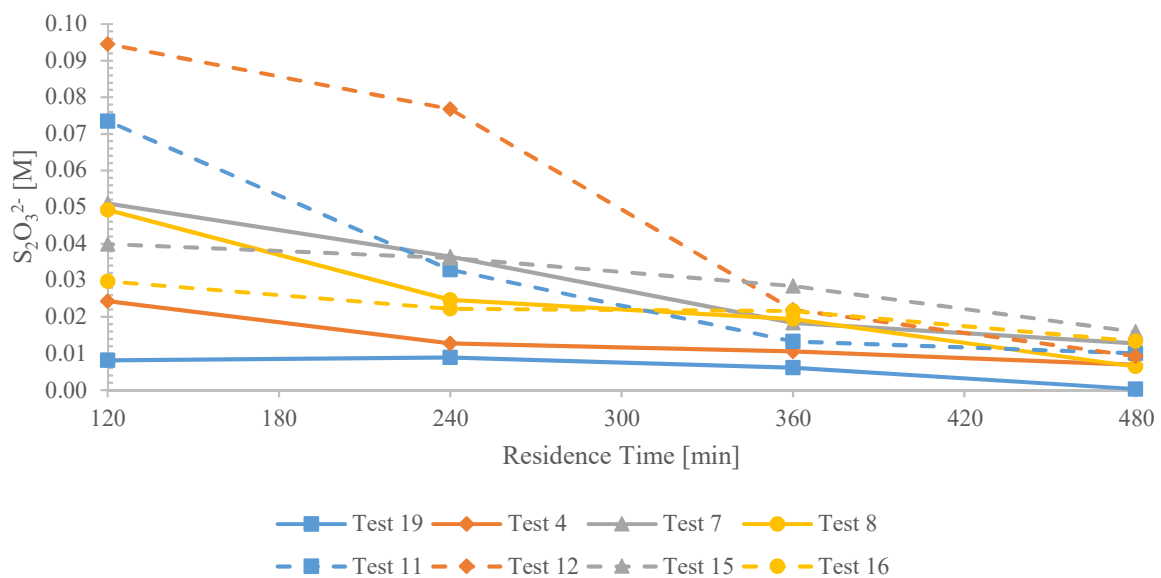


Figure 31: Thiosulphate degradation during tests which used $0.2 \text{ M S}_2\text{O}_3^{2-}$

A faster degradation rate was expected in the tests that used higher temperatures (from literature). The tests that implemented the same $\text{S}_2\text{O}_3^{2-}$, NH_3 and Cu(II) concentrations were used to compare the effects of temperature on $\text{S}_2\text{O}_3^{2-}$ degradation/consumption. These comparisons were used to see if the effect of a change in temperature was prominent enough (due to Au leaching being chemically controlled) to ignore a change in leftover Cu on the PCBs, pulp density and pH.

The expected increase in the rate of degradation/consumption (due to a rise in temperature) was encountered from test 7 to 8, 9 to 10, 12 to 11, 14 to 13 and 15 to 16. The same could not be said for the rise in temperature from test 1 to 2, 4 to 3 and 6 to 5.

4.3.1.4. Copper Behaviour

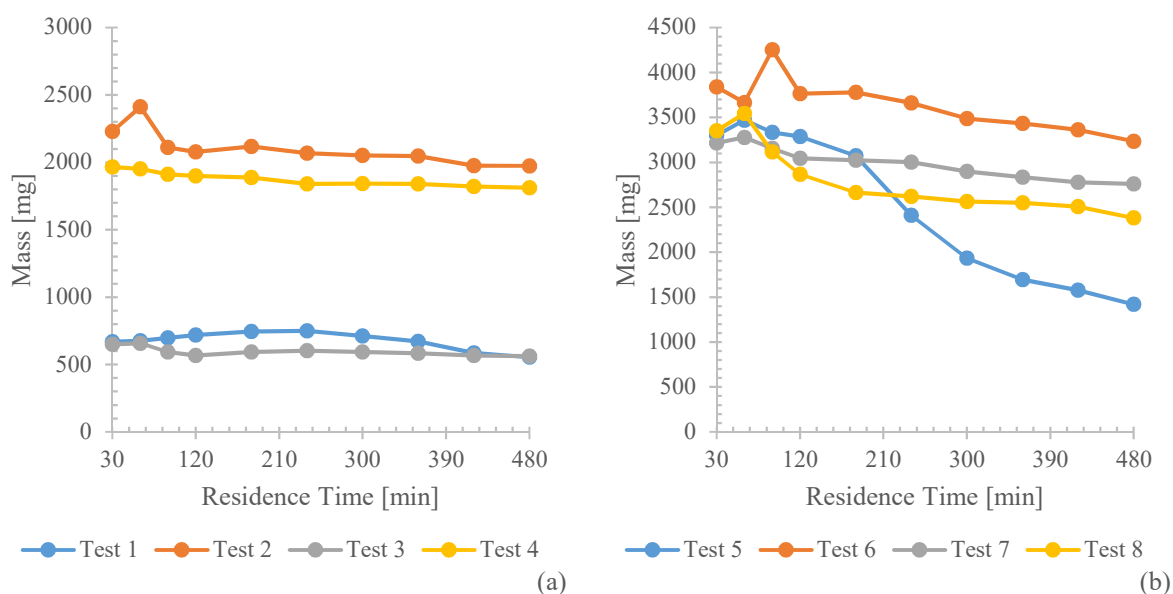


Figure 32: Copper behaviour as a function of time during (a) tests 1 to 4 and (b) tests 5 to 10

In tests 1 to 16 the Cu content was analysed to illustrate the behaviour of Cu during the precious metal leaching stage. The starting Cu content during these tests varied considerably, as different amounts of Cu(II) and leftover Cu were present. Figure 32 and Figure 33 shows that Cu generally decreases with time. This was expected as Cu(II) was used as an oxidant during the leaching reactions. There were some areas where Cu increased or sharply decreased. The initial increase in Cu content was probably due to the leaching of Cu layers that covered the Au and Ag in the PCBs. This consequently caused slower leaching of Ag from 30 to 60 minutes in tests 2, 8, and 10 and from 30 to 90 minutes in test 12. Initial Au leaching appeared to be slower than initial Ag leaching for most of the tests.

The sharp decreases in Cu content could be due to precipitation per Reaction 37 or Reaction 38. Interestingly when the Cu content decreased, the Ag extraction generally decreased until the rate of Cu decrease slowed down. This can be seen in tests 2 (60 to 90 minutes), 3 (60 to 120 minutes), 5 (60 to 90 and 180 to 300 minutes), 6 (90 to 120 minutes), 8 (60 to 180 minutes), 10 (90 – 120 minutes), 11 (120 – 180 minutes), 13 (30 to 120 minutes) and 16 (30 to 90 minutes). The corresponding decreases in Ag extraction can be seen in Figure 26 for tests 2 and 3, Figure 27 for tests 5, 6 and 8, Figure 28 for tests 10 and 11 and Figure 29 for tests 13 and 16. This could suggest that Ag precipitates according to a different reaction than Reaction 39, as Cu_2S is converted to aqueous form in this reaction but the Cu content does not increase when Ag precipitates.

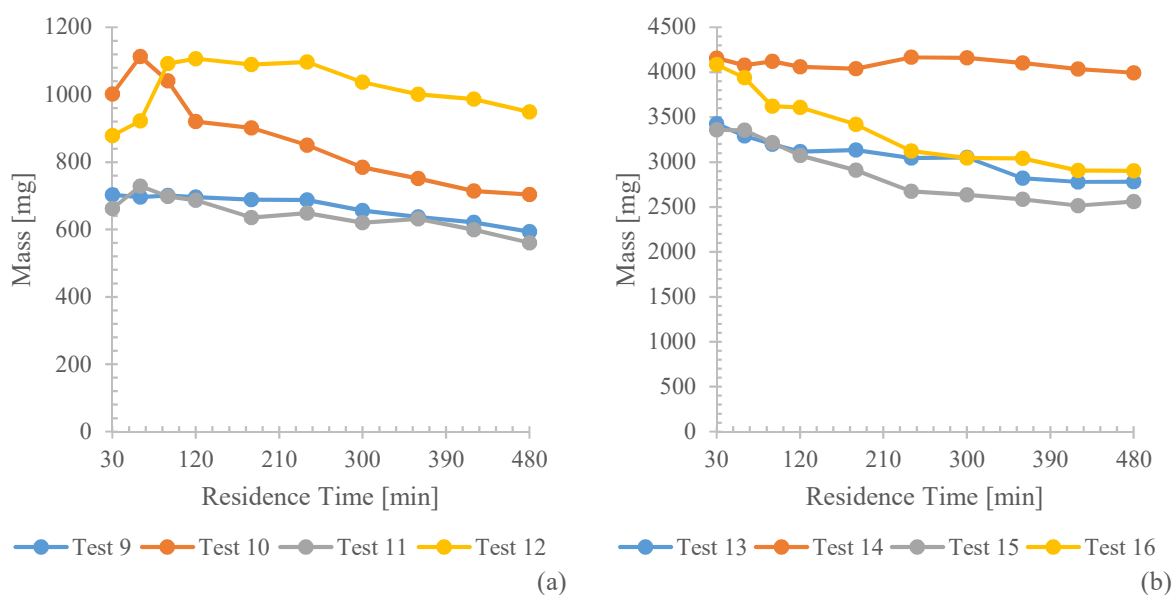


Figure 33: Copper behaviour as a function of time during (a) tests 9 to 12 and (b) tests 13 to 16

4.3.1.5. ICP-OES vs ICP-MS

The detection limits of ICP-OES for Au and Ag are normally around 50 and 5 $\mu\text{g/L}$, while the detection limit for both Au and Ag is around 0.1 $\mu\text{g/L}$ for ICP-MS (assuming no spectral interferences affecting the best isotope or wavelength) [91]. To confirm the results from ICP-OES, the final Au and Ag extraction was determined from the ICP-MS analyses of the 480 minute samples of tests 17 to 32, and compared to the final extraction values determined from ICP-OES. The results are given in Table 27.

Table 27: Comparison of Au and Ag detection capabilities ICP-OES and ICP-MS

Test	Au Extraction [%]			Ag Extraction [%]		
	ICP-OES	ICP-MS	Difference	ICP-OES	ICP-MS	Difference
17	8.88	10.54	-1.66	57.71	56.29	1.42
18	10.68	6.61	4.07	27.88	34.13	-6.25
19	44.88	67.76	-22.88	65.38	68.41	-3.03
20	20.37	25.09	-4.72	64.49	60.31	4.18
21	8.23	10.57	-2.34	37.90	44.43	-6.53
22	7.19	9.67	-2.47	54.39	41.36	13.03
23	13.55	15.00	-1.45	46.87	49.03	-2.16
24	10.58	6.93	3.65	42.26	44.61	-2.34
25	26.08	21.00	5.07	56.98	50.34	6.64
26	6.57	11.36	-4.79	45.07	49.07	-4.00
27	31.01	24.71	6.30	60.15	59.85	0.30
28	10.50	18.06	-7.57	65.65	64.92	0.73
29	9.62	2.68	6.94	58.78	60.30	-1.53
30	21.61	8.34	13.28	62.43	65.42	-2.99
31	12.24	10.95	1.29	53.10	52.57	0.52
32	26.38	29.73	-3.35	57.73	54.38	3.35

The results indicated maximum Au and Ag extraction differences of 22.88 % and 13.03 %, but absolute average differences of 5.74 % and 3.69 % respectively. It was expected that the average difference in Ag extraction would be lower than that of Au, as Ag was more prominent than Au and consequently easier to detect. Despite the low Au and Ag concentrations that were near the detection limits of the ICP-OES, the results obtained with the ICP-OES were realistic and compared relatively well with the extractions that were calculated based on the results obtained from the ICP-MS.

4.3.1.6. Statistical Analysis

The initial statistical analysis on the $2^{(7-3)}$ fractional factorial design produced an ANOVA table which is given in Table 28. The Au extraction was used as the response variable. Due to the analysis being a fractional factorial design, only certain interaction effects could be investigated. The confounding of effects is illustrated in Table 48 in Appendix C. The redundant effects, which were linear combinations of other effects and could consequently not be estimated, are given in Table 49.

Table 28: Initial ANOVA table of $2^{(7-3)}$ fractional factorial design phase

Factor	SS	df	MS	F	p
(1) Cu on PCB	16.632	1	16.632	0.529	0.477
(2) S ₂ O ₃ [M]	352.385	1	352.385	11.214	0.004
(3) Cu(II) [M]	125.018	1	125.018	3.978	0.063
(4) NH ₃ [M]	51.233	1	51.233	1.630	0.220
(5) T [°C]	0.079	1	0.079	0.003	0.961
(6) pH	166.212	1	166.212	5.289	0.035
(7) Pulp Density [g/L]	365.513	1	365.513	11.632	0.004
1 by 2	6.151	1	6.151	0.196	0.664
1 by 3	570.629	1	570.629	18.159	0.001
1 by 4	13.507	1	13.507	0.423	0.521
1 by 5	121.096	1	121.096	3.854	0.067
1 by 6	0.167	1	0.167	0.005	0.943
1 by 7	159.892	1	159.892	5.088	0.038
2 by 4	71.611	1	71.611	2.279	0.151
1*2*4	28.558	1	28.558	0.909	0.355
Error	502.787	16	31.424		
Total SS	2551.468	31			

The p-values in Table 28 suggested that a change in S₂O₃ concentration, pH range and pulp density each had a statistically significant effect on the Au extraction (these values were < 0.05). A change in the leftover Cu on the PCBs, temperature, Cu(II) - and NH₃ concentrations did not have statistically significant effects on the Au extraction. This seemed to indicate that the difference in leftover Cu on the PCBs was too small to make a significant impact on the amount of Au extraction.

To confirm this, additional tests were conducted in the optimisation phase in section 4.3.3 during which the Cu content left on the PCBs was increased. Previous literature could not agree on the optimum temperature for Au extraction but seemed to point to the optimum being either 25 or 40°C. This was probably the reason why no significant difference in Au extraction was encountered between these two temperatures. It is unknown why the analysis did not indicate the significance of a change in NH₃ concentration and Cu(II) concentration.

The p-values also indicated that the only significant interaction existed between the Cu on the PCBs and Cu(II) concentration; and the Cu on the PCBs and pulp density. Literature suggested that a fine balance existed between the S₂O₃/NH₃ ratio and Au extraction, but the statistical analysis did not indicate this. The fact that higher order interactions were not significant was expected, as these interactions are normally of little importance. This fractional factorial design reduced the number of tests from 128 to 16, which meant that it was only an indication of what was significant.

Table 29: 2⁴ full factorial experimental design

Test	A - S ₂ O ₃ [M]	B - NH ₃ [M]	C - pH	D - Pulp Density [g/L]
1	0.1	0.2	9 - 9.5	25
2	0.2	0.2	9 - 9.5	25
3	0.1	0.4	9 - 9.5	25
4	0.2	0.4	9 - 9.5	25
5	0.1	0.2	10 - 10.5	25
6	0.2	0.2	10 - 10.5	25
7	0.1	0.4	10 - 10.5	25
8	0.2	0.4	10 - 10.5	25
9	0.1	0.2	9 - 9.5	50
10	0.2	0.2	9 - 9.5	50
11	0.1	0.4	9 - 9.5	50
12	0.2	0.4	9 - 9.5	50
13	0.1	0.2	10 - 10.5	50
14	0.2	0.2	10 - 10.5	50
15	0.1	0.4	10 - 10.5	50
16	0.2	0.4	10 - 10.5	50

The full factorial design is illustrated in Table 29. The screening tests were used to check repeatability. No repeat tests were planned for the full factorial phase. Only the test that produced the optimum Au extraction was planned to be repeated. The parameters that were chosen to carry on to the full factorial phase were S₂O₃ concentration, pH range and pulp density. The NH₃ concentration was also included, as literature suggested that changes in this parameter have significant effects on the Cu-NH₃-S₂O₃ system. Cu(II) concentration was not included in the next phase as most of the results in Table 12 indicated that a S₂O₃/Cu(II) ratio between 2.5 and 20 provided optimum Au leaching. With the S₂O₃²⁻ concentration varying between 0.1 and 0.2 M, a Cu(II) concentration of 0.02 M seemed sufficient.

The fixed parameters were therefore 1 – 10 % Cu on PCBs, Cu(II) concentration of 0.02 M, temperature of 25°C, agitation rate of 500 rpm and residence time of 8h. All the studies that implemented a prior base metal leaching stage seemed to agree that to achieve significant Au extraction most of the base metals needed to be removed. This was most likely not encountered because the Cu leftover ranges were too close to each other. Ranges of 1 – 10 % and 11 – 20 % could mean that in most tests the leftover Cu was in fact very close.

4.3.2. Full Factorial Phase

4.3.2.1. Effect of Thiosulphate Concentration

There exists a fine balance between using too much $S_2O_3^{2-}$ and too little $S_2O_3^{2-}$. If the $S_2O_3^{2-}$ concentration is too high it may result in the stabilisation of $Cu(S_2O_3^{2-})_3^{5-}$, which would consequently limit the catalytic action on Au extraction. Higher $S_2O_3^{2-}$ concentrations also lead to increased consumption of $S_2O_3^{2-}$, which in turn leads to increased $S_2O_3^{2-}$ degradation [4]. The effect of a change in $S_2O_3^{2-}$ concentration on Au leaching during the full factorial phase is illustrated in Figure 34.

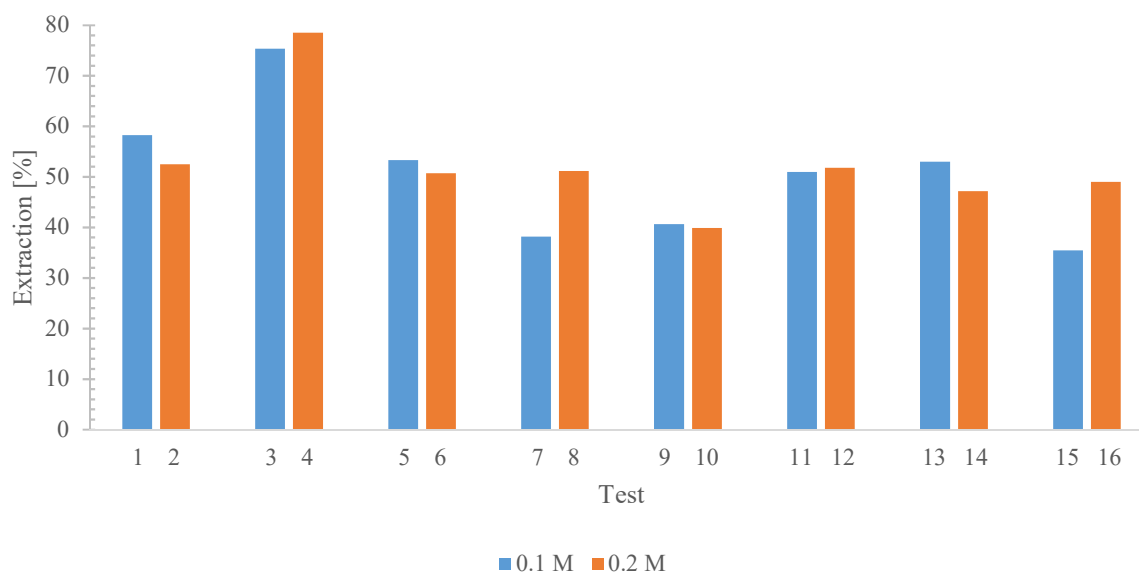


Figure 34: Effect of change in thiosulphate concentration on gold leaching

An increase in $S_2O_3^{2-}$ concentration lead to increased Au extraction from tests 3 to 4, 7 to 8, 11 to 12 and 15 to 16. The Au extraction decreased from tests 1 to 2, 5 to 6, 9 to 10 and 13 to 14. This could be explained by looking at the $S_2O_3^{2-}/NH_3$ ratios. Recall that [75] proposed that a $S_2O_3^{2-}/NH_3$ ratio between 0.5 and 1 was necessary to provide sufficient stability for $Cu(NH_3)_4^{2+}$ while still providing an adequate rate of Au leaching. The $S_2O_3^{2-}/NH_3$ ratio increased from 0.5 to 1 from tests 1 to 2, 5 to 6, 9 to 10 and 13 to 14, which meant that $S_2O_3^{2-}$ became more prominent relative to NH_3 . This meant that the $Cu(S_2O_3^{2-})_3^{5-}$ complex is more prominent which hindered Au dissolution.

The $S_2O_3^{2-}/NH_3$ ratio increased from 0.25 to 0.5 from tests 3 to 4, 7 to 8, 11 to 12 and 15 to 16. This correlated with the increase in Au extraction as the $S_2O_3^{2-}/NH_3$ ratio of 0.25 fell outside the desired range of 0.5 to 1. An increase in $S_2O_3^{2-}$ was still beneficial at this stage. Literature reported that with increasing $S_2O_3^{2-}$ concentrations, Au extraction increased initially, reached a maximum and then decreased [2], [4].

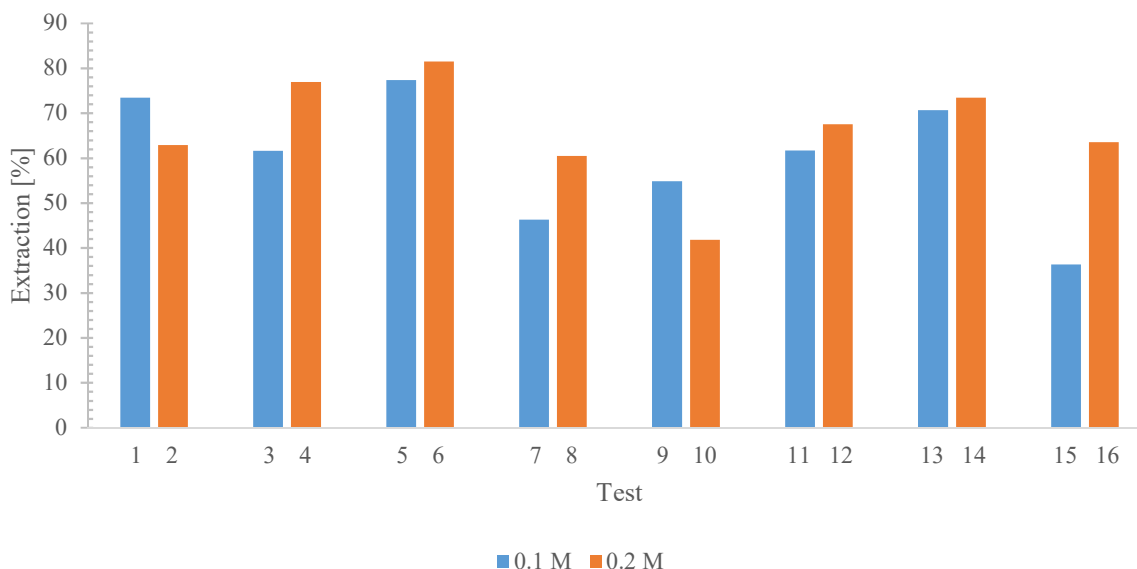


Figure 35: Effect of change in thiosulphate concentration on silver leaching

Ag extraction behaved like Au extraction, except for the increase in Ag extraction due to a rise in $S_2O_3^{2-}$ concentration from test 5 to 6, 13 to 14. Ag leaching chemistry is comparable to Au leaching chemistry, which means that Ag should behave in the same way as Au to a change in $S_2O_3^{2-}$ concentrations.

4.3.2.2. Effect of Ammonia Concentration

As with $S_2O_3^{2-}$, NH_3 concentrations must not be too high or too low. If the NH_3 concentration is too high, it will decrease the oxidation potential of the Cu(II)-Cu(I) couple and in doing so reduce the driving force for Reaction 16 [57], [74]. At NH_3 concentrations that are too low most of the Cu(II) reacts with $S_2O_3^{2-}$ which reduces the amount of $Cu(NH_3)_4^{2+}$ that is available for Reaction 16.

In section 4.3.2.1 it was determined that a $S_2O_3^{2-}/NH_3$ ratio of 0.5 provided the best Au leaching. The ratio decreased from 0.5 to 0.25 from tests 1 to 3, 5 to 7, 9 to 11 and 13 to 15, while it decreased from 1 to 0.5 from tests 2 to 4, 6 to 8, 10 to 12 and 14 to 16. The Au extraction should increase when the $S_2O_3^{2-}/NH_3$ ratio is decreased from 1 to 0.5 and decrease when the $S_2O_3^{2-}/NH_3$ ratio is decreased from 0.5 to 0.25. Figure 36 confirmed this for an increase in Au extraction due to an increase in NH_3 concentration from tests 2 to 4, 6 to 8, 10 to 12 and 14 to 16. A decrease in Au extraction was also confirmed from tests 5 to 7 and 13 to 15. An unexpected increase in Au extraction was encountered from tests 1 to 3 and 9 to 11. These tests were conducted at the lower pH range of 9 – 9.5, which might explain why the Au extraction increased even though the $S_2O_3^{2-}/NH_3$ ratio decreased from 0.5 to 0.25.

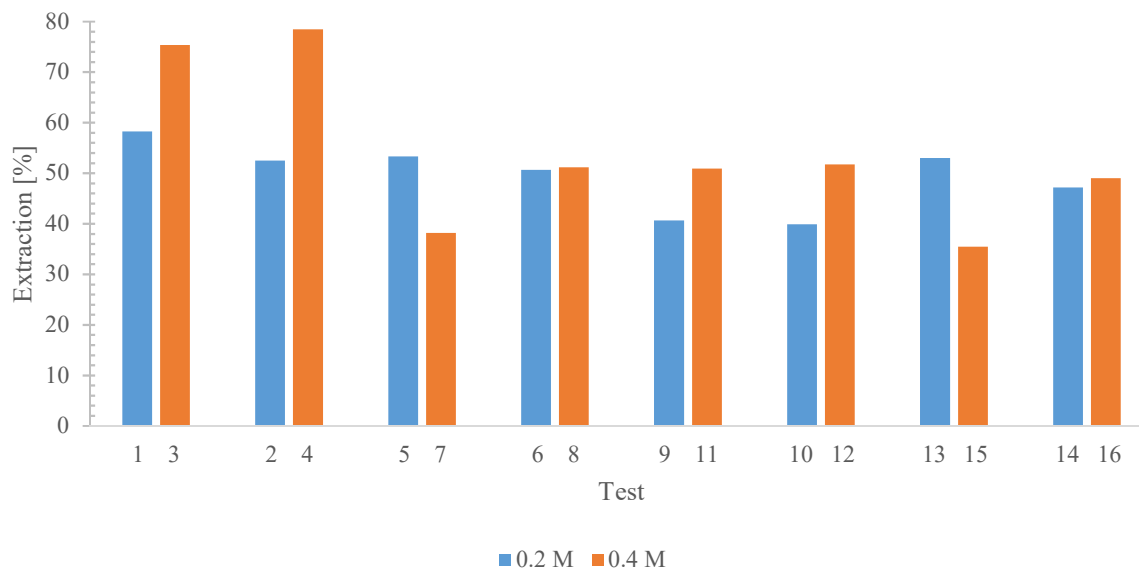


Figure 36: Effect of change in ammonia concentration on gold leaching

Interestingly, all the tests in which the lower pH range of 9 – 9.5 was used seemed to have a significant effect on Au extraction with a change in NH₃ concentration (tests 1 to 3, 2 to 4, 9 to 11, 10 to 12). This might be explained by looking at the amount of NH₄ present in solution. Thurston et al. [92] claimed that the amount of NH₃ dissolved in H₂O was dependent on the pH and temperature and that it existed in un-ionized form (NH₃) and ionized form (NH₄⁺). They found that at lower pH values the ionized form was more present than at higher pH values. Breuer and Jeffrey [54] found that Au leaches faster at higher NH₄ concentrations. They suggested that at low pH values Cu(NH₃)₄²⁺ was stabilized by hydroxide ions, which made Cu(II) more oxidizing and consequently increased Au leaching.

Ag extraction in Figure 37 generally exhibited similar behaviour to Au extraction due to a change in NH₃ concentration. Tests 1 to 3, 6 to 8 and 14 to 16, however, showed different changes in Ag extraction. The decrease in Ag extraction from tests 1 to 3 was the expected outcome of a decrease in S₂O₃²⁻/NH₃ ratio from 0.5 to 0.25. The unexpected decrease in Ag extraction from tests 6 to 8 and 14 to 16 could possibly be due to precipitation that occurred.

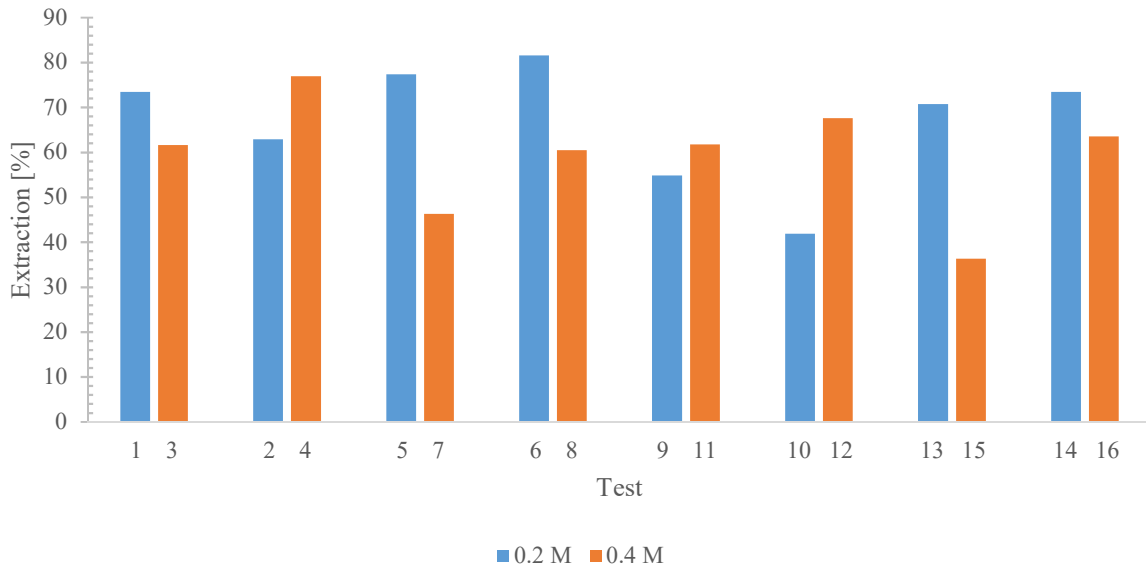


Figure 37: Effect of change in ammonia concentration on silver leaching

4.3.2.3. Effect of Pulp Density

Figure 38 and Figure 39 showed that an increase in pulp density from 25 g/L to 50 g/L resulted in a decrease in both Au and Ag extraction for all tests. This was expected as the amount of reagent per unit weight of PCB decreased. Similar results were reported by [2], [93]. A noticeably larger decrease in Au extraction was encountered in tests that utilized the lower pH range, which means that a possible explanation could be linked to the fact that more NH_4 was present (see section 4.3.2.2). The difference in actual Au content could also possibly be the cause of the large differences in Au extraction, as the standard deviation of total Au content for these tests was 0.72 mg. This large standard deviation could indicate significant differences in the placement of Au on the PCB particles.

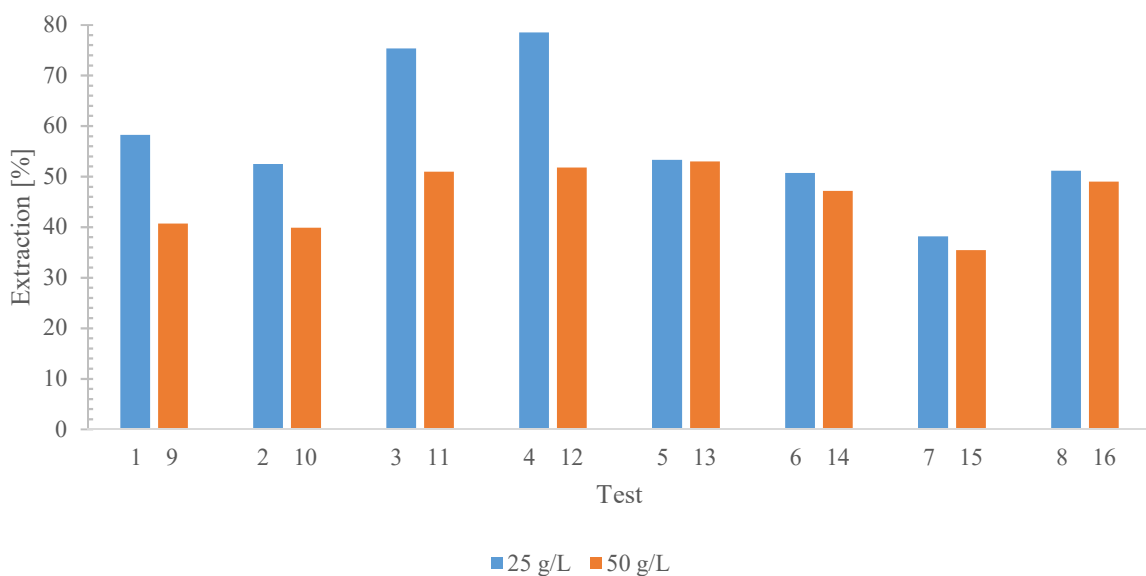


Figure 38: Effect of change in pulp density on gold leaching

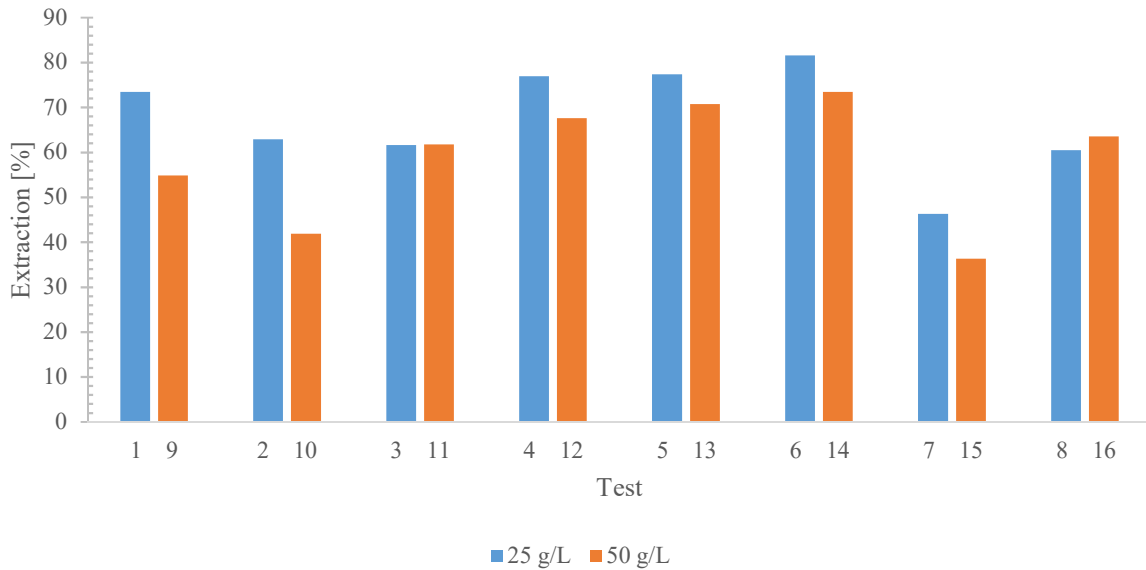


Figure 39: Effect of change in pulp density on silver leaching

4.3.2.4. Effect of pH Range

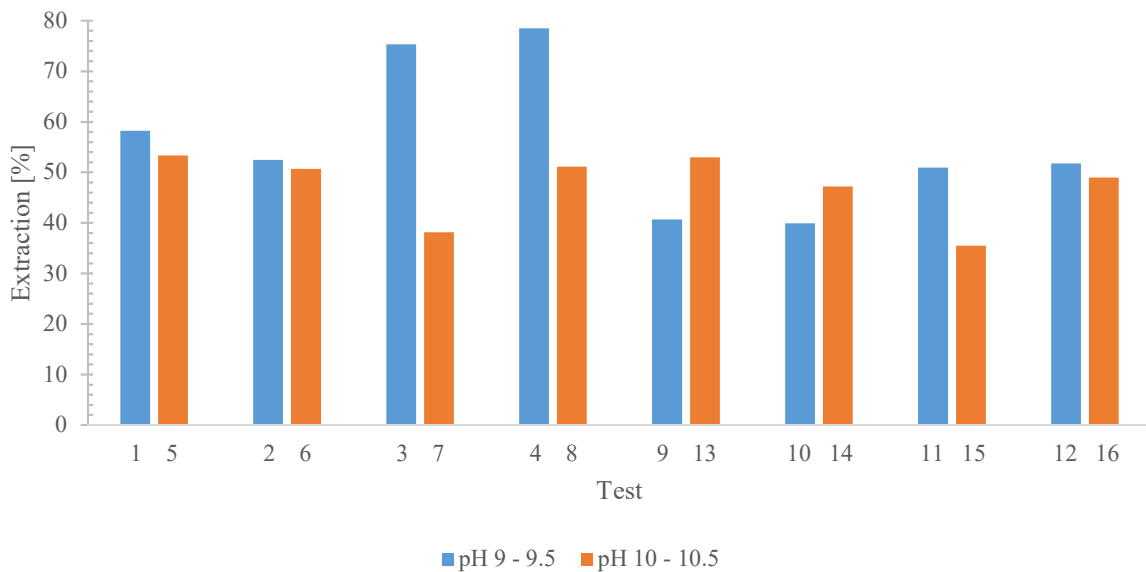


Figure 40: Effect of change in pH range on gold leaching

A decrease in Au extraction was encountered when the higher pH range was used in most of the tests. Decreased Au extraction at higher pH values has been reported by Breuer & Jeffrey [54], which was attributed to an increased rate of $S_2O_3^{2-}$ degradation at higher pH values. This could not be confirmed as $S_2O_3^{2-}$ degradation tests could not be completed during the full factorial phase. There have also been studies that reported increased Au extraction at higher pH values [2]. Higher pH values increased the stability of $Cu(NH_3)_4^{2+}$ and $Cu(S_2O_3)_3^{5-}$ in their tests, which resulted in increased dissolution of Au. The Ag extraction generally followed the same trend as the Au extraction due to changes in the pH range.

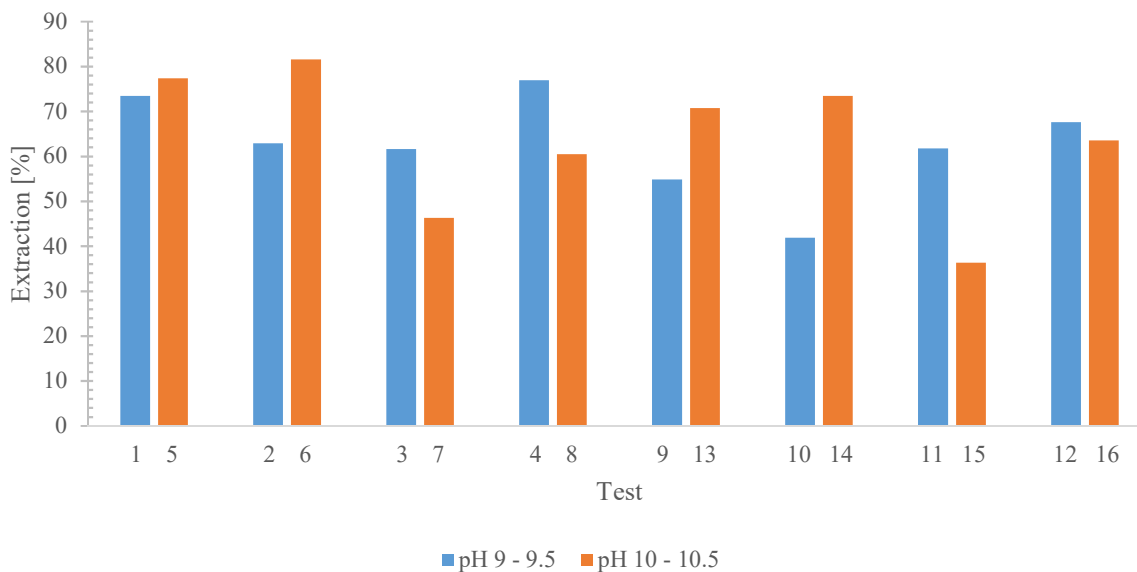


Figure 41: Effect of change in pH range on silver leaching

4.3.2.5. Rate Limiting Step

Three general rate limiting steps are mentioned by Prosser [80], namely chemical reaction [Equation (1)], mass transport in the boundary layer [Equation (2)] and mass transport in the porous product layer [Equation (3)]. To determine which was the rate limiting step, Equations (1), (2) and (3) were plotted against time and fitted with linear trendlines.

Table 30: Comparison of three different rate limiting models

Test	Chemical Reaction		Mass Transport in Boundary Layer		Mass Transport in Product Layer	
	R ²	k [min ⁻¹]	R ²	k [min ⁻¹]	R ²	k [min ⁻¹]
1	0.590	0.0006	0.544	0.0011	0.825	0.0001
2	0.793	0.0005	0.754	0.0009	0.979	0.00009
3	0.899	0.0009	0.839	0.0015	0.988	0.0002
4	0.909	0.001	0.858	0.0016	0.969	0.0003
5	0.687	0.0006	0.646	0.001	0.921	0.0001
6	0.397	0.0006	0.374	0.001	0.565	0.0001
7	0.557	0.0004	0.534	0.0007	0.794	0.00004
8	0.204	0.0006	0.199	0.001	0.234	0.0001
9	0.373	0.0004	0.357	0.0008	0.536	0.00006
10	0.420	0.0004	0.403	0.0008	0.587	0.00006
11	0.583	0.0005	0.547	0.001	0.536	0.00009
12	0.697	0.0005	0.659	0.001	0.911	0.0001
13	0.455	0.0006	0.425	0.001	0.659	0.0001
14	0.559	0.0005	0.529	0.0009	0.782	0.00008
15	0.384	0.0004	0.370	0.0007	0.558	0.00004
16	0.523	0.0005	0.492	0.0009	0.752	0.00008

Table 30 seemed to indicate that the rate limiting step was mass transport in the porous product layer, as the R^2 values were generally higher than the other two. Diffusion through a product layer normally cannot control the reaction rate at the start of a reaction [80], but this could be an indication that Au is not exposed. The average rate constant for the mass transport in the product layer was 0.0001 min^{-1} . Section 7.3.2.3 in Appendix C contains a comparison of the different rate limiting steps for tests 1 to 4.

4.3.2.6. Statistical Analysis

The p-values in Table 31 suggested that a change in pH range and pulp density each had a significant effect on the Au extraction and that significant interactions existed between $\text{S}_2\text{O}_3^{2-}$ concentration and NH_3 concentration; NH_3 concentration and pH range; and pH range and pulp density. The significance of the interaction between the $\text{S}_2\text{O}_3^{2-}$ and NH_3 concentrations was mentioned in section 4.3.2.1. A significant interaction between NH_3 concentration and pH range was also expected, as a change in NH_3 concentration directly affects the pH. The pH was only adjusted once it reached the boundaries of each specific range (the system could progress without interference inside the predetermined ranges). The differences in $\text{S}_2\text{O}_3^{2-}$ concentration and NH_3 concentration may be insignificant according to the p-value test, but the normal probability plot in Figure 42 suggested that these factors could be included in the model. The values touching the line represent insignificant factors. A new statistical analysis was conducted by excluding the interactions between $\text{S}_2\text{O}_3^{2-}$ concentration and pH; $\text{S}_2\text{O}_3^{2-}$ concentration and pulp density; and NH_3 concentration and pulp density.

Table 31: Initial ANOVA table for 2^4 full factorial design phase

Factor	SS	df	MS	F	p
(1) $\text{S}_2\text{O}_3^{2-}$ [M]	16.606	1	16.606	1.160	0.331
(2) NH_3 [M]	72.335	1	72.335	5.054	0.074
(3) pH	297.735	1	297.735	20.801	0.006
(4) Pulp Density [g/L]	514.609	1	514.609	35.952	0.002
1 by 2	134.444	1	134.444	9.393	0.028
1 by 3	24.751	1	24.751	1.729	0.246
1 by 4	0.046	1	0.046	0.003	0.957
2 by 3	561.453	1	561.453	39.225	0.002
2 by 4	32.433	1	32.433	2.266	0.193
3 by 4	336.539	1	336.539	23.512	0.005
Error	71.568	5	14.314		
Total SS	2062.519	15			

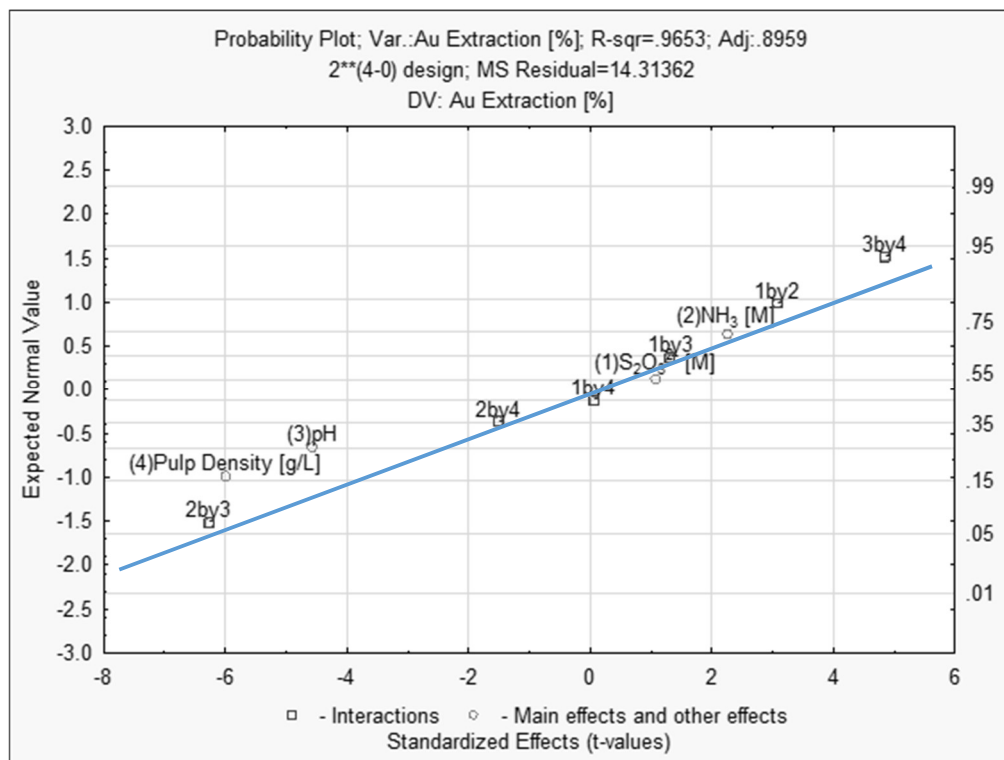


Figure 42: Initial normal probability plot

The adjusted ANOVA table is given in Table 32. The R^2 value for the new model is 0.94, which is acceptable.

Table 32: Adjusted ANOVA table of 2^4 full factorial phase

Factor	SS	df	MS	F	p
(1) $S_2O_3^{2-}$ [M]	16.606	1	16.606	1.031	0.400
(2) NH_3 [M]	72.335	1	72.335	4.493	0.067
(3) pH	297.735	1	297.735	18.493	0.003
(4) Pulp Density [g/L]	514.609	1	514.609	31.964	0.0004
1 by 2	134.444	1	134.444	8.351	0.020
2 by 3	561.453	1	561.453	34.873	0.0004
3 by 4	336.539	1	336.539	20.903	0.002
Error	128.798	8	16.100		
Total SS	2062.519	15			

The calculated regression coefficients are shown in Table 33. These coefficients were used to determine the model equation (4).

$$y = 85.475 - 153.550x_1 - 6.462x_2 - 0.602x_3 - 0.821x_4 + 579.750x_1x_2 - 118.475x_2x_3 + 0.734x_3x_4 \quad (4)$$

The residuals appear to be normally distributed (Figure 43) and generally random (Figure 44).

Table 33: Adjusted regression coefficients of 2⁴ full factorial phase

Factor	Regression Coefficient	Std.Err.	t(8)	p	-95 %	+95 %
Mean/Interc.	85.475	11.349	7.532	0.00007	59.304	111.646
(1)S ₂ O ₃ ²⁻ [M]	-153.550	63.442	-2.420	0.042	-299.848	-7.252
(2)NH ₃ [M]	-6.462	33.270	-0.194	0.851	-83.182	70.257
(3)pH	-0.602	8.745	-0.069	0.947	-20.768	19.563
(4)Pulp Density [g/L]	-0.821	0.114	-7.231	0.0001	-1.082	-0.559
1 by 2	579.750	200.623	2.900	0.020	117.114	1042.386
2 by 3	-118.475	20.062	-5.905	0.0004	-164.739	-72.211
3 by 4	0.734	0.161	4.572	0.002	0.364	1.104

The optimum Au extraction was obtained at a temperature of 25°C, agitation rate of 500 rpm, leftover Cu on PCB of 1 to 10 %, Cu(II) concentration of 0.02 M, S₂O₃²⁻ concentration of 0.2 M, NH₃ concentration of 0.4 M, pulp density of 25 g/L and pH range of 9 – 9.5. The predicted optimum Au extraction at these conditions is 78.04 %, which compares well with the actual value of 78.47 %. This statistical model is only valid for the concentration ranges that were implemented in the full factorial design, as it does not consider any of the complex interactions that occur beyond those concentration ranges. The Au extraction fitted surface plots are given in Appendix C section 7.3.2.

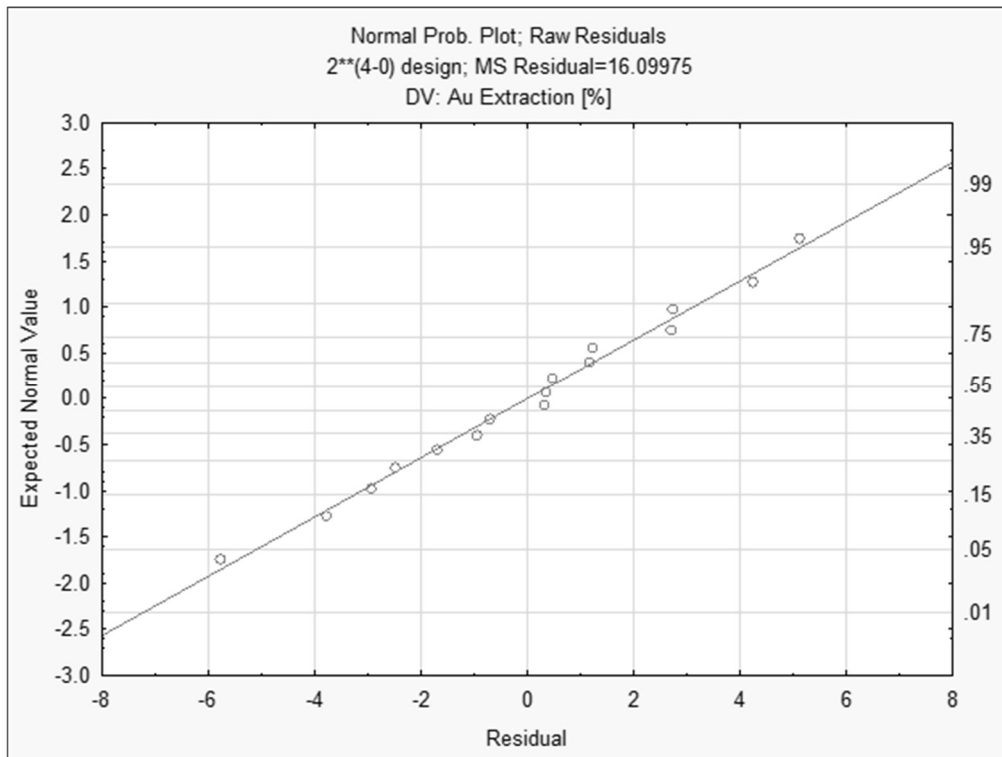


Figure 43: Normal probability plot of residuals

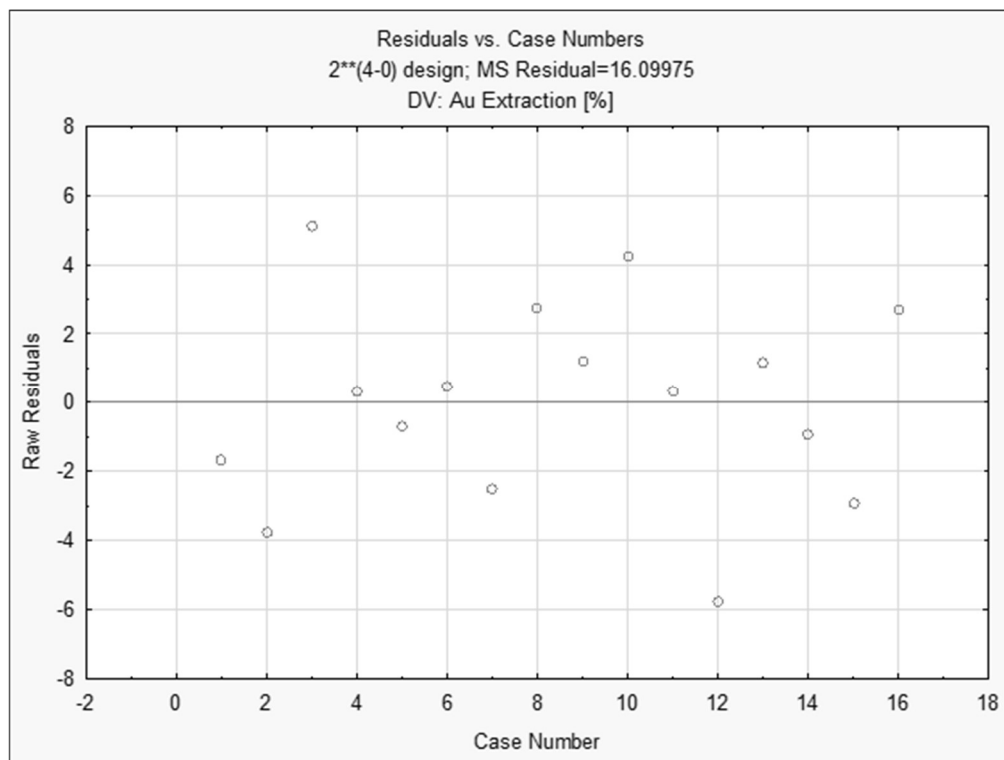


Figure 44: Raw residuals vs case numbers

An attempt was made to generate a model that could be a better indication of the fundamental/chemical effects, by excluding pulp density as a factor. This resulted in a model with R^2 value of 0.69 that predicted 67.78 % Au extraction at the optimum conditions, which is not comparable. Further testing at a wider parameter range with multiple replicates would be required to produce a more accurate model.

4.3.3. Optimization Phase

The optimization phase had two main goals. The first goal was to determine the effect of a larger change in leftover Cu on Au extraction, as the change in this parameter had no effect in previous tests. A change in temperature and Cu(II) concentration were included as additional parameters. The second goal was to see what the effect of changing these parameters would have on thiosulphate degradation/consumption. The parameters that produced the optimum Au extraction in section 4.3.2 were used as a baseline to see if a change in these parameters would improve the Au leaching further. The possibility of counter-current leaching was also investigated in this section to attempt to achieve complete Au dissolution.

4.3.3.1. Repeatability of Optimum Gold Extraction

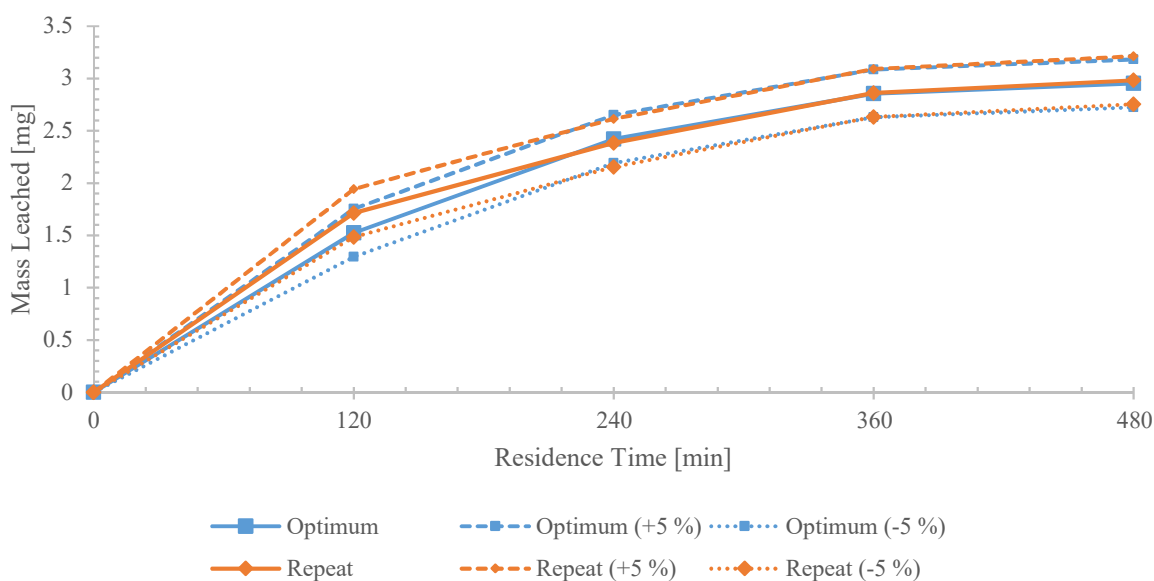


Figure 45: Repeatability test of optimum Au extraction

The heterogeneous nature of PCBs made it difficult to produce samples that contained an even distribution of metals. The repeatability of the test that achieved the optimum Au extraction in section 4.3.2 was therefore tested. The total Au content from the six characterisation tests in section 4.1, the 32 screening tests in section 4.3.1, the 16 tests in section 4.3.2 and the five tests in the optimization phase were used to calculate a 95 % confidence interval ($\alpha = 0.05$) of 0.23 mg. This was used to quantify the variation in feed composition. Figure 45 shows that the Au dissolution was within the range of what could be attributed to a variation in total Au content. The Au extraction of the repeat test was 74.1 %, which compared well with the Au extraction encountered in section 4.3.2 of 78.5 %.

4.3.3.2. Effect of Temperature

Figure 46 shows that an increase in temperature resulted in an initial increase in Au extraction from 25 - 50°C. After 120 minutes, however, the Au extraction rate reached a maximum for both 40 and 50°C and started to decrease. The Au leaching reaction was considered to be endothermic, as the system required heat to maintain the temperatures at the set values. The Au extraction continued for 25°C and seemed to reach an equilibrium at 480 minutes.

Literature reports were contradicting, as there were studies that claimed an increase in temperature resulted in an increase in Au extraction ([93], [94]) while other studies claimed that a decrease in temperature resulted in an increase in Au extraction [8], [95]. Zipperian et al. [94] did, however, experience a decrease in Au extraction rate at higher temperatures after 1 h of leaching. Ha et al. [5] found that Au leaching increased from 20 to 40°C, but decreased when the temperature was increased further to 50°C.

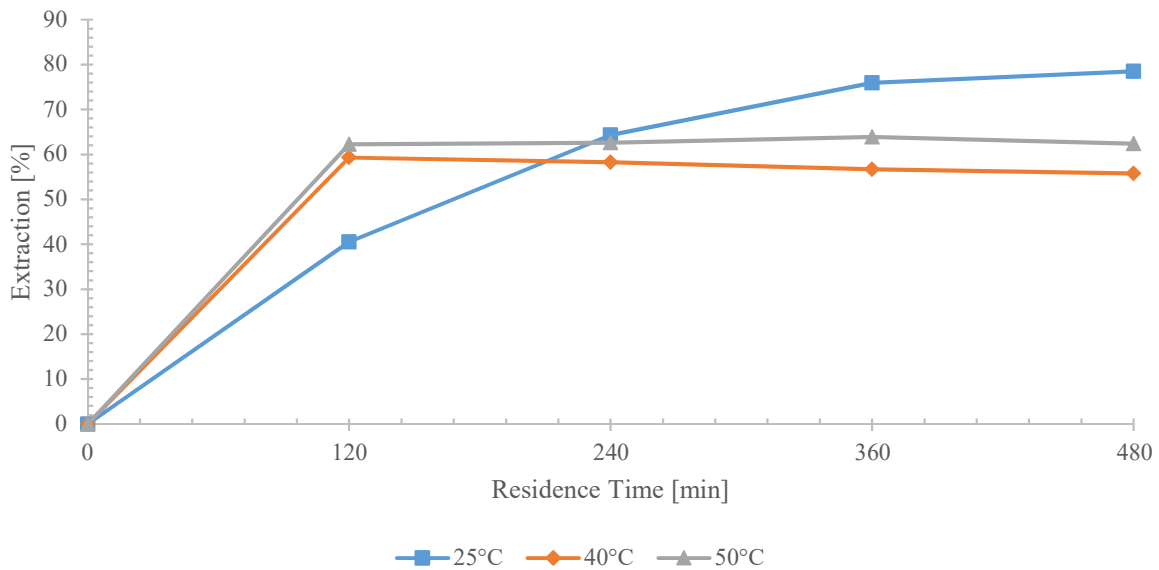


Figure 46: Effect of temperature on Au extraction

Figure 47 shows that the $S_2O_3^{2-}$ degradation increased with an increase in temperature from 25 to 50°C, which was also reported in literature [75]. Breuer & Jeffrey [54] reported that apart from the Au leaching reaction, the Cu(II) reduction reaction is also chemically controlled with a larger activation energy. They suggested that the system should not be operated at much higher temperatures than 25°C to avoid the unwanted consumption of thiosulphate.

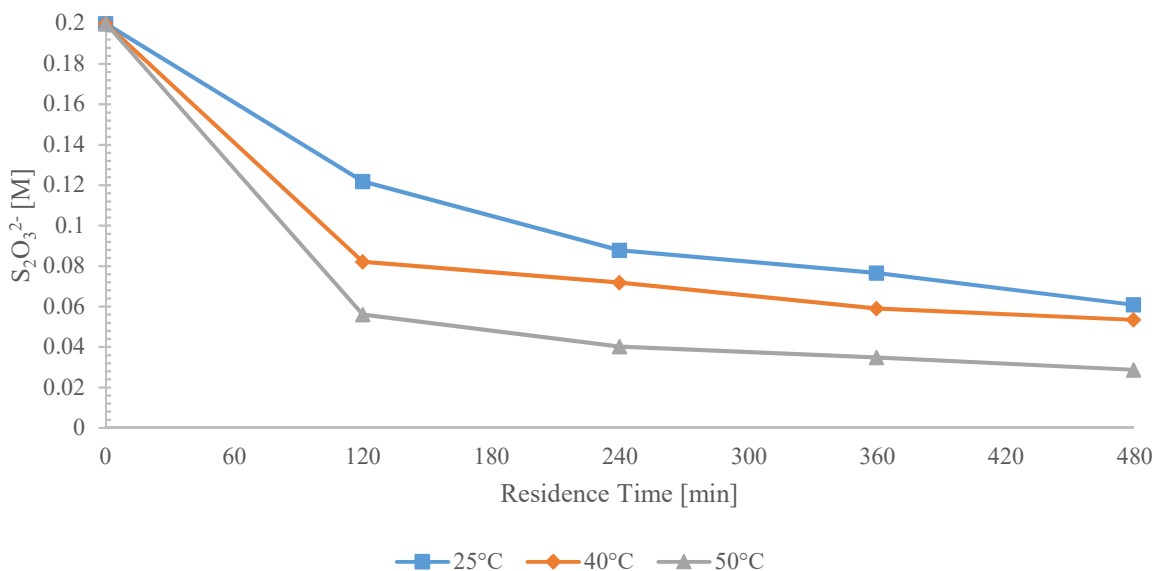


Figure 47: Effect of temperature on thiosulphate degradation

4.3.3.3. Effect of Cu(II) Concentration

Figure 48 illustrates that an increase in Cu(II) concentration initially led to an increase in Au extraction at 120 minutes, after which the Au dissolution rate became slower than the test in which 0.02 M Cu(II) was used. Literature reported an increase in Au extraction when Cu(II) concentration was increased [2], [8], [4]. Arslan & Sayiner [88] reported an increase in Au extraction up to 0.01 M, after which the Au extraction decreased. They implemented 0.5 M $S_2O_3^{2-}$ and 0.1 M NH_3 . Increased $S_2O_3^{2-}$ consumption was encountered up to 120 minutes for an increase in Cu(II) concentration from 0.02 M to 0.06 M. This corresponds to the initial increase in Au extraction. Higher Cu(II) concentrations lead to higher losses of thiosulphate through its conversion to tetrathionate according to Reaction 24 [52].

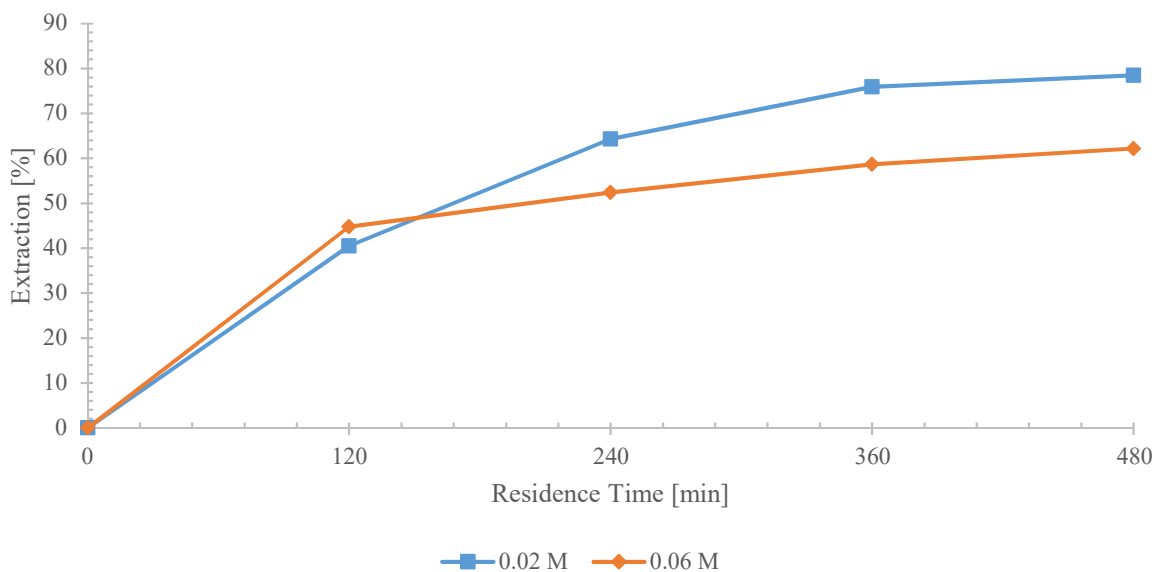


Figure 48: Effect of Cu(II) concentration on Au extraction

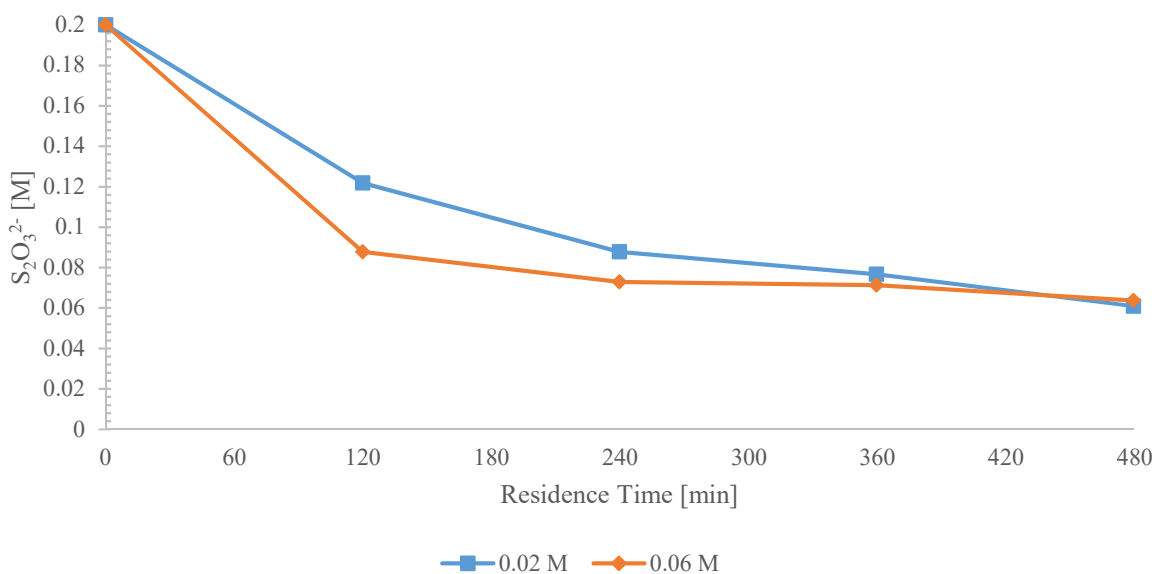


Figure 49: Effect of Cu(II) concentration on thiosulphate degradation

4.3.3.4. Effect of Leftover Copper on PCB

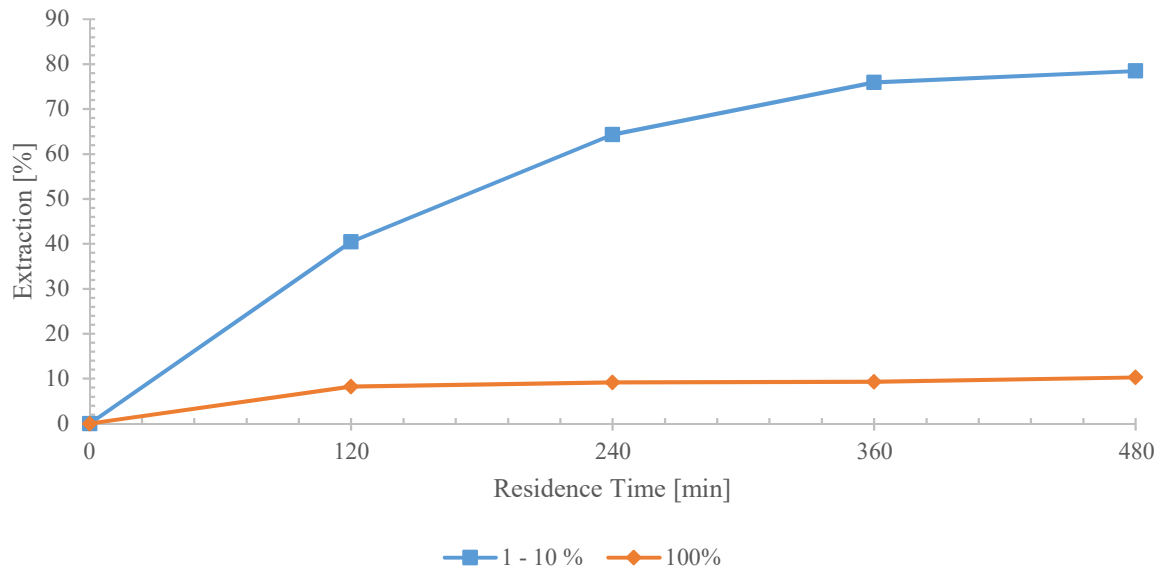


Figure 50: Effect of leftover Cu on Au extraction

Figure 50 illustrates the importance of a complete base metal leaching stage. When no Cu was extracted during the base metal leaching stage the Au dissolution was noticeably reduced in the precious metal leaching stage. The results in which no Cu was extracted is comparable to what Petter et al. [7] found. Figure 51 shows that increased $S_2O_3^{2-}$ degradation was present when all the Cu was left in the PCBs. This was probably due to the increased base metal leaching that took place, as the base metals are placed more superficially in PCBs. This could not be confirmed as results for base metals were not available.

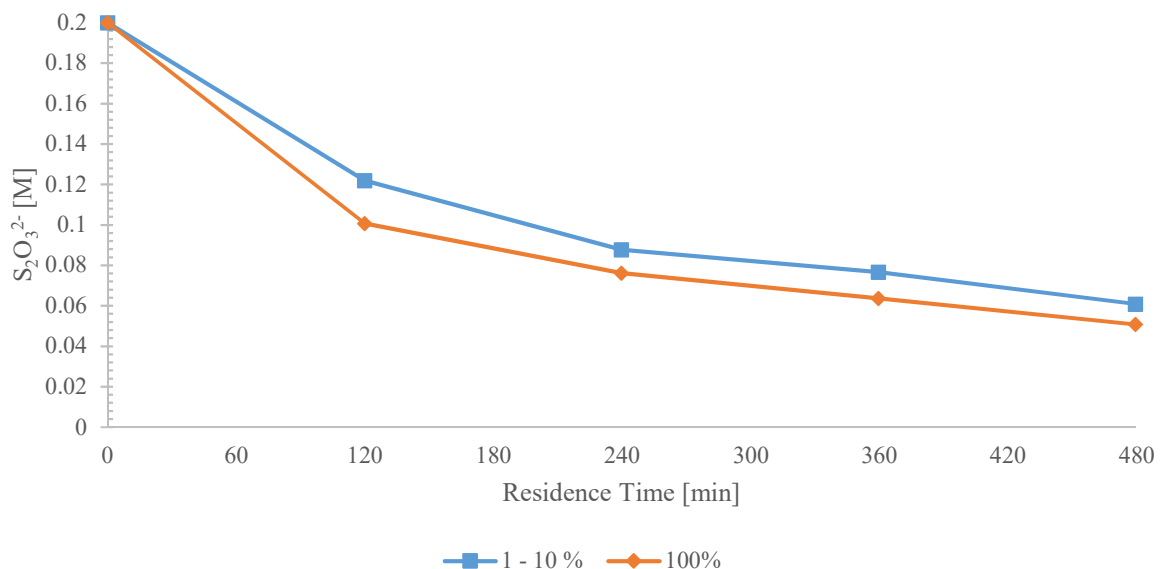


Figure 51: Effect of leftover Cu on thiosulphate degradation

4.3.3.5. Possibility for Counter-Current Leaching

The possibility for counter-current leaching was investigated by using the residue from the test that provided the optimum Au leaching (74.1 %) and re-leaching it in a second step at the same conditions. The second step leached only 11.1 % of the total Au, which brought the Au extraction during the precious metal leaching stage to 85.2 %. This suggested that counter-current leaching would not be efficient for 2 stages, as the lower Au content seemed to inhibit the ability of the lixiviant to extract the remainder of the Au. Increasing the number of stages could potentially lead to the complete extraction of Au, but utilising too many stages would not be economical.

5. Conclusions and Recommendations

5.1. Conclusions

By utilizing recommendations from literature and statistical results from the screening phase, it was determined that the $S_2O_3^{2-}$ concentration, NH_3 concentration, pH range and pulp density were significant factors that needed further investigation. A change in $S_2O_3^{2-}$ concentration and NH_3 concentration provided results that were consistent with literature in the sense that each species has an optimum point at which Au leaching is maximized. Excessive $S_2O_3^{2-}$ concentrations lead to a more prominent $Cu(S_2O_3^{2-})_3^{5-}$ complex which inhibits Au dissolution, while excessive NH_3 concentrations decrease the oxidation potential of the Cu(II)-Cu(I) couple which in turn reduces the driving force for the Au leaching reaction. It was found that a $S_2O_3^{2-}/NH_3$ ratio of 0.5 provided optimum Au leaching. Variation of the NH_3 concentration was found to be more significant at the lower pH range of 9 – 9.5. This was believed to be due to a higher concentration of NH_4^+ relative to NH_3 being present at lower pH values, which caused faster Au leaching.

More effective Au leaching was encountered at the lower pH range of 9 – 9.5, which could suggest that $Cu(NH_3)_4^{2+}$ was stabilized by hydroxide ions, which made Cu(II) more oxidizing and consequently increased Au leaching. Literature also suggests that a decreased rate of $S_2O_3^{2-}$ degradation is present at lower pH values. It was determined that a decrease in pulp density from 50 to 25 g/L resulted in increased Au leaching as the amount of reagent per unit weight of PCB increased. The full factorial phase achieved an optimum Au extraction of 78.47 % when PCB residue was leached at 0.2 M $S_2O_3^{2-}$, 0.4 M NH_3 , 0.02 M Cu(II), 25 g/L, 25°C, 1 – 10 % leftover Cu, pH range of 9 – 9.5 and 500 rpm for 8 h.

During the screening phase, it was determined that the variation in leftover Cu between 1 – 10 % and 11 – 20 % could not properly determine the effect that this parameter has on Au leaching. This could be attributed to the large deviation in feed composition that is commonly encountered with PCBs. The leftover Cu was investigated further by using the optimum conditions that were identified in the full factorial phase and substituting 100 % leftover Cu. The results confirmed the initial theory that the presence of Cu inhibits Au dissolution. The test in which 100 % Cu was left over produced only 10.28 % Au extraction. Increased amounts of Cu inhibit Au leaching through the dissolution of Cu to $Cu(NH_3)_2^+$ with the consumption of $Cu(NH_3)_4^{2+}$, which is the oxidizing agent for gold.

Three different rate models were compared in the full factorial phase to determine the rate limiting step. It was found that the rate of Au leaching was limited by the mass transport in the porous product layer. Diffusion through a product layer cannot normally control the reaction rate at the start of a reaction, but this could just be an indication of the fact that Au is not fully exposed in the PCBs.

During testing in the optimization phase, faster Au leaching was achieved in the first 120 minutes when the temperature was increased from 25 to 50°C. An increase in Cu(II) concentration initially led to an

increase in Au extraction at 120 minutes, after which the Au dissolution rate became slower. This was consistent with certain literature.

Investigation into the degradation of $S_2O_3^{2-}$ indicated that increased degradation/consumption is encountered at higher temperatures, higher Cu(II) concentrations and higher leftover Cu.

5.2. Recommendations

Au extraction could possibly be improved by including a pre-treatment process for the PCBs. Jha et al. [96] reported that by swelling the PCBs with an organic solution, you can separate Cu layers from epoxy resin. The organic solution, n-methyl-2-pyrrolidone, seeps into the PCBs and dissolves a variety adhesives and certain chemicals present in the PCB resin. The epoxy resin contains solder that consists mostly of Pb and Sn. By utilising this pre-treatment method, the selective leaching of base metals can be improved as well.

$S_2O_3^{2-}$ degradation is an important factor that needs to be minimized to achieve efficient leaching of precious metals. The degradation and consumption of $S_2O_3^{2-}$ are often referred to as a single factor when determining the influence of various parameters. Investigation into what part is due to degradation of $S_2O_3^{2-}$ and what part is due to metal complex formation, would provide a way to determine at what conditions $S_2O_3^{2-}$ could be efficiently utilized for metal extraction (by minimizing the loss due to degradation).

Counter-current leaching is a method that was briefly touched during this investigation. Further study could provide an answer as to how many stages are required to achieve complete Au dissolution and determine if the process is economically viable when utilized at those conditions.

6. References

- [1] G. Senanayake, "Gold leaching in non-cyanide lixiviant systems: critical issues on fundamentals and applications," *Minerals Engineering*, vol. 17, no. 6, pp. 785-801, 2004.
- [2] A. Tripathi, M. Kumar, D. C. Sau, A. Agrawal, S. Chakravarty and T. R. Mankhand, "Leaching of gold from the waste mobile phone printed circuit boards (PCBs) with ammonium thiosulphate," *International Journal of Metallurgical Engineering*, vol. 1, pp. 17-21, 2012.
- [3] J. Ficeriova, P. Balaz and E. Gock, "Leaching of gold, silver and accompanying metals from circuit boards (PCBs) waste," *Acta Montanistica Slovaca*, vol. 16, pp. 128-131, 2011.
- [4] V. H. Ha, J.-c. Lee, J. Jeong, H. T. Hai and M. K. Jha, "Thiosulfate leaching of gold from waste mobile phones," *Journal of Hazardous Materials*, vol. 178, pp. 1115-1119, 2010.
- [5] V. H. Ha, J.-c. Lee, T. H. Huynh, J. Jeong and B. D. Pandey, "Optimizing the thiosulfate leaching of gold from printed circuit boards of discarded mobile phone," *Hydrometallurgy*, vol. 149, pp. 118-126, 2014.
- [6] C. J. Oh, S. O. Lee, H. S. Yang, T. J. Ha and M. J. Kim, "Selective leaching of valuable metals from waste printed circuit boards," *Journal of the Air & Waste Management Association*, vol. 53, no. 7, pp. 897-902, 2003.
- [7] P. M. H. Petter, H. M. Veit and A. M. Bernardes, "Leaching of gold and silver from printed circuit board of mobile phones," *Metallurgy and Materials*, vol. 68, no. 1, pp. 61 - 68, 2015.
- [8] C. Abbruzzese, P. Fornari, R. Massidda, F. Veglio and S. Ubaldini, "Thiosulphate leaching for gold hydrometallurgy," *Hydrometallurgy*, vol. 39, pp. 265-276, 1995.
- [9] S. Camelino, J. Rao, R. L. Padilla and R. Lucci, "Initial studies about gold leaching from printed circuit boards (PCB's) of waste cell phones," *Procedia Materials Science*, vol. 9, pp. 105 - 112, 2015.
- [10] Empa, "ewasteinfo," 2009. [Online]. Available: <http://ewasteguide.info/>. [Accessed 07 March 2015].
- [11] POST, "Electronic waste," London, 2007.
- [12] A. Finlay and D. Liechti, "e-Waste assessment South Africa," 2008.

- [13] APME, *Plastics—A Material of Choice for the Electrical and Electronic Industry-Plastics Consumption and Recovery in Western Europe 1995*, Brussels: APME, 2004.
- [14] P. Kiddee, R. Naidu and M. H. Wong, “Electronic waste management approaches: An overview,” *Waste Management*, vol. 33, pp. 1237-1250, 2013.
- [15] J. K. Y. Chan, G. H. Xing, Y. Xu, Y. Liang, L. X. Chen, S. C. Wu, C. K. C. Wong, C. K. M. Leung and M. H. Wong, “Body loadings and health risk assessment of polychlorinated dibenzo-p-dioxins and dibenzofurans at an intensive electronic waste recycling site in China,” *Environmental Science & Technology*, vol. 41, pp. 7668-7674, 2007.
- [16] X. Huo, L. Peng, X. Xu, L. Zheng, B. Qui, Z. Qi, B. Zhang, D. Han and Z. Piao, “Elevated blood lead levels of children in Guiya, an electronic waste recycling town in China,” *Environmental Health Perspectives*, vol. 115, pp. 1113-1117, 2007.
- [17] W. Qu, X. Bi, G. Sheng, S. Lu, J. Fu, J. Yuan and L. Li, “Exposure to polybrominated diphenyl ethers among workers at an electronic waste dismantling region in Guangdong, China,” *Environment International*, vol. 33, pp. 1029-1034, 2007.
- [18] T. Wang, J. Fu, Y. Wang, C. Liao, Y. Tao and G. Jiang, “Use of scalp hair as indicator of human exposure to heavy metals in an electronic waste recycling area,” *Environmental Pollution*, vol. 157, pp. 2445-2451, 2009.
- [19] G. H. Xing, J. K. Y. Chan, A. O. W. Leung, S. C. Wu and M. H. Wong, “Environmental impact and human exposure to PCBs in Guiyu, an electronic waste recycling site in China,” *Environment International*, vol. 35, pp. 76-82, 2009.
- [20] G. Zhao, Z. Wang, M. H. Dong, K. Rao, J. Luo, D. Wang, J. Zha, S. Huang, Y. Xu and M. Ma, “PBBs, PBDEs, and PCBs levels in hair of residents around e-waste disassembly sites in Zhejiang Province, China, and their potential sources,” *Science of the Total Environment*, vol. 397, pp. 46-57, 2008.
- [21] L. Zheng, K. Wu, Y. Li, Z. Qi, D. Han, B. Zhang, C. Gu, G. Chen, J. Liu, S. Chen, X. Xu and X. Huo, “Blood lead and cadmium levels and relevant factors among children from an e-waste recycling town in China,” *Environmental Research*, vol. 108, pp. 15-20, 2008.
- [22] K. A. Asante, T. Agusa, C. A. Biney, W. A. Agyekum, M. Bello, M. Otsuka, T. Itai, S. Takahashi and S. Tanabe, “Multi-trace element levels and arsenic speciation in urine of e-waste recycling workers from Agbogbloshie, Accra in Ghana,” *Science of the Total Environment*, vol. 424, pp. 63-73, 2012.

- [23] A. Eguchi, K. Nomiyama, G. Devanathan, A. Subramanian, K. A. Bulbule, P. Parthasarathy, S. Takahashi and S. Tanabe, "Different profiles of anthropogenic and naturally produced organohalogen compounds in serum from residents living near a coastal area and e-waste recycling workers in India," *Environmental International*, vol. 47, pp. 8-16, 2012.
- [24] N. N. Ha, T. Agusa, K. Ramu, N. P. C. Tu, S. Murata, K. A. Bulbule, P. Parthasaraty, S. Takahashi, A. Subramanian and S. Tanabe, "Contamination by trace elements at e-waste recycling sites in Bangalore, India.," *Chemosphere*, vol. 76, pp. 9-15, 2009.
- [25] I. O. Ogunniyi, M. K. G. Vermaak and D. R. Groot, "Chemical composition and liberation characterization of printed circuit board comminution fines for beneficiation investigations," *Waste Management*, vol. 29, pp. 2140-2146, 2009.
- [26] M. Kaya, "Recovery of metals and nonmetals from electronic waste by physical and chemical recycling processes," *Waste Management*, vol. 57, pp. 64-90, 2016.
- [27] A. Khaliq, M. A. Rhamdhani, G. Brooks and S. Masood, "Metal extraction processes for electronic waste and existing industrial routes: A review and Australian perspective," *Resources*, vol. 3, pp. 152-179, 2014.
- [28] J. Hao, H. F. Wang, S. L. Song and X. Wang, "Status of recycling scrap printed circuit boards by pyrolysis," *China Resources Comprehensive Utilization*, vol. 26, pp. 30-33, 2008.
- [29] N. T. Yu, Z. X. Tie and F. H. Wang, "The methods for recycling of waste printed circuit boards," *China Resources Comprehensive Utilization*, vol. 29, pp. 21-24, 2011.
- [30] I. O. Ogunniyi and M. K. G. Vermaak, "Investigation of froth flotation for beneficiation of printed circuit board comminution fines," *Minerals Engineering*, vol. 22, pp. 378-385, 2009.
- [31] I. O. Ogunniyi and M. K. G. Vermaak, "Froth flotation for beneficiation of printed circuit boards comminution fines: An overview," *Mineral Processing and Extractive Metallurgy Review: An International Journal*, vol. 30, pp. 101-121, 2009.
- [32] I. O. Ogunniyi and M. K. G. Vermaak, "Improving printed circuit board physical processing - an overview," in *European Metallurgical Conference*, Dusseldorf, Germany, 2007.
- [33] C. Hagelucken, "Improving metal returns and eco-efficiency in electronics recycling - A holistic approach for interface optimisation between pre-processing and integrated metals smelting and refinery," *IEEE International Symposium on Electronics and the Environment*, pp. 218-223, 2006.

- [34] M. Iji and S. Yokoyama, "Recycling of printed wiring boards with mounted electronic components," *Circuit World*, vol. 23, pp. 10-15, 1997.
- [35] H. Yang, J. Liu and J. Yang, "Leaching copper from shredded particles of waste printed circuit boards," *Journal of Hazardous Materials*, vol. 187, pp. 393-400, 2011.
- [36] A. Mecucci and K. Scott, "Leaching and electrochemical recovery of copper, lead and tin from scrap printed circuit boards," *Journal of Chemical Technology and Biotechnology*, vol. 77, pp. 449-457, 2002.
- [37] I. Birloaga, I. De Michelis, F. Ferella, M. Buzatu and F. Veglio, "Study on the influence of various factors in the hydrometallurgical processing of waste printed circuit boards for copper and gold recovery," *Waste Management*, vol. 33, pp. 935-941, 2013.
- [38] J. Guo, J. Guo and Z. Xu, "Recycling of non-metallic fractions from waste printed boards: a review," *Journal of Hazardous Materials*, vol. 168, no. 2-3, pp. 567-590, 2009.
- [39] Y. J. Park and D. J. Faray, "Recovery of high purity precious metals from printed circuit boards," *Journal of Hazardous Materials*, vol. 164, pp. 1152-1158, 2009.
- [40] M. Goosey and R. Kellner, A scoping study: End-of-life printed circuit boards, Makati City: Intellect and the Department of Trade and Industry, 2002.
- [41] A. Akcil, C. Erust, C. S. Gahan, M. Ozgun, M. Sahin and A. Tuncuk, "Precious metal recovery from waste printed circuit boards using cyanide and non-cyanide lixivants - A review," *Waste Management*, vol. 45, pp. 258-271, 2015.
- [42] M. Laubertova, M. Novicky and T. Vindt, "The possibilities of hydrometallurgical treatment of discarded mobile phones," *International Student's Day of Metallurgy*, pp. 412-418, 2011.
- [43] A. Behnamfard, M. M. Salarirad and F. Veglio, "Process development for recovery of copper and precious metals from waste printed circuit boards with emphasize on palladium and gold leaching and precipitation," *Waste Management*, vol. 33, pp. 2354-2363, 2013.
- [44] M. I. Reyes, I. Rivera, F. Patino, M. U. Flores and M. Reyes, "Total recovery of gold contained in computer printed circuit boards. Leaching kinetics of Cu, Zn and Ni," *Journal of the Mexican Chemical Society*, vol. 56, pp. 144-148, 2012.
- [45] P. M. H. Petter, H. M. Veit and A. M. Bernardes, "Evaluation of gold and silver leaching from printed circuit board of cellphones," *Waste Management*, vol. 34, pp. 475-482, 2014.

- [46] I. Birloaga, V. Coman, B. Kopacek and F. Veglio, "An advanced study on the hydrometallurgical processing of waste computer printed circuit boards to extract their valuable content of metals," *Waste Management*, vol. 34, pp. 2581-2586, 2014.
- [47] Y. Zhang, S. Liu, H. Xie, X. Zeng and J. Li, "Current status on leaching precious metals from waste printed circuit boards," *Procedia Environmental Sciences*, vol. 16, pp. 560-568, 2012.
- [48] Y. Lu and Z. Xu, "Precious metals recovery from waste printed circuit boards: A review for current status and perspective," *Resources, Conservation and Recycling*, vol. 113, pp. 28-39, 2016.
- [49] A. C. Kasper, J. C. Abad, M. G. Gabaldon, H. M. Veit and V. P. Herranz, "Determination of the potential gold electrowinning from an ammoniacal thiosulphate solution applied to recycling of printed circuit board scraps," *Waste Management & Research*, vol. 34, pp. 47-57, 2016.
- [50] A. C. Grosse, G. W. Dicoski, M. J. Shaw and P. R. Haddad, "Leaching and recovery of gold using ammoniacal thiosulfate leach liquors (a review)," *Hydrometallurgy*, vol. 69, pp. 1-21, 2003.
- [51] M. G. Aylmore and D. M. Muir, "Thermodynamic analysis of gold leaching by ammoniacal thiosulfate using Eh/pH and speciation diagrams," *Minerals & Metallurgical Processing*, vol. 18, pp. 221-227, 2001.
- [52] M. G. Aylmore and D. M. Muir, "Thiosulfate leaching of gold - A review," *Minerals Engineering*, vol. 14, pp. 135-174, 2001.
- [53] P. L. Breuer and M. I. Jeffrey, "An electrochemical study of gold oxidation in solutions containing thiosulfate, ammonia and copper," in *Electrochemistry Meeting*, Toronto, 2000.
- [54] P. L. Breuer and M. I. Jeffrey, "Thiosulfate leaching kinetics of gold in the presence of copper and ammonia," *Minerals Engineering*, vol. 13, no. 10-11, pp. 1071-1081, 2000.
- [55] P. L. Breuer and M. I. Jeffrey, "Copper catalyzed oxidation of thiosulphate by oxygen in gold leach solutions.," *Minerals Engineering*, vol. 16, no. 1, pp. 21-30, 2003.
- [56] C. K. Chu, P. L. Breuer and M. I. Jeffrey, "The impact of thiosulfate oxidation products on the oxidation of gold in ammonia thiosulfate solutions," *Minerals Engineering*, vol. 16, no. 3, pp. 265-271, 2003.
- [57] M. I. Jeffrey, P. L. Breuer and C. K. Chu, "The importance of controlling oxygen addition during thiosulfate leaching of gold ores," *International Journal of Mineral Processing*, vol. 72, no. 1-4, pp. 323-330, 2003.

- [58] N. Naseri Joda and F. Rashchi, "Recovery of ultra fine grained silver and copper from PC board scraps," *Separation and Purification Technology*, vol. 92, pp. 36-42, 2012.
- [59] M. K. Jha, J.-c. Lee, A. Kumari, P. K. Choubey, V. Kumar and J. Jeong, "Pressure leaching of metals from waste printed circuit boards using sulfuric acid," *Journal of The Minerals, Metals, & Materials Society*, vol. 63, pp. 29-32, 2011.
- [60] K. Koyama, M. Tanaka and J.-c. Lee, "Copper leaching behaviour from waste printed circuit board in ammoniacal alkaline solution," *Metrials Transactions*, vol. 47, pp. 1788-1792, 2006.
- [61] H. L. Le, J. Jeong, J.-C. Lee, B. D. Pandey, J.-M. Yoo and T. H. Huyunh, "Hydrometallurgical process for copper recovery from waste printed circuit boards (PCBs)," *Mineral Processing & Extractive Metallurgy Review*, vol. 32, pp. 90-104, 2011.
- [62] R. Vijayaram, D. Nesakumar and K. Chandramohan, "Copper extraction from the discarded printed circuit board by leaching," *Research Journal of Engineering Sciences*, vol. 2, pp. 11-14, 2013.
- [63] W. A. Rossouw, *Effect of mechanical pre-treatment on leaching of base metals from waste printed circuit boards*, Stellenbosch: Stellenbosch University, 2015.
- [64] F. Habashi, *Textbook of Hydrometallurgy*, Metallurgie Extractive Quebec, 1999.
- [65] S. Gos and A. Rubo, *The relevance of alternative lixivants with regard to technical aspects, work safety and environmental safety*, Hanau: Cyplus. Degussa AG, 2001.
- [66] F.-R. Xiu, Q. Yingying and Z. Fu-Shen, "Leaching of Au, Ag, and Pd from waste printed circuit boards of mobile phone by iodide lixiviant after supercritical water pre-treatment," *Waste Management*, no. 41, pp. 134-141, 2015.
- [67] F.-R. Xiu, Q. Yingying and F.-S. Zhang, "Recovery of metals from waste printed circuit boards by supercritical water pre-treatment combined with acid leaching process," *Waste Management*, no. 33, pp. 1251-1257, 2013.
- [68] J. W. Ahn, D. W. Chung, K. W. Lee, J.-G. Ahn and H. Y. Sohn, "Nitric Acid Leaching of Base Metals from Waste PDP Electrode Scrap and Recovery of Ruthenium Content from Leached Residues," *Materials Transactions*, vol. 52, no. 5, pp. 1063-1069, 2011.
- [69] A. Chaurasia, K. K. Singh and T. R. Mankhand, "Extraction of Tin and Copper by Acid Leaching of PCBs," *International Journal of Metallurgical Engineering*, no. 2, pp. 243-248, 2013.

- [70] McGraw Hill Education, Complete Chemistry: JEE Main, India: Paperback Press, 2016.
- [71] F. R. Carillo-Pedroza, M. J. Soria-Aguilar, E. Salinas-Rodriguez, A. Martinez-Luevanos, T. E. Pecina-Trevino and A. Davalos-Sanchez, "Oxidative hydrometallurgy of sulphide minerals," in *Recent researches in metallurgical engineering - from extraction to forming*, M. Nusheh, Ed., Shanghai, InTech, 2012, pp. 25-42.
- [72] R. H. Petrucci, W. S. Harwood, G. E. Herring and J. Madura, General Chemistry : Principles and Modern Applications, 9th ed., New Jersey: Prentice Hall, 2006.
- [73] D. Feng and J. S. J. van Deventer, "The effect of iron contaminants on thiosulphate leaching of gold," *Minerals Engineering*, vol. 23, pp. 399-406, 2010.
- [74] M. I. Jeffrey, "Kinetic aspects of gold and silver leaching in ammonia-thiosulfate solutions," *Hydrometallurgy*, vol. 60, no. 1, pp. 7-16, 2001.
- [75] E. Molleman and D. Dreisinger, "The treatment of copper-gold ores by ammonium thiosulfate leaching," *Hydrometallurgy*, vol. 66, pp. 1-21, 2002.
- [76] F. K. Crundwell, "The dissolution and leaching of minerals. Mechanisms, myths and misunderstandings," *Hydrometallurgy*, vol. 139, pp. 132-148, 2013.
- [77] C. Cao, J. Hu and Q. Gong, "Leaching of gold by low concentration thiosulfate solution," *The Transactions of Nonferrous Metals Society of China*, vol. 2, pp. 21-25, 1992.
- [78] M. I. Jeffrey, P. L. Breuer and W. L. Choo, "A kinetic study that compares the leaching of gold in the cyanide, thiosulfate, and chloride systems," *Metallurgical and Materials Transactions*, vol. 32B, pp. 979-986, 2001.
- [79] G. Senanayake, "Review of rate constants for thiosulphate leaching of gold from ores, concentrates and flat surfaces: Effect of host minerals and pH," *Minerals Engineering*, vol. 20, pp. 1-15, 2007.
- [80] A. P. Prosser, "Review of uncertainty in the collection and interpretation of leaching data," *Hydrometallurgy*, vol. 41, pp. 119-153, 1996.
- [81] B. F. G. Johnson and R. Davis, Gold in comprehensive inorganic chemistry, vol. 5, J. C. Bailar, H. J. Emeleus, R. Nyholm and A. F. Trotman-Dickenson, Eds., Oxford: Pergamon Press, 1973.

- [82] R. D. Hancock, N. P. Finkelstein and A. Evers, "Linear free energy relationships in aqueous complex-formation reactions of the d10 metals ions," *Journal of Inorganic Nuclear Chemistry*, vol. 36, pp. 2539-2543, 1974.
- [83] R. Y. Wan, "Importance of solution chemistry for thiosulfate leaching of gold," in *Proceedings of the World Gold 97*, Singapore, 1997.
- [84] D. Feng and J. S. J. van Deventer, "Ammoniacal thiosulfate leaching of gold from waste mobile phones," *Journal of Hazardous Materials*, vol. 82, pp. 126-132, 2006.
- [85] D. Feng and J. S. J. van Deventer, "The role of oxygen in thiosulphate leaching of gold," *Hydrometallurgy*, vol. 85, pp. 193-202, 2007.
- [86] L. F. Kozin and V. T. Melekhin, "Extraction of gold from ores and concentrates by leaching with the use of cyanides and alternative reagents," *Russian Journal of Applied Chemistry*, vol. 77, pp. 1573-1592, 2004.
- [87] K. M. Habib Al Razi, "Resourceful recycling process of waste desktop computers: A review study," *Resources, Conservation and Recycling*, vol. 110, pp. 30-47, 2016.
- [88] F. Arslan and B. Sayiner, "Extraction of gold and silver from turkish gold ore by ammoniacal thiosulphate leaching," *Mineral Processing & Extractive Metallurgy Review*, vol. 29, pp. 68-82, 2008.
- [89] G. Senanayake, "The role of ligands and oxidants in thiosulfate leaching of gold," *Gold Bulletin*, no. 38, pp. 170-179, 2005.
- [90] D. M. Puente-Siller, J. C. Fuentes-Aceituno and F. Nava-Alonso, "A kinetic-thermodynamic study of silver leaching in thiosulfate-copper-ammonia-EDTA solutions," *Hydrometallurgy*, Vols. 134-135, pp. 124-131, 2013.
- [91] EAG Laboratories, "EAG Laboratories," 2014. [Online]. Available: www.eag.com. [Accessed 15 July 2016].
- [92] R. V. Thurston, R. C. Russo and K. Emerson, "Aqueous Ammonia Equilibrium - Tabulation of Percent Un-Ionized Ammonia," United States Environmental Protection Agency, Minnesota, 1979.

- [93] R. K. Rath, N. Hiroyoshi, M. Tsunekawa and T. Hirajima, "Ammoniacal thiosulphate leaching of gold ore," *The European Journal of Mineral Processing and Environmental Protection*, vol. 3, pp. 344-352, 2003.
- [94] D. Zipperian, S. Raghavan and J. P. Wilson, "Gold extraction by ammoniacal thiosulfate leaching from a rhyolite ore," *Hydrometallurgy*, vol. 19, pp. 136-375, 1988.
- [95] T. Fujita, W. T. Yen, B. Jeyadevan, S. Takano, E. Toyota and E. Kuzuno, "Gold leaching from electric machine part scraps using thiosulphate or hypochlorite," in *4th International Symposium on East-Asian Resources Recycling Technology*, Kunming, 1997.
- [96] M. K. Jha, A. Kumari, P. K. Choubey and J.-c. Lee, "Leaching of lead from solder material of waste printed circuit boards (PCBs)," *Hydrometallurgy*, Vols. 121-124, pp. 28-34, 2012.

7. Appendices

7.1. Appendix A: PCB Characterisation

7.1.1. Aqua Regia Preparation

To illustrate the required quantities of HNO₃ and HCl for the preparation of a 200 mL solution of Aqua Regia, refer to Table 34.

Table 34: Calculation of required quantities of aqua regia components per 200 mL digestion

Substance	Concentration [wt%]	Mw [g/mol]	Molar Ratio	Required [mol]	Required [g]	Density [g/L]	Required [mL]	Volume Ratio
HNO ₃	55.00	63.01	1.00	0.53	60.24	1339.30	44.98	1.00
HCl	32.00	36.46	3.00	1.58	179.72	1159.30	155.02	3.45

7.1.2. Experimental Data

The values contained in Table 35 show the amount of metals leached during Aqua Regia residence time tests of 20 g PCB samples.

Table 35: Results of Aqua Regia residence time tests of 6 different PCB samples

Aqua Regia Test	Time [h]	Mass Leached [mg]									
		Ag	Al	Au	Co	Cu	Fe	Ni	Pb	Sn	Zn
1	4	7.14	74.16	2.06	0.58	5259.61	281.74	116.41	251.33	1181.42	369.13
	6	8.55	75.45	2.40	0.52	5395.86	271.95	112.03	239.68	1165.12	349.04
	10	9.02	90.41	2.89	0.58	5381.96	294.35	117.92	251.27	1200.22	363.67
	14	8.56	99.36	3.20	0.56	5453.96	289.77	115.23	244.11	1164.32	351.82
	22	16.15	133.42	3.39	0.55	5444.30	298.65	117.74	244.71	1189.12	346.46
	24	17.24	143.86	3.51	0.51	5499.37	297.09	118.58	246.03	1196.91	349.03
2	4	6.39	54.92	1.84	0.29	4917.44	69.87	73.23	183.73	915.25	322.61
	6	6.40	58.85	2.39	0.32	4982.93	77.49	74.99	196.57	986.66	329.91
	10	6.07	67.32	2.56	0.31	4962.93	77.21	75.56	195.30	976.05	323.79
	14	6.96	83.25	2.97	0.33	5211.24	84.65	82.24	211.07	1045.79	339.59
	22	8.41	106.30	3.15	0.33	5197.67	86.62	85.10	211.36	1067.52	330.14
	24	8.49	114.79	3.38	0.34	5213.83	88.70	88.20	216.47	1106.85	338.60
3	4	5.38	100.41	1.65	0.69	5310.99	47.14	65.09	209.91	900.73	578.94
	6	5.64	104.59	1.80	0.68	5412.43	48.81	66.64	211.20	908.86	574.08
	10	7.63	114.03	2.04	0.69	5378.01	50.59	69.21	215.07	925.32	584.23
	14	6.65	116.46	2.02	0.64	5362.13	48.64	65.50	202.31	900.99	545.56
	22	7.50	148.82	2.45	0.74	5426.71	53.20	71.48	218.18	941.11	586.48
	24	9.09	151.18	2.35	0.71	5418.94	52.66	70.44	216.69	947.30	583.22
4	4	5.34	41.30	1.88	0.47	4415.37	102.81	62.95	192.60	954.04	355.49
	6	8.39	47.43	2.23	0.52	4778.09	119.34	69.74	209.49	1049.52	377.67
	10	9.04	56.66	2.79	0.54	4747.98	122.54	72.09	210.23	1044.08	374.60
	14	10.16	63.79	2.96	0.55	4687.17	209.91	72.24	209.35	1058.45	368.03
	22	10.57	80.21	3.19	0.52	4793.27	129.14	74.69	214.58	1065.60	373.72
	24	12.35	88.36	3.40	0.57	5002.32	132.41	77.47	223.10	1105.47	387.67
5	30	13.75	128.37	2.38	1.15	4373.95	125.56	70.92	221.93	1439.92	374.13
6	30	11.5	135.08	2.43	0.9	4063.47	83.48	49.79	176.8	932.9	281.03

Figure 52 illustrates the average metal content found in the PCBs.

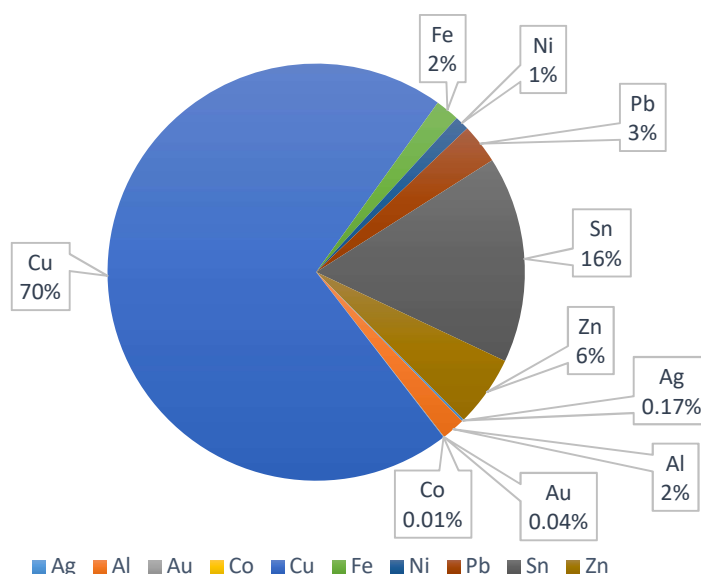
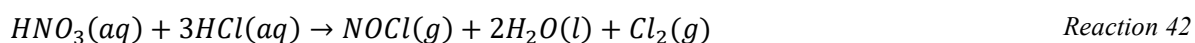


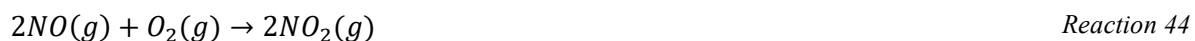
Figure 52: PCB metal content

7.1.3. Aqua Regia Safety

Aqua Regia is an oxidative, acidic and corrosive mixture that is used to dissolve metals. This means that it is extremely important to know the risks associated with the preparation of Aqua Regia, as well as the proper handling procedures. The chemical reaction associated with the preparation is given in Reaction 42.



Nitrosyl chloride (NOCl) will decompose over time which leads to the production of nitric oxide (NO₂) and additional chlorine gas. The NO will auto-oxidise to nitrogen dioxide (NO₂). Cl₂, NO and NO₂ are poisonous gasses. The gas build-up will eventually lead to a container rupture if the container is closed.



During preparation, the following guidelines must be adhered to:

- Wear appropriate PPE
- Work inside a fume hood
- Never add any form of organics to Aqua Regia as it might cause an explosion
- Make sure that HNO₃ is added to HCl each time a solution is prepared

7.2. Appendix B: Base Metal Leaching

7.2.1. Initial Base Metal Leaching Tests

The extent of leaching during initial base metal leaching tests are given in Table 36.

Table 36: Initial base metal leaching tests

Test	Step	Mass Leached [mg]									
		Ag	Al	Au	Co	Cu	Fe	Ni	Pb	Sn	Zn
1	1	0.05	141.82	0.00	1.43	53.49	293.25	165.16	715.11	211.97	1002.76
	2	1.63	246.41	0.00	1.17	18334.25	197.64	129.25	6.90	10.67	1563.73
	Aqua Regia	16.80	470.50	7.58	0.34	735.41	41.77	49.05	12.60	876.63	70.85
2	1	0.28	121.06	0.02	1.43	46.70	309.37	109.19	749.24	109.82	972.49
	2	1.24	221.22	0.01	0.36	16668.32	143.38	143.62	0.99	29.69	1737.47
	Aqua Regia	18.17	752.96	8.16	0.60	866.47	40.15	49.81	23.68	651.19	98.48

Table 37 contains the comparison of the initial base metal leaching tests with results obtained from [63].

Table 37: Base metal leaching comparison

Source	Step	Extraction [%]									
		Ag	Al	Au	Co	Cu	Fe	Ni	Pb	Sn	Zn
[63]	1	1.30	15.30	0.00	-	0.20	76.20	33.60	97.90	7.00	1.70
	2	8.50	18.40	0.00	-	96.50	16.30	57.80	0.00	7.50	93.40
	Total	9.80	33.70	0.00	-	96.70	92.50	91.40	97.90	14.50	95.10
Test 1	1	0.30	16.52	0.00	48.50	0.28	55.05	48.09	97.35	19.28	38.02
	2	8.82	28.69	0.00	39.91	95.87	37.10	37.63	0.94	0.97	59.29
	Total	9.12	45.21	0.00	88.40	96.15	92.16	85.72	98.28	20.25	97.31
Test 2	1	1.43	11.05	0.19	59.88	0.27	62.77	36.08	96.81	13.89	34.63
	2	6.31	20.20	0.18	14.89	94.81	29.09	47.46	0.13	3.75	61.87
	Total	7.74	31.25	0.37	74.77	95.07	91.85	83.54	96.94	17.64	96.49

7.2.2. Large-Scale HNO₃ Leaching

Table 38 contains the amount of metals leached from 2 kg of PCBs during the large scale HNO₃ leaching step. Negative values indicate unreadable values, i.e. very low or no metal content.

Table 38: Amount of metals leached from 2 kg of PCBs during large scale HNO₃ leaching step

Residence Time [min]	Mass Leached [g]									
	Ag	Al	Au	Co	Cu	Fe	Ni	Pb	Sn	Zn
80	-0.01	0.75	0.00	0.00	0.42	5.95	0.72	9.76	32.56	1.97
120	0.00	0.98	0.00	0.01	0.45	6.37	1.09	12.72	51.48	2.67
420	0.00	2.07	0.00	0.03	0.92	7.55	2.89	19.25	34.53	7.92
480	0.00	2.19	0.00	0.03	1.17	7.61	2.98	19.62	32.12	8.17
510	0.00	2.30	0.00	0.03	1.34	7.59	3.24	19.71	25.50	8.21
540	0.01	2.53	0.00	0.03	1.33	7.60	3.58	19.53	21.86	8.58
600	0.02	2.43	0.00	0.03	1.31	7.64	3.87	19.85	26.11	9.91
660	0.02	2.58	0.00	0.03	1.34	7.70	3.97	19.89	13.08	10.36

The extent of leaching during the large scale HNO₃ leaching step is illustrated in Table 39.

Table 39: Metal extraction at various times during large scale HNO₃ leaching step

Residence Time [min]	Extraction [%]									
	Ag	Al	Au	Co	Cu	Fe	Ni	Pb	Sn	Zn
0	0.00	0.00	0.00	0.00	0.00	0.00	0.00	0.00	0.00	0.00
80	-0.62	5.87	0.03	7.03	0.08	45.80	9.12	44.99	29.03	5.12
120	-0.38	7.75	0.00	12.02	0.09	49.01	13.71	58.67	45.90	6.91
420	-0.05	16.32	0.00	36.87	0.19	58.07	36.43	88.79	30.79	20.53
480	-0.01	17.29	0.00	40.74	0.24	58.56	37.59	90.46	28.64	21.20
510	0.11	18.11	0.00	41.77	0.27	58.41	40.91	90.90	22.74	21.28
540	0.58	19.91	0.06	45.34	0.27	58.47	45.24	90.05	19.49	22.25
600	1.98	19.13	0.00	48.05	0.27	58.80	48.84	91.55	18.63	25.70
660	1.82	20.36	0.09	48.60	0.27	59.22	50.04	91.73	11.66	26.88

7.2.3. Small Scale H₂SO₄ Leaching

Table 40 shows the amount of metals leached from 80 g of PCBs during the small scale H₂SO₄ leaching step.

Table 40: Amount of metals leached from 80 g of PCBs during small scale H₂SO₄ leaching step

Residence Time [min]	Mass Leached [mg]									
	Ag	Al	Au	Co	Cu	Fe	Ni	Pb	Sn	Zn
0	0.00	0.00	0.00	0.00	0.00	0.00	0.00	0.00	0.00	0.00
180	0.85	87.53	-0.05	0.55	16559.67	147.59	112.68	-0.85	11.95	997.45
240	1.15	92.65	0.02	0.63	17389.53	152.96	118.56	-1.16	39.52	1025.59
300	1.21	105.37	0.01	0.69	18614.89	150.55	120.59	0.02	41.45	1011.82
360	4.19	122.01	0.02	0.74	18800.77	178.42	120.69	-0.49	64.52	1021.60
480	1.27	144.22	-0.06	0.82	18763.06	155.18	121.57	-2.68	102.73	1030.43
540	1.73	153.89	0.01	0.94	18817.59	164.48	120.71	-1.61	234.87	1043.76

The extent of leaching during the small scale H₂SO₄ leaching step is given in Table 41.

Table 41: Metal extraction at various times during small scale H₂SO₄ leaching step

Residence Time [min]	Extraction [%]									
	Ag	Al	Au	Co	Cu	Fe	Ni	Pb	Sn	Zn
0	0.00	0.00	0.00	0.00	0.00	0.00	0.00	0.00	0.00	0.00
180	1.76	17.24	0.00	19.57	84.00	28.39	35.55	-0.10	0.27	64.67
240	2.39	18.25	0.15	22.58	88.21	29.42	37.41	-0.13	0.88	66.49
300	2.50	20.75	0.11	24.72	94.42	28.96	38.05	0.00	0.92	65.60
360	8.67	24.03	0.14	26.51	95.36	34.32	38.08	-0.06	1.44	66.23
480	2.64	28.40	0.00	29.48	95.17	29.85	38.36	-0.31	2.29	66.81
540	3.58	30.31	0.12	33.79	95.45	31.64	38.08	-0.19	5.24	67.67

7.3. Appendix C: Precious Metal Leaching

7.3.1. Screening Phase

7.3.1.1. Gold and Silver Leaching

The final Au and Ag leaching during the screening phase experiments are given in Table 42 and Table 43.

Table 42: Calculating the Au extraction at the end of the screening phase

Test	Au leached [mg]					Total Extraction [%]	PML Stage Extraction [%]
	Residue	BML Tests		PML Test	Highest Amount in PML Test		
		HNO ₃ Leaching	H ₂ SO ₄ Leaching				
1	1.227	0.002	0.002	0.218	0.257	14.89	14.64
2	1.938	0.003	0.004	0.246	0.775	9.31	9.03
3	1.237	0.002	0.002	0.307	0.307	20.09	19.84
4	2.127	0.003	0.004	0.934	0.934	30.69	30.45
5	1.149	0.003	0.004	0.183	0.435	11.96	11.48
6	0.821	0.002	0.002	0.165	0.182	16.80	16.43
7	3.096	0.003	0.004	0.528	0.528	14.75	14.54
8	1.704	0.002	0.002	0.182	0.234	9.58	9.38
9	1.631	0.003	0.004	0.491	0.491	23.43	23.07
10	0.658	0.002	0.002	0.087	0.216	10.38	9.95
11	2.367	0.003	0.004	0.676	0.676	22.41	22.16
12	1.150	0.002	0.002	0.190	0.209	14.19	13.91
13	1.515	0.002	0.002	0.152	0.187	9.13	8.91
14	1.590	0.003	0.004	0.531	0.534	25.29	24.93
15	1.916	0.002	0.002	0.282	0.282	12.97	12.80
16	1.303	0.003	0.004	0.586	0.586	31.30	30.90
17	1.604	0.002	0.002	0.157	0.165	9.09	8.88
18	1.042	0.003	0.004	0.144	0.300	11.24	10.68
19	0.226	0.002	0.002	0.187	0.187	45.79	44.88
20	1.586	0.003	0.004	0.408	0.408	20.75	20.37
21	1.287	0.003	0.004	0.127	0.246	8.72	8.23
22	0.864	0.002	0.002	0.071	0.119	7.58	7.19
23	1.817	0.003	0.004	0.286	0.286	13.91	13.55
24	1.224	0.002	0.002	0.145	0.145	10.86	10.58
25	1.013	0.003	0.004	0.360	0.360	26.63	26.08
26	1.548	0.002	0.002	0.112	0.159	6.79	6.57
27	1.965	0.003	0.004	0.887	0.887	31.27	31.01
28	0.955	0.002	0.002	0.112	0.112	10.85	10.50
29	1.030	0.002	0.002	0.114	0.155	9.94	9.62
30	1.187	0.003	0.004	0.330	0.330	22.11	21.61
31	2.548	0.002	0.002	0.356	0.356	12.37	12.24
32	1.057	0.003	0.004	0.382	0.382	26.91	26.38

Table 43: Calculating the Ag extraction at the end of the screening phase

Test	Ag leached [mg]					Total Extraction [%]	PML Stage Extraction [%]
	Residue	BML Tests		PML Test	Highest Amount in PML Test		
		HNO ₃ Leaching	H ₂ SO ₄ Leaching				
1	0.703	0.138	0.270	3.223	3.382	80.80	71.73
2	7.026	0.275	0.540	3.872	7.576	30.40	25.11
3	0.806	0.138	0.270	2.823	3.392	70.15	61.30
4	1.845	0.275	0.540	8.032	8.032	82.74	75.11
5	1.439	0.275	0.540	3.059	5.286	51.39	40.57
6	0.784	0.138	0.270	1.572	1.683	68.86	54.67
7	3.607	0.275	0.540	4.758	4.832	60.23	51.42
8	1.598	0.138	0.270	2.756	5.768	40.70	35.45
9	4.115	0.275	0.540	7.329	8.181	62.12	55.90
10	1.065	0.138	0.270	1.399	2.160	49.73	38.50
11	3.386	0.275	0.540	6.285	6.285	67.71	59.93
12	1.363	0.138	0.270	6.039	6.039	82.54	77.32
13	0.623	0.138	0.270	1.767	2.284	65.61	53.31
14	4.951	0.275	0.540	8.996	8.996	66.46	60.94
15	1.472	0.138	0.270	2.670	2.681	67.48	58.54
16	1.526	0.275	0.540	3.503	4.856	60.00	48.67
17	2.113	0.138	0.270	3.439	3.439	64.55	57.71
18	3.307	0.275	0.540	2.090	3.373	38.76	27.88
19	0.416	0.138	0.270	1.767	1.879	80.47	65.38
20	0.914	0.275	0.540	3.419	3.571	79.87	64.49
21	1.570	0.275	0.540	1.818	2.411	54.90	37.90
22	0.658	0.138	0.270	1.292	1.309	71.57	54.39
23	2.982	0.275	0.540	3.351	3.351	58.29	46.87
24	1.540	0.138	0.270	1.511	1.627	53.67	42.26
25	2.321	0.275	0.540	4.155	4.155	68.16	56.98
26	1.089	0.138	0.270	1.397	1.603	58.23	45.07
27	2.924	0.275	0.540	6.228	6.615	68.03	60.15
28	0.786	0.138	0.270	2.282	2.282	77.38	65.65
29	0.986	0.138	0.270	2.021	2.044	70.64	58.78
30	1.254	0.275	0.540	3.609	3.711	76.54	62.43
31	2.867	0.138	0.270	3.707	3.707	58.94	53.10
32	2.761	0.275	0.540	4.884	4.884	67.37	57.73

The extent of Au and Ag leaching during screening test 1 - 16 are given in Table 44.

Table 44: Extent of Au and Ag leaching during the screening phase experiments

Test	Residence Time [min]	Mass Leached [mg]		Extraction (%)	
		Ag	Au	Ag	Au
1	0	0.000	0.000	0.00	0.00
	30	3.146	0.126	70.03	8.45
	60	3.050	0.138	67.89	9.25
	90	3.044	0.199	67.76	13.37
	120	3.229	0.194	71.86	13.02
	180	3.283	0.243	73.06	16.33
	240	3.266	0.228	72.68	15.35
	300	3.281	0.246	73.03	16.50
	360	3.382	0.257	75.28	17.25
	420	3.323	0.217	73.97	14.58
	480	3.223	0.218	71.73	14.64

2	0	0.000	0.000	0.00	0.00
	30	6.091	0.653	39.51	26.40
	60	7.576	0.756	49.14	27.81
	90	5.049	0.774	32.75	28.47
	120	5.243	0.765	34.01	28.10
	180	5.326	0.775	34.55	28.47
	240	5.490	0.706	35.61	25.93
	300	5.197	0.655	33.71	24.08
	360	5.003	0.447	32.45	16.44
	420	3.804	0.298	24.67	10.95
	480	3.872	0.246	25.11	9.03
3	0	0.000	0.000	0.00	0.00
	30	3.221	0.265	69.95	17.13
	60	3.392	0.256	73.65	16.51
	90	3.107	0.285	67.47	18.43
	120	2.755	0.274	59.83	17.67
	180	2.760	0.262	59.93	16.90
	240	2.757	0.294	59.87	18.99
	300	2.704	0.276	58.71	17.86
	360	2.672	0.292	58.01	18.88
	420	2.473	0.292	53.70	18.86
	480	2.823	0.307	61.30	19.84
4	0	0.000	0.000	0.00	0.00
	30	6.132	0.454	57.35	14.79
	60	7.001	0.634	65.47	20.67
	90	7.398	0.721	69.19	23.50
	120	7.517	0.748	70.30	24.39
	180	7.736	0.770	72.35	25.09
	240	7.742	0.878	72.40	28.61
	300	7.860	0.893	73.51	29.09
	360	7.777	0.894	72.74	29.15
	420	7.754	0.900	72.52	29.33
	480	8.032	0.934	75.11	30.45
5	0	0.000	0.000	0.00	0.00
	30	2.439	0.095	32.34	5.99
	60	5.286	0.346	70.10	21.73
	90	4.272	0.378	56.64	23.75
	120	4.235	0.403	56.16	25.33
	180	4.163	0.435	55.20	27.32
	240	3.482	0.362	46.17	22.78
	300	3.111	0.328	41.25	20.63
	360	3.112	0.258	41.27	16.21
	420	3.078	0.189	40.82	11.85
	480	3.059	0.183	40.57	11.48
6	0	0.000	0.000	0.00	0.00
	30	0.894	0.015	31.11	1.45
	60	1.165	0.075	40.52	7.44
	90	1.683	0.182	58.55	18.09
	120	1.489	0.146	51.81	14.48
	180	1.487	0.166	51.74	16.45
	240	1.515	0.165	52.72	16.38
	300	1.613	0.158	56.13	15.67
	360	1.554	0.170	54.08	16.88
	420	1.622	0.165	56.42	16.38
	480	1.572	0.165	54.67	16.43

7	0	0.000	0.000	0.00	0.00
	30	4.380	0.495	47.33	13.63
	60	4.388	0.471	47.42	12.96
	90	4.786	0.508	51.71	13.99
	120	4.399	0.491	47.54	13.53
	180	4.346	0.518	46.96	14.26
	240	4.440	0.495	47.98	13.63
	300	4.832	0.495	52.21	13.64
	360	4.738	0.466	51.20	12.82
	420	4.759	0.483	51.42	13.30
	480	4.758	0.528	51.42	14.54
	8	0	0.000	0.000	0.00
30		4.394	0.118	56.53	6.06
60		5.768	0.142	74.20	7.30
90		4.658	0.210	59.92	10.81
120		4.037	0.175	51.93	9.01
180		3.381	0.181	43.50	9.34
240		3.530	0.213	45.42	10.98
300		3.204	0.234	41.22	12.06
360		3.230	0.200	41.55	10.32
420		2.792	0.207	35.92	10.68
480		2.756	0.182	35.45	9.38
9		0	0.000	0.000	0.00
	30	5.973	0.297	45.56	13.94
	60	6.456	0.354	49.24	16.62
	90	6.933	0.355	52.88	16.66
	120	8.181	0.424	62.39	19.91
	180	7.159	0.431	54.60	20.24
	240	7.364	0.423	56.17	19.84
	300	7.191	0.439	54.85	20.59
	360	6.845	0.459	52.21	21.55
	420	7.495	0.485	57.16	22.75
	480	7.329	0.491	55.90	23.07
	10	0	0.000	0.000	0.00
30		1.431	0.146	39.40	16.58
60		1.488	0.148	40.97	16.81
90		2.160	0.216	59.47	24.65
120		1.645	0.160	45.29	18.27
180		1.548	0.149	42.60	16.93
240		1.671	0.134	45.99	15.27
300		1.530	0.150	42.11	17.08
360		1.456	0.145	40.07	16.53
420		1.425	0.103	39.23	11.74
480		1.399	0.087	38.50	9.95
11		0	0.000	0.000	0.00
	30	5.167	0.473	49.27	15.51
	60	4.934	0.488	47.05	16.01
	90	5.161	0.521	49.22	17.10
	120	5.123	0.542	48.85	17.78
	180	4.639	0.550	44.24	18.03
	240	5.810	0.608	55.41	19.93
	300	5.054	0.596	48.19	19.55
	360	5.979	0.641	57.02	21.03
	420	6.105	0.644	58.22	21.11
	480	6.285	0.676	59.93	22.16

12	0	0.000	0.000	0.00	0.00
	30	1.733	0.079	22.19	5.83
	60	2.681	0.115	34.33	8.44
	90	3.057	0.121	39.13	8.87
	120	3.687	0.143	47.21	10.52
	180	4.017	0.137	51.43	10.01
	240	4.137	0.143	52.96	10.49
	300	5.689	0.205	72.83	15.06
	360	5.747	0.187	73.58	13.74
	420	5.746	0.209	73.57	15.35
	480	6.039	0.190	77.32	13.91
	13	0	0.000	0.000	0.00
30		2.284	0.067	68.91	3.94
60		2.010	0.107	60.64	6.28
90		1.828	0.121	55.13	7.12
120		1.750	0.142	52.78	8.33
180		1.721	0.156	51.91	9.13
240		1.768	0.151	53.32	8.84
300		1.840	0.187	55.49	10.96
360		1.796	0.154	54.18	9.03
420		1.770	0.167	53.40	9.82
480		1.767	0.152	53.31	8.91
14		0	0.000	0.000	0.00
	30	8.539	0.094	57.84	4.39
	60	8.004	0.195	54.22	9.17
	90	8.107	0.256	54.92	12.02
	120	8.052	0.322	54.54	15.10
	180	8.323	0.361	56.38	16.95
	240	8.452	0.511	57.25	23.98
	300	8.807	0.534	59.66	25.05
	360	8.609	0.520	58.32	24.41
	420	8.637	0.523	58.51	24.52
	480	8.996	0.531	60.94	24.93
	15	0	0.000	0.000	0.00
30		2.304	0.157	50.51	7.11
60		2.447	0.140	53.66	6.37
90		2.527	0.180	55.41	8.19
120		2.538	0.227	55.65	10.31
180		2.495	0.217	54.71	9.87
240		2.623	0.246	57.51	11.19
300		2.617	0.259	57.39	11.77
360		2.681	0.261	58.78	11.85
420		2.522	0.262	55.30	11.89
480		2.670	0.282	58.54	12.80
16		0	0.000	0.000	0.00
	30	4.788	0.179	66.52	9.43
	60	4.856	0.266	67.46	14.03
	90	2.754	0.331	38.26	17.43
	120	3.159	0.394	43.89	20.79
	180	3.158	0.422	43.88	22.25
	240	2.797	0.519	38.85	27.38
	300	3.100	0.570	43.07	30.04
	360	3.353	0.580	46.58	30.60
	420	3.487	0.575	48.44	30.31
	480	3.503	0.586	48.67	30.90

The extent of Au and Ag leaching during screening tests 17 - 32 are given in Table 45.

Table 45: Extent of Au and Ag leaching during the screening phase repeat experiments

Test	Residence Time [min]	Mass Leached [mg]		Extraction (%)	
		Ag	Au	Ag	Au
17	0	0.000	0.000	0.00	0.00
	120	3.349	0.163	56.20	9.19
	240	3.046	0.165	51.11	9.33
	360	3.171	0.150	53.20	8.47
	480	3.439	0.157	57.71	8.88
18	0	0.000	0.000	0.00	0.00
	120	3.373	0.300	45.00	22.20
	240	2.738	0.298	36.53	22.05
	360	2.402	0.245	32.05	18.16
	480	2.090	0.144	27.88	10.68
19	0	0.000	0.000	0.00	0.00
	120	1.879	0.167	69.53	39.93
	240	1.824	0.160	67.50	38.28
	360	1.817	0.168	67.24	40.21
	480	1.767	0.187	65.38	44.88
20	0	0.000	0.000	0.00	0.00
	120	3.395	0.337	64.05	16.83
	240	3.571	0.390	67.37	19.49
	360	3.297	0.350	62.19	17.48
	480	3.419	0.408	64.49	20.37
21	0	0.000	0.000	0.00	0.00
	120	2.411	0.238	50.26	15.46
	240	2.320	0.246	48.38	15.97
	360	1.731	0.222	36.10	14.39
	480	1.818	0.127	37.90	8.23
22	0	0.000	0.000	0.00	0.00
	120	1.275	0.114	53.70	11.52
	240	1.309	0.119	55.11	12.03
	360	1.274	0.112	53.63	11.32
	480	1.292	0.071	54.39	7.19
23	0	0.000	0.000	0.00	0.00
	120	2.997	0.121	41.92	5.73
	240	3.238	0.207	45.30	9.79
	360	3.177	0.211	44.44	10.01
	480	3.351	0.286	46.87	13.55
24	0	0.000	0.000	0.00	0.00
	120	1.627	0.124	45.51	9.02
	240	1.525	0.134	42.66	9.78
	360	1.482	0.128	41.47	9.35
	480	1.511	0.145	42.26	10.58
25	0	0.000	0.000	0.00	0.00
	120	3.921	0.247	53.78	17.88
	240	4.126	0.276	56.58	20.01
	360	4.119	0.315	56.49	22.79
	480	4.155	0.360	56.98	26.08
26	0	0.000	0.000	0.00	0.00

	120	1.520	0.138	49.04	8.07
	240	1.603	0.159	51.71	9.32
	360	1.495	0.141	48.23	8.26
	480	1.397	0.112	45.07	6.57
27	0	0.000	0.000	0.00	0.00
	120	6.615	0.654	63.88	22.88
	240	5.972	0.729	57.67	25.49
	360	6.075	0.777	58.67	27.16
	480	6.228	0.887	60.15	31.01
28	0	0.000	0.000	0.00	0.00
	120	1.800	0.098	51.78	9.12
	240	2.050	0.105	58.98	9.81
	360	2.137	0.107	61.47	9.98
	480	2.282	0.112	65.65	10.50
29	0	0.000	0.000	0.00	0.00
	120	2.041	0.119	59.36	10.05
	240	2.044	0.155	59.46	13.02
	360	1.992	0.118	57.93	9.91
	480	2.021	0.114	58.78	9.62
30	0	0.000	0.000	0.00	0.00
	120	3.711	0.139	64.20	9.10
	240	3.612	0.186	62.48	12.22
	360	3.516	0.226	60.82	14.83
	480	3.609	0.330	62.43	21.61
31	0	0.000	0.000	0.00	0.00
	120	3.592	0.158	51.45	5.44
	240	3.669	0.266	52.55	9.14
	360	3.699	0.312	52.98	10.73
	480	3.707	0.356	53.10	12.24
32	0	0.000	0.000	0.00	0.00
	120	3.952	0.240	46.71	16.57
	240	4.083	0.296	48.26	20.48
	360	4.492	0.336	53.10	23.23
	480	4.884	0.382	57.73	26.38

7.3.1.2. Thiosulphate Degradation

The results from thiosulphate degradation analyses are illustrated in Table 46.

Table 46: Thiosulphate degradation/consumption of screening tests

Test	Thiosulphate [M]				
	0 min	120 min	240 min	360 min	480 min
1	0.100	0.008	0.003	0.001	0.000
2	0.100	0.019	0.002	0.000	0.000
19	0.200	0.008	0.009	0.006	0.000
4	0.200	0.024	0.013	0.011	0.007
5	0.100	0.004	0.001	0.000	0.000
6	0.100	0.003	0.001	0.000	0.000
7	0.200	0.051	0.036	0.018	0.013
8	0.200	0.049	0.025	0.019	0.006
9	0.100	0.045	0.031	0.006	0.000
10	0.100	0.028	0.008	0.000	0.000
11	0.200	0.074	0.033	0.013	0.010
12	0.200	0.095	0.077	0.022	0.009
13	0.100	0.002	0.000	0.000	0.000
14	0.100	0.007	0.005	0.001	0.000
15	0.200	0.040	0.036	0.028	0.016
16	0.200	0.030	0.022	0.022	0.013

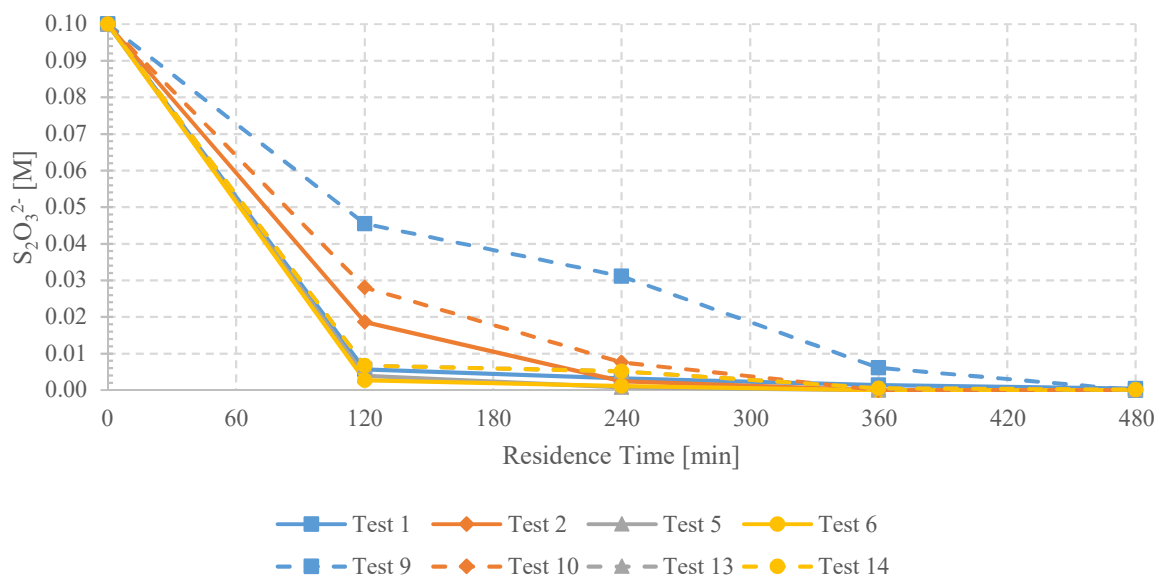


Figure 53: Thiosulphate degradation during tests which used 0.1 M $S_2O_3^{2-}$ (extended)

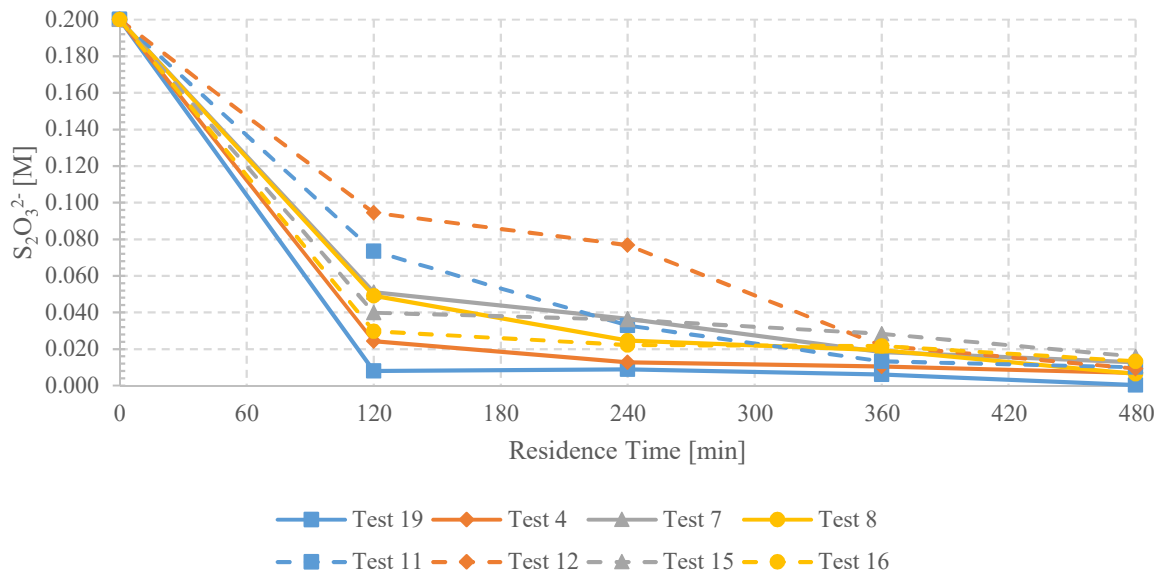


Figure 54: Thiosulphate degradation during tests which used $0.2 \text{ M S}_2\text{O}_3^{2-}$ (extended)

Several degradation tests reported minute concentrations of thiosulphate due to the time between the end of each test and the thiosulphate degradation analyses being too long. This resulted in the repetition of several tests to generate plausible degradation curves. The tests which provided thiosulphate concentrations that were detectable beyond 120 minutes were chosen to represent the best set of 16 tests for the screening phase. Tests 1, 2, 19 and 4 to 16 were chosen.

7.3.1.3. pH Regulation

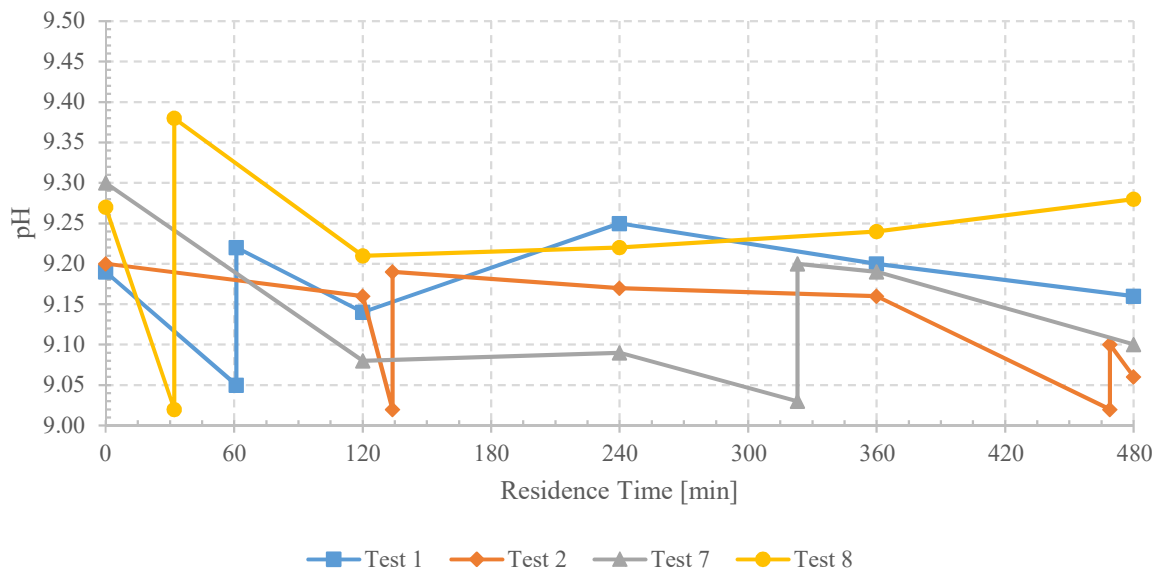


Figure 55: Change in pH for tests 1, 2, 7 and 8

The addition of NaOH shows a sudden rise in pH, while the addition of H₂SO₄ shows a sudden drop in pH. The screening tests in which the pH was controlled between 9 and 9.5 are tests 1, 2, 7, 8, 11, 12, 13 and 14. The change in pH of these tests are illustrated in Figure 55 and Figure 56.

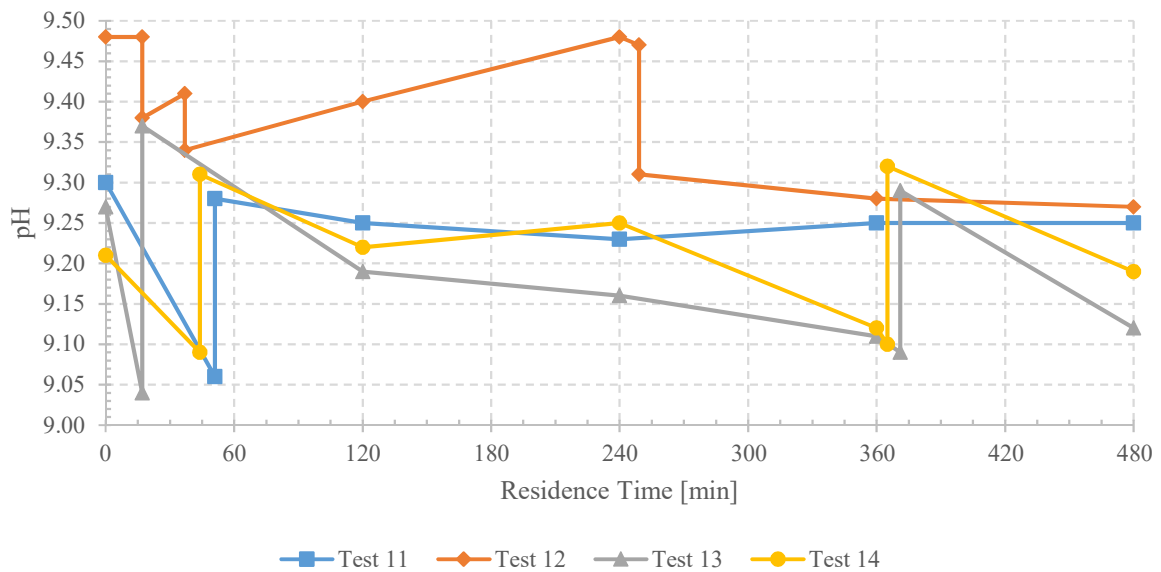


Figure 56: Change in pH for tests 11, 12, 13 and 14

The screening tests in which the pH was controlled between 10 and 10.5 are tests 3, 4, 5, 6, 9, 10, 15 and 16. The change in pH of these tests are illustrated in Figure 57 and Figure 58.

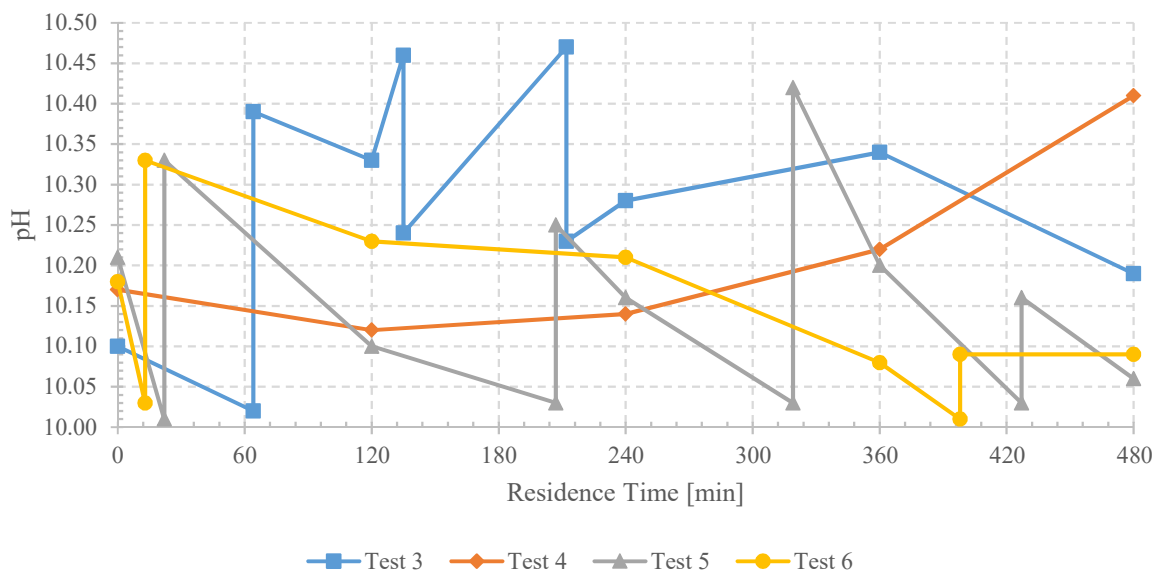


Figure 57: Change in pH for tests 3, 4, 5 and 6

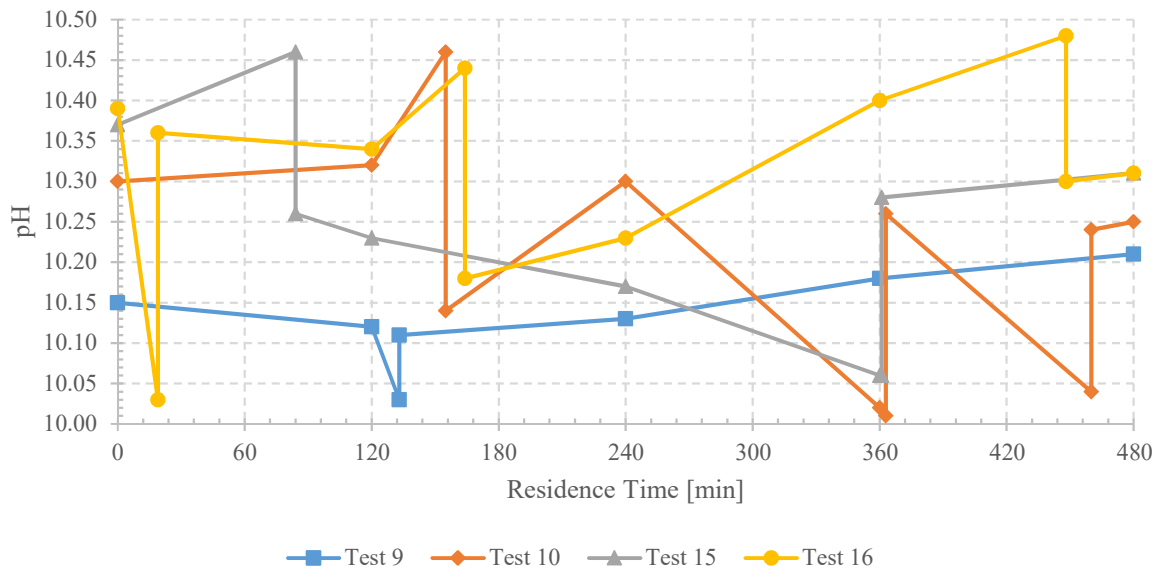


Figure 58: Change in pH for tests 9, 10, 15 and 16

7.3.1.4. Gold and Silver Extraction According to ICP-MS

The calculation of the Au and Ag extraction from results of ICP-MS were completed in the same manner as the results from ICP-OES. The only difference being that the mass of leached Au and Ag were determined by results from ICP-MS.

Table 47: Calculation of Au and Ag extraction (ICP-MS)

Test	Mass Leached		Extraction	
	Au [mg]	Ag [mg]	Au [%]	Ag [%]
17	0.189	3.246	10.537	56.288
18	0.074	2.136	6.605	34.129
19	0.483	1.784	67.760	68.412
20	0.534	2.628	25.091	60.307
21	0.153	1.907	10.566	44.428
22	0.093	0.752	9.669	41.362
23	0.322	3.653	15.000	49.032
24	0.091	1.569	6.930	44.607
25	0.271	3.180	21.004	50.337
26	0.199	1.442	11.361	49.066
27	0.647	5.575	24.709	59.849
28	0.211	2.210	18.064	64.916
29	0.028	2.118	2.683	60.305
30	0.109	3.915	8.339	65.419
31	0.314	3.630	10.947	52.574
32	0.451	4.262	29.733	54.375

7.3.1.5. Statistical Analysis

Table 48: Confounding of effects in the screening analysis

Factor	Confounding of Effects					
	Alias	Alias	Alias	Alias	Alias	Alias
(1) Cu on PCB	2*3*5	2*6*7	3*4*7	4*5*6		
(2) S ₂ O ₃ [M]	1*3*5	1*6*7	3*4*6	4*5*7		
(3) Cu(II) [M]	1*2*5	1*4*7	2*4*6	5*6*7		
(4) NH ₃ [M]	1*3*7	1*5*6	2*3*6	2*5*7		
(5) T [°C]	1*2*3	1*4*6	2*4*7	3*6*7		
(6) pH	1*2*7	1*4*5	2*3*4	3*5*7		
(7) Pulp Density [g/L]	1*2*6	1*3*4	2*4*5	3*5*6		
1 by 2	3*5	6*7				
1 by 3	2*5	4*7				
1 by 4	3*7	5*6				
1 by 5	2*3	4*6				
1 by 6	2*7	4*5				
1 by 7	2*6	3*4				
2 by 4	3*6	5*7				
1*2*4	1*3*6	1*5*7	2*3*7	2*5*6	3*4*5	4*6*7

Table 49: Redundant effects in the screening analysis

Number	Effect	Number	Effect	Number	Effect	Number	Effect	Number	Effect
1	2*3	11	4*7	21	1*3*6	31	2*3*6	41	3*4*7
2	2*5	12	5*6	22	1*3*7	32	2*3*7	42	3*5*6
3	2*6	13	5*7	23	1*4*5	33	2*4*5	43	3*5*7
4	2*7	14	6*7	24	1*4*6	34	2*4*6	44	3*6*7
5	3*4	15	1*2*3	25	1*4*7	35	2*4*7	45	4*5*6
6	3*5	16	1*2*5	26	1*5*6	36	2*5*6	46	4*5*7
7	3*6	17	1*2*6	27	1*5*7	37	2*5*7	47	4*6*7
8	3*7	18	1*2*7	28	1*6*7	38	2*6*7	48	5*6*7
9	4*5	19	1*3*4	29	2*3*4	39	3*4*5		
10	4*6	20	1*3*5	30	2*3*5	40	3*4*6		

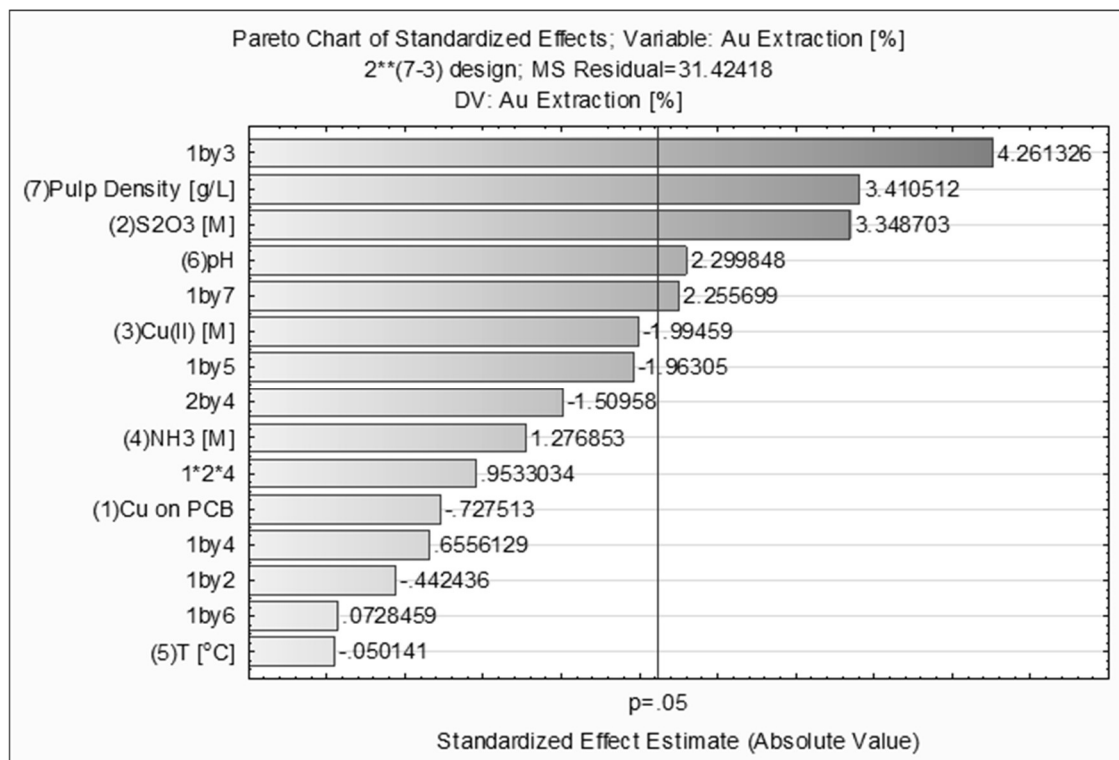


Figure 59: Initial Pareto chart of standardized effects

7.3.2. Full Factorial Phase

7.3.2.1. Gold and Silver Extraction

Table 50: Calculating the Au extraction at the end of the full factorial phase

Test	Au Leached [mg]				Total Extraction [%]	PML Stage Extraction [%]
	Residue	BML Tests		PML Test		
		HNO ₃ Leaching	H ₂ SO ₄ Leaching			
1	1.114	0.002	0.002	1.557	58.36	58.22
2	1.299	0.002	0.002	1.437	52.59	52.45
3	0.684	0.002	0.002	2.099	75.46	75.32
4	0.806	0.002	0.002	2.953	78.57	78.47
5	1.163	0.002	0.002	1.332	53.47	53.32
6	1.327	0.002	0.002	1.367	50.82	50.67
7	1.322	0.002	0.002	0.818	38.31	38.14
8	1.633	0.002	0.002	1.712	51.24	51.13
9	2.527	0.002	0.002	1.734	40.75	40.66
10	1.126	0.002	0.002	0.749	40.06	39.86
11	1.360	0.002	0.002	1.416	51.06	50.93
12	1.236	0.002	0.002	1.330	51.90	51.75
13	1.874	0.002	0.002	2.115	53.06	52.96
14	1.654	0.002	0.002	1.479	47.27	47.15
15	1.320	0.002	0.002	0.727	35.64	35.45
16	2.115	0.002	0.002	2.033	49.07	48.98

The final Au and Ag leaching during the full factorial phase experiments are given in Table 50 and Table 51.

Table 51: Calculating the Ag extraction at the end of the full factorial phase

Test	Ag Leached [mg]				Total Extraction [%]	PML Stage Extraction [%]
	Residue	BML Tests		PML Test		
		HNO ₃ Leaching	H ₂ SO ₄ Leaching			
1	0.488	0.138	0.270	2.480	85.54	73.45
2	0.864	0.138	0.270	2.155	74.80	62.90
3	0.420	0.138	0.270	1.329	80.50	61.60
4	0.720	0.138	0.270	3.762	85.27	76.93
5	0.787	0.138	0.270	4.082	85.09	77.36
6	0.599	0.138	0.270	4.441	89.01	81.52
7	0.563	0.138	0.270	0.836	68.85	46.28
8	1.142	0.138	0.270	2.371	70.88	60.48
9	1.522	0.138	0.270	2.343	64.38	54.84
10	1.663	0.138	0.270	1.489	53.29	41.83
11	1.830	0.138	0.270	3.608	68.69	61.71
12	1.452	0.138	0.270	3.873	74.68	67.56
13	1.731	0.138	0.270	5.159	76.29	70.70
14	1.612	0.138	0.270	5.580	78.79	73.42
15	1.566	0.138	0.270	1.125	49.47	36.31
16	1.553	0.138	0.270	3.421	71.14	63.56

7.3.2.2. Change in pH and Eh

The change in pH and Eh (standard hydrogen electrode) during tests are given in Table 52. The Eh values were considered to be unreliable however.

Table 52: Change in pH and Eh during full factorial tests

Test	Time [min]							
	120		240		360		480	
	pH	Eh [mV]	pH	Eh [mV]	pH	Eh [mV]	pH	Eh [mV]
1	9.33	12	9.29	20	9.29	25	9.36	31
2	9.29	-11	9.29	-7	9.31	-7	9.3	-7
3	9.31	0	9.29	6	9.28	11	9.26	17
4	9.24	-17	9.32	-15	9.33	-13	9.34	-16
5	10.17	8	10.29	21	10.39	20	10.27	23
6	10.23	-34	10.29	-27	10.29	-25	10.35	-18
7	10.17	1	10.15	9	10.16	14	10.11	12
8	10.26	-54	10.26	-48	10.28	-48	10.3	-48
9	9.25	23	9.25	28	9.25	41	9.3	46
10	9.06	-4	9.022	-12	9.21	-11	9.21	-3
11	9.29	-12	9.29	12	9.22	18	9.28	18
12	9.28	-12	9.25	-16	9.2	-20	9.16	-7
13	10.38	-1	10.25	7	10.22	12	10.29	15
14	10.25	-33	10.19	-25	10.19	-25	10.13	-21
15	10.15	-12	10.12	-6	10.14	-3	10.18	-6
16	10.11	-45	10.1	-45	10.33	-47	10.33	-45

7.3.2.3. Rate Limiting Step

The comparison of the different rate limiting steps are given in Figure 60 to Figure 62 for tests 1 to 4.

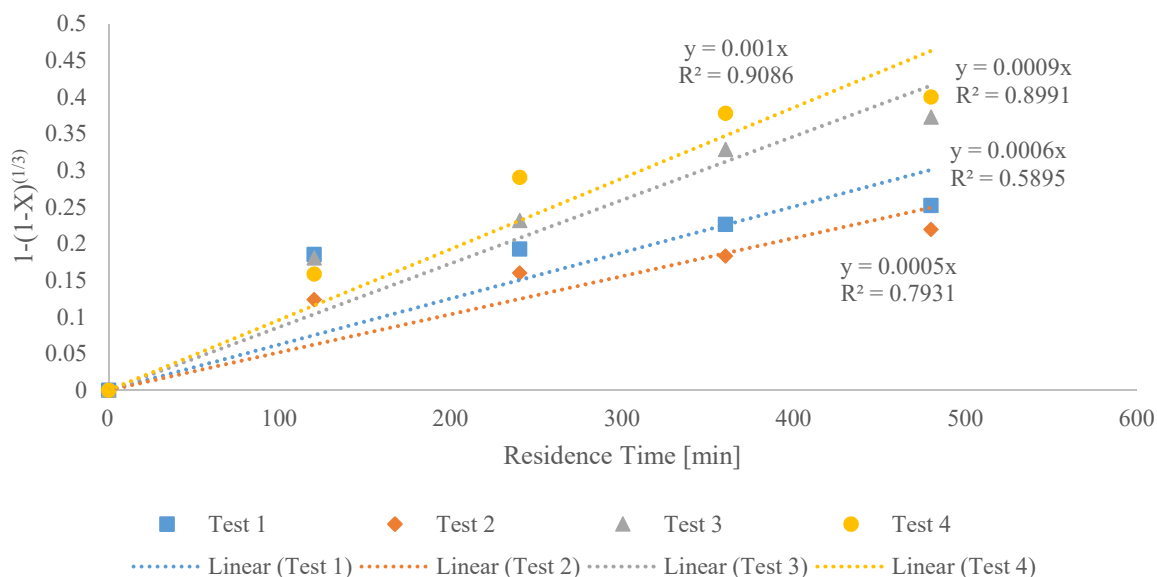


Figure 60: Rate controlled by surface chemical reaction

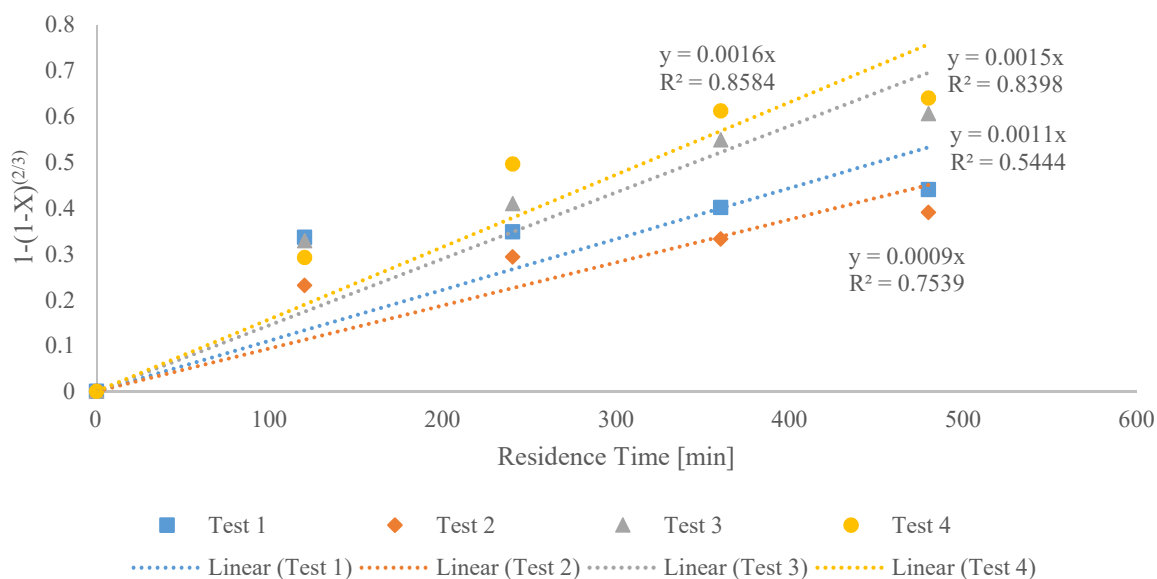


Figure 61: Rate controlled by diffusion in the boundary layer

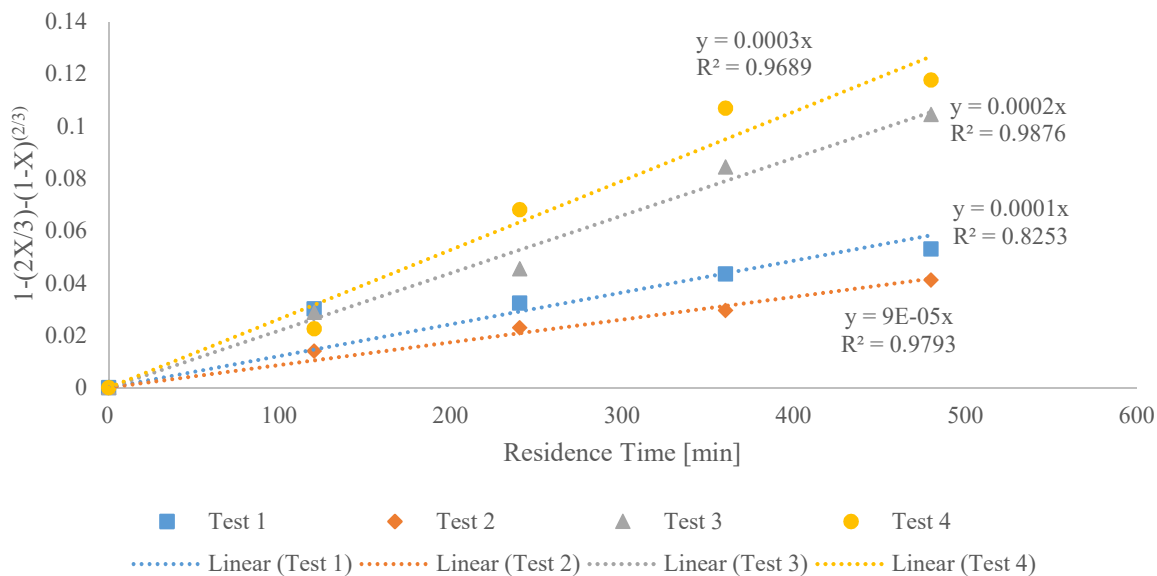


Figure 62: Rate controlled by diffusion in the porous product layer

7.3.2.4. Au Extraction Fitted Surface Plots

The Au extraction fitted surface plots that were generated from the statistical model are given below. Note that a value of 0 represented the low pH range, while 1 represented the high pH range.

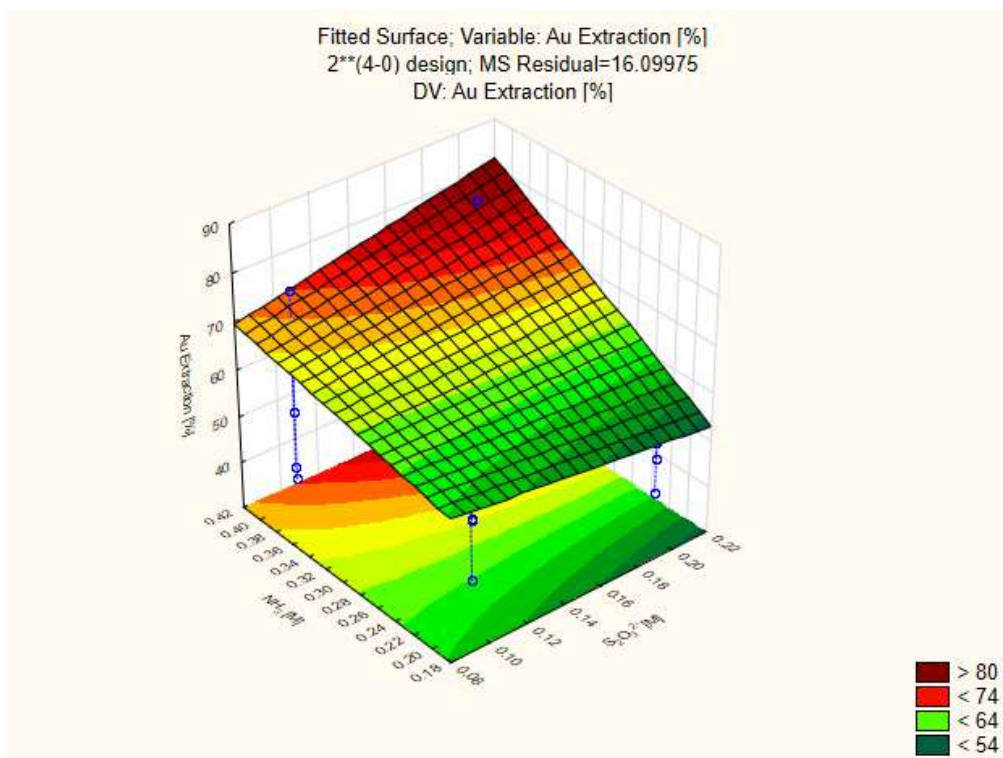


Figure 63: $\text{NH}_3 - \text{S}_2\text{O}_3^{2-}$ fitted surface plot (pH 9 – 9.5, 25 g/L)

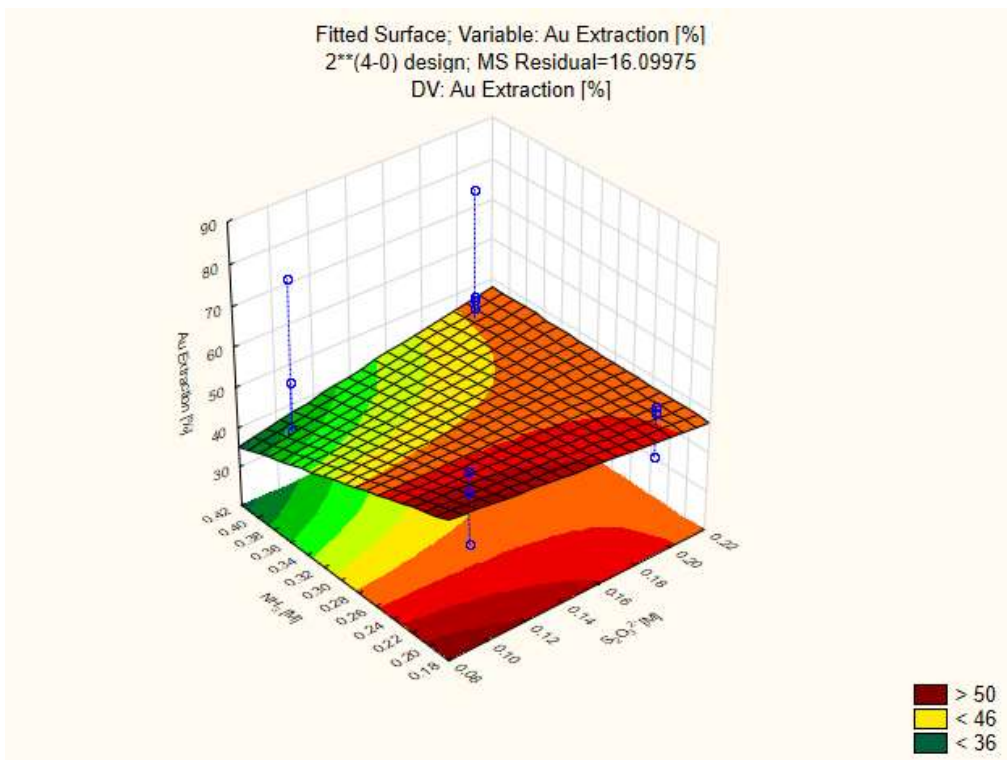


Figure 64: $\text{NH}_3 - \text{S}_2\text{O}_3^{2-}$ fitted surface plot (pH 10 – 10.5, 50 g/L)

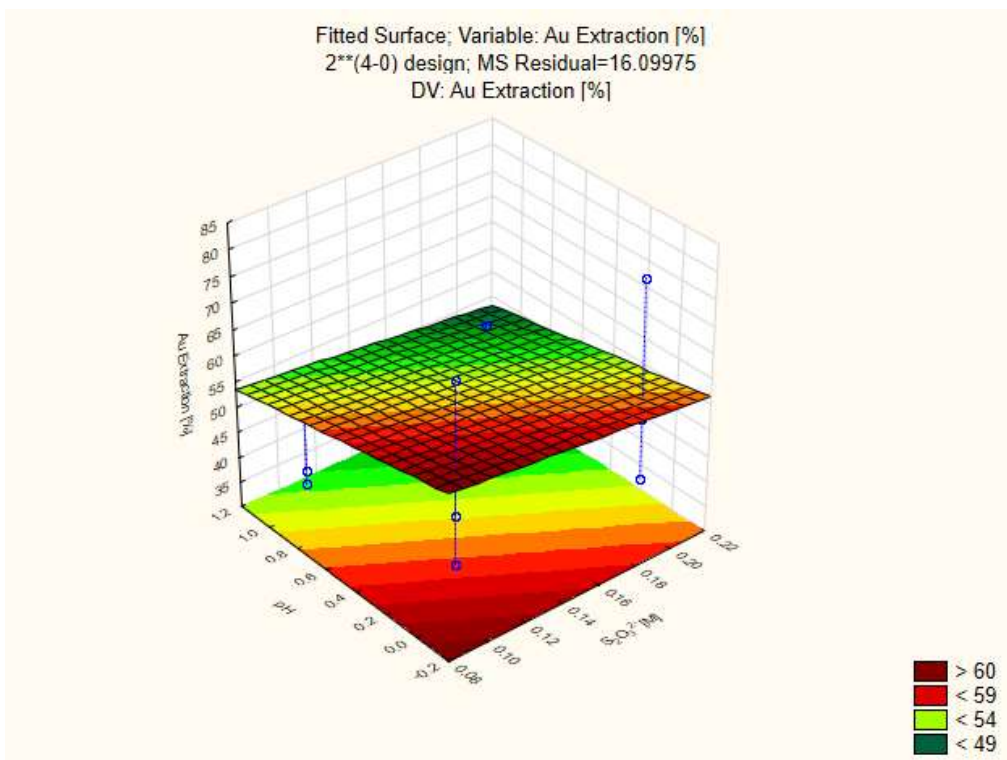


Figure 65: $\text{pH} - \text{S}_2\text{O}_3^{2-}$ fitted surface plot (0.2 M NH_3 , 25 g/L)

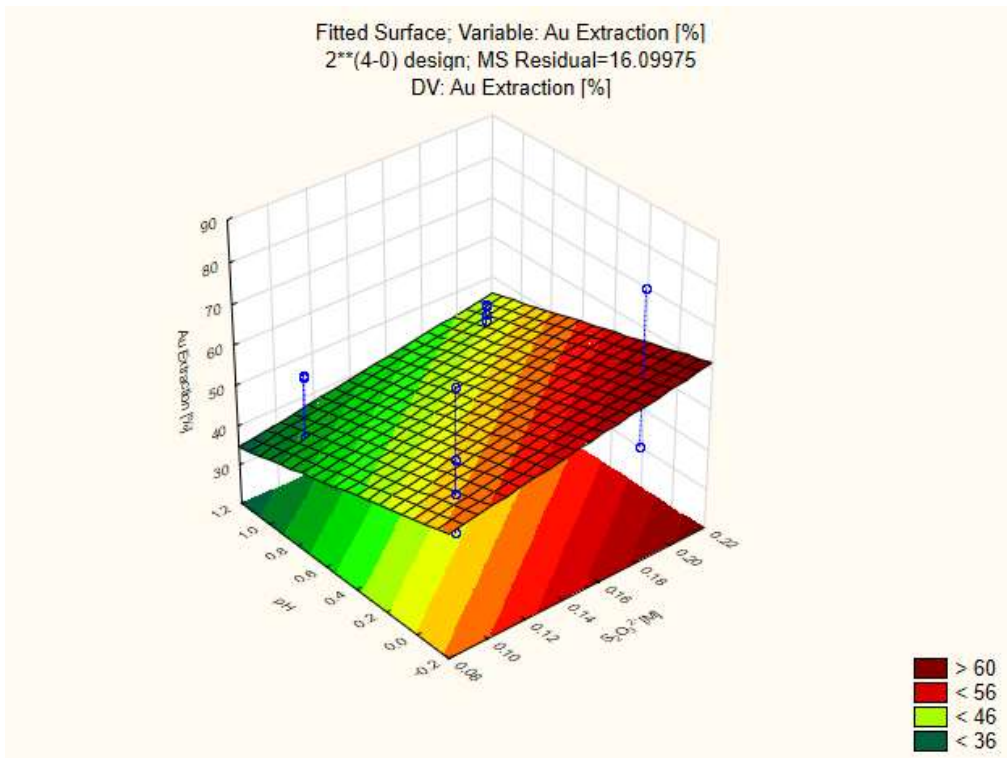


Figure 66: pH – $S_2O_3^{2-}$ fitted surface plot (0.4 M NH_3 , 50 g/L)

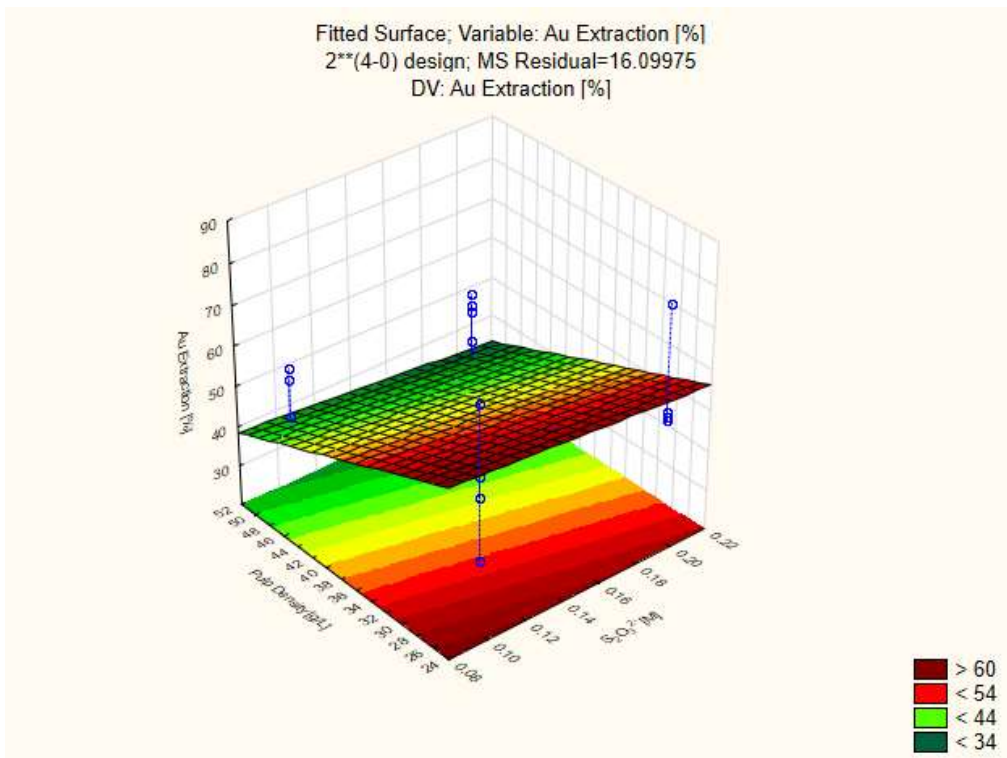


Figure 67: Pulp density – $S_2O_3^{2-}$ fitted surface plot (pH 9 – 9.5, 0.2 M NH_3)

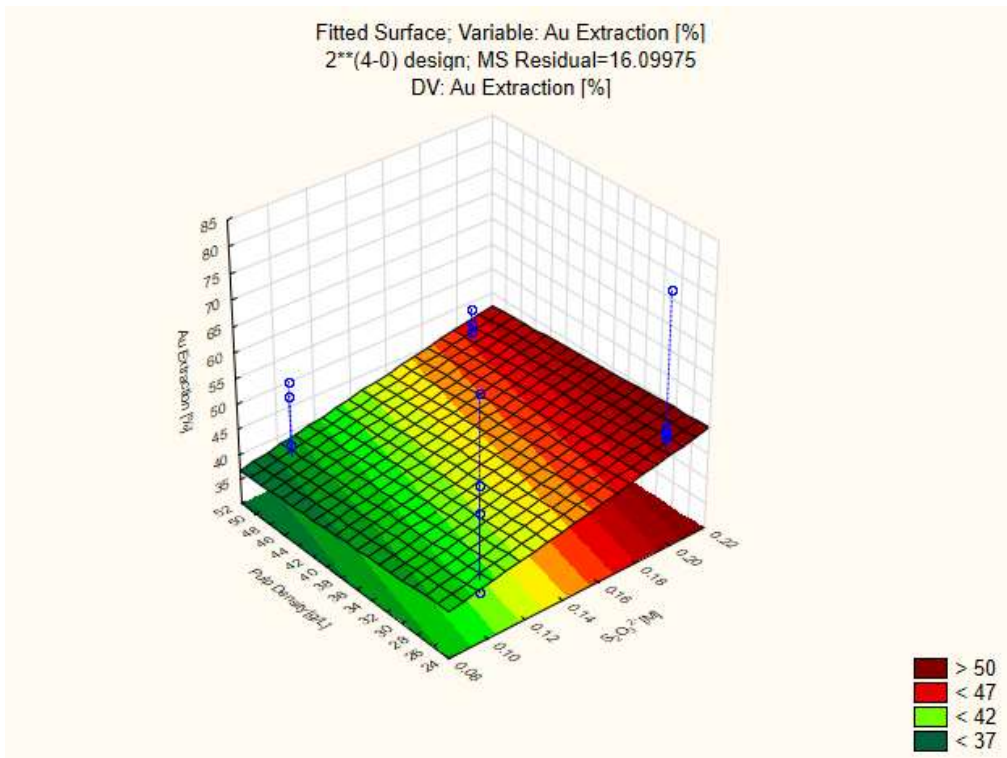


Figure 68: Pulp density – $S_2O_3^{2-}$ fitted surface plot (pH 10 – 10.5, 0.4 M NH_3)

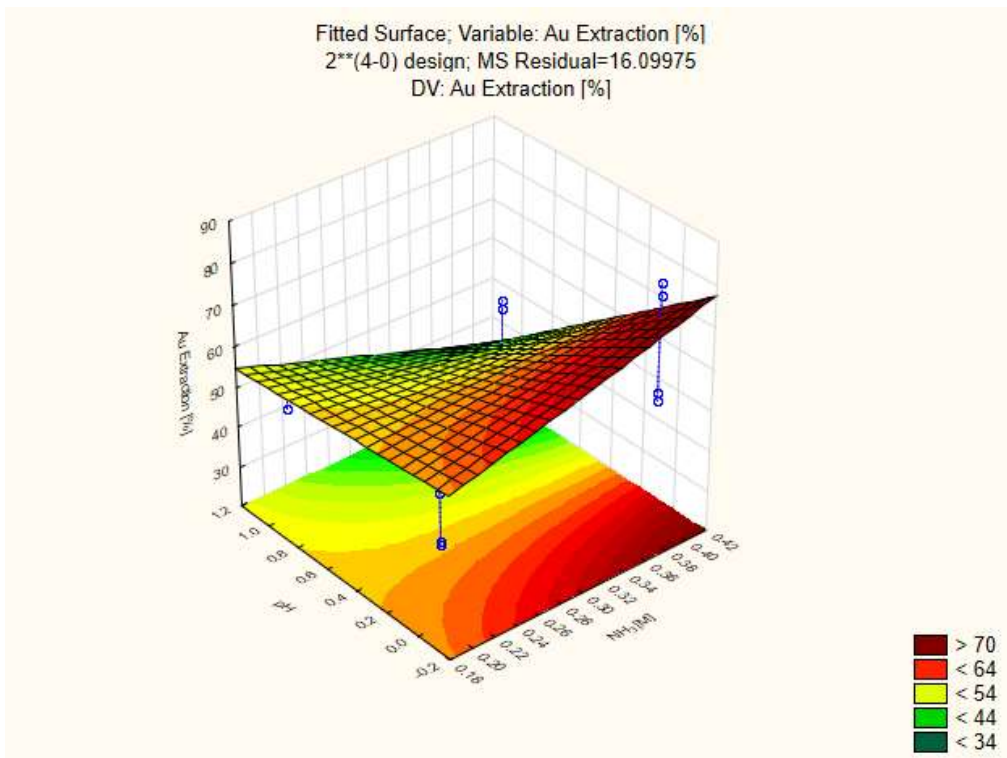


Figure 69: pH – NH_3 fitted surface plot (0.1 M $S_2O_3^{2-}$, 25 g/L)

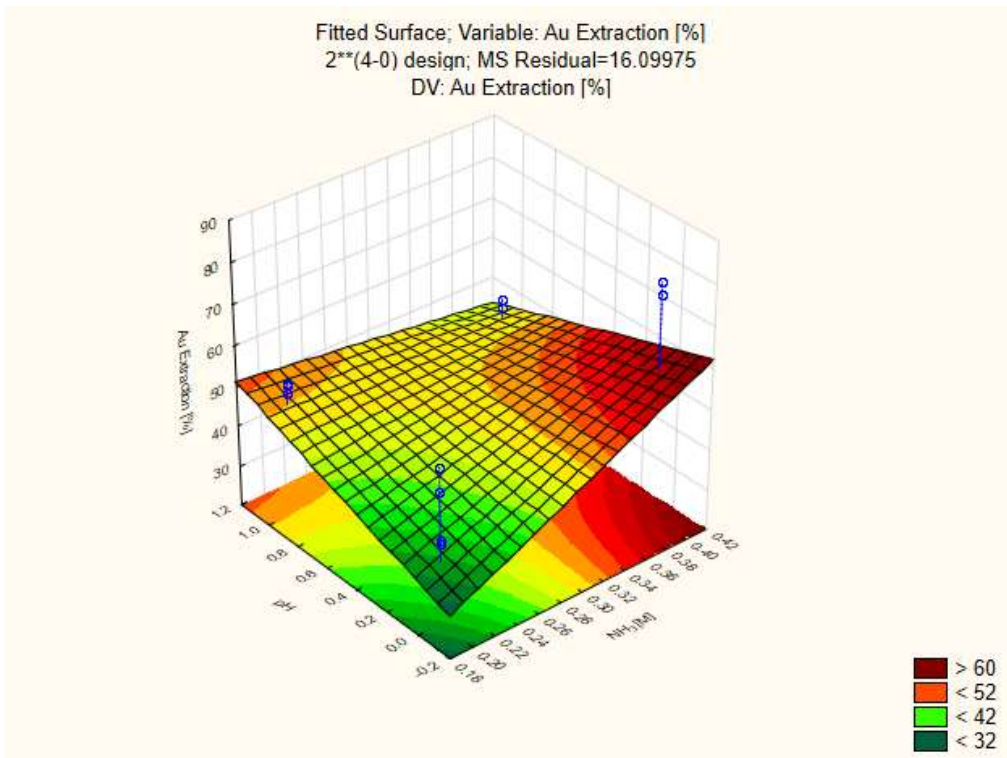


Figure 70: pH – NH₃ fitted surface plot (0.2 M S₂O₃²⁻, 50 g/L)

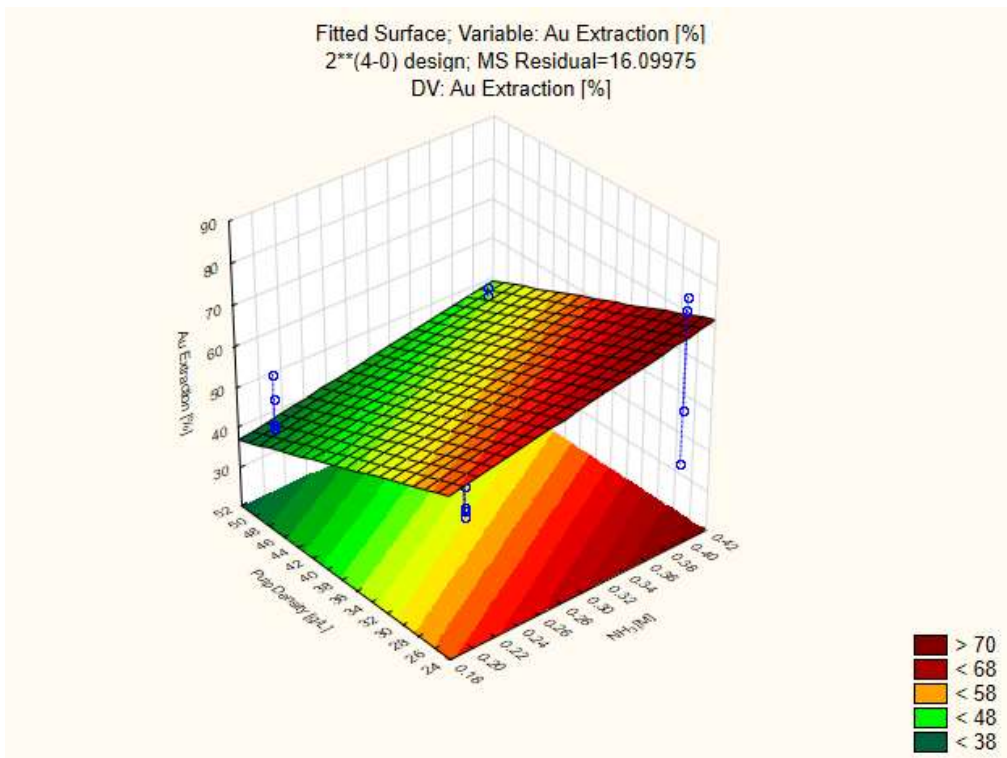


Figure 71: Pulp density – NH₃ fitted surface plot (pH 9 – 9.5, 0.1 M S₂O₃²⁻)

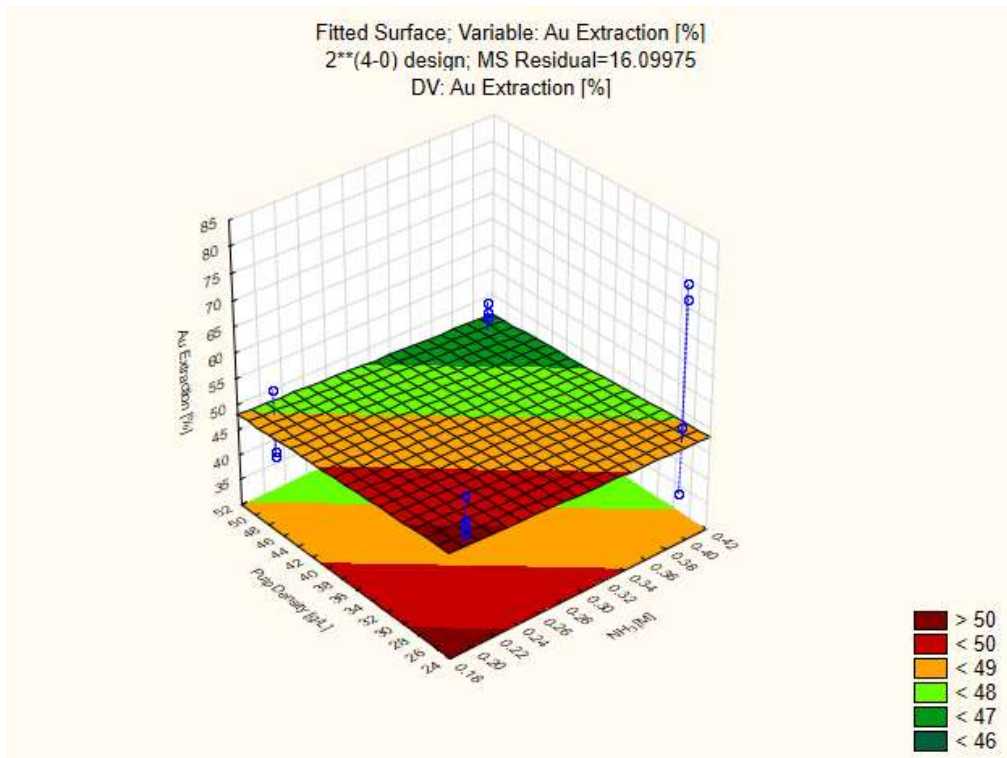


Figure 72: Pulp density – NH₃ fitted surface plot (pH 10 – 10.5, 0.2 M S₂O₃²⁻)

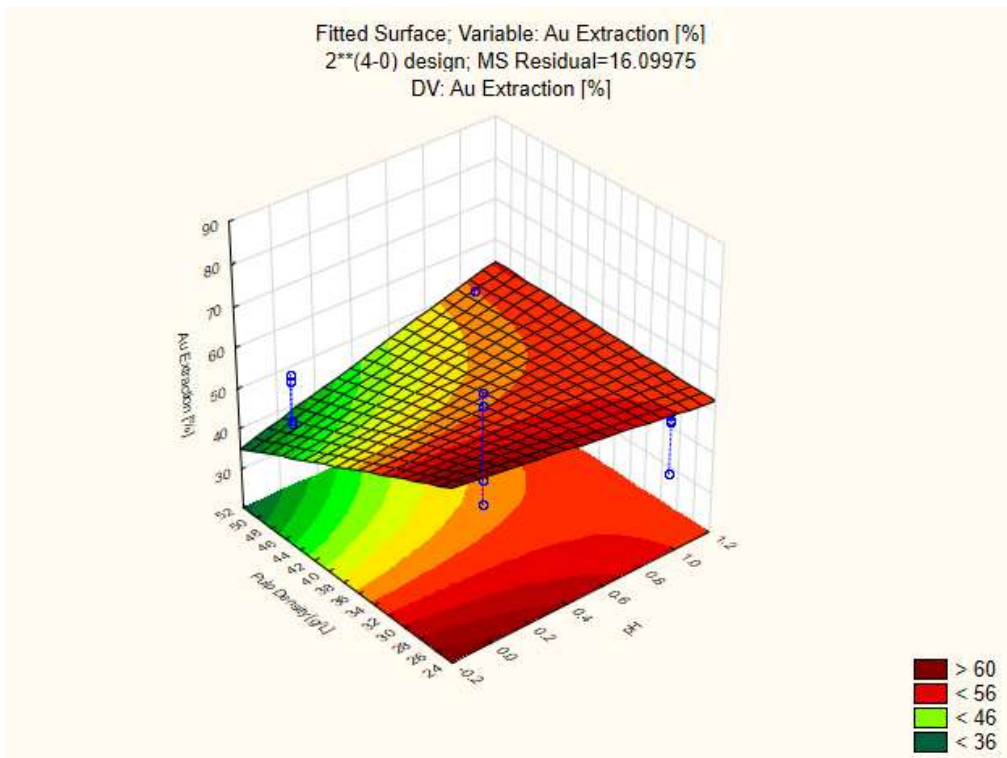


Figure 73: Pulp density – pH fitted surface plot (0.1 M S₂O₃²⁻, 0.2 M NH₃)

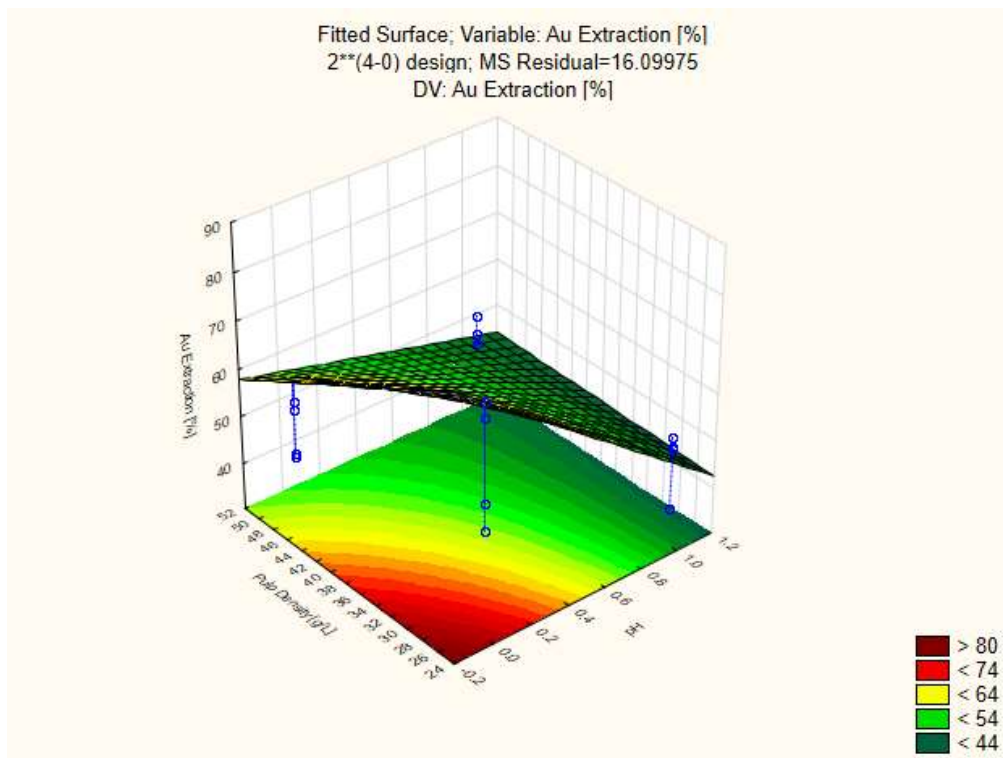


Figure 74: Pulp density – pH fitted surface plot (0.2 M $S_2O_3^{2-}$, 0.4 M NH_3)

7.3.3. Optimisation Phase

Table 53 illustrates the six tests that were conducted in the optimization phase. The test constants were $S_2O_3^{2-}$ concentration (0.2 M), NH_3 concentration (0.4 M), pulp density (25 g/L) and pH range (9 – 9.5). The residue from test 1 was used as feed material for test 3, which implemented the same conditions as test 1.

Table 53: Test conditions for the optimization phase

Test	Leftover Cu [%]	T [°C]	Cu(II) [M]
1	1 - 10	25	0.02
2	1 - 10	50	0.02
3	-	25	0.02
4	100	25	0.02
5	1 - 10	25	0.06
6	1 - 10	40	0.02

7.3.3.1. Gold and Silver Extraction

The final Au and Ag extraction during the optimization phase are given in Table 54 and Table 55. The extent of Au and Ag leaching throughout the duration of each test is given in Table 56.

Table 54: Calculating the Au extraction at the end of the optimization phase

Test	Au Leached [mg]				Total Extraction [%]	PML Stage Extraction [%]
	Residue	BML Tests		PML Test		
		HNO ₃ Leaching	H ₂ SO ₄ Leaching			
1		0.002	0.002	2.984	74.17	74.07
2	0.520	0.002	0.002	0.927	64.14	62.37
3	0.594	0.002	0.002	0.447	11.19	11.09
4	1.855	0.002	0.002	0.213	10.46	10.28
5	0.802	0.002	0.002	1.324	62.35	62.18
6	0.653	0.002	0.002	0.957	59.53	55.75

Table 55: Calculating the Ag extraction at the end of the optimization phase

Test	Ag Leached [mg]				Total Extraction [%]	PML Stage Extraction [%]
	Residue	BML Tests		PML Test		
		HNO ₃ Leaching	H ₂ SO ₄ Leaching			
1		0.138	0.270	5.292	75.69	70.27
2	0.745	0.138	0.270	2.367	78.83	62.75
3	0.837	0.138	0.270	0.994	18.62	13.21
4	2.756	0.138	0.270	1.278	37.95	28.77
5	1.517	0.138	0.270	5.086	78.36	72.54
6	1.089	0.138	0.270	2.698	74.05	63.87

Table 56: Extent of Au and Ag leaching during the optimization phase experiments

Test	Residence Time [min]	Mass Leached [mg]		Extraction [%]	
		Ag	Au	Ag	Au
1	120	5.015	1.715	66.597	42.583
	240	5.235	2.386	69.508	59.221
	360	5.198	2.862	69.023	71.055
	480	5.292	2.984	70.270	74.072
2	120	2.294	0.904	65.156	62.267
	240	2.367	0.908	67.243	63.585
	360	2.287	0.927	64.967	63.877
	480	2.209	0.905	62.755	62.374
3	120	0.973	0.378	12.927	9.380
	240	0.985	0.393	13.074	9.762
	360	0.965	0.430	12.820	10.682
	480	0.994	0.447	13.205	11.095
4	120	1.015	0.171	22.848	8.262
	240	1.117	0.190	25.152	9.191
	360	1.232	0.193	27.725	9.298
	480	1.278	0.213	28.770	10.281
5	120	4.890	0.953	69.741	44.752
	240	4.855	1.116	69.247	52.401
	360	5.036	1.250	71.823	58.694
	480	5.086	1.324	72.543	62.176
6	120	2.620	0.957	62.453	59.295
	240	2.698	0.940	64.324	58.223
	360	2.541	0.915	60.591	56.687
	480	2.679	0.900	63.871	55.746

7.3.3.2. Silver Extraction Curves

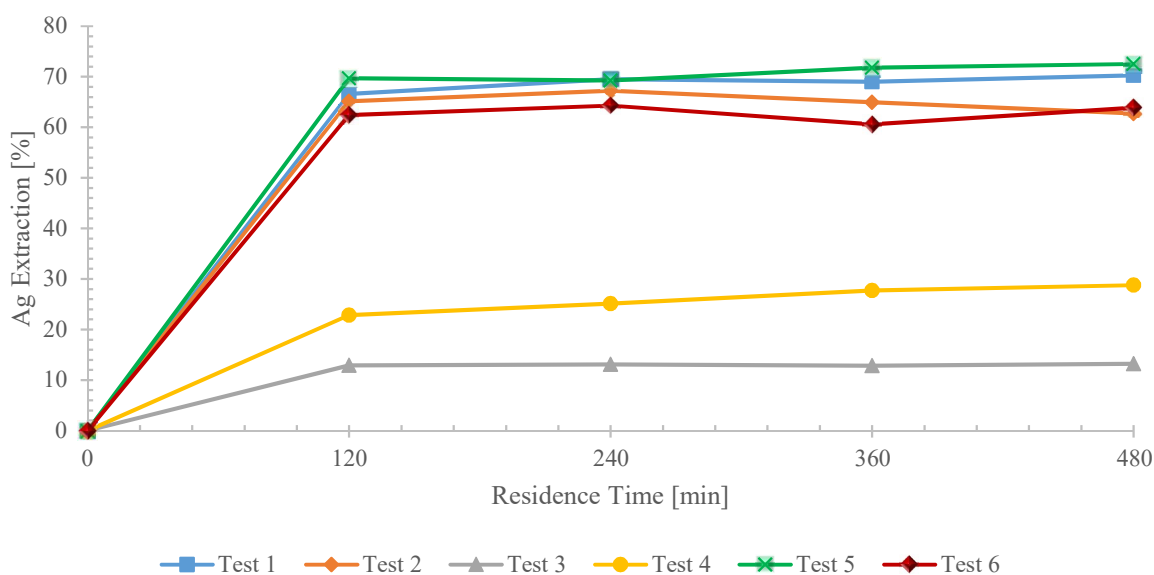


Figure 75: Silver extraction during optimization phase tests

Figure 75 indicated that a total Ag extraction of 83.5 % could be achieved in a two-step precious metal leaching stage. An increase in temperature from 40 to 50°C provided an initial increase in Ag extraction but increased precipitation. This meant that the final Ag extraction increased when the temperature was decreased from 50 to 25°C. An increase in Cu(II) concentration from 0.02 M to 0.06 M resulted in increased Ag extraction. Increased amounts of Cu leftover from the base metal leaching stage resulted in reduced Ag extraction.

7.3.3.3. Thiosulphate Degradation/Consumption

The thiosulphate degradation/consumption encountered during the optimization phase tests is given in Table 57.

Table 57: Thiosulphate degradation/consumption of optimization phase tests

Test	Thiosulphate [M]				
	0 min	120 min	240 min	360 min	480 min
1	0.200	0.122	0.088	0.077	0.061
2	0.200	0.056	0.040	0.035	0.029
3	0.200	0.115	0.106	0.095	0.087
4	0.200	0.101	0.076	0.064	0.051
5	0.200	0.088	0.073	0.071	0.064
6	0.200	0.082	0.072	0.059	0.053

7.3.3.4. Change in pH

The change in pH during these tests are given in Table 58.

Table 58: Change in pH during optimization phase test

Test	pH			
	120 min	240 min	360 min	480 min
1	9.34	9.35	9.42	9.41
2	9.21	9.09	9.12	9.02
3	9.17	9.26	9.25	9.28
4	9.37	9.32	9.37	9.34
5	9.2	9.22	9.17	9.12
6	9.13	9.08	9.13	9.12